Environment Canada Environnement Canada

National Hydrology Research Institute

NHRI PAPER NO. 13
IWD SCIENTIFIC SERIES NO. 116

Hydrogeological and Hydrochemical Investigation of the Waste Disposal Basin at I.M.C.C. K2 Potash Plant, Esterhazy, Saskatchewan

J. A. Vonhof

NHRI

NATIONAL HYDROLOGY RESEARCH INSTITUTE
INLAND WATERS DIRECTORATE
OTTAWA, CANADA, 1985

Environment Canada Environnement Canada

National Hydrology Research Institute

*Present address:

Vonhof Consulting Ltd.,
5228 Veronica Rd. N.W.,
Calgary, Alberta.
T3A 0T3

NHRI PAPER NO. 13
IWD SCIENTIFIC SERIES NO. 116

Hydrogeological and Hydrochemical Investigation of the Waste Disposal Basin at I.M.C.C. K2 Potash Plant, Esterhazy, Saskatchewan

J. A. Vonhof*

NHRI

NATIONAL HYDROLOGY RESEARCH INSTITUTE
INLAND WATERS DIRECTORATE
OTTAWA, CANADA, 1983

© Minister of Supply and Services Canada 1983

Cat. No. En 36-502/116E

ISBN 0-662-12894-7

Contents

	Page
ABSTRACT	xi
RÉSUMÉ	xii
ACKNOWLEDGMENTS	xiii
1. INTRODUCTION	1
General remarks	1
Objectives	1
Location of study area, physiography, and climate	1
2. PRAIRIE EVAPORITE FORMATION	3
General stratigraphy	3
Relationship between ore and waste products	4
3. WASTE DISPOSAL TECHNIQUES	5
4. PROBLEMS RELATED TO WASTE DISPOSAL	6
General	6
Evaporation	6
Erosion	6
5. REGIONAL STRATIGRAPHY	8
Introduction	8
Regional bedrock stratigraphy and topography	8
Surficial features	9
6. STRATIGRAPHY OF I.M.C.C. K2 POTASH MINE DISPOSAL BASIN	10
Introduction	10
Riding Mountain Formation	11
Pleistocene stratigraphy	11
Battleford Formation	12
Floral Formation	12
Fluvial deposits	12
Evolution of bedrock topography and depositional history	13
Summary	14
7. OBSERVATION WELL NETWORK	15
Introduction	15
Well construction	15
Operating experience	16
Fuel requirements	17
Hydrodynamic response of wells and changes with time	17
Observation well record 1971-1975 (incl.)	19
Barometric efficiency	20
Long-term water level fluctuations	20
Summary	22

Contents (Cont.)

Page

8. AN ELECTRIC ANALOG SIMULATION OF GROUNDWATER FLOW PATTERNS (D.R. Bourne and J.A. Vonhof) 23
Introduction. 23
Steady state 23
Transient case. 24
Hydraulic conductivity distribution 24
Till 24
Buried valley fluvial deposits 25
Pump tests 25
Theis recovery method 25
Hydraulic conductivity estimates from grain size distributions 27
Hydrodynamic response tests. 27
Transmissibility estimates from well logs 27
Porosity and compressibility 28
Electric analog model 29
Analog model simulations 29
Steady state results 30
Transient results 30
Effect of flowing seismic shothole 31
Summary 31

9. GROUNDWATER CHEMISTRY (C.C. Davison and J.A. Vonhof) 33
Introduction. 33
1971 Groundwater sampling program 33
1972 Groundwater sampling program 34
1973 and 1974 Groundwater sampling program 36
Sampling schedule 36
Field methods. 36
Laboratory methods 38
Sample preservation during storage 38
Chemical equilibria 38
Solid phase equilibria 39
Spatial distribution of major constituents. 39
Speciation and mineral equilibria 40
Chemical processes occurring within the aquifer 41
Temporal distribution of dissolved constituents. 42
(a) flowing well 1 43
(b) flowing well 2 43
(c) ferric oxyhydroxide stability 44
Error analysis 45
Introduction. 45
Analytical inaccuracy 45
Variability 46
Sampling variation. 47
Distribution of variations 47
Uncertainty 48
Saturation index calculations. 50
Summary 50

Contents (Cont.)

Page

10. SEQUENTIAL SAMPLING OF OBSERVATION WELL NETWORK AND MONITORING 52

11. CONCLUSIONS 55

REFERENCES 57

APPENDIX I. Hydrodynamic response or slug-testing equipment (J. A. Banner and J. A. Vonhof) 137

APPENDIX II. Pump-test data for observation wells A to G 141

APPENDIX III. Theis recovery method data sheets for observation wells A to G 151

APPENDIX IV. Electric analog modeling (R. A. Bourne and J. A. Vonhof) 167

APPENDIX V. Summary field analyses hydrochemical sampling program 1972-1974 177

APPENDIX VI. Indirect determination of Cl and SO_4 in aqueous solutions by atomic absorption spectroscopy 195

APPENDIX VII. Standard addition method to detect and correct for interference effects in flame atomic absorption spectroscopy determinations of Ca, Mg, and K (R. R. Barefoot) 197

APPENDIX VIII. Calcium and magnesium analyses of unpreserved stored groundwater samples (C. C. Davison) 199

APPENDIX IX. Field laboratory and Western Laboratory analyses of split groundwater samples, summer 1973 201

Tables

1. Chemical composition of brine. 5

2. Barometric efficiencies of observation wells 20

3. Hydrogeologic components of the steady state and transient groundwater electric analog model 24

4. Hydraulic conductivity values for till and shale in Saskatchewan and other geologically similar areas 26

5. Transmissibility and storage coefficient values for the Theis and Jacob methods 27

6. Hydraulic conductivity estimates from the Theis recovery method for observation wells A to G 28

Tables (Cont.)

Page

7. Hydraulic conductivity values from hydrodynamic response tests for observation wells A to G 28
8. Injection well combinations and their injection rates. Each injection rate was simulated for 5, 10, 20, and 50 years 31
9. Quantity of water flowing through cross sections F-F' and H-H' for various brine level elevations 31
10. Travel times of brine from the brine pond to the flowing seismic shothole with the seismic shothole both plugged and unplugged 31
11. Iron concentration (mg/l) in pump discharge water 33
12. Major ion analyses of frozen and unfrozen samples, flowing well 1 and 2 35
13. Lead content in frozen and unfrozen surface water samples 36
14. Summary of sample bottle-sample solution analysis, unacidified groundwater samples 39
15. Major ion analyses for November 1973 groundwater samples 40
16. Summary of chemical saturation, November 1973 groundwater samples from WATEQF 40
17. Comparison of calculated bicarbonate and analyzed bicarbonate concentrations for November 1973 groundwater samples 42
18. pΩ Calculations for Eh range observed in flowing well 1 and flowing well 2 during 1973-1974 44
19. U.S. Geological Survey interlaboratory quality control study 45
20. Inland Waters interlaboratory quality control study 46
21. Mean, standard deviation and total coefficient of variation for major ions in field determinations: flowing well 1, 1972-1974 47
22. Mean, standard deviation and total coefficient of variation for major ions in field determinations: flowing well 2, 1972-1974 47
23. Mean, standard deviation and total coefficient of variation for major ions, Western Laboratory: flowing wells 1 and 2, 1973 48
24. Distribution of coefficients of variation for 1973 sampling program: flowing wells 1 and 2 48
25. Comparison of split groundwater samples, 1973, between field laboratory and Western Laboratory analyses: flowing wells 1 and 2 49
26. Saturation index uncertainty arising from analytical/storage uncertainties of the chemical species: flowing wells 1 and 2 49
27. Summary of analytical/storage uncertainty in the Western Laboratory determination of Ca, Mg, Fe, and HCO_3 during this study: flowing wells 1 and 2 49
28. Range of ionic concentration in surface and groundwater 50
29. Sequential analyses of observation wells A to G 53

Illustrations

Page

Figure 1. Location of area under investigation 62
Figure 2. Distribution of Prairie Evaporite Formation in prairie provinces 63
Figure 3. Structural cross section of Prairie Evaporite Formation, Saskatchewan 64
Figure 4. Kind and origin of wastes in the Saskatchewan potash industry 65
Figure 5. Waste disposal basin, I.M.C.C. K2 potash plant, Esterhazy, Saskatchewan . . . 66
Figure 6. Dyke erosion 67
Figure 7. Dyke protection 68
Figure 8. Pre-1969 bedrock topography 70
Figure 9. Bedrock topography after 1969 drilling program 71
Figure 10. Bedrock topography after 1969-1970 drilling program 72
Figure 11. Bedrock topography after 1970-1971 and 1972-1973 drilling program 73
Figure 12. Total carbonate content in Battleford and Floral Formations 74
Figure 13. Oxidized fractures in till (Floral Formation) 75
Figure 14. Plan view and polar projection of fracture pattern in Floral Formation 76
Figure 15. Location of observation wells 77
Figure 16. Observation well A: completion zone and record 78
Figure 17. Observation well B: completion zone and record 79
Figure 18. Observation well C: completion zone and record 80
Figure 19. Observation well D: completion zone and record 81
Figure 20. Observation well E: completion zone and record 82
Figure 21. Observation well F: completion zone and record 83
Figure 22. Observation well G: completion zone and record 84
Figure 23. Hydrograph data recovery for each observation well and cause of record loss 85
Figure 24. Summary of record loss for each observation well over total recording period and source of record loss 86
Figure 25. Propane gas consumption for each observation well: winter 1971-1972 87
Figure 26. Propane gas consumption for each observation well: winter 1972-1973 88
Figure 27. Transmissivities of observation wells from slug tests at different times over period 1971-1974 89
Figure 28. Consecutive slug tests with different size slug in observation well A and damped oscillation 90
Figure 29. Consecutive slug tests with different size slug in observation well B and damped oscillation 91
Figure 30. Sequential hydrodynamic response tests with different volumes added in observation wells F and G, Dec. 10 and 11, 1974 92
Figure 31. Instantaneous rise in brine level versus rise in water level in each well 93

Illustrations (Cont.)

Page

Figure 32. Lines of best fit of instantaneous rise in brine level versus water level in each well and correlation factors 94

Figure 33. Cross section J-J' illustrating the essential components of the study site boundary value problem 95

Figure 34. Cross section G-G' illustrating the essential components of the study site boundary value problem 96

Figure 35. Location of observation wells and flowing holes 97

Figure 36. Jacob method applied to observation well A with observation well B pumping at 8.3 lgpm (37.7 l/min) 98

Figure 37. Theis recovery method applied to observation well F 99

Figure 38. Transmissibility estimate (lgpd/ft) in the buried valley fluvial deposits 100

Figure 39. Steady state groundwater flow pattern in the till layer for a brine elevation of 1671 ft 101

Figure 40. Steady state groundwater flow pattern in the buried valley aquifer for a brine elevation of 1671 ft 102

Figure 41. Steady state groundwater flow pattern along cross section J-J' for a brine elevation of 1671 ft 103

Figure 42. Steady state groundwater flow pattern along cross section J-J' for a brine elevation of 1666 ft 104

Figure 43. Steady state groundwater flow pattern along cross section J-J' for a brine elevation of 1661 ft 105

Figure 44. Steady state groundwater flow pattern along cross section J-J' with no brine pond present 106

Figure 45. Graph of the travel time of brine moving from the brine pond plotted against distance from the eastern dyke of the brine pond 107

Figure 46. Location of injection wells and flowing seismic shothole (FW1) 108

Figure 47. Change in hydraulic head in the buried valley aquifer after 50 years of injection at 30 lgpm (136 l/min) per well 109

Figure 48. Resultant hydraulic head distribution in the buried valley aquifer after 50 years of injection at 30 lgpm (136 l/min) per well 110

Figure 49. Change in hydraulic head in the buried valley aquifer after 5 years for the seismic shothole (FW1) discharging at a rate of 20 lgpm (91 l/min) 111

Figure 50. Change in hydraulic head in the buried valley aquifer after 10 years for the seismic shothole (FW1) discharging at a rate of 20 lgpm (91 l/min) 112

Figure 51. Change in hydraulic head in the buried valley aquifer after 20 years for the seismic shothole (FW1) discharging at a rate of 20 lgpm (91 l/min) 113

Figure 52. Analytical results of water samples taken during the pump test at observation wells A and B which froze prior to analysis 114

Illustrations (Cont.)

Page

Figure 53. Daily analyses of alkalinity, calcium, and total hardness of samples from flowing wells 1 and 2 subjected to temperature cycles and shaking 115

Figure 54. Histogram of concentration of alkalinity, calcium, and total hardness of frozen versus unfrozen samples 116

Figure 55. Sampling flow sheet for heavy metal preservation study 117

Figure 56. Analytical results, heavy metal samples, flowing well 1 118

Figure 57. Analytical results, heavy metal samples, flowing well 3 119

Figure 58. Successive analyses, frozen heavy metal samples, flowing well 1 120

Figure 59. Successive analyses, frozen heavy metal samples, flowing well 3 121

Figure 60. Summary of hydrochemical sampling schedule, 1973 and 1974 122

Figure 61. Comparison of field and laboratory measured pH values of groundwater samples (after Davison, 1974) 123

Figure 62. Comparison of field and laboratory pCO_2 values of groundwater samples (after Davison, 1974) 124

Figure 63. Calcite saturation in stored groundwater samples (after Davison, 1974) 125

Figure 64. Na-SO_4 ion plot of aquifer water samples 126

Figure 65. Na-Cl plot of aquifer water samples 127

Figure 66. Modified Piper ion plot of aquifer water samples 128

Figure 67. Temporal ion plots for water samples collected from flowing well 1 during November 1972 and June, July, and August 1973 129

Figure 68. Temporal ion plots for water samples collected from flowing well 2 during November 1972 and June, July, and August 1973 130

Figure 69. Comparison of AAS-EDTA determination of Ca in groundwater samples . . . 131

Figure 70. Comparison of AAS-EDTA determination of Mg in groundwater samples . . . 132

Figure 71. Comparison of saturation indices obtained from WATEQF II program and Wang computer: flowing well 1 133

Figure 72. Comparison of saturation indices obtained from WATEQF II program and Wang computer: flowing well 2 134

Figure 73. Comparison of saturation indices obtained from WATEQF II program and Wang computer: Cutarm Creek north of K1 mine and plant runoff K2 mine site 135

PLATE 1. Bedrock topography and regional stratigraphy . . . . . (in pocket)
PLATE 2. Detailed bedrock topography near I.M.C.C. K2 mine . . . . . (in pocket)
PLATE 3. Geologic cross sections E-E', F-F', G-G', H-H', I-I', and J-J' . . . . . (in pocket)
PLATE 4. Sand and gravel isopach . . . . . (in pocket)
PLATE 5. Total till isopach . . . . . (in pocket)
PLATE 6. Hydrographs observation wells A to G and still well in brine pond: 1971 (in pocket)
PLATE 7. Hydrographs observation wells A to G and still well in brine pond: 1972 (in pocket)

Illustrations (Cont.)

Page

PLATE 8. Hydrographs observation wells A to G and still well in brine pond: 1973 (in pocket)
PLATE 9. Hydrographs observation wells A to G and still well in brine pond: 1974 (in pocket)
PLATE 10. Hydrographs observation wells A to G and still well in brine pond: 1975 (in pocket)
PLATE 11. Hydrograph observation well A, barometric efficiencies, mean daily temperature, and hydrograph still well: 1971-1975 . . . . . (in pocket)

Abstract

Large volumes of both solid and liquid wastes are generated by the potash industry in Saskatchewan. The waste, consisting primarily of NaCl, is stored on the surface near the plants in waste disposal basins which are artificially constructed lagoons and/or natural depressions. Several of the mines use deep-well injection to dispose of some of the excess brine in conjunction with surface storage.

The waste disposal basins are underlain by Pleistocene sediments. Infiltration of brine from the waste disposal basins into the underlying sediments and subsequent incorporation into groundwater flow systems present a potential hazard of contamination of the groundwater resources in the vicinity of the mines. Ultimately, if pollution of groundwater cannot be contained, the surface water systems will be contaminated.

To determine the effect of the waste disposal basins on the groundwater and surface water regime, a study was undertaken by the Hydrology Research Division, Inland Waters Directorate, from 1968 to 1975, near one of the potash mines: International Minerals and Chemical Corporation (Canada) Ltd., K2 potash plant, Esterhazy, Saskatchewan. The study involved the definition of the hydrogeological and hydrochemical environment and subsequent monitoring of both environments. In addition, detailed studies were conducted on the spatial and temporal variation of the groundwater chemistry and an electric analog model was constructed.

The results of the various investigations show that, first, the waste disposal basin is underlain by a semi-confined buried valley aquifer. However, a major facies change in the fill of the buried valley between the waste disposal basin and Cutarm Creek significantly retards movement of contaminants towards Cutarm Creek. Secondly, electric analog simulations indicate that within 30 years considerable contamination of an area several hundred acres in size, immediately east of the brine pond, could occur. The analog simulations do not incorporate the effect of the difference in density between the brine and the groundwater on the flowpath of the brine, nor do they take the physicochemical effects of the brine on the permeability of the sediments into account. The stated time period for pollution to occur appears therefore to be a minimum rather than a maximum. Transient results of the analog simulations show that high injection rates will be necessary for hydrodynamic containment. Thirdly, significant temporal variations were found to be present in the groundwater chemistry. Analytical/storage uncertainties associated with groundwater samples analyzed outside the field were found to be of such magnitude that they masked the temporal chemical variations and caused significant uncertainties in subsequent calculations of mineral equilibria. Fourthly, sequential sampling of the observation well network shows that at the point of sampling no contamination of the aquifer has occurred. However, although the observation well network is adequate for monitoring the hydrodynamic response of the aquifer to natural and man-made inputs, it is inadequate for the monitoring of pollutant movement in this hydrogeological environment. Different methods, which provide more continuous coverage between individual points, will have to be used to monitor the position and rate of movement of a brine front in the subsurface.

Further research will have to be conducted on the effect of brine on the permeability of the sediments underlying the waste disposal basins. Proper definition of the processes involved and the rate of progress of these processes is mandatory for long-term waste management.

Résumé

En Saskatchewan, l'industrie de la potasse produit beaucoup de résidus solides et liquides. Ces résidus, du NaCl surtout, sont stockés à la surface près des installations, dans des bassins spécialement construits ou dans des dépressions naturelles. Plusieurs mines éliminent également une partie de l'excès de la saumure par injection dans un puits profond.

Les bassins reposent sur des sédiments du pléistocène. L'infiltration de saumure dans ces sédiments représente un risque de pollution des eaux souterraines aux environs des mines. Si cette pollution parvient à se répandre, les eaux de surface seront également contaminées.

Afin de déterminer les répercussions des bassins à résidus sur le régime des eaux souterraines et des eaux de surface, la Division de recherche en hydrologie, de la Direction générale des eaux intérieures, a réalisé de 1968 à 1975 une étude près de l'une des mines de potasse, soit l'installation K2 de l'International Minerals and Chemical Corporation (Canada) Ltd. à Esterhazy, en Saskatchewan. Cette étude comportait la détermination des caractéristiques de l'environnement hydrogéologique et de l'environnement hydrochimique ainsi que la surveillance des paramètres de ces environnements. On a, de plus, étudié de façon détaillée les fluctuations spatio-temporelles des paramètres chimiques des eaux souterraines et construit un modèle électrique analogique.

Les résultats indiquent que le bassin à résidus se trouve au-dessus d'une couche aquifère de vallée enfouie et à nappe semi-captive. Toutefois, une modification importante du faciès du sol recouvrant cette vallée entre le bassin et le ruisseau Cutarm retarde de façon importante le mouvement des contaminants vers le ruisseau. D'autre part, d'après les simulations analogiques électriques, il pourrait se produire une contamination considérable sur une étendue de plusieurs centaines d'acres immédiatement à l'est du bassin à saumure d'ice trente ans. Cependant, ces simulations ne tiennent pas compte de l'effet de la différence de densité entre la saumure et les eaux souterraines sur le trajet de la saumure, ni des effets physico-chimiques de la saumure sur la perméabilité des sédiments. Le délai indiqué pourrait donc être plutôt un minimum qu'un maximum. Les résultats provisoires des simulations analogiques indiquent que le confinement hydrodynamique exigera des injections massives. Par ailleurs, on a observé des variations temporelles significatives dans les caractéristiques chimiques des eaux souterraines. Les incertitudes relativement aux méthodes de conservation et d'analyse en laboratoire des échantillons d'eaux souterraines sont toutefois telles qu'elles ont masqué les variations chimiques temporelles et rendu notablement imprécis les calculs des équilibres minéraux. Enfin, l'échantillonnage continu du réseau de puits d'observation indique qu'au point d'échantillonnage aucune contamination de l'aquifère ne s'est produite. Toutefois, bien que le réseau de puits d'observation convienne à la surveillance de la réaction hydrodynamique de l'aquifère face aux apports naturels et anthropiques, il ne convient pas à la surveillance du déplacement des polluants dans cet environnement hydrogéologique. On devra recourir à des méthodes différentes, permettant d'obtenir une plus grande continuité de surveillance entre les points, pour contrôler la position et la vitesse de déplacement du front de saumure dans le sous-sol.

Des recherches supplémentaires devront être effectuées sur l'effet de la saumure sur la perméabilité des sédiments sur lesquels reposent les bassins à résidus. Il est essentiel pour la gestion à long terme des résidus que les processus en cause et la vitesse de déroulement de ces processus soient bien connus.

Acknowledgments

Very special thanks are hereby extended to Mr. and Mrs. L. Martinovsky of Gerald, Saskatchewan, for their hospitality. Their yard became the centre of operations for all the field studies. It was through Mr. Martinovsky's attention and interest that continuity of data collection was achieved. Furthermore, his workshop was always available for use when things had to be built or repaired, and Mr. Martinovsky was always ready to lend a helping hand.

The cooperation of the management and the excellent working relationship with the employees of International Minerals and Chemical Corporation Ltd. are gratefully acknowledged; without their interest this study would not have been possible.

The assistance of Mr. J.A. Banner, Hydrology Research Division, Inland Waters Directorate, Calgary, during various phases of this study is gratefully acknowledged.

The author expresses his sincere thanks to Mr. R.A. Bourne, presently with B.C. Hydro, Vancouver, and Mr. C.C. Davison, presently with the Hydrology Research Division, Inland Waters Directorate, Ottawa, who both worked on different aspects of this study for use in an M.Sc. thesis, for their able assistance, research, and legwork. Thanks are also extended to Mrs. J. Hooke-Davison for her able assistance in the field.

The author had many helpful discussions on various aspects of this study with Dr. C.A. Baar, Calgary; Dr. G.E. Caldwell, Dept. of Earth Sciences, University of Saskatchewan, Saskatoon; Dr. A.E. Foscolos, Institute for Sedimentary and Petroleum Geology, Calgary; Dr. R.A. Freeze, Department of Geology, University of British Columbia, Vancouver; Dr. W.A. Meneley, Saskatchewan Research Council, Saskatoon; and Dr. R.O. van Everdingen, Hydrology Research Division, Inland Waters Directorate, Calgary. Mr. R.R. Barefoot, while working for the Institute of Sedimentary and Petroleum Geology, provided expert advice concerning atomic absorption spectroscopy analytical techniques used in this study.

Finally, special thanks are due Dr. R.O. van Everdingen, Hydrology Research Division, Inland Waters Directorate, Calgary, for critically reading the manuscript.

Introduction

GENERAL REMARKS

The element Potassium is basic to life; without this element there would be no plant and animal life. In plants potassium is essential to the formation of organic compounds during photosynthesis, whereas in animals it is a vital element in the tissue. Lack of potassium in animal diets stops growth, results in muscular weakness, degeneration of such vital organs as the kidneys and heart, etc.

The term "potash" was derived from the method of producing potassium carbonate in the early days. Prior to the discovery of soluble potassium salt in Germany in 1839, practically all potassium was obtained by leaching wood ashes and evaporating the leachate collected in large iron pots. The white residue left in the pot was called "pot ash". The name potash has since become a generic term which refers to soluble salts that are used by agriculture and industry for their potassium content.

Most potash (90 to 95 per cent of the world production) is used for fertilizers. Muriate of potash (KCl) is the common commercial form of potash used as fertilizer. When pure, it contains 63.2 per cent K_2O equivalent.

Potash mineralization in Saskatchewan was first discovered in a core from the Norcanol Radville No. 1 well, drilled early in 1943 by Imperial Oil Ltd., near the town of Radville in southeastern Saskatchewan (Anonymous, 1965, p. 3). Since the potash-bearing beds in this well occurred at a depth of 7650 feet (2330 m), the discovery was not considered commercial. In 1946 ore grading 21.6 per cent K_2O over 11 ft (3.3 m) was recovered from the Verbata No. 2 well drilled near Unity in west-central Saskatchewan. In this well the potash-bearing beds were encountered at a depth of approximately 3465 ft (1055 m) and the possibility of commercial production was considered.

The first commercial production of potash in Saskatchewan was attempted in 1951 by Western Potash Corporation Ltd. by using solution mining on land acquired in the Unity district (Anonymous, 1965, p. 9). After an unsuccessful attempt at solution mining, a shaft-sinking operation was begun in 1952. By 1960, after several delays, a depth of 1800 ft (550 m) had been reached at which depth the Blairmore Formation was encountered. Water from the Blairmore Formation flooded the shaft with sand and water to within 360 ft (110 m) of the surface. The project was subsequently abandoned. During the period 1950 to 1960 exploration for potash accelerated dramatically in Saskatchewan, resulting in the first exploitation; the first commercial shipment of muriate of potash was made in March 1959, by the mine of the Potash Company of America, which is located east of the city of Saskatoon.

International Minerals & Chemical Corporation (Canada) Ltd. entered the field in 1955 in a lease near the town of Esterhazy in eastern Saskatchewan. Shaft sinking was begun in 1957 and the potash deposit was reached in 1962. Since that time this mine, the world's largest potash mine, has been in continuous operation. In 1965 a second shaft and plant were started, which became the I.M.C.C. K2 operation.

The study described in this report was carried out around the I.M.C.C. K2 plant and is concerned with the disposal of both the solid and liquid wastes and their effect on the environment. The study was started during the summer of 1967.

OBJECTIVES

The objectives of this research project were

1. To study the effects of the waste disposal basin on the groundwater regime
2. To evaluate the long-term effects of the waste disposal basin on both the groundwater and surface water resources in the area
3. To determine if and when remedial measures must be taken to limit the spread of subsurface pollution
4. To recommend possible alternative solutions to the waste disposal problem around potash mines.

LOCATION OF STUDY AREA, PHYSIOGRAPHY, AND CLIMATE

The study area, which includes the I.M.C.C. K2 waste disposal basin, is located approximately 9 miles (14 km) east of the town of Esterhazy in southeastern Saskatchewan

(Fig. 1). The area is located within the Assiniboine River Plains physiographic division (Acton *et al.*, 1960). Regional drainage in the area is through several northwest-southeast trending creeks. These creeks discharge into the Qu'Appelle River, which in turn discharges into the Assiniboine River system. The topography is level to gently rolling and contains numerous temporary and permanent sloughs.

The waste disposal basin at the I.M.C.C. K2 mine is located approximately 1 mile (1.6 km) west of Cutarm Creek. Cutarm Creek valley, a relatively wide and flat-bottomed glacial meltwater channel, is the only significant topographic feature in the area. The elevation of the terrain around the K2 plant is about 1650 ft (502 m) above mean sea level, whereas the bottom of Cutarm Creek valley is at 1510 ft (460 m) above mean sea level. The maximum relief in the area is approximately 140 ft (42 m).

The climate for the area is classified as a Dfb or "Cold Forest" climate (Richards and Fung, 1969). Annual precipitation as measured at the Broadview meteorological station, which is located approximately 40 miles (64 km) southwest from the study area ranges from 9 to 27 in. (229 to 682 mm) with an average of 17.5 in. (445 mm) per year. Most of the annual precipitation, 50 to 70 per cent, occurs during the summer season. The temperatures range from +109°F to -50°F (+43°C to -46°C) with a mean of +35°F (+1.7°C).

Prairie Evaporite Formation

GENERAL STRATIGRAPHY

The Prairie Evaporite Formation is part of the Upper Elk Point Subgroup of Middle Devonian age. The Upper Elk Point Subgroup is continuously present in the subsurface over a wide area that extends from North Dakota northwestward through Manitoba, Saskatchewan, Alberta, and into the Northwest Territories. The Upper Elk Point Subgroup consists of a cyclical carbonate and evaporite sequence with thin clastic beds. The carbonates are commonly reefoid (Grayston *et al.*, 1966). The sediments were laid down in a continuous basin. Present limits are erosional (pre-Cretaceous in the northeastern part of the basin and pre-Jurassic in that part of the basin located in southern Manitoba and adjacent parts of North Dakota) or depositional. Since deposition considerable removal of the salt beds by solution has taken place along the edges and within the basin, resulting in salt collapse structures (Grayston *et al.*, 1966; Holter, 1969; Christiansen, 1967, 1970, 1971b; van Everdingen, 1971).

The Upper Elk Point Subgroup consists, in ascending order, of the Winnipegosis-Keg River Formations, the Prairie Evaporite and Muskeg Formations, and the Dawson Bay Formation. The Winnipegosis-Keg River interval is composed of reef and non-reef carbonates ranging from less than 50 ft (15 m) thick in the inter-reef areas to more than 600 ft (180 m) in the thickest reef sections (Grayston *et al.*, 1966). The Prairie Evaporite and Muskeg Formations overlie the Winnipegosis-Keg River carbonate sequence. The formations range up to 1000 ft (305 m) thick, filling in the depressions between the Winnipegosis and Keg River reefs and forming a cover up to 250 ft (75 m) thick over the highest reefs. These formations consist predominantly of evaporites and are known as the Prairie Evaporite Formation in central Alberta, Saskatchewan, and North Dakota (Bailey, 1953) and Muskeg Formation in northern Alberta and the Northwest Territories (Law, 1955). The distribution of the Prairie Evaporite Formation in Alberta, Saskatchewan, and Manitoba is shown in Figure 2. The Prairie Evaporite Formation consists essentially of halite (NaCl), and only in the top 100 to 200 ft (30 to 60 m) of the section near the centre of the basin located in Saskatchewan, Manitoba, and North Dakota do potash beds interbedded with halite occur (Grayston *et al.*, 1966; Holter, 1969). Sylvite (KCl) and carnallite ($KCl\ MgCl_2 \cdot 6H_2O$) are the most common potash minerals present.

Three main potash-bearing beds are recognized in the upper part of the Prairie Evaporite Formation in Saskatchewan. These are named in ascending order the Esterhazy, Belle Plaine and Patience Lake Members (Fig. 3). Intervening halite units are unnamed and contain little or no potassium mineralization (Holter, 1969).

The Prairie Evaporite Formation is overlain by the Dawson Bay Formation. This formation attains a maximum thickness of 240 ft (72 m) in southeastern Saskatchewan. In the areas where the Dawson Bay Formation is thick, three units can be recognized: a basal clastic unit ("Second Red Beds"), a carbonate sequence, and an upper unit comprising evaporites (Lane, 1959). The "Second Red Beds" consist of thick-bedded red and green dolomitic shales. This unit directly overlies the Prairie Evaporite Formation. The contact between the two formations is generally gradational except in those areas where the Prairie Evaporite Formation has been removed by solution. In these areas the "Second Red Beds" rest directly on the Winnipegosis Formation.

At I.M.C.C. Ltd. potash ore is being mined from the Esterhazy Member. The Patience Lake Member is not present in this region and appears to have been removed by erosion. The second potash ore zone is present but immediately underlies the "Second Red Beds" of the Dawson Bay Formation. Mining of this potash ore bed is not considered because it could result in fracturing of the overlying formations caused by subsidence, which would lead to water inflow problems in the mine. The Esterhazy Member lies approximately 100 ft (30 m) below the shales of the "Second Red Beds". The ore mined at Esterhazy is sylvinite (a mechanical mixture of halite and sylvite). The ore is low in insoluble content but contains carnallite in some areas. In ore with low carnallite content, milky halite crystals occur in a groundmass of clear waxy sylvite. Carnallite, where present, fills interstices between halite and sylvite crystals and also fills fractures in the ore bed. The insoluble material consists of finely divided dolomite, anhydrite, and clay (Keys and Wright, 1966; Wardlaw, 1968; Baar, 1972).

RELATIONSHIP BETWEEN ORE AND WASTE PRODUCTS

The volume and type of waste produced during the mining and refining of potash ore is a function of the type and grade of ore, the depositional environment, and penecontemporaneous and post-depositional changes in the ore beds.

The bulk of the waste is directly related to the type and grade of ore. Two end members can be recognized in the type of ore. These are sylvite and carnallite, which contain 63.2 per cent and 16.9 per cent K_2O equivalent respectively. The ore that is present in Saskatchewan does not consist of the end members only, but is composed of a mixture of sylvite and/or carnallite and halite. Thus far, all mining activity in Saskatchewan has concentrated on those areas where the ore is primarily sylvinite and has no or only a low carnallite content. In addition to a much lower K_2O equivalent than sylvite, carnallite ore has another disadvantage because it contains $MgCl_2$, which is undesirable in the finished end product and must be removed. This is readily achieved by selective solution, but as a result, larger volumes of waste brine are produced than during the processing of sylvinitic ore. Since carnallitic ore prevails and constitutes the major resource for potassium in the Prairie Evaporite Formation, a shift toward the mining of carnallitic ores will be inevitable in the future (Baar, 1977, pers. comm.). This will result in waste brine volumes far exceeding present levels of brine production per ton of KCl produced.

Another source of waste, albeit a minor one, which, like the grade and type of the ore, is determined by the original depositional environment, is the insolubles. The insolubles consist primarily of clays and minor amounts of anhydrite, gypsum, quartz, and carbonate minerals (Streeton, 1967). The clays are either interspersed with the ore or they occur as discrete thin layers in the ore bed. The other minerals generally occur interspersed with the ore. If the location of the mines in Saskatchewan is considered with respect to type of ore and insoluble content, then it can be seen that the ore in southeastern Saskatchewan contains approximately 1-5 per cent carnallite, whereas the ore mined by the various companies in central Saskatchewan is essentially free from carnallite but contains a higher percentage of insolubles (Holter, 1969; Baar, 1972).

Although the bulk of the waste is determined by the type and grade of the ore, additional sources of waste within the ore bed have been created by penecontemporaneous and post-depositional processes. In both cases the processes have resulted in the formation of barren zones, primarily composed of halite, within the ore.

The penecontemporaneous changes in the ore bed are the result of the effect of surface water or groundwater flow (undersaturated brine) on existing deposits of evaporites. These are

1. erosion of the ore bed during periods of exposure, and subsequent deposition of halite in eroded areas;
2. leaching of ore beds just after their deposition by inflowing diluted brines;
3. leaching of carnallite beds below the sylvite-bearing beds shortly after deposition.

With respect to point 3 the following comments can be made. Conversion of carnallite to sylvite by infiltrating brines is accompanied by a volume reduction in the rock mass of approximately 50 per cent. Subsequent collapse or subsidence of the overlying salt and potash beds in the leached area will result in considerable disruption in the continuity of the overlying potash beds. For a more detailed description of the above phenomena the reader is referred to a report by Baar (1972).

Post-depositional changes, caused by deep groundwater flow systems, have resulted in considerable removal of salt and subsequent collapse of the overlying strata. In many areas the entire section of the Prairie Evaporite Formation has been removed (Holter, 1969; Baar, 1972; Christiansen, 1971b; Gendzwill and Hajnal, 1971). A number of documented cases are present where blocks of the overlying formations have been found within the potash mining horizon in these solution areas (Baar, 1972).

Depending on the size of the barren zones as well as their distribution and frequency, many of the smaller ones have to be mined for technical and economic reasons and the waste salt thus obtained is transported with the ore to the surface.

Waste Disposal Techniques

In addition to the volume of waste generated during the milling and refining of the potash ore three other sources can be recognized. These are: "wash" water in the mill, shaft water, and spent mill chemicals. All wastes from these various sources are discharged in a waste disposal basin. Figure 4 summarizes the origin and kind of wastes.

Table 1. Chemical Composition of Brine (Sept. 2, 1972).

Parameter	Concentration
Specific conductance (μmhos/cm)	264 000
pH (units)	7.6
Density (g/cm^3)	1.19
Ca (ppm)	1 980
Mg	7 940
Na	88 500
K	39 500
HCO_3	120
SO_4	2 100
Cl	200 000
Fe	<0.02
Mn	8.4
Pb	0.018
Cu	0.012
Zn	0.045
F	0.1

The waste, both liquid and solid, from the mill and other sources is pumped as a slurry into the waste disposal basins. The waste disposal basins consist of artificially constructed lagoons and/or natural depressions. Figure 5 shows the waste disposal basin at I.M.C.C. K2 plant, which is of the constructed type. The solid particles in the slurry build "alluvial" fans above and deltas below the brine level from the point of discharge in the waste disposal basin. A chemical analysis of the brine in the waste disposal basin at I.M.C.C. K2 is shown in Table 1.

Waste volume production is in the order of 1.5 tons of solid waste per ton of finished product, and 20 to 40 gallons of brine per ton of ore milled. The size of the individual disposal lagoons ranges from 400 to 1000 acres (160-400 ha).

In addition to the storage of waste in disposal lagoons most mines also use deep-well injection to reduce the volume of liquid waste (Dennison and Simpson, 1973). The disposal formations are all located below the Prairie Evaporite Formation. Injection rates range from 150 to 1200 (US) gpm (0.5-4.5 m^3/min).

Problems Related to Waste Disposal

GENERAL

In Saskatchewan the potash industry is not allowed to discharge brine at any time during the year into bodies of fresh water. This is contrary to practices in other potash mining districts in the world. For example, in the Werra area in West Germany, discharge is allowed into streams until a certain concentration level is reached (Poschke, 1965).

The companies operating in Saskatchewan, therefore, must retain the waste within the boundaries of the mine property (i.e. waste disposal basins) or dispose of part of the waste by other means, such as backfill of solid waste in mined-out areas (not practiced at this time), or disposal of brine by deep-well injection. The biggest disadvantage of the present waste disposal method, if no other techniques such as deep-well injection are used to reduce the waste volume, is the constant need for increased storage capacity. This means that existing lagoons will have to be expanded constantly in future years to supply the necessary storage space.

Besides the physical storage problem of the waste, the waste disposal basins present a number of other problems which have to be considered. These will be discussed briefly in the following sections.

EVAPORATION

Evaporation (Anonymous, 1970) in southeastern Saskatchewan ranges, according to a five-year average (1964-1969), from 425 to 450 mm (16.7-17.7 in.). This amount equals the average annual precipitation. Furthermore, tests using class A evaporation pans have shown that evaporation from brine surfaces (pans) during the summer season exceeds annual precipitation by a factor of 1.2-1.5 (Maybank and Calvert, 1970). Unfortunately, results obtained from evaporation pans are not really compatible with evaporation from large surfaces of water or brine (Wartena, 1974). Similar experience has been gained by the potash industry. Originally it was thought that evaporation would be an important factor in brine volume reduction, however, surface roughness, turbulence, unfavourable temperature gradients (too great a depth in most brine ponds), and the very high salt content of the brine have resulted in far less evaporation than expected. Several years of operating experience have shown that evaporation from brine ponds approximately equals the annual precipitation; therefore, evaporation is no longer regarded as a factor in the reduction of brine volume.

One method to increase evaporation, which has not been employed in Saskatchewan, is the use of spray systems. According to Smoak *et al.* (1969), spray systems, as used in experimental brine ponds, showed a considerable increase in evaporation rates. The main disadvantage of the method is the possibility of driftage of droplets, which could result in airborne transport of pollutants.

EROSION

The dykes of the brine ponds undergo severe erosion. The dykes are built from till and are compacted during construction. Initially, in most cases special measures, such as riprap covers or wave breaker booms, were not taken to protect the dykes from wave erosion. The combination of strong winds (wind speeds of 30-50 km/hr are common), wide open prairie with little or no protective forest cover in the vicinity of the lagoons, the relatively large brine storage areas, and the absence of a protective wave-breaking cover near the dykes caused severe erosion by wave action (Fig. 6, A and B). This problem is further aggravated by the brine itself. The brine has an average specific gravity of 1.19, which in comparison with water not only results in greater impact energy of the waves on the dykes, but also tends to keep more material in suspension, thereby further increasing the impact energy. This combined effect has resulted in accelerated erosion of the unprotected dykes by wave action. Rates of erosion observed over a period of one year are as high as 3 ft (90 cm) in places.

To alleviate some of the problems of dyke erosion several methods have been used such as lining the dykes with scrap iron and/or old cars, discarded conveyor belts, straw bale booms, and waste salt (Fig. 7, A, B, C, and D). The most successful of these methods is the deposition of waste salt against the dyke. Although the exposed salt is subjected to minor karst type erosion by rainfall, intermittent spraying of the surface with brine results in precipitation of

halite in the interstices of the granular waste salt. The "cemented" waste salt forms a hard crust at the surface and wave action has little effect on the stability of this surface. Another beneficial effect of the waste salt on the inside of the dykes is that it reduces the surface area subjected to brine infiltration in the immediate vicinity of the dyke.

The long-term effect of potassium-rich NaCl brines on the montmorillonitic clays may be more serious than dyke erosion. Montmorillonitic clays are abundant in the sediments underlying the brine and in the fill used for dyke construction. The effect of the saturated, potassium-rich NaCl brines on these clays is twofold. Initially, it will cause dispersion of the clay minerals (Baver, 1959) and subsequently it will induce mineralogical changes from montmorillonites to illites (Foscolos, 1977, pers. comm.). In the first instance this will result in a decrease in the permeability, whereas in the second instance an increase in the permeability can be expected. The increase in permeability in the latter case is caused by the reduction in the original "mineral" volume that occurs during the transformation from montmorillonite to illite.

To the writer's knowledge no detailed studies have been conducted on the rate of change in the mineralogy, permeability, and porosity of the sediments subjected to brine infiltration. This problem, however, warrants further study, because a progressive increase in the permeability of the sediments would result in higher brine infiltration rates, which may become environmentally unacceptable.

Regional Stratigraphy

INTRODUCTION

All waste disposal basins near the various potash mines are underlain by glacial drift deposits of Pleistocene age. The drift deposits comprise all sediments overlying "bedrock", which in most of southern Saskatchewan consists of sediments such as shales, clays, silts and sands of Upper Cretaceous age. The drift deposits comprise till, clay, silts, sand, gravel, and various admixtures, depending on the mode of deposition. The thickness of the drift deposits varies from less than 1 ft (30 cm) to greater than 1000 ft (300 m). The aquifers and aquifer systems within the Pleistocene section are the most important units within the section. Not only do the aquifers constitute potential freshwater resources of great magnitude, they also represent the permeable paths for migration of pollutants in the shallow subsurface (Meneley, 1965, Vonhof, 1975a). Since almost all surface water bodies receive a considerable volume of water through discharge from these aquifers (Weyer, 1972, 1973; Fritz *et al.*, 1976), pollutant transport into the aquifers will not only contaminate the subsurface freshwater resources, but would eventually also lead to pollution of surface water.

The origin of the aquifers, their position in the section, areal extent, development, type and uniformity of sediment, and interrelationship is directly related to the glacial history of the Pleistocene Epoch. Because of the lack of surface exposures, extensive drilling programs, both on a regional and local scale, are necessary to obtain the data to define the complex stratigraphic relationships and to correlate the various lithologic units within the Pleistocene section. In addition to the information on the Pleistocene section, data on the underlying bedrock, in terms of type of sediment, preglacial topography, structural pattern, etc., have to be considered because of their effect on depositional and erosional pattern during Pleistocene time.

Excellent studies on the regional Pleistocene stratigraphy were conducted by Christiansen (1967, 1968a, 1968b, 1969, 1972). These studies greatly facilitate the correlation of local and regional stratigraphy.

The regional stratigraphy and bedrock topography of the area under study (Plate 1) was determined by using data collected by the Saskatchewan Research Council (Christiansen, 1971a; Cherry and Whitaker, 1969), the Geological Survey of Canada (Klassen, 1972), consultants' published (Beckie and Balzer, 1970) and unpublished reports, Saskatchewan Water Resources Commission (Anonymous, 1964-1967), Saskatchewan Department of Environment (Anonymous, 1968-1975), testhole information from wildcats (oil industry) and potash exploration programs, and from testdrilling programs conducted by the Inland Waters Branch, Environment Canada, in 1968, 1969, 1970, 1971, and 1973.

The size of the area considered for the regional stratigraphy is approximately 2500 square miles (6500 km^2).

REGIONAL BEDROCK STRATIGRAPHY AND TOPOGRAPHY

The regional bedrock stratigraphy is shown in the cross sections on Plate 1. As can be seen, the various formations dip gently toward the southwest. The sediments of the Swan River Group of Lower Cretaceous age are composed of sand, clay, carbonaceous shale, and, locally, coal. The Swan River Group has created considerable difficulties during shafting operations for the various potash mines because it is a good aquifer, which upon penetration caused a number of shafts to flood temporarily. The Swan River Group is overlain by the Ashville Group, which consists primarily of shale. The upper beds of the Ashville Group are considered to be of Upper Cretaceous age (Wickenden, 1945). The Favel Formation, which overlies the Ashville Group, comprises shales, impure limestones, and bentonite beds. Because of its varied composition in comparison to the over- and underlying formations, the Favel Formation can be easily recognized on geophysical logs and is an excellent stratigraphic marker in this area. The Favel Formation is in turn overlain by the Vermillion River Formation of Upper Cretaceous age. The latter formation consists primarily of shales. The youngest formation of Upper Cretaceous age present in the area is the Riding Mountain Formation. This formation overlies the Vermillion River Formation and unconformably underlies the Pleistocene sediments. The upper beds of this formation outcrop in the area, in the Qu'Appelle and Assiniboine river valleys. Near the top of the Riding Mountain Formation a distinct hard siliceous shale can be found, which is called the

Odanah Member. The distribution of this member is restricted to an area along the Qu'Appelle valley between Esterhazy and Rocanville (Christiansen, 1972). The reference section for this bed is located in lsd. 14, sec. 5, T. 18, R. 33, W 1 mer., in the southern part of the area (Wright, 1972). The Odanah Member appears to have undergone considerable shearing and thrusting during Pleistocene time as indicated by Christiansen (1971a, 1972). Where the siliceous shale of the Odanah Member is subjected to erosion by surface water, it forms distinct deposits of shale-pebble gravel in the stream beds. The Odanah Member is absent in the vicinity of the I.M.C.C. K2 potash plant (Christiansen, 1971a); however, the presence of thick beds of shale-pebble gravel in the fill of glacial valleys cut into bedrock, which drained in the direction of or parallel to the present-day contact configuration of the Odanah Member, suggests the following possible sources of origin. First, the areal extent of the Odanah Member could have been much larger during pre-Pleistocene time and considerable erosion of the member took place during Pleistocene time, providing the shale pebbles. Secondly, the shale-pebble gravels could represent reworked pre-Pleistocene alluvial and/or colluvial deposits, or, thirdly, the siliceous shale pebbles in the valley fill could have been derived locally. Since the base level of these glacial valleys is several hundred feet below the contact of the Odanah Member, this would imply that siliceous shales are not restricted to the Odanah Member only, but also occur in older sections of the Riding Mountain Formation.

Although the Riding Mountain Formation is described as primarily composed of shales and clays, during the drilling program conducted in the vicinity of the I.M.C.C. K2 potash plant several thick sections, up to 75 ft (25 m) thick, of silt and very fine grained sand were found. Microfauna collected from these sections seem to indicate that these beds are correlative with the upper part of the Pakowki Formation in western Saskatchewan (Caldwell, 1976, pers. comm.).

The very fine grained nature of the sediments in the Riding Mountain Formation strongly suggests that the pre-glacial topography was a badland type of topography. On a gross scale this is reflected in the bedrock topography as shown in Plate 1, which is characterized by uplands and valley systems. The pre-Pleistocene bedrock surface has been strongly modified by glacial erosion. In addition, dissolution of the Prairie Evaporite Formation by deep groundwater flow systems has resulted in salt collapse features, which locally have caused the formation of major depressions in the bedrock surface. Studies of the bedrock stratigraphy in this area show that salt collapse occurred in post-Cretaceous time and during the Pleistocene Epoch (Christiansen, 1971a, 1971b, 1972).

The valley systems shown on the bedrock surface in Plate 1 are part of the regional Hatfield Valley system (Christiansen, 1971a, 1972). The Hatfield Valley is one of the major glacial meltwater valleys in Saskatchewan, running from the northwestern part to the southeastern part of the province. The Hatfield Valley is a major aquifer and in this area it functions as a major subsurface drain which collects water from a large area and diverts it into the Qu'Appelle Valley (Christiansen, 1972). In the eastern part of the area (Plate 1) it most likely also supplies water to the Assiniboine river system. The cross sections on Plate 1 show that the fill is highly irregular: in places the fill is primarily till, whereas in other parts of the area it consists of thick beds of well-sorted sand and gravel. The considerable variation in fill and rapid facies changes are also indicated by several areas with flowing wells. The I.M.C.C. K1 plant near Yarbo obtains all its water, 450-650 lgpm (2000-2900 l/m), from these aquifers. No appreciable decline in the static level or increase in drawdown has occurred since these wells were first operated in 1962.

Drift thickness in this area varies from less than 1 ft (0.3 m) to 450 ft (135 m). The thin drift cover occurs in the bedrock upland area in the vicinity of the Qu'Appelle Valley, whereas thick drift sections are present in salt collapse areas and bedrock valleys.

SURFICIAL FEATURES

Most of the area under investigation (Plate 1) is characterized by ridged ground moraine with a relief of 5 to 15 ft (1.5-4.5 m). Flutings are present northeast of the I.M.C.C. K2 potash plant. The southeastern part of the area is characterized by a sand plain, the Welby Sand Plain, which was formed in an interlobe area (Christiansen, 1972). Kaposvar, Cutarm and Deerhorn Creeks are southeasterly trending meltwater channels.

Stratigraphy of I.M.C.C. K2 Potash Mine Disposal Basin

INTRODUCTION

Once the regional stratigraphic setting of the Pleistocene drift deposits and the bedrock sediments was determined, the investigation was focused on a small area, approximately 6 square miles (15 km^2) in size, in the vicinity of the disposal basin. A total of 96 testholes were drilled in this area (Plate 2), 15 of which were drilled for and funded by I.M.C.C. Ltd. The latter testholes are all located in sec. 28, T. 19, R. 32, W 1 mer., and were drilled to determine the suitability of this area for future brine pond expansion (Vonhof, 1970). Because of yearly funding limitations the testdrilling program was conducted over the period 1969 to 1973.

The regional setting showed that the I.M.C.C. K2 waste disposal basin was located on the northern flank of a bedrock upland. Furthermore, information available up to the end of 1968 suggested that a buried valley was present southeast of the existing waste disposal basin (Fig. 8). Based on this information, a testdrilling program was conducted during the summer of 1969 to prove the existence and location of this buried valley and its relationship to the sediments in the vicinity of and below the brine pond. A total of 41 testholes were drilled, with an average spacing of approximately 0.25 miles (400 m). The results are shown in Figure 9. As can be seen in Figure 9, the bedrock topography differs considerably from that determined from the regional setting (Fig. 8). Not only is the buried valley south of the brine pond nonexistent, but the true position is found to be under the brine pond. Considerable difficulties were experienced in the definition of the position of this buried valley immediately east of the brine pond, because of terrain conditions (soft, muddy, swampy) during the drilling program conducted in the summer. To overcome this problem of mobility, further drilling programs were conducted during the winter. No major time loss was experienced as a result of climatic conditions. Only a few days, when the temperature dropped below -30°C or when blizzard conditions occurred, were lost. During the winter of 1969-1970 an additional 40 testholes, including 15 testholes drilled for I.M.C.C. Ltd., were completed. The results of this drilling program are shown in Figure 10. A comparison of Figures 9 and 10 shows the existence of a second eastwest trending buried valley under the northern part of the brine pond. This valley, immediately west of the brine pond, is only 1000 ft (300 m) wide and approximately 250 ft (75 m) deep. There is a considerable difference in the fill between the two buried valleys. Details of this difference will be discussed in one of the following chapters.

An evaluation of the fill characteristics in the east-west trending main buried valley in the vicinity of Cutarm Creek and the projected valley gradients of the second buried valley under the centre of the brine pond suggested that two types of valleys cut into bedrock were present in this area. In order to prove or disprove these suspicions a further 10 testholes were drilled during the winter of 1970-1971. An additional five testholes were drilled during the winter of 1972-1973 northwest of the brine pond to better define the position of the buried valley in this part of the area. The results of the final phase of subsurface data collection are shown in Figure 11 and Plate 2. The major difference between Figures 10 and 11 is that the northern buried valley, instead of draining toward the east-northeast, drains toward the west. Furthermore, the confluence of the two buried valleys is essentially under the brine pond.

Based on the experience gained during the data-gathering process and the drastic changes in the perceived configuration of the bedrock topography with each increase in information, and taking into account that in most cases budget restraints predetermine the number of data points, the writer offers the following suggestions which may aid in future exploration programs in similar geological settings:

1. If problems with mobility are expected in summer drilling programs, drilling can be done in the winter, after freeze-up
2. A reconnaissance testdrilling program should be conducted to obtain preliminary information on the type and distribution of Pleistocene drift deposits and bedrock sediments and on the bedrock topography. With this information, for example the type of bedrock sediments and the relief, a fair idea of the preglacial type of erosion and, consequently, landform can be obtained. In case of badland topography, analogies with present-day exposed surfaces can be made and based on studies of valley width versus depth; in these areas estimates can be

made of the testhole spacing required for the detection of these valleys in the subsurface. Furthermore, the preliminary information on the local relief of the bedrock surface in relation to regional features, in combination with glacial process models (Clayton and Moran, 1974), should provide insight into the type of processes which may occur and the type and distribution of sediments which could be found. Once this information is available, the appropriate drilling program can be designed to obtain the necessary information to properly define the geologic model in the area.

The distribution of testholes in this area is such that the position of the buried valleys in the immediate vicinity of the waste disposal basin is reasonably well defined. However, if the area in section 26, T. 19, R. 32, W 1 mer. is considered, the testhole density is insufficient for proper definition, and conclusions with respect to distribution of sediment and evolution of the Pleistocene geological model for this part of the area are based mainly on conjecture. With respect to pollutant movement in the buried valley system, the lack of data in this area is not considered too serious, because if brine movement is detected in the buried valley east of the pond, remedial measures should be taken long before the brine reaches this area.

The results of the geological investigation are shown as the bedrock topography (Plate 2), six cross sections (Plate 3), sand and gravel isopach map (Plate 4), and total till isopach (Plate 5).

RIDING MOUNTAIN FORMATION

The Riding Mountain Formation underlies unconformably the Pleistocene drift deposits in the area. Outcrops of the formation occur approximately 0.75 miles (1.2 km) south of the Highway 22 in the valley walls of Cutarm Creek. Outcrops were also found in the valley walls near the dam during its construction in the northeast part of the area. Subsequent slumping has obliterated these occurrences.

The Riding Mountain Formation comprises primarily non-calcareous, gray (5Y, 5/1)*, unoxidized mudstone and clay. In places large siliceous concretions are present. Within the clay section the formation contains beds of very fine grained, silty, greenish gray (5GY, 5/1), non-calcareous to slightly calcareous sands. The very fine grained sands and silts are common in the western part of the area (west of sections 26 and 35, T. 19, R. 32, W 1 mer.). The position of these beds has been indicated on cross sections E-E', F-F', and H-H' (Plate 3). The contacts with the overlying and underlying clays are gradational and the contacts shown in the cross sections should be considered as such. The thickness of these beds varies from 10 to 90 ft (3-27 m). In the eastern part of the area it appears that most of these beds have been removed by erosion.

*Munsell Colour Code, dry samples.

PLEISTOCENE STRATIGRAPHY

The Pleistocene drift deposits comprise tills and fluvial sediments. Two tills are recognized in the area. According to Christiansen (1968a, 1971b, 1972), the tills in most of Saskatchewan can be divided into the Saskatoon Group and the older Sutherland Group. The tills in these groups can be differentiated and correlated on the basis of their total carbonate content. The tills in the Sutherland Group invariably have a total carbonate content approximately 30 per cent less than the tills in the Saskatoon Group. The total carbonate content in the tills of the Saskatoon Group varies from a mean content of 41.6 ml/g (ml CO_2 gas evolved upon testing, per gram of sample) in the Saskatoon area (Christiansen, 1968b) to 41.3 ml/g in a section from Saskatoon to Echo Lake, Qu'Appelle Valley (Christiansen, 1972) to 52 ml/g near Crater Lake, south of Yorkton (Christiansen, 1971b). The corresponding mean total carbonate values for the Sutherland Group are 26.7, 30.4, and 35 ml/g, respectively. According to Christiansen (1972), the variation in the total carbonate content in both groups can be attributed to systematic areal differences, which most likely relate to differences in source areas for the tills. Christiansen (1968a) has shown that the Saskatoon Group could be further divided into the Battleford and Floral Formations. The till of the Floral Formation is hard and generally jointed and stained, whereas the Battleford Formation is typically soft, friable, and unjointed. According to Christiansen (1972), there is no consistent difference in total carbonate content between tills of the Floral and Battleford Formations.

To determine the total carbonate content in the tills, 240 sidehole cores from 17 testholes were analyzed by the Saskatchewan Research Council; 87 samples were from the upper till and 153 samples from the lower till. The mean total carbonate content in the upper till is 31.5 ml/g with a standard deviation of ± 3.1 ml/g, whereas the lower till has a mean value of 45.3 ± 6.0 ml/g (Fig. 12). The mean value for both tills combined is 40.1 ml/g. If these values are compared with those published by Christiansen (1968a, 1968b, 1971b, 1972), then both tills in the area under investigation belong to the Saskatoon Group. Furthermore, based on the physical characteristics of the two tills, it is reasonable to assume that the upper till is equivalent to the till of the Battleford Formation and the lower till is correlative with the till of the Floral Formation.

The difference in total carbonate content between the Battleford and Floral Formations would seem to indicate that in this area a significant difference exists in the total carbonate content between the two tills, which contradicts the conclusion reached by Christiansen (1972). However, a close examination of the carbonate profiles in the testholes (see for example cross section F-F', I-I', and J-J', Plate 3) shows that the major shift in carbonate content does not correspond to the position of the contact between the two tills in most testholes. Rather, it coincides much more closely with the change from oxidized to unoxidized till in the Floral Formation. It appears, therefore, that the lower total carbonate profile in the Battleford Formation and in places in the upper part of the Floral Formation could be the result of post-depositional weathering, or the source for the till in the Battleford Formation was mainly weathered Floral Formation. If the total carbonate profiles in testholes with multiple till beds and thick till sections are examined (testholes 7, 18, 19, and 35), it appears that no tills of the Sutherland Group are present in the area. Only two samples near the base of the till section, testholes 9 and 21, showed total carbonate contents less than 30 ml/g, however, each sample in both testholes was taken immediately above the Riding Mountain Formation. The lower carbonate content in these samples is most likely caused by a high percentage of non-calcareous bedrock sediment in the till.

Battleford Formation

The Battleford Formation comprises friable, oxidized, calcareous, sandy and silty till. The thickness varies from 6 to 17 ft (2-5.5 m) and averages 10 ft (3 m). The contact with the underlying Floral Formation more or less parallels the present surface.

Floral Formation

The Floral Formation, which underlies the Battleford Formation, consists of oxidized to unoxidized, calcareous, hard, pebbly till. The upper part of the formation is oxidized and the thickness of the oxidized zone ranges from 8 to 20 ft (2.5-6.5 m). The Floral Formation is generally fractured with fractures extending at least 30 ft (10 m) below the contact with the overlying Battleford Formation. The fractures can be easily recognized because their surfaces are always more oxidized than the matrix (Fig. 13). Excellent examples of fracture patterns were found and measured in two borrow pits within the northern part of the brine pond (NOTE: the northern half of the brine pond was still under construction when this investigation started, and the patterns were measured prior to flooding). Additional patterns were measured in road cuts during the construction of new approaches into Cutarm Creek from Highway 22. The results of these measurements are shown in Figure 14. In all locations well-developed fracture patterns were found. There is a considerable difference in the density of the fractures, as shown by the plan views, between the Cutarm Creek locality and the borrow pits. Polar projections of the fracture traces show that in both localities orthogonal sets of near vertical fractures are present. A reasonably well developed set of near horizontal fractures is also present in the borrow pit sections. The significance of the fractures in terms of groundwater flow and, consequently, pollutant transport will be discussed in detail in another section of this report.

The thickness of the Floral Formation varies considerably. This is illustrated in the total till isopach map (Plate 5) and the cross section in Plate 3. Although the map shows the combined till thickness of the tills of both the Battleford and Floral Formations, since the thickness of the Battleford Formation can be considered uniform, this map shows mainly the variation in thickness of the tills of the Floral Formation. As can be seen in Plate 5, the thickness of the total till section in most of the area is less than 50 ft (15 m) and, consequently, the thickness of the Floral Formation is less than 40 ft (12 m). Two areas, however, show a considerable deviation. One is the buried valley under the central part of the brine pond where the Floral Formation thickens to 150 ft (45 m). The other is the buried valley system east of the brine pond, in the east half of section 27 and southwest quarter of section 35, T. 19, R. 32, W 1 mer., where the tills of the Floral Formation reach a combined thickness of 250 ft (75 m). Also in this part of the area the thickness of the tills outside the buried valley system is greater than in the western half of the area under investigation.

Fluvial Deposits

The fluvial deposits comprise silt, sand, polymict gravel, and gravel that consists mainly of siliceous shale pebbles. Generally, the individual beds are well sorted and the particles subangular to subrounded. The sand size ranges from very fine to very coarse with medium sizes predominating. The gravels vary in size from 2 to 40 mm. The shale-pebble gravel beds consist of subrounded to rounded siliceous shale fragments which were derived from the Riding Mountain Formation. The pebbles range in size from 2 mm to at least 50 mm. The shale pebbles are generally embedded in a sandy matrix. Furthermore, several of the very coarse grained sands consist entirely of rounded to well-rounded shale particles.

The fluvial deposits occur mainly as extensive valley fills (cross sections E-E', F-F', G-G', H-H', I-I', and J-J', Plate 3). In most of the area west of sections 26 and 35, T. 19, R. 32, W 1 mer., the deposits rest unconformably

on the Riding Mountain Formation and underlie the tills of the Floral Formation. East of sections 27 and 34, T. 19, R. 32, W 1 mer., the fluvial deposits occur as thin discontinuous (?) layers and lenses interbedded with till layers of the Floral Formation. Minor occurrences of fluvial deposits, lenses, and thin discontinuous beds are present at the contact between the Battleford and Floral Formations.

The thickness of the fluvial deposits below and within the Floral Formation is shown in the sand and gravel isopach map (Plate 4). As can be seen in Plate 4, thick deposits of fluvial sediments are present in the buried valley under the northern part of the brine pond and in part of the northwesterly trending buried valley located in section 27, T. 19, R. 32, W 1 mer., east of the plant site. Thicknesses of 150-200 ft (45-60 m) are common in these areas. The thickness of the fluvial deposits in the buried valley located under the central part of the brine pond, the reach of buried valley near Cutarm Creek and the eastern part of the northwesterly trending valley in sections 26 and 27, T. 19, R. 32, W 1 mer., differs markedly from the other portions of the buried valley system. In these areas fluvial deposits are more haphazard in distribution and the thickness varies greatly. A comparison of Plate 4 with the total till isopach map (Plate 5) shows essentially a mirror image. The most significant change from a hydrologic point of view occurs in the reach of buried valley near Cutarm Creek (cross sections I-I' and J-J', Plate 3). Not only does the continuity of the fluvial deposits change in this area but also the degree of sorting and uniformity of the sediments. The sections in this area are characterized by rapid vertical facies changes, inclusion of till and shale fragments in the fluvial deposits and a generally unsorted appearance. Correlation and extent of individual sand and gravel beds in this area, as shown on the cross sections, is completely hypothetical and for illustrative purposes only. A much more detailed drilling program would be required to resolve the stratigraphic complexities in the geological model in these areas.

In many parts of the buried valley system colluvial deposits occur near the bedrock surface. These deposits are composed of unsorted admixtures of angular shale fragments, sand, and gravel.

EVOLUTION OF BEDROCK TOPOGRAPHY AND DEPOSITIONAL HISTORY

It is apparent, if the distribution and type of Pleistocene sediments are considered, that two generations of bedrock valleys are present in this area, i.e. preglacial and glacial in origin. It appears that the bedrock valley under the central part of the brine pond which shows closure west of the brine pond in sections 28 and 33, T. 19, R. 32, W 1 mer., is preglacial in origin. Similarly, part of the northwesterly trending valley in sections 26 and 27, T. 19, R. 32, W 1 mer., is thought to be preglacial in origin, although the latter valley has undergone considerable change during Pleistocene time. Both valleys drained the upland and their confluence was most likely in the northeasterly corner of section 27, T. 19, R. 32, W 1 mer., from where the joint valley continued in a northeasterly direction towards the present position of Cutarm Creek. During glaciation several events occurred which led to the formation of a newly cut valley. The new valley used part of the existing valley system—the portion of the buried valley system filled with thick deposits of fluvial sediments. It is unfortunate that no tills or other sediments are present in the area below the fluvial deposits, which would define the time stratigraphic interval of the deposition of these fluvial deposits, however, their occurrence under the till of the Floral Formation and their incorporation in the tills of the Floral Formation in the eastern part of the area definitely indicates that the fluvial deposits are older than the tills. They may, however, still have been deposited during the glacial period which deposited the tills of the Floral Formation, because stratigraphic relationships in the eastern part of the area suggest that the fluvial deposits were laid down just prior to the deposition of the tills. If this contention is true, then the following events must have taken place. During the advance of the ice, drainage from the existing valley system was blocked, resulting in considerable ponding and deposition in the portions of the existing valley system. Simultaneous with the upslope advance of the ice onto the bedrock upland considerable thrusting, accompanied by excavation, took place in the reach of the buried valley near Cutarm Creek. During this time the existing fluvial deposits were incorporated in the tills of the Floral Formation. Ice thrusting is common in those areas in Saskatchewan where pre-Pleistocene bedrock uplands, with or without existing valleys, were present (Kupsch, 1962; Clayton and Moran, 1974; Christiansen and Whitaker, 1976).

Concomitant with the thrusting, thick deposits of till were deposited south of the buried valley on the west flank of a small bedrock upland (west to southwest half of section 26, T. 19, R. 32, W 1 mer.), partly infilling a valley. The deposition of thick sequences of till in this location confirms the theoretical glacial processes proposed by Clayton and Moran (1974). It should be pointed out, however, that ice thrusting could also be partly responsible for the thickening of the drift deposits in this area. During this time the ice front appears to have been quasi stationary and it is thought that the "glacial" bedrock valley was cut as an ice marginal meltwater channel draining towards the northwest. Its position and trend correspond to the marginal position of the ice in this area. The direction of thrusting indicates a southwesterly direction of ice flow, and if the configuration of the bedrock topography is considered

with respect to the ice flow direction, then the marginal position of the ice will be more or less perpendicular, i.e. northwesterly. The proximity of the meltwater channel to a thrust zone would explain the heterogeneity of the sediments in that vicinity (NE corner sec. 27, T. 19, R. 32, W 1 mer.). Furthermore, a gradual increase in the degree of sorting can be observed in a northwesterly direction along the "glacial" bedrock valley.

The preglacial bedrock valley under the central part of the brine pond apparently was not used as a drainage path by the meltwater. The distribution of fluvial deposits in this valley is at least spotty in those portions that could be investigated. Its relationship to the glacial bedrock valley to the north is not known because its assumed confluence is located under the brine pond and could not be investigated. It appears that during the period when the tills of the Floral Formation were deposited, which was also the time when the fluvial deposits in the "glacial" bedrock valley were covered, the valley was mainly filled with till. Another possibility is that, since the trend of this valley is more or less parallel to the direction of ice flow, most of the fluvial fill was removed by thrusting.

Subsequent to the deposition of the tills of the Floral Formation, the till of the Battleford Formation was deposited. Little or no modification of the existing topography in most of the area occurred during the glacial period, as is indicated by the uniformity in thickness of the Battleford Formation. It is not known whether Cutarm Creek Valley was formed during the retreat of the last glaciation or whether Cutarm Creek was already in existence and reactivated as a meltwater channel during that time.

SUMMARY

Two different tills belonging to the Battleford and Floral Formations respectively can be recognized in the area. No tills of the older Sutherland Group have been found. Thick deposits of fluvial sediments are present in most of the valleys cut into the bedrock. The age of these deposits is not known, but stratigraphic relationships suggest that they were deposited just prior to the tills of the Floral Formation.

A major facies change occurs in the fill of the bedrock valleys in the eastern part of the area, where continuity has been severely disrupted and modified by glacial thrusting. Part of the preglacial valley system appears to have been preserved in the area.

The major discontinuity in the buried valley fill between the brine pond and Cutarm Creek is of utmost importance when contaminant movement is considered.

Observation Well Network

INTRODUCTION

A total of seven observation wells were installed near the waste disposal basin. The inside diameter of the wells is 6.5 in. (16.5 cm), and all wells were instrumented with continuous water level recorders with a 5 in. (12.7 cm) diameter float. The recorder platforms are attached to the casing. A concrete pad, 6 in. (15 cm) thick, was poured around each well, and a metal shed, 48 in. (D) x 68 in. (W) x 65 in. (H) (that is 122 cm (D) x 173 cm (W) x 165 cm (H)), was constructed on the pad over each observation well. Since the water level in most of the observation wells is near or above surface, the sheds were insulated with 2 in. (5 cm) thick fibreboard and propane heaters with outside venting were installed. Access to the wells for well maintenance purposes could easily be achieved by removing a roof panel.

Six wells were completed in the upper part of the aquifer, and one well, located next to a shallow well, was completed in the lower part of the aquifer. The proximity of the waste disposal basin to Cutarm Creek, a distance of less than 1 mile (1.6 km), necessitated an adequate definition of the hydrological environment in the area between the waste disposal basin and Cutarm Creek. Six of the seven wells were therefore installed in the main buried valley east of the waste disposal basin and the seventh well was located west of the waste disposal basin. The location of the wells is shown in Figure 15.

Accessibility of the observation well sites is poor because of wet terrain conditions. Well construction and maintenance work were therefore conducted during the late fall and winter months.

In addition to the seven observation wells, a still well was installed in the brine pond to record the fluctuations of the brine level.

WELL CONSTRUCTION

The procedures used for test drilling and well construction in the glacial aquifers were those developed over many years by the contractor, Elk Point Drilling Ltd. (Topilka, 1967). Prior to well construction a testhole is drilled to determine the texture, sorting, and stratification of the material in the completion zone. The selection of the completion interval is based on the description of the cutting samples, the single point resistance and spontaneous potential electrical logs, and the driller's log. After this information is obtained, the testhole is abandoned and, if necessary, is plugged with bentonite-cement grout. The well is then constructed within a 10-ft (3 m) radius of the testhole. This procedure is designed to eliminate formation damage resulting from drilling fluid entering the completion zone.

The hole for the well is drilled to the top of the completion zone. Before the casing is installed, a landing ring is welded to the bottom of the casing. This landing ring engages on the bushing at the box of the lead packer and prevents the screen assembly from passing entirely through the bottom of the casing. The casing is run, and the annulus is filled with a bentonite-cement grout. After the grout has set (about 24 hours) the completion zone is drilled out using clean water as drilling fluid. The water is run off to waste rather than being recirculated during the drilling of the completion zone. A very detailed driller's log is kept of the drilling character; the colour of the returning fluid (a qualitative measure of the silt and clay content) is noted; and samples are collected from each 1-ft (30 cm) interval in the completion zone. After the completion zone has been drilled, the screen assembly is made up, using screens with the desired slot size and the necessary fittings and blank extension pipe as the situation requires. Following screen installation, the position of the screen is verified by measurement with a weighted steel tape and then the packer is swedged. The well construction details are shown in Figures 16-22. Johnson stainless steel screens were used in all wells.

When the screen assembly has been installed, the well is developed. The objective of well development is to bring a well to its maximum designed production capacity. This is achieved by reducing the skin effect, increasing the permeability, and creating a natural "gravel" pack close to the screened interval. The procedures and techniques involved in the development of screened wells in unconsolidated sediments are therefore designed to (Anonymous, 1966, p. 294):

1. Correct any damage to or clogging of the water-bearing formation occurring as a side effect from drilling (skin effect);

2. Increase the porosity and permeability of the natural formation in the vicinity of the well;
3. Stabilize the formation around the screened interval so that the well will yield water free of sand, silt, etc. (creation of natural gravel pack).

The techniques employed for the observation wells include high-velocity hydraulic jetting in the screen, wir-lift pumping, mechanical surging, and, in one well, hydraulic jetting with a dispersing agent (sodium acid polyphosphate). At the outset, development procedures are carried out gently to allow the sand to collapse around the screen. As development proceeds, the energy applied to the completion zone is increased. Development is continued until the discharge water is essentially sand-free, sequential hydrodynamic response tests show no further increase in the transmissivity, and the electrical conductivity has stabilized. The successful use of hydrodynamic response testing as a means to measure the progress of well development has been described elsewhere (Vonhof, 1975b).

OPERATING EXPERIENCE

Each observation well was equipped with a Leupold Stevens Type F recorder with a weight-driven clock. The maximum continuous recording period for this type of installation is 32 days. The observation well network was operational on May 1, 1971, and recording continued until December 20, 1975. Figure 23 shows the data recovery for the wells in each year and the source of the record loss, whereas Figure 24 shows a summary of the record loss for each well over the total recording period (1702 days) and the magnitude and source of the record loss over the total number of recording days (11 914).

Before discussing the causes of the record losses, it should be pointed out that the regular maintenance program consisted of:

1. replacement of the clocks once a year
2. cleaning of moving parts once a month
3. cleaning and/or replacement of pens once every 3 months

The loss of record attributed to human error refers to those occasions when the charts were not changed on time. With respect to observation well D (Fig. 23) additional recording days were lost because the propane heater was not lit early enough in the fall, and since the water level in observation well D is approximately 7 ft above ground level, this resulted in freezing of the water column in the well. The record loss designated as mechanical failure consisted mainly of clock failure. Although the clocks were replaced regularly on a yearly basis, the record (Fig. 23) shows that a shorter replacement interval, for example, 6 months, would have been desirable for this type of clock. Another type of mechanical failure was caused by the malfunctioning of the thermostats on the propane heaters. This resulted in either freezing of the well or overheating of the well housing. The overheating caused the ink in the pen nibs to dry up. In one instance the temperature was so high that the plastic ink reservoir actually melted. The total number of recording days lost to malfunctioning of the thermostats on the propane heaters was in the order of 75 days, which represents approximately 10 per cent of the record loss attributed to mechanical failure.

The record loss was worst in 1975. A number of phenomena occurred in that year which were not foreseen:

1. A severe storm (small twister) destroyed the well shed at observation well B (June, 1975). The shed was completely ripped off the foundation and the propane tank (500 gal) located behind the shed was rolled off its foundation blocks.
2. A change in the waste disposal practice was initiated by I.M.C.C. during the late summer of 1975, which resulted in very rapid rises in the water levels in the observation wells. Loss of record was caused by insufficient free fall space for the counterweight of the recorder. In addition, a number of the wells, D, F, and G, overflowed.

In summary, the main source of record loss can be attributed to mechanical failure of the clocks, which accounts for approximately 70 per cent of the total number of days lost.

The operating performance of the still wells in the brine pond was disappointing, to say the least. Since no still well was present in the brine pond when this program started, a number of makeshift installations were constructed. All of these were built near the high brine level mark, at the time of construction, on the inside of the dykes. As the result of rising brine levels, the recorder housing became partially submerged and wave action demolished the housing. In addition to this inconvenience, a host of other problems caused loss of recording days. These were:

1. severe corrosion
2. deposition of brine films on moving parts
3. deposition of thin salt crusts on moving parts
4. crystallization of halite between the float and the inside of the casing, plugging of intake pipe by salt crystallization and slime buildup, etc.

As a result of these problems the data recovery over the period 1971 to 1976 was as follows:

1971	78.4 per cent
1972	91.2 per cent
1973	81.3 per cent
1974	59.1 per cent
1975	50.9 per cent

The overall data recovery for the period was 73.2 per cent.

FUEL REQUIREMENTS

As was pointed out before, six of the seven wells had water levels close to or above ground surface. In order to avoid freezing of the water in the casing, which could have caused damage to the casing and would have resulted in interruption of the hydrograph records, heaters were installed in the sheds. It was hoped that sufficient heat would be conducted downward through the concrete floor and the casing to prevent frost from reaching the casing from the outside. The depth of the frost line varies from 7 to 9 ft (210 to 275 cm) below surface, depending on the climatic conditions during each winter. No loss of record as a result of freezing was experienced during the winter months when the heaters were operational. The heaters used were propane heaters vented to the outside. The capacity of these heaters was 8000 Btu/hr. The inside temperature of the sheds was thermostatically controlled and kept at approximately 70°F (21°C). It is not known what the minimum temperature was which would have prevented freezing of the water in the casing. Since the area where the wells are located is essentially inaccessible for vehicles during the winter months, sufficient propane had to be delivered in the fall to each well site to last for the winter and early spring. Based on experience gained during the construction of the wells, when the non-insulated metal sheds were heated and propane was supplied in 100-lb (45 kg) bottles, it was felt that 500 gal (2270 l) of propane per well would be sufficient. Figures 25 and 26 show the propane consumption for the winters 1971/1972 and 1972/1973 respectively. As can be seen in Figures 25 and 26, sufficient propane was on site to assure continuous operation of the heaters from the late fall to the following spring. The mean daily temperatures in Figures 25 and 26 show that the winter of 1971/1972 was much cooler than the winter of 1972/1973, which is also reflected in the propane consumption. Of all the wells in Figures 25 and 26 well B shows the highest propane consumption. This is caused by the location of well B, which is on a small knoll in an open area, whereas the other wells are much more sheltered from the wind by bushes.

HYDRODYNAMIC RESPONSE OF WELLS AND CHANGES WITH TIME

The hydrodynamic response of a finite-diameter well to an instantaneous charge of water is a measure of the transmissivity of the aquifer (Hvorslev, 1951; Ferris and Knowles, 1954; Ferris *et al.*, 1962; Cooper *et al.*, 1967; Van der Kamp, 1976). However, as Ferris *et al.* (1962, p. 104-105) properly warned: "The duration of a 'slug' test is very short, hence the estimated transmissibility determined from the test will be representative only of the water-bearing material close to the well. Serious errors will be introduced unless the . . . well is fully developed and completely penetrates the aquifer".

Few wells completely penetrate an aquifer. According to Cooper *et al.* (1967), the vertical permeability of most stratified aquifers is only a small fraction of their horizontal permeability; therefore, when flow is induced within a cylindrical volume of indeterminate radius around the well bore by adding or withdrawing a relatively small volume of water, then that flow will be essentially radial. In this case, the aquifer thickness can thus be considered equal to the length of the inlet section, and the transmissivity value can be considered to represent that part of the aquifer in which the well is completed. Because the volume of water added or removed during a hydrodynamic response test is small, the radius of investigation will be relatively small. A hydrodynamic response test is thus uniquely suited to measure the transmissivity immediately surrounding the inlet section, which is the region most affected by formation damage, well development and changes which occur with time as the result of clogging of the well screen. The use of hydrodynamic response tests as a means of monitoring the progress of well development has been described elsewhere (Vonhof, 1975b).

From 1971 to 1974 hydrodynamic response tests were conducted at different times on the various observation wells to determine whether a reduction in the transmissivity was occurring with time. Also, in the summer of 1973, new testing equipment was obtained which made it possible to evaluate different methods of hydrodynamic response testing. Before the summer of 1973, the equipment used to conduct the hydrodynamic response tests was that developed by the Saskatchewan Research Council as described in Vonhof (1975b). The new testing equipment that became available in the summer of 1973 used an electric pressure transducer for measuring the change in the water level during the tests. A complete description of the equipment is included in Appendix I.

The instantaneous charge for the hydrodynamic response test was provided by a solid slug, a bailer, and various

volumes of water which could be added to the well. The solid slug was used in conjunction with the equipment developed by the Saskatchewan Research Council, whereas the other methods were used with the pressure transducer equipment. The charge would result in the following changes in the water level in a well with a 6.5 in. (16.5 cm) inside diameter:

Slug	+ 0.775 ft (23.6 cm)
Bailer	- 0.590 ft (18.0 cm)
Large addition	+ 0.805 ft (24.5 cm)
Small addition	0.609 ft (18.5 cm)

The results of the various hydrodynamic response tests from 1971 to 1974 are shown in Figure 27. During 1971 and 1972 only one set of transmissivity values was obtained in each year for the various wells, whereas in 1973 two sets of values were obtained for all wells except observation well D. Furthermore, a series of sequential tests, using different charges, were conducted on both dates in 1973. It is obvious from the data in Figure 27 that some care has to be exercised in the interpretation of transmissivity values obtained from hydrodynamic response tests. This became especially apparent when sequential tests were run over short time intervals (a few hours or less). The value of the transmissivity varies not only with the type of charge but also with the sequence of the charges. Almost invariably an increase can be noted in the magnitude of the transmissivity between the first and the last test of a series of tests irrespective of the type of charge. Furthermore, a change in the type of charge, addition or withdrawal, in a series of tests is generally accompanied by an apparent change in the transmissivity. This strongly suggests that minor well development takes place during the hydrodynamic response tests.

Figures 28 and 29, observation wells A and B respectively, show examples of a series of hydrodynamic response tests conducted on December 4, 1973. In addition, both figures show damped oscillations which took place during the first few seconds of the test. (Note: the damped oscillations were only observed on the tests with the solid slug). According to the criteria outlined by Bredehoeft *et al.* (1966) and Van der Kamp (1976), the aquifer-well system should be overdamped and the wells should not undergo force-free oscillation following an instantaneous change in the water level. Meneley (1970) ascribes these oscillations to the relative movement of the float on the water surface after the slug has been lowered. Observations of the start of hydrodynamic response tests with different types of charges and recording methods on the same wells show that this type of oscillation is indeed absent, and the contention that the oscillations are inherent to the slug test method is in all likelihood true.

To better define the effect of a particular type of charge on the magnitude of the transmissivity, another series of hydrodynamic response tests was run on December 10 and 11, 1974. These tests were conducted on observation wells F and G, and different volumes of water were added. The volumes were varied from 0.53 to 5.25 l, which resulted in a change of 0.081 ft (2.5 m) to 0.805 ft (24.5 cm) in the water level. The results are shown in Figure 30. As can be seen in Figure 30,

- a rather large difference is present in the magnitude of the transmissivity values for the different sizes of the charges,
- the magnitude of the transmissivity in each volume class remains more or less the same, although a slight increase can be noted with the progression of several tests in one volume class.

The above observations would suggest that the magnitude of the transmissivity as determined by hydrodynamic response tests is volume dependent. Furthermore, the results indicate that in observation well F the transmissivity increases when the volume of the charge is reduced, whereas for observation well G more or less the opposite is true. This could indicate that zones with different transmissivity are present around the screen section; however, the number of tests conducted with small volumes is insufficient to ascertain that conclusion. A much more detailed study would have to be conducted, with a large number of tests with different charges on several wells with different transmissivities, to determine whether a relationship between volume (size of charge) and magnitude of the transmissivity indeed exists. It is questionable whether this would be worthwhile. Examination of the data in Figures 12 and 15 shows that the variation within one particular charge is comparable to differences between charges of different sizes. It may therefore very well be that many of the differences in transmissivity values obtained from these tests are inherent in the system which is used for conducting the hydrodynamic response tests. In other words, the observed variation may be a measure of the accuracy of the system. If the groups of sequential measurements are considered, then for most of the wells the transmissivity values vary with respect to the mean value of each group from ±3 to ±15 per cent. This type of variation is insignificant if it is compared to the natural variation in the transmissivity of the fluvial deposits.

If sequential hydrodynamic response tests are to be used to monitor deterioration of the well, differences between consecutive tests should be at least larger than the inherent variability of the method. This means that multiple measurements should be made each time the method is used to determine the transmissivity. Furthermore, for comparative purposes, the size of the charge should be the same in all the tests.

OBSERVATION WELL RECORD 1971-1975 (INCL.)

The water levels in seven observation wells completed in a small buried valley aquifer and one still well in the brine pond were measured continuously from April 1, 1971, to December 20, 1975. The hydrograph record of the wells for each year is shown in Plates 6, 7, 8, 9, and 10.

The objective of the data collection was to determine the response of the hydrogeological environment to input changes, specifically the activities in the waste disposal basin. Plates 6-10 show that the behaviour of the water level in each of the observation wells is essentially the same. The water level traces are parallel and each trace shows the same fluctuations at the same time. The only difference between the traces is a difference in the fine structure, i.e. very small fluctuations (0.01 ft (3 mm)) of short duration. Hydrographs of the wells with the higher transmissivity have more fine structure than the other wells. The hydrographs of two wells show considerable noise at times. The hydrograph trace of well D shows a large number of vertical spikes. These are caused by short-term loading of the aquifer by railroad transport. The main railroad for shipping the product from the mine is located approximately 200 ft (61 m) west of well D. Well A, which is located approximately 100 ft (30 m) from the east dyke of the brine pond, shows, at several times during the years of observation, small oscillations with an amplitude of up to 0.015 ft (4.5 mm) along portions of the hydrograph trace. These oscillations are caused by wave action on the brine pond. Occasionally, for example in April and June of 1972, these oscillations, albeit much smaller, can also be noted on the hydrograph records of well G, which is located about 1400 ft (426 m) east of the brine pond.

Another form of short time loading which can be recognized on the hydrographs of all wells is high intensity precipitation from rapidly passing rainstorms, for example, to cite a few, June 13, August 1, and August 15, 1972; July 23/24, August 8, and August 18, 1973. A comparison between the "instantaneous" rise in the level of the brine pond and the simultaneous rise of the water levels in the wells strongly suggests that the latter is primarily caused by the instantaneous loading of the aquifer as a result of the rapid rise of the brine level and not by precipitation. Figure 31 shows a plot of the rise in the brine pond versus the simultaneous rise in each observation well. Linear regression analysis was used to determine the line of best fit. The correlation coefficient was also calculated. For easy comparison the lines of best fit for the plots are shown in Figure 32. As can be seen in Figure 32, the correlation coefficients show that the "degree of fit" of the given points to the least-squares straight line is excellent. The position of the line of best fit for each observation well shows that with an increase in the distance between the location of a well and the brine pond, the resultant response in the well to an instantaneous increase in brine level decreases. This is a typical response of an aquifer to "point" loading. Furthermore, the brine pond acts as a giant rain gauge. However, the rise in the brine level as measured in the still well is not a true measure of the amount of rainfall, because of the differences in density between the rainwater and the brine, and the observed rise should be multiplied by approximately 1.19 to obtain the true amount of precipitation. If the aquifer would react to the instantaneous loading of the surface by precipitation, then the rise in the water levels in the wells would be greater than the rise in the brine level (if the total load caused by the precipitation is transmitted). In addition, the decrease in response in the wells with an increase in distance from the brine pond should not be present.

The temporary rise in the water levels in the wells is dissipated with time and acts independently of the behaviour of the brine level subsequent to the instantaneous rise. This is well illustrated, for example, on the hydrographs of the observation wells and the still well over the period July 22 to August 23, 1972. Gentle rises in the brine pond level as a result of prolonged low intensity rainfall cannot be detected on the observation well hydrographs.

Another major example of the effect of loading on the water levels in the wells is shown by the hydrograph records of the latter part of 1975 (Plates 6-10). During this time, I.M.C.C. Ltd. changed the disposal practice in the waste disposal basin. Prior to this time, the waste from the mill was discharged into the brine pond, where the solid portion of the waste built an alluvial fan near its discharge point above the brine level, and a deltaic deposit below the brine level. The slope of the surface of both types of deposits was at a low angle. As a result, the solid portion of the waste occupied a considerable area of the waste disposal basin and reduced the effective storage for the brine over the years. During the second half of 1975 the discharge of waste into the waste disposal basin was modified to the extent that the settlement of the solid waste was controlled. This resulted in a rapid localized buildup of solid waste, which in turn resulted in increased localized loading of the surface. Although the hydrograph record of the still well in the brine pond is missing for the latter part of 1975 for reasons outlined before, visual observation of the brine pond during that period showed that only minor changes took place in the brine level. The localized loading of the surface within the waste disposal basin had an immediate effect on the water levels in the observation wells as is shown in Plate 10. For example, from September to December, 1975, the water level in observation well A rose by 2.2 ft (66 cm).

The rise in observation well D, which is the farthest from the brine pond, over the same period is 2 ft (60 cm). This rapid rise in the water levels of the wells caused a number of wells to overflow, which, as mentioned previously, resulted in a considerable loss of record. At the time when this study was ended the water levels in the wells were still rising. It is not known what has happened to the water levels since that time.

Barometric Efficiency

The barometric efficiency of a well is the ratio of the change in the water level in the well to the change in atmospheric pressure. The barometric efficiency of the various observation wells was calculated according to the method outlined by Clark (1967). A record of the barometric pressures was made with a recording barometer over the years 1971 to 1976, at a location within one mile (1.6 km) from the wells. Table 2 shows the barometric efficiencies for the various wells on different dates in 1971 and 1972. The first three columns show barometric efficiencies calculated at 4-hr intervals over a 10-day period, whereas the last four columns show barometric efficiencies based on single barometric events of short duration (less than 2 hr). Except for the values obtained on August 14, 1972, the other values are low for a confined aquifer. Also, a considerable variation exists in the magnitude of the barometric efficiency for each well. To investigate further the variation in the barometric efficiency of the wells, the barometric efficiencies of observation well A were calculated over the period 1971-1976. Each segment of the hydrograph record used in the calculation comprises 10 consecutive days and the time between the segments is approximately 20 days. A total of 52 barometric efficiencies were calculated. The results are shown in Plate 11. The barometric efficiency varies considerably throughout the year with the highest values occurring during the "winter" period (Plate 11). (Note: the temperature trace on Plate 11 shows the mean daily temperature; the "winter" period runs from the first to the last day with recorded frost; at the start and end of the "winter" period the minimum temperatures are indicated by dots). The lowest values are found during both the "winter" period and "summer" period. No specific trends can be found in the barometric efficiency values over the 5-year period. There appears to be no correlation with precipitation, nor is the onset of freezing and the subsequent growth of the frost layer a significant factor, contrary to the findings of Gilliland (1969). In actual fact the magnitude of barometric efficiency appears to be randomly distributed.

The aquifer in which the wells are completed is confined, and large portions show artesian conditions. Within the areas with artesian conditions there are several perennially wet areas, which indicate that considerable discharge is taking place. According to Mr. Martinovsky (pers. comm.), the former owner of the land where the mine site is located, these conditions were present long before the start of mining operations. The till deposits which overlie the aquifer and which are at least 35 ft (10 m) thick can therefore at best be considered semi-confining. This is also confirmed by the low barometric efficiency values (Gilliland, 1969). It is unfortunate that no wells were completed at different depths in the till, because information on the interrelationship between the water level fluctuations in these wells and the observation wells in the underlying aquifer would undoubtedly have shed more light on the various factors controlling the barometric efficiency of the aquifer.

Long-term Water Level Fluctuations

Plate 11 also shows the hydrographs of observation well A and the still well in the brine pond from April 1971 to December 1975. The comments on the behaviour of the water level in well A apply equally to all observation wells because of the similarity and parallelism in the trend of the water levels (Plates 6-10). Several observations can be made:

1. The water level trace of well A shows clearly the instantaneous response to rainfall and the subsequent dissipation.

Table 2. Barometric Efficiencies of Observation Wells (per cent).

Observation well	April 2-12, 1971	Aug. 8-18, 1971	April 4-14, 1972	July 2, 1971 03.00-04.00 hr	July 6, 1971 19.00-21.00 hr	July 7, 1971 02.00 hr	Aug. 14, 1972 10.30-12.30 hr
A	14.7	10.8	14.7	14.7	17.6	15.8	26.9
B	14.6	11.2	14.9	15.9	15.6	11.2	29.4
C	13.7	11.5	15.9	17.2	15.6	9.1	21.2
D	14.4	11.8	13.7	12.3	14.6	9.1	–
E	12.9	12.8	15.9	23.3	16.5	15.2	32.7
F	16.2	10.9	12.6	15.9	17.4	16.3	27.0
G	15.7	9.3	13.4	17.2	16.5	15.2	20.4

2. The highest water level in well A is recorded during the "winter" months.
3. Decline of the water level from its highest point coincides with the time when the mean daily temperature during the "winter" period starts to increase. This is true for all years except 1974, when this decline started earlier.
4. Increases in the water levels coincide with the end of the "winter" period in 1971, 1973, 1974, and 1976.
5. The amplitude of the highest water level decreased from 1972 to 1975.
6. From April 1971 to April 1975 only a modest net increase of approximately 0.5 ft (15 cm) can be noted.
7. The level in the brine pond increased 3.90 ft (119 cm) from April 1971 to June 1973, at which time it peaked.
8. From June 1973 the brine level has been gradually decreasing.
9. There is *no* relationship between the long-term changes in the brine level of the waste disposal basin and the water levels in the observation wells.

The decline in the brine level corresponds approximately with the time a deep disposal well became operational.

The hydraulic head measured in an observation well under natural conditions is a function of the hydrodynamic equilibrium between recharge and discharge. When the net water level in a well is rising, it indicates that the rate of recharge to the aquifer exceeds the rate of discharge. Conversely, a decline in the water level would signify that discharge exceeds recharge. Since the peak water levels occur during the "winter" period in all years and recharge is negligible during this period, the peaking could indicate delayed recharge. On the other hand, it is known from the barometric efficiency that the "confining" layer is semi-confining at best and furthermore that large portions of the aquifer are artesian. It is therefore conceivable that peaking of the water levels indicates a partial blockage of discharge as the result of the buildup of the frost layer or it could be a combination of both. Why the decline of the water level more or less coincides with the time when the mean daily temperature during the "winter" period starts to increase is not known, and only some highly speculative hypotheses can be advanced to explain this phenomenon. It is known that during freezing of water several salts precipitate, whereas others stay in solution and become more concentrated into brines. These super-cooled liquids could therefore be the cause of a large number of "holes" in the frost layer. However, with a further reduction in the temperature, further precipitation of salt will occur. This phenomenon has been observed on many occasions in the brine pond, which is essentially an open body of "water" during the winter. When the air temperature dropped to below -30°C, considerable crystallization of NaCl took place in the shallow portions of the brine pond. A similar process could take place in the zone where the frost layer is formed every winter in the discharge areas, which would result in a progressive blocking of the discharge. Once the mean air temperature reverses its decline and starts to increase again, the process would be reversed and the discharge would increase, resulting in a decline in the water levels. The decline would be relatively rapid, because recharge is not occurring.

The increase in the water level at the end of the "winter" period, which more or less corresponds with the spring melt period, in almost all years indicates that recharge is occurring relatively rapidly, which strongly suggests a relatively open system.

The lack of correlation between the hydrographs of observation wells and the brine level is puzzling. Two contradictory lines of evidence are shown by the data. On the one hand, the loading phenomena strongly suggest that the aquifer is confined and does not have a direct hydraulic connection with the brine pond (based on the criteria outlined by van Everdingen (1968)). On the other hand, the barometric efficiency and the behaviour of the water levels in reaction to natural input parameters strongly suggest that the aquifer is semi-confined at best. Although no testdrilling was conducted in the area occupied by the brine pond, projection of stratigraphic information collected around the brine pond does not indicate any major changes. It is therefore reasonable to assume that the semi-confined condition is also present under the brine pond. According to van Everdingen (1968), in the case of a confined aquifer in hydraulic connection with a reservoir, movement of water between the reservoir and the aquifer affects the water levels in the aquifer. Initially, the rise in aquifer water level may be partly due to loading by water in the reservoir. Since the aquifer in this area is semi-confined, it would be reasonable to assume that at least some influence of the reservoir (brine pond) would be detectable; however, the hydrographs of the observation wells show otherwise. A possible explanation for this contradiction may be that the hydraulic connection in the semi-confining layer between the bottom of the brine pond and the top of the aquifer has been destroyed by the effect of the brine on the sediment in the semi-confining layers. It is a well-known fact that a solution with a high concentration of Na-ions will cause cation exchange in Ca-Mg montmorillonites and subsequent dispersion, which in turn will cause a drastic reduction in the transmissivity of the sediment. The tills contain a considerable amount of montmorillonitic clays. Infiltration of brine into these sediments could therefore have resulted in destruction of transmissivity and a change from

a semi-confined to a locally confined condition. If this contention is correct, it would explain the apparently contradictory behaviour of the semi-confined aquifer.

As was pointed out in a previous chapter, evaporation from a brine pond is negligible in comparison with annual precipitation. An indication of the rate of evaporation from the brine pond was obtained from the hydrographs of the still well from May 19, 1973, to August 19, 1973 (Plate 8). During this time little or no waste was discharged in the brine pond, and the instantaneous small rises that can be observed are caused by high-intensity rainstorms. It is therefore reasonable to assume that the decline in the rise of the brine level after the rainstorms is due to evaporation. Based on the rate of decline, the evaporation rate over this period is in the order of 0.0115 ft (3.5 mm) per day.

SUMMARY

Loss of record in observation wells that have water levels above or close to the ground surface and that are located in areas inaccessible for servicing during the winter months can be prevented by using propane heaters in the observation well houses and on-site fuel storage. Fuel requirements are less than 500 gal of propane per house per season.

The operating experience with the Leupold Stevens Type F recorder with a weight-driven clock over a total of approximately 11 900 recording days shows a loss of record of 10.7 per cent. The main cause of loss of record was mechanical failure of clocks (5.9 per cent).

The results of a large number of hydrodynamic response tests using different volumes and different recording equipment show that minor well development occurs during consecutive tests and that the magnitude of the transmissivity is, to a minor degree, dependent on the volume of the slug.

The hydrographs of the observation wells show that the water level traces are essentially parallel and show similar responses to input changes. Continuous recording in a few wells (three) supplemented by spot measurements in the other wells would therefore be more than sufficient for long-term monitoring of the water levels. A significant saving in the operating and maintenance cost of the long-term monitoring program can thus be realized.

A comparison between the long-term fluctuations of the water levels in the observation wells and the brine level in the waste disposal basin shows that there is no relationship; however, short-term loading events within the brine pond cause an immediate response in the observation wells.

An extensive study of the barometric efficiency of the wells in conjunction with the response of the water levels in the wells to input changes shows that the aquifer is semi-confined at best.

An Electric Analog Simulation of Groundwater Flow Patterns (D. R. Bourne and J. A. Vonhof)

INTRODUCTION

In order to calculate convective travel times and the direction of pollutant movement within the sedimentary deposits, groundwater flow nets are required. Flow nets can be constructed by mapping key hydrologic phenomena in the field (Meyboom, 1963) or by solving a mathematical model of the hydrogeological system (Toth, 1963; Freeze and Witherspoon, 1966, 1967). Once the mathematical model has been calibrated against field measurements, the model can be used for predictive purposes.

The mathematical model approach involves replacing the hydrogeological system with an equivalent mathematical model in the form of a boundary value problem. Once the problem is formulated in a mathematical model, then accepted mathematical techniques for solving boundary value problems can be employed.

Boundary value problems consist of five essential components:

1. the partial differential equation which governs the system
2. the shape of the region
3. the boundary conditions
4. the initial conditions
5. the hydrogeological parameter distributions for K, α, and n in the region of flow.

The two most common methods for solving boundary value problems are by analytical and numerical techniques. Analytical techniques produce the most satisfactory form of solution, but these techniques are only effective if geometries, hydrogeologic parameter distributions, and boundary conditions are all relatively simple (Bear, 1972). Any complex boundary value problem must be solved using numerical techniques, either by the finite difference method or the finite element method. The finite difference method is adopted in this study.

To solve the boundary value problem numerically, either a digital computer or an analog model may be employed. A digital computer is the most efficient method of solution, but the electric analog offers several advantages in practical situations:

1. A very large one-, two-, or three-dimensional grid can be used, whereas in a digital computer storage may be limited or computation time may become excessive.
2. The hydraulic conductivity variation either within or between geologic formations can exceed four orders of magnitude in an electric analog model. Digital solutions for such cases may require excessive computer time (Freeze, 1975, pers. comm.).
3. Analogs are more effective as a communication tool with practicing engineers, administrators, and laymen (Meneley, 1975, pers. comm.).
4. Non-technical personnel can operate the analog at a minimum cost.

The solution or output of an electric analog model of a steady state groundwater flow problem is a hydraulic head value for each nodal point in the system, namely $\varphi(x,y,z)$. In the transient case, the output is $\Delta\varphi(x,y,z,t)$, the change in hydraulic head from time zero to time t.

Both a steady state and transient analysis have been applied to the study site analog model. A short description of the essential components of these two boundary value problems is necessary before proceeding. Figures 33 and 34 illustrate the study site boundary value problem.

Steady State

The nonlinear partial differential equation describing steady state groundwater flow through a heterogeneous, anisotropic, saturated porous medium in three dimensions is

$$\frac{\delta}{\delta x}\left[K(x,y,z)\frac{\delta\varphi}{\delta x}\right]+\frac{\delta}{\delta y}\left[K(x,y,z)\frac{\delta\varphi}{\delta y}\right]+\frac{\delta}{\delta z}\left[K(x,y,z)\frac{\delta\varphi}{\delta z}\right]=0 \quad (1)$$

where φ = hydraulic head, L

$K(x,y,z)$ = hydraulic conductivity, L/T

x,y,z = Cartesian coordinates, L

Both impermeable and constant head boundary conditions are present at the site. Impermeable boundaries are located in two places: (1) the contact of the shale bedrock and the unconsolidated deposits, and (2) under Cutarm Creek.

The water table is assumed to be a constant head boundary, the hydraulic head along the water table being equal to its average elevation.

The region of flow is restricted to the unconsolidated deposits.

Of the three hydrogeologic parameters (K,α,n), only K is needed for the steady state case. The K distribution in the region of flow is obtained by employing a number of techniques, which are described in the following sections.

Transient Case

The nonlinear partial differential equation describing transient, three-dimensional flow through a heterogeneous, anisotropic, saturated porous medium is

$$\frac{\delta}{\delta x}\left[K(x,y,z)\frac{\delta \varphi}{\delta x}\right]+\frac{\delta}{\delta y}\left[K(x,y,z)\frac{\delta \varphi}{\delta y}\right]$$

$$+\frac{\delta}{\delta z}\left[K(x,y,z)\frac{\delta \phi}{\delta z}\right]=\gamma\left[\alpha(x,y,z)+n(x,y,z)\beta\right]\frac{\delta \phi}{\delta t}$$

$$+Q(x,y,z,t) \qquad (2)$$

where γ = specific weight of water (M/L^2T^2)

$\alpha(x,y,z)$ = compressibility of medium, (L/MT^2)

$n(x,y,z)$ = porosity

β = compressibility of water (L/MT^2)

t = time (T)

$Q(x,y,z,t)$ = volume rate of withdrawal or injection at any node (L^3/T)

Two types of boundary conditions, impermeable and constant flux, are present. The region of flow is, as in the steady state case, confined to the unconsolidated deposits.

The distribution of the hydrogeologic flow parameters, K, α, and n, must be known in order to obtain a transient solution. The K distribution is the same as that in the steady state case. The distributions of compressibility, α, and porosity, n, can be obtained indirectly from pump tests and will be discussed later. Table 3 summarizes the hydrogeologic flow parameters required for the steady state and transient cases.

HYDRAULIC CONDUCTIVITY DISTRIBUTION

Several methods were employed to estimate the hydraulic conductivity distribution within the subsurface geologic units. Pump tests, hydrodynamic response tests, hydraulic conductivity estimates from grain size analyses, electric logs, and the published literature provided a good basis for selecting K-values.

Till

No K-measurements of the till were made at the study site. Freeze (1969) noted that in the absence of actual field measurements of K two approaches could be followed:

1. Estimating K from the texture of the sediment using empirically or experimentally justified relations.
2. The use of K-measurements from geologically similar areas.

Since there were insufficient data available on the textural characteristics of the till at the study site, the hydraulic conductivity was based on values determined for geologically similar areas. Table 4 summarizes K-measurements of fractured and unfractured till from Saskatchewan and other geologically similar areas. Note that there is a distinct difference in K-values between fractured and unfractured till. Although the fracture density and orientation was measured in two borrow pits where the Floral Formation was

Table 3. Hydrogeologic Components of the Steady State and Transient Groundwater Electric Analog Model.

	Groundwater flow equations	Boundary conditions			Hydrogeologic parameters		
		Imperm.	Constant head	Constant flux	K	α	n
Steady state	$\nabla^2(K(X,Y,Z)\phi)=0$	X	X		X		
Transient	$\nabla^2(K(X,Y,Z)\phi)=\gamma(\alpha+n\beta)\frac{\delta \phi}{\delta t}+Q$	X		X	X	X	X

exposed, no information was obtained on the aperture of the fractures. Consequently, the permeability of the tills in the Floral Formation could not be calculated. A value of $K = 1$ lgpd/ft^2 (5.7×10^{-5} cm/sec) was selected for the till at the study site on the basis of Table 4. In the subsequent calculations the hydraulic conductivity in the tills is assumed to be isotropic and homogeneous.

Buried Valley Fluvial Deposits

The hydraulic conductivity of the buried valley fluvial deposits was calculated, from a variety of methods, to have an average value of 330 lgpd/ft^2 (19×10^{-2} cm/sec). These fluvial deposits are composed basically of sand and gravel. The average K-value of the sand was measured at 200 lgpd/ft^2 (1.1×10^{-2} cm/sec). The average K-value for the gravel was estimated and measured at 1000 lgpd/ft^2 (5.7×10^{-2} cm/sec). Once again, the hydraulic conductivity within the buried valley fluvial deposits is assumed to be isotropic and homogeneous. The methods used to estimate and measure the hydraulic conductivity are discussed in detail in the following sections.

Pump Tests

Pump test data were analyzed by the authors using the Theis, Jacob, and Theis recovery methods. These methods provide determination of the derived formation parameters transmissibility (T) and storage coefficient (S), where

$$T = K.b \tag{3}$$

and $$S = b.\gamma\,(\alpha + n\beta) = bS_s \tag{4}$$

where b = thickness of the geological formation (L)

S_s = the specific storage (1/L)

The pump test data are included in Appendix II.

The Theis and Jacob non-equilibrium methods are approximate solutions to boundary value problems describing transient groundwater flow. These methods are based on analytical mathematical solutions that relate the lowering of the hydraulic head in a pumping well to T and S of the aquifer. The theory and assumptions behind these methods are discussed by Todd (1959). An especially helpful engineering guide is the one by Kruseman and de Ridder (1970).

Three important assumptions in the theory of pump tests are

1. the aquifer is of infinite areal extent
2. the pumping well fully penetrates the aquifer
3. there is no leakage from adjacent geologic units.

At Esterhazy, none of these assumptions are satisfied, so there are limitations on the direct application of the methods to the data. The first assumption restricted the analysis to very early drawdown-versus-time data to match the Theis type curve properly. Noticeable deviations from the type curve for large times due to leakage and boundary effects make these data unsuitable for direct calculation.

In aquifers that are only partially penetrated by a pumping well, flow lines around discharging wells are not horizontal but radially oriented around the bottom of the well screen. Only at some distance from the pumping well is the flow horizontal. Kruseman and de Ridder (1970) specify this distance as approximately 2.b, where b is the saturated thickness of the aquifer. At the site, the buried valley fluvial deposits have a maximum thickness of 250 ft (76 m), so a partial penetration correction method should be utilized for any observation well within 500 ft (152 m) of a pumped well. As it turns out, all distances between observation wells and pumping wells in the Esterhazy tests are greater than 500 ft (152 m), therefore, the Theis and Jacob methods hold without correction.

Results of the Theis and Jacob methods are summarized in Table 5. Observation well locations are illustrated in Figure 35. An example of a plot of the Jacob method is illustrated in Figure 36. There is a wide variation in the results both between and within each method. In general, the Jacob method gives a better estimate of the T-value because boundary effects can be readily determined on the graphs and affected data identified.

Theis Recovery Method

After pumping of a well has stopped, the water level will rise again, ultimately to its original position. The rate at which the water level rises reflects the transmissibility of the aquifer. The limiting assumptions are the same as in the Theis and Jacob methods. Kruseman and de Ridder (1970) describe the theoretical and practical aspects of the method.

The Theis recovery method was applied to each of the pumping wells. The results are listed in Table 6 and a sample plot of the Theis recovery method is illustrated in Figure 37. The values indicated are of the same order of magnitude as those obtained with the Theis and Jacob methods.

Hydraulic conductivities (K_s) are usually calculated by dividing transmissibility by the length of the well screen (B_s). However, in this case of partially penetrating well screens, dividing T by the average saturated thickness of the aquifer (b_a) resulted in hydraulic conductivity (K_a) values closer to those arrived at by other methods than if

Table 4. Hydraulic Conductivity Values for Till and Shale in Saskatchewan and Other Geologically Similar Areas (after Bourne, 1976).

Geological formation	Fractured	Unfractured	Unknown	Location	Source	Method							Depth (ft)	Hydraulic conductivity (Igpd/ft^2) range or average		
						Pump test	Slug test	Laboratory	Tritium	Grain size estimate	Digital simulation	Estimated		Mean K	Horizontal K	Vertical K
Till			X	Allan Hills, Sask.	Meyboom (1966b)		X						0-50	0.025-6.75		
Till			X	Gravelbourg, Sask.	Freeze (1964)	X							75			0.05 to 3.0
Till			X	South Central Sask.	Meyboom		X						0-50	0.125 to 12.5		
Till and Shale			X	South Central Sask.	Meyboom (1966a)				X				0-250	0.4		
Till	X			Southern Sask.	Mawson (1961)				X				0-30	0.17 to 1.7		
Till			X	Ohio	Norris (1962)	X		X					0-110	0.75		
Till				Saskatoon, Sask.	Meneley (1970)								Shallow			0.002 to 0.02
Till			X	Good Spirit Lake, Sask.	Freeze (1969a)	X								7.9×10^{-9} to 3.0		
Till			X	North Dakota	Sloan (1972)	X							Shallow	0.012 to 0.12		
Till			X	Southeastern, Manitoba	Clister (1973)		X						Shallow	0.17×10^{-3} to 0.17		
Till	X			Alberta, Sask. & Manitoba	Grisak et al. (1975)								5-65	5.6×10^{-3}		
Till	X			Eastern Manitoba	Grisak & Cherry (1975)				X		X		0-75	3×10^{-3}		
Till		X		Eastern Manitoba	Grisak & Cherry (1975)			X					0-75	9×10^{-5}		
Till			X	Regina, Sask.	Lissey (1962)	X							Shallow	0.024 to 0.6		
Bearpaw Shale			X	South Central Sask.	Meyboom		X						0-200	0.018-0.125		
Bearpaw Shale			X	South Central Sask.	Meyboom		X						300	0.009		
Bearpaw Shale			X	South Sask. Reservoir	Peterson (1954)			X					100		10^{-3}-10^{-7}	10^{-3}-10^{-7}

Table 5. Transmissibility and Storage Coefficient Values for the Theis and Jacob Methods.

Observation well	Pumped well	Theis method		Jacob method	
		Average T lgpd/ft	S	T lgpd/ft	S
A	B	15 000	2.9×10^{-4}	67 000	2.0×10^{-4}
	C	12 000	1.3×10^{-4}	40 000	0.9×10^{-4}
	F	15 000	1.8×10^{-4}	89 000	1.8×10^{-4}
	G	11 000	1.2×10^{-4}	64 000	1.2×10^{-4}
B	A	18 000	2.6×10^{-4}	73 000	2.2×10^{-4}
	C	15 000	2.7×10^{-4}	62 000	2.4×10^{-4}
	F	24 000	3.2×10^{-4}	426 000*	6.4×10^{-4}
	G	13 000	1.9×10^{-4}	377 000*	6.0×10^{-4}
C	A	38 000	2.7×10^{-4}	188 000	2.5×10^{-4}
	B	6 000	3.3×10^{-4}	76 000	5.6×10^{-4}
	F	19 000	2.1×10^{-4}	22 000	3.3×10^{-4}
	G	3 000	5.3×10^{-4}	347 000	5.7×10^{-4}
D	F	72 000	2.3×10^{-4}	183 000	1.4×10^{-4}
	G	12 000	0.9×10^{-4}	213 000	1.6×10^{-4}
F	A	7 000	1.1×10^{-4}	88 000	1.7×10^{-4}
	B	45 000	3.1×10^{-4}	96 000	1.9×10^{-4}
	C	49 000	2.4×10^{-4}	94 000	1.3×10^{-4}
	D	29 000	2.0×10^{-5}	191 000	1.6×10^{-4}
	G (vertical)	18 000	4.0×10^{-3}	36 000	0.37
G	A	2 000	4.8×10^{-5}	69 000	1.6×10^{-4}
	B	18 000	2.4×10^{-4}	172 000*	3.5×10^{-4}
	C	23 000	1.7×10^{-4}	259 000*	2.6×10^{-4}
	D	10 000	1.4×10^{-4}	126 000	2.1×10^{-4}
	F (vertical)	17 000	5.3×10^{-3}	36 000	0.7

*Not enough points to make a reliable prediction.

the transmissibility was divided by the length of the well screen. Both values, K_a and K_s, are reported in Table 6. The Theis recovery calculations are included in Appendix III.

Hydraulic Conductivity Estimates from Grain Size Distributions

Hydraulic conductivity estimates derived from grain size distribution curves have been successfully applied to unconsolidated sands, ranging in diameter from 2.0 mm to 0.0625 mm (Masch and Denny, 1966). This technique involves the determination of the median grain size (MD_{50}) and the inclusive graphic standard deviation (σ_I) from grain size distribution curves. A set of type curves is then used to translate these two measurements, MD_{50} and σ_I, into an estimate of the hydraulic conductivity K.

Hydraulic conductivity values for approximately 60 samples were determined by this method. The K-values ranged from 66 to 1000 lgpd/ft^2 (3.8×10^{-3} to 5.7×10^{-2} cm/sec), and averaged 200 lgpd/ft^2 (1.1×10^{-2} cm/sec). These figures compare well with published figures on K-values for unconsolidated sands (Todd, 1959; Bear, 1972). Also, these results agree with the K-values calculated for the buried valley fluvial deposits from the pump tests.

Hydrodynamic Response Tests

Hydrodynamic response tests were conducted on all observation wells using the method outlined by Cooper *et al.* (1967). The results are shown in Table 7. These results indicate K-values in the same range as determined by pump tests and grain size estimation techniques. Hydraulic conductivity estimates were obtained by dividing the calculated transmissibilities (T) of each well by the length of their well screen. This method of calculating hydraulic conductivity values from transmissibilities contrasts with the Theis recovery method, where reasonable K-values were obtained by dividing T by the average saturated thickness of the aquifer.

Transmissibility Estimates from Well Logs

A total transmissibility estimate for each testhole in the buried fluvial deposit can be determined using lithologic and geophysical well logs. The method is as follows: total thickness of both sand and gravel is calculated using the

Table 6. Hydraulic Conductivity Estimates from the Theis Recovery Method for Observation Wells A to G.

Pumping well	Well screen length b_s (ft)	Average aquifer thickness b_a (ft)	Q Igpm	T Igpd/ft	$K_s = \frac{T}{b_s}$ Igpd/ft^2	$K_a = \frac{T}{b_a}$ Igpd/ft^2
A	8	60	49.9	57 000	7 125	950
B	10	180	8.3	55 000	5 500	305
C	8	165	16.6	66 000	8 250	400
D	10	190	16.6	68 000	6 800	358
E	8	230	49.9	110 000	13 750	478
F	14	220	49.9	38 000	2 715	173
G	8	220	49.9	33 000	4 125	150

Table 7. Hydraulic Conductivity Values from Hydrodynamic Response Tests for Observation Wells A to G.

Observation well	T cm^2/sec	T Igpd/ft	Well screen length, ft	K Igpd/ft^2	K cm/sec
A	12.9	80×10^2	8	1000	3.8×10^{-3}
B	2.5	14×10^2	10	140	8.0×10^{-3}
C	2.3	13×10^2	8	162	9.2×10^{-3}
D	1.9	11×10^2	10	110	6.3×10^{-3}
E	9.7	56×10^2	8	700	4.0×10^{-2}
F	2.0	12×10^2	14	86	4.9×10^{-3}
G	6.6	38×10^2	8	475	2.7×10^{-2}

available well logs, assuming these are the only lithologic units present. Using the hydraulic conductivity estimates previously determined for the sand and gravel, the total transmissibility at a well is estimated from

$$T_{total} = (b_{total\ sand} \cdot K_{sand}) + (b_{total\ gravel} \cdot K_{gravel}) \quad (5)$$

Total transmissibility values, T_{total}, were plotted at each well in the buried aquifer, then contoured to give an initial T estimate for the aquifer (Fig. 38). The average K-value of the aquifer is calculated by dividing the transmissibility by the saturated thickness of the aquifer at a number of points. This method of calculation produced an average K-value for the buried valley fluvial deposits of 330 Igpd/ft^2 (1.9×10^{-2} cm/sec).

Subsequent to this study, Vandenberg (1978) analyzed pump test data from the Esterhazy area by matching time-drawdown curves obtained from pump tests with simulated time-drawdown curves obtained from an analytical expression for drawdown in a leaky strip aquifer. Results of his investigations indicate K-values for the buried valley aquifer ranging from 4.9 to 8.5×10^{-2} cm/sec (860-1500 Igpd/ft^2), assuming that the average thickness of the aquifer is 38 m (125 ft). These values are somewhat higher than results obtained by this study; however, considering that K-values range over 2 orders of magnitude, the results between the two independent investigations are in reasonable agreement.

Porosity and Compressibility

In addition to the hydraulic conductivity, transient simulations require values of the distribution of porosity, n, and compressibility of the geological units, α, in the region of flow. No direct measurements of n and α were made at the site, however, an indirect measurement of these parameters is the storage coefficient (S), where

$$S = b.\gamma\ (\alpha + n\beta) \quad (4)$$

and b, γ, and β are known constants. The storage coefficient was measured in the buried valley fluvial deposits during pump tests. An initial average value of $S = 2.3 \times 10^{-4}$ was selected from Table 5 for the buried valley fluvial deposits. Assuming the average saturated thickness for the fluvial deposits is 125 ft (38 m), $S_s = 2 \times 10^{-6}$ 1/ft.

Since the storage coefficient or specific storage was not measured during pump tests for the till, an estimate of 7×10^{-4} was adopted (Domenico, 1970).

ELECTRIC ANALOG MODEL

The electric analog model approach was used to solve the previously outlined boundary value problem at the study site. A review of the theory, the design criteria and the construction methods is given in Appendix IV.

Four main sources of errors are inherent in an electric analog analysis of a hydrogeological problem. These are:

1. Errors owing to the replacement of a continuous field by a finite difference model.
2. Errors in the electrical equipment.
3. Leakage of electricity in the electric analog model.
4. Errors in the hydrogeological model, i.e. in the configuration of the hydrogeologic parameters K, α, and n.

Karplus (1958) discusses items (1) and (2) in detail. Discretizing errors can be kept within reason by selecting small enough nodal distances. Inaccuracies owing to (2) above seldom exceed 3% according to Karplus (1958). The more sophisticated electrical equipment of recent years has probably reduced this figure even further.

As discussed in Appendix IV, leakage of electricity in the electric analog model is negligible.

The largest errors in a hydrogeological model study are in the estimation of the hydrogeologic parameter distributions (K, α, and n). These errors are difficult to measure, therefore, a complete error analysis of these parameter distributions was not undertaken.

We have assumed that the two hydrogeologic formations are homogeneous and isotropic, although in nature they are heterogeneous and anisotropic. Errors owing to this assumption are probably small within a highly permeable buried valley aquifer.

ANALOG MODEL SIMULATIONS

The results of the analog model simulations are presented in two parts: steady state and transient flow. However, before proceeding with the discussion of the results, a number of observations must be made. First, an important hydrological feature at the study site is a flowing seismic shothole located between observations wells D and F (Fig. 35). This shothole, which presently flows at 20 Igpm and has been flowing for at least 15 years, is completed in the buried valley fluvial deposits. It provides an escape route for some of the subsurface flow and reduces the travel time of a small portion of the brine from its source to the location of the flowing hole. All steady state solutions are simulated with the flowing seismic shothole plugged. Secondly, all measurements of the depth of brine in the brine pond are multiplied by the brine density of 1.19, so that the hydraulic heads of the brine and fresh water are consistent. Lastly, all calculations of brine travel were made for a true scale cross section (J-J'). This cross section corresponds with stratigraphic cross section J-J' (Plate 3).

Steady state results include both the calculation of convective travel times and the direction of brine migration from the brine pond to its discharge points.

Darcy's law provides the specific discharge $v = Q/A$. The actual velocity of fluid movement is $v' = Q/nA$, where n is the porosity. Calculation of steady state brine travel times are therefore based on:

$$v' = \frac{-K\delta h}{n\delta l}$$

Since the velocity of groundwater varies with the hydraulic gradient, each flow line is divided into several constant-hydraulic-gradient segments. The travel time for each segment is then calculated from:

$$t = \frac{(6.23)\,l.n}{K\dfrac{\delta h}{\delta l}}$$

where

n = porosity (dimensionless)

t = time (days)

l = distance (feet)

K = hydraulic conductivity (Igpd/ft^2)

$\dfrac{\delta h}{\delta l}$ = hydraulic gradient (dimensionless)

Total travel time for each flow line, from its source to its discharge point, is calculated by adding the travel times of the various segments.

Steady state results were recorded for the two horizontal layers of the electric analog model.

Once the travel times and directions of brine migration have been established, it is possible to carry out a transient

analysis of some possible remedial measures that have been suggested to prevent the brine from migrating to the surface waters of Cutarm Creek. Transient results were recorded only for the horizontal buried sand and gravel layer of the electric analog model.

Steady State Results

Four steady state cases were investigated:

(A) brine pond at present elevation of 1671 ft

(B) brine pond at an elevation of 1666 ft

(C) brine pond at an elevation of 1661 ft

(D) the natural groundwater flow system with no brine pond.

Figures 39 and 40 illustrate the measured hydraulic head values in the two horizontal layers of the electric analog model for case A. Figures 41, 42, 43, and 44 show the groundwater flow pattern along cross section J-J' for cases A, B, C, and D, respectively. Flow lines are not drawn on these cross sections because the diagrams are vertically exaggerated 16 times. Therefore, flow lines are not at right angles to the equipotential lines and it is a time-consuming task to locate them accurately. For the reader's convenience, approximate direction of groundwater flow is indicated.

In the steady state cross sections the hydraulic head measurements which intersect the ground surface do not all correspond to the ground elevation. There are two reasons for this:

1. the maximum hydraulic head in the brine pond is higher than the ground elevation because of the high density of the brine
2. the water table is approximated as a step function rather than a continuous function.

This problem of inconsistent hydraulic head measurements at the water table is particularly noticeable near Cutarm Creek and around the brine pond.

Recharge and discharge areas for each case are also indicated on the cross sections. For cases A, B, and C, the recharge and discharge areas are identical, with recharge occurring west of point X and discharge east of this point.

Since the discharge areas are the same, total travel times for a number of flow lines are plotted against the distance from the eastern dyke of the brine pond to Cutarm Creek (Fig. 45). Note in this figure that the surface area from point X east to the facies change in the buried valley aquifer will be polluted by brine within 30 years for all brine pond elevations. From the facies change (about 5600 ft east of the brine pond) to Cutarm Creek, the brine travel times increase significantly. Also, as the brine pond elevation is decreased a slight increase in brine travel time is apparent.

Direct brine contamination of Cutarm Creek by any of the cases A, B, and C will take between 640 and 1260 years, therefore, this mechanism of surface water pollution does not pose an immediate problem. The area of greatest concern is located between point X, the recharge-discharge boundary, and the position of the facies change in the buried valley sediments (approximately 5600 ft (1707 m) east of the brine pond) on Figures 41, 42, and 43. In this area long-term discharge could result in the contamination of the surface. The surface drainage characteristics are such that the pollutant would be transported to Cutarm Creek.

Another area of concern is the buried valley aquifer to the west of the brine pond. The steep hydraulic gradient there ensures that the brine will be readily convected through this area. Contamination of the aquifer is almost certain unless remedial measures are undertaken.

Preventive measures designed to solve these problems are investigated in the following section on transient results.

Figure 44 shows the simulated steady state groundwater flow pattern before the construction of the brine pond. A comparison between Figure 44 and Figures 41, 42, and 43 shows that the discharge area has increased considerably since the construction of the brine pond, but the position of the groundwater divide has changed only slightly, because the position of the centre of the brine pond coincides closely with the topographic divide.

Transient Results

Vonhof (1975b) has suggested that a few low rate injection wells, properly located, might reverse the hydraulic gradient, thereby limiting the migration of the brine in the buried valley aquifer. Only low injection rates were considered because only small volumes of potable water are available for injection in the area.

Several combinations of injection wells, of which the locations are shown in Figure 46, were simulated with the electric analog model. Table 8 summarizes the injection well combinations, their pumping rate and duration of pumping. None of the injection well combinations investigated were successful in reversing the hydraulic gradient in either the east or west portions of the buried valley aquifer. Two examples are shown in Figures 47 and 48.

To understand why low-rate injection wells are not effective in reversing the hydraulic gradient one must look

Table 8. Injection Well Combinations and Their Injection Rates. Each Injection Rate was Simulated for 5, 10, 20, and 50 Years.

Injection well combinations	Injection rate/well lgpm
I, II	5
	10
	15
	30
	50
III, IV, V, VI	5
	10
	30
	50
I, II, VII, VIII	5
	10
	30
	50
VII, VIII	5
	10
	15
	30
	50

at the amount of water being transmitted through the buried valley aquifer at various brine level elevations. The quantity of water flowing through the buried valley aquifer is calculated by

$$Q = KA \frac{\delta h}{\delta l}$$

where K = 330 lgpd/ft^2. Table 8 shows the volume of water flowing through stratigraphic cross sections F-F' and H-H' (Plate 3). Cross-sectional areas for F-F' and H-H' are 88 000 ft^2 and 200 000 ft^2 respectively. The figures in Table 9 range from 370 to 565 lgpm, indicating that a minimum of 370 to 565 lgpm would have to be injected into the buried valley aquifer to reverse the hydraulic gradient. At this site, injection wells of this magnitude are not feasible because of the reasons previously stated.

To check the validity of the water volume calculations a transient electric analog simulation was undertaken with a brine level elevation of 1671 ft. Results show that a combined injection rate of 500 lgpm at well locations I and II (Fig. 46) is necessary to reverse the hydraulic gradient in the western portion of the aquifer. This analysis supports the results in Table 9.

Effect of Flowing Seismic Shothole

The flowing seismic shothole was simulated on the electric analog model to examine its effect on the flow paths and pollutant travel times indicated by the steady state solutions. Changes in hydraulic head after 5, 10, and 20 years, with the seismic shothole flowing at 20 lgpm, are illustrated in Figures 49, 50, and 51. In order to examine the effect of the seismic shothole on various steady state solutions, pollutant travel times from the brine pond to the seismic shothole were calculated with the shothole both plugged and unplugged (see Table 10). There is very little difference in pollutant travel times for various brine pond elevations.

Table 9. Quantity of Water Flowing Through Cross Sections F-F' and H-H' for Various Brine Level Elevations.

Brine pond elevation, feet above mean sea level	Hydraulic gradient		Quantity flowing through aquifer, lgpm	
	F-F'	H-H'	F-F'	H-H'
1661	0.023	0.008	465	370
1666	0.025	0.010	505	460
1671	0.028	0.011	565	505

When last checked (March 1976), brine-contaminated water had not reached the seismic shothole. Fresh water was flowing from the shothole at 29 000 lgpd.

As the brine pond elevation is increased, there is an increase in the hydraulic gradient around the seismic shothole. This results in an increase in the discharge from the shothole.

Although the effect of the flowing shothole on the travel time of brine from the brine pond to the shothole is negligible (Table 10), the presence of the flowing shothole provides an easy escape route for the brine once it has reached this location.

Table 10. Travel Times of Brine from the Brine Pond to the Flowing Seismic Shothole with the Seismic Shothole both Plugged and Unplugged.

Brine pond elevation, feet above mean sea level	Years to reach flowing seismic shothole	
	Plugged	Unplugged
1661	10.5	9.9
1666	9.8	9.3
1671	8.7	8.6

SUMMARY

The steady state electric analog simulations of the groundwater flow conditions near the brine pond show

that from the point of view of potential pollution two problem areas can be recognized.

1. It appears that an area of approximately 340 acres (135 ha) east of the brine pond could be polluted by discharging brine within 30 years.
2. Brine pollution by groundwater discharge directly into Cutarm Creek does not appear to be a major pollution hazard because of the presence of a major facies change in the buried valley deposits west of Cutarm Creek. This results in a drastic increase in the travel time of the brine.
3. If brine infiltrates into the portion of the buried valley west of the groundwater divide, it will flow through this section more quickly than through any other part of the buried valley aquifer because the hydraulic gradient is steepest here. This would result in fairly extensive pollution of this aquifer.

The transient electric analog simulations show that low-rate injection wells (up to 50 Igpm) would not reverse the hydraulic gradient in the buried valley aquifer. Calculations indicate that injection rates of between 350 and 575 Igpm would be required.

A word of caution must be expressed on the interpretation of the significance of the calculated travel times. First, it was assumed that the brine infiltrating the till sediments under the brine pond would not cause any changes in the sediments. This is not true because the introduction of brine in this type of sediment will have a drastic effect on the permeability. Initially, it will reduce the permeability significantly, whereas continued exposure of the sediment to the brine will cause major mineralogical changes, which in turn may increase the permeability again. At this time, insufficient information is available on the effect of the brine on this type of sediment and on the rate of progress of these processes. Considerable research will have to be conducted to define the rate of change, both in terms of the mineralogy and the permeability in the sediments. It should be pointed out that these processes take place not only in the recharge area under the brine pond, but also in the discharge areas when the brine reaches the aquifer. This means that if these processes are indeed slow, a considerable delay of the emergence of brine in the discharge areas can be expected.

Secondly, although the density of the brine was taken into account as an input parameter in establishing the hydraulic head in the brine pond, the difference in density between the water and the brine was not considered in the analog simulations. The problem of flow of two fluids with different density cannot be handled by the analog model. Since it is known (observation wells G and F) that the upward gradient is negligible at least in a portion of the aquifer, the brine, once it has reached the aquifer, will have a tendency, under the influence of gravity, to concentrate in the lower portion of the aquifer. Whether the brine will flow upwards depends largely on the hydraulic gradients. At this time it appears that these gradients may indeed be present in the vicinity of the brine pond near the east dyke. The distribution of the completion zones of the existing observation wells in the aquifer is adequate to define the gradient distribution in the vicinity of the brine pond. This distribution is, however, insufficient for monitoring changes in the hydrochemical environment caused by brine infiltration. This will be discussed in more detail later.

The travel times for brine in the aquifer, arrived at by the various analog model simulations, should be considered as the worst possible case, representing a minimum rather than a maximum value.

CHAPTER 9

Groundwater Chemistry (C. C. Davison and J. A. Vonhof)

INTRODUCTION

An integral part of any study in an area with a potential groundwater pollution problem is the collection of water samples for chemical analysis. Since the representativeness of the chemical analysis of a water sample is not only dependent on the accuracy of the analytical methodology, but is also strongly influenced by the medium to be sampled (groundwater versus surface water), the sampling procedures, and the handling of the samples, a number of studies were conducted over a period of several years to determine the effect of some of these parameters. The major impetus for these studies was the analytical results for samples taken during a series of pump tests (1971) which subsequently froze during storage.

It should be pointed out that the main interest was focused on changes that occur during storage and shipment. It was realized that little or no control could be exercised over the changes that take place in the chemical equilibria in the groundwater during extraction from the aquifer, i.e. the effect of differential pressure gradients across the screen, pump, and discharge point, turbulent flow regimes, etc. However, since the extraction technique did not change during the course of the studies, the sum total of these effects was considered to be constant. Furthermore, it was thought that if the samples for the various studies were taken from the flowing wells in the area, many of the deleterious effects of pumping would be eliminated.

At no time was any sediment observed in any of the discharges from either the pump wells or the flowing wells, and the water samples were as a rule not filtered. Although filtering of water appears to be more and more of a recommended practice (Weyer and Feder, 1978), the effects of filtering on the distribution of the major ions is poorly documented. According to Demayo *et al.* (1978), considerable care must be exercised in the interpretation of the trace metal content of water in filtered samples. Depending on the analytical technique that will be used for the determination of the major cations, considerable variation can be introduced in the concentration of the ions, for example by acidification of the sample (filtrate or raw sample), because the acid can dissolve portions of or all of the suspended materials and various colloids. Filtering of a sample does *not* provide any guarantee that the filtrate is free from suspended and/or colloidal material and as such is of questionable value.

1971 GROUNDWATER SAMPLING PROGRAM

A total of seven observation wells were constructed in January and February of 1971. Subsequent to their completion a pump test was run on each observation well. These tests were conducted in March, 1971. During the pump tests water samples were collected at various times to determine whether any changes took place in the water chemistry. Furthermore, the electric conductivity of the pump discharge was measured continuously. Figure 52 shows an example of the analytical results of the water samples from observation wells A and B. During the pump test, only a slight change was noted in the specific conductance values, however, when the results from the laboratory analyses were received, it was found that the specific conductance values were much lower and that considerable variation in the concentrations of especially bicarbonate and calcium existed. Furthermore, trace element concentrations showed an even greater variation as is shown for iron in Table 11.

Table 11. Iron Concentration (mg/l) in Pump Discharge Water.

Observation well A		Observation well B	
Time (min)	Concentration (mg/l)	Time (min)	Concentration (mg/l)
1	14.6	3.5	13.8
15	3.9	10	4.2
100	3.6	35	3.1
500	0.4	60	0.04
1065	5.9	180	4.3
		335	0.04
		1245	3.7

It should be pointed out that the water samples for trace element analysis were acidified to a pH < 1.5. The magnitude of the variation was puzzling, to say the least, especially if the short duration of the pump test and the type of aquifer were considered. Further checking with the

laboratory revealed that the samples on arrival were in various stages of freezing, from completely to partially frozen. It appeared that the observed variability in the ionic composition was frost-induced and the true concentration of several ionic species could not be determined.

1972 GROUNDWATER SAMPLING PROGRAM

To evaluate further the effect of freezing and to determine which values of the 1971 sampling program could be considered correct, a more extensive study was conducted in the fall of 1972. At the same time unfrozen samples were subjected to temperature cycles and shaken for various time periods to simulate transport and storage. The sources of the water were two flowing wells. The samples collected from each well were all taken within one hour and were divided into five classes. These are

1. Samples kept at a constant temperature of 75°F (23.9°C)
2. Samples subjected to fluctuating daily temperature cycle from 40-75°F (4.4-23.9°C)
   (a) analyzed at 40°F (4.4°C)
   (b) analyzed at 75°F (23.9°C)
3. Samples subjected to shaking and fluctuating daily temperature cycle from 40-75°F (4.4-23.9°C)
   (a) analyzed at 40°F (4.4°C)
   (b) analyzed at 75°F (23.9°C)

Triplicate samples were taken for each class and analyzed in a field laboratory over a consecutive 6-day period.

One triplicate set of samples was analyzed immediately and is referred to as the field value. Also several samples were forwarded to the Western Laboratory, Water Quality Branch, Environment Canada, in Calgary, Alberta. The analyses conducted in the field were calcium, total hardness, alkalinity, iron, and pH, and the method used for analysis is the same as that employed by the Western Laboratory. Concurrent with the above-mentioned program, a large number of samples were frozen and also analyzed over six consecutive days; daily samples of the two wells were collected for immediate analysis. In addition, acidified samples were collected for heavy metal analysis by the Western Laboratory. Some of these samples were allowed to freeze.

The results of the analyses of the samples in the five classes of unfrozen samples from flowing wells 1 and 2 are shown in Figure 53. Only the average value of the analysis of the three samples in each class for each day is plotted in Figure 53. None of the classes show a specific trend, but if the groups of daily results are compared over the 6-day period, a slight decrease in the alkalinity and total hardness values can be detected. No such changes are indicated by the calcium values. These observations show that temperature fluctuations and shaking do not materially change the composition of groundwater samples for the ions analyzed here, but that length of storage time will affect the composition, albeit in a small way, of a groundwater sample.

Figure 53 also shows that the immediate field value is almost always larger than the Calgary Laboratory value. This difference is particularly noticeable for the alkalinity data. In addition, Figure 53 shows that the most significant changes take place in less than a day. Again, this is especially noticeable for the alkalinity data. Although the pH values are not shown in Figure 53, considerable changes were noted between the immediate field value, the consecutive 6 days of field analysis, and the Calgary Laboratory value. Increases of up to 0.3 pH units were noted between the immediate field value and the samples which were analyzed in the field, whereas increases in the order of 0.5 pH units were present between the immediate field sample and the Calgary Laboratory value.

Since it is apparent from Figure 53 that no significant trends are present between the five sample classes, the results of the daily analyses of the samples in each class can thus be regarded as multiple samples from the same population. In other words, the results are a measure of the accuracy of the analytical methods. The ranges of the relative standard deviation (standard deviation x 100/mean value) for daily results over the 6 days of analysis are:

	Flowing well 1	Flowing well 2
Alkalinity	0.4-1.1%	0.3-0.9%
Calcium	1.6-5.4	0.8-2.1
Total Hardness	0.2-2.5	0.4-1.8

The values of the relative standard deviation are in general smaller than those obtained by Carron and Aspila (1978) from round-robin quality control studies. The analytical methods used in the field can therefore be considered relatively accurate.

The results of the daily analyses of the frozen samples are summarized in Figure 54, which also shows the frequency distribution of the analytical results of the frozen and the unfrozen samples. The frozen samples show a much greater degree of scatter than the unfrozen samples, and the analytical results of water samples that have been frozen are unreliable. Since not all the parameters could be checked in the field laboratory, several frozen samples were sent to the laboratory in Calgary. The results of the analyses are shown in Table 12. Table 12 indicates changes for alkalinity, total hardness, and calcium similar to Figure 54. In addition to

these parameters, sulphate also undergoes drastic changes during freezing, whereas sodium, potassium, and chloride are essentially not affected. Therefore the only data that can be salvaged from all the analyses made on the water samples collected during the pump tests in the various observation wells which froze during transport to the laboratory in Calgary are the results on the concentration of chloride, potassium, and sodium ions.

The effect of freezing on acidified samples taken for heavy metal analysis was investigated further in the following controlled experiment. The "sampling flow sheet" is shown in Figure 55. Heavy metal samples were acidified with one of three acids (HCl, HNO_3, or H_2SO_4) to determine whether any one acid had superior preserving qualities for heavy metals. Two sets of samples, one with no air space or full and the other with 25% air space, were collected for treatment with each acid. Each set consists of three bottles. This was done to determine whether the presence of an expansion space (25% air space) during freezing made any difference in the analytical results. For one experiment a complete series of samples consists of 36 prepared samples. Eighteen of these samples were subsequently frozen. Two complete series were collected from two different groundwater sources: flowing well 1 and flowing well 3, respectively.

All samples were analyzed by the Western Laboratory, Water Quality Branch, Calgary.

The prepared water samples were analyzed for Fe, Mn, Zn, Cu, Pb, Cd, and the pH was measured. The results are shown in Figures 56 and 57. The following observations can be made:

Iron

(A) Unfrozen samples: little or no difference between full and "air space" samples (less than 2% for flowing well 1, 3-10% for flowing well 3).

(B) Frozen samples: considerable difference between full and "air space" samples. Considerable difference between full frozen and unfrozen samples.

Little difference between "air space" frozen and unfrozen samples (up to 5%).

Manganese

(A) Unfrozen samples: no difference between full and "air space" samples

(B) Frozen samples: considerable difference between frozen and unfrozen samples for both the full and "air space" samples.

Zinc and Copper

Only trace amounts were present in the two sources, however, it appears that both zinc and copper are best preserved by nitric acid. Their trace distribution in the frozen samples is erratic.

Lead and Cadmium

Neither metal was detected.

All samples were again analyzed approximately 2 weeks later, on January 10, 1973, to determine whether any change had taken place in the heavy metal content. The result of this second analysis is shown in Figures 58 and 59. Except for the manganese values of the frozen samples, no changes were observed. Both the "air space" and full sample values showed changes in the manganese content. The most drastic

Table 12. Major Ion Analyses of Frozen and Unfrozen Samples, Flowing Wells 1 and 2.

	Flowing well 1				Flowing well 2			
	Unfrozen		Frozen		Unfrozen		Frozen	
	Immediate field	Calgary laboratory	Calgary laboratory		Immediate field	Calgary laboratory	Calgary laboratory	
	5/11/72	15/11/72	18/11/72	13/02/73	12/11/72	20/11/72	18/11/72	13/02/73
Spec. cond. (μmhos/cm)	1620	1544	1107	882	2700	2685	2430	2458
pH	7.00	7.80	8.00	8.30	7.85	7.90	8.30	8.30
Ca (mg/l)	196	189	123	78.9	129	129	103	87
Total hardness (mg/l)	733	730	556	403	425	427	344	281
Na (mg/l)		86.5	84	85		421	430	460
K (mg/l)		9.6	9.6	9.2		7.0	6.4	7.0
Alkalinity (mg/l)	515	495	331	169	333	317	239	170
SO_4 (mg/l)		418	377	394		1036	924	1009
Cl (mg/l)		13.8	13.3	14.0		60.9	54.0	61.5

NOTE: All samples were collected at the same time.

change occurred in the "air space" frozen samples. The second set of values approximates the values of the unfrozen samples. Further analyses of these samples for manganese did not show any more changes. No explanation can be given for this phenomenon.

Another set of samples immediately frozen at the time of collection and kept frozen for 2½ months was analyzed March 1, 1973 (Figs. 58 and 59). The results of the analyses are similar to those obtained from earlier frozen samples.

A number of water samples were collected from Bragg Creek in Bragg Creek Provincial Park and from the Bow River at Cochrane. These samples were subjected to the same procedures as the groundwater samples. The only detectable heavy metal present in these waters is lead (Table 13).

Table 13. Lead Content in Frozen and Unfrozen Surface Water Samples.

		Frozen	
	Unfrozen	No air space	25% air space
Bragg Creek at	0.030	0.003	0.027
Bragg Creek,	0.029	0.003	0.019
Alberta	0.027	0.003	0.003
Bow River at	0.012	0.003	0.015
Cochrane,		0.003	0.015
Alberta	0.013	0.003	0.004

As can be seen from Table 13, a similar variability between frozen and unfrozen samples is present in surface water as was found previously for groundwater.

It is obvious both from the major ion and the heavy metal analyses of water samples which froze that the results of such analyses are almost invariably unreliable. The ions that seem least affected by freezing are chloride, potassium, and sodium.

In addition to the experiments on the effect of storage, shipping, and freezing on the ionic content of a water sample, the sources—flowing wells 1 and 2—were also sampled daily for immediate analysis. Flowing well 1 was sampled daily from November 5 to 18, 1972, and flowing well 2 from November 12 to 18, 1972. The results of the daily immediate analyses are shown in Figures 67 and 68. The daily variation in the ionic content of the analyzed parameters is greater than the analytical variability, which therefore suggests that temporal variations exist. The temporal variations were investigated in detail during the summer of 1973, at which time further work was also conducted on analytical variability. The latter experiments were expanded in 1974.

1973 AND 1974 GROUNDWATER SAMPLING PROGRAM

An extensive groundwater sampling program was continued in 1973 and 1974 in order to describe the chemical characteristics of the groundwater flow through the buried valley aquifer in the study area. The main aims of the program were:

1. To establish the spatial distributions of the concentrations of major chemical constituents (Ca, Mg, Na, K, HCO_3, SO_4, Cl), conductance, and pH.
2. To define the probable physico-chemical factors controlling 1.
3. To investigate the temporal variations of the major chemical species, Eh, Fe, and Mn.
4. To define the probable physico-chemical factors controlling 3.
5. From the results of 1-4 to establish the baseline water quality criteria for the aquifer in the study area.

A comprehensive statistical assessment of the experimental errors associated with discrete measurements of the chemical constituents is a prerequisite in any discussion of chemical water quality (Wainerdi and Uken, 1971). This allows one to eliminate the risk of misinterpretation and also to establish the range of statistically probable interpretations these measurements represent. Such a treatment is especially critical in discussions of variations (either spatial or temporal), since random sampling, preservation, or analytical errors may obscure existing natural trends. During this study several quality control experiments were carried out to appraise the importance of these undesired sources of variation.

Sampling Schedule

Figure 60 shows a flowchart representation of the sampling schemes undertaken to measure the major hydrochemical constituents of the buried valley aquifer in the study area. A complete listing of the results of the chemical analyses is given in Appendix V.

Field Methods

Water samples were collected in November 1973 from the seven observation well installations and three flowing wells located in the study area (Fig. 35). The observation wells were pumped with a 4-in. OD (10 cm) submersible pump located immediately above the screened portion of the well, and water samples were collected from the discharge outlet after approximately one hour of pumping.

During the 1974 summer sampling period a manual pump was operated for approximately five minutes to bail air-contaminated water from the observation wells prior to sampling. Water samples were taken from the screened interval of the wells by means of a brass downhole Nansen sampler (capacity one litre) activated from the surface by a weighted messenger. Water samples were taken directly from the well heads at the flowing localities.

Temperature, pH, Eh, and specific conductance were all measured at the sample sites at the time of sampling. Values for pH were determined using a portable, temperature-compensating, Eh-pH meter (Corning model 610 A) and combination pH electrode (Sargent Welch Mfg. Co.). The electrode was calibrated before each measurement with the standard buffer solutions, pH = 7.00 and pH = 4.00. Drifting readings were eliminated by shading the instrument from direct sunlight and equilibrating the electrode with the temperature of a "dummy" solution before immersing the electrode in the "fresh" solution to be analyzed. With proper care, field pH can be measured in well-buffered aqueous samples to a precision of ±0.02 units and an accuracy of ±0.05 units (Langmuir, 1971). During this particular study, calibration with the pH = 7.00 buffer was not made with the buffer at the same temperature as the sample. Instead, the meter was adjusted to read pH = 7.10 when inserted in the pH = 7.00 buffer to compensate for the temperature difference between the buffer and sample solutions.

The Eh of the water samples was measured in the field using a portable Corning model 610 A combination Eh-pH meter, and platinum metal and calomel reference electrodes (Corning Mfg. Co.). The temperature of the electrodes was allowed to equilibrate with that of the sample before a fresh sample was collected for the Eh determination. The fresh sample aliquot was transferred immediately from the wellhead (for flowing wells) or the airtight Nansen sampler (for observation wells) to a measuring beaker containing the Eh electrodes. A plot of the meter-reading versus time allowed the Eh of the sample to be estimated; the lowest reading was taken to represent the best estimate of the Eh of the sample. The measured potentials were converted to Eh by adding the potential of the calomel reference electrode (cre):

$$E^{\circ}_{(cre)} = 0.2415 - [(0.00076)\ (T\text{-}25)\ ]$$

Several other improved methods for measuring the field Eh of anoxic groundwater samples have been reported in the literature (Back and Barnes, 1965; Edmunds, 1970; McNaughton, 1975). In these methods, Eh measurements are made in airtight plastic chambers to eliminate the risk of oxygen being added to the sample. If the samples are transferred to the measuring cell by peristaltic pumps, special precautions must be taken to reduce interference effects such as streaming potentials and external electrical interferences. Minute gas bubbles coating the electrode surfaces can also create interference problems.

Temperature measurements were made in the field at the sampling site with a Fisher brand mercury thermometer calibrated in 0.2°C intervals. The performance of the field thermometer was periodically checked against two identical spare thermometers. Field determinations of specific conductance were made with a portable battery-powered, temperature-compensating conductivity meter (Beckman, RB3). The electrode was calibrated in the field against the standard 0.01 *M* KCl solution (1413 μmhos/cm @ 25°C). Water samples from the observation wells were filtered to remove particulate matter (greater than 2 μm) before being placed in polyethylene sample bottles and saved for further chemical analysis. The water samples collected from the flowing wells were not filtered.

During the summer of 1973, a 2-litre sample was collected daily from flowing well 1 and flowing well 2, so that total alkalinity, total hardness, calcium, and total iron could be determined at a central field laboratory. With these methods the calcium, magnesium, iron, and bicarbonate concentrations of the samples were known within one hour of sampling. Alkalinity was measured by titration with 0.01 *N* H_2SO_4 to the two end points pH 4.2 and 4.5 (Traversy, 1971). Total hardness and calcium were analyzed by titration with disodium ethylenediamine tetraacetate (sodium EDTA) and the appropriate dye indicator: Eriochrome Black T for total hardness; Calver II for calcium (Traversy, 1971). Total iron was determined by the 2,4,6,-tripyridyl-s-triazine (TPTZ) colorimetric method (Traversy, 1971), using a Bausch and Lomb Spectronic 20 colorimeter. These procedures were calibrated daily with laboratory-prepared standards. Replicate aliquots were analyzed routinely and a reproducibility of ±1% - ±2% was established for each technique. In addition to the daily sampling of wells, a 2-litre sample for wet analysis and a 250-ml sample for atomic absorption spectrophotometry were collected once a week from flowing well 1 and flowing well 2 and shipped to the Western Laboratory in Calgary for complete analysis. Two ml conc. HNO_3 was added to the 250-ml sample (for atomic absorption spectroscopy analysis) to guard against chemical precipitation during storage.

During the summer of 1974 a compact single-beam atomic absorption unit (Jarrell-Ash: Dial Atom II), with a single-slot premix burner head, was installed at the central field laboratory to complement the wet analytical techniques. Wet techniques were used to determine Ca, Mg, and HCO_3 concentrations; Ca, Mg, Na, K, Fe, Mn, SO_4 and

Cl concentrations were analyzed by atomic absorption spectroscopy (AAS) techniques. Standard solutions for AAS analyses were prepared beforehand in a Calgary laboratory and checked against U.S. Geological Survey Standard Reference Water Samples. Water samples for field AAS determinations were prepared with the addition of 0.6 ml conc. HNO_3 per 100 ml to normalize both the samples and standards. Na, K, Fe, and Mn were analyzed by AAS following the methods of Kahn (1968) and Fishman (1966) in conjunction with "Atomic Absorption Analytical Methods" supplied with the Jarrell-Ash spectrophotometer. Cl and SO_4 were determined by indirect AAS techniques (Dunk *et al.*, 1969). A detailed description of these indirect AAS methods is presented in Appendix VI. Careful Standard Addition techniques (Barefoot, written comm.) were adopted to detect and correct for matrix interference effects in the determination of both Ca and Mg (Angino and Billings, 1972). Appendix VII outlines the main features of the Standard Addition Method. Rapid and accurate dilutions for AAS methods in the field laboratory were made with disposable micropipette and macropipette systems (accurate to ±0.1% of total volume). Small disposable plastic pharmaceutical vials were used to prepare samples for analysis.

Laboratory Methods

Samples sent to the Western Laboratory in Calgary were analyzed for pH, specific conductance, Ca, Mg, Fe, Mn, Na, K, HCO_3, SO_4, Cl, and SiO_2. Ca and Mg concentrations were determined by EDTA complexometric titration methods; Fe and Mn were determined by AAS; Na and K determinations were carried out by automated flame photometric techniques; HCO_3 was determined by titration with a standard acid to the double end points pH 4.5 and pH 4.2; SO_4 was determined by barium chloride titration using Thorin as an indicator; Cl determinations were carried out by an automated thiocyanate method; and SiO_2 was determined by automated heteropoly blue method (Traversy, 1971). Ideally, in a complete and correct chemical analysis of a sample, the sum of the anions in milliequivalents per litre (meq/l) should be equal to the sum of the cations in milliequivalents per litre. Complete laboratory analyses which had a cation-anion difference (in meq/l) greater than 5% of the sum of cations and anions (in meq/l) were rejected because of the possibility of significant analytical inaccuracies (Hem, 1970).

Sample Preservation During Storage

Preservation of the chemical character of water samples during storage prior to laboratory analysis is of prime concern, especially when dealing with groundwater samples. Groundwater can be highly enriched in CO_2 (up to 10 to 100 times atmospheric equilibrated sample concentrations), and CO_2 losses from the sample to the atmosphere during periods of storage can result in a pH increase in the sample, according to the reactions

$$CO_2 + H_2O \rightleftarrows H_2CO_3 \rightleftarrows HCO_3^- + H^+$$

Increases in pH of up to 1.0 pH unit have been recorded in groundwater samples after a few weeks of storage (Robertson *et al.*, 1963; Davison, 1974, 1976). Figures 61 and 62 illustrate the pH and pCO_2 changes occurring as a result of CO_2 losses during storage in water samples from flowing wells 1 and 2 (FW1 and FW2). Increases of pH can result in extreme supersaturation of the sample with respect to carbonate mineral phases (Fig. 63), and precipitation of these phases can occur during storage if proper preservation techniques are not used. To evaluate this possibility a group of samples from FW1 and FW2, which had been stored unpreserved for 3 months in polyethylene bottles at ambient temperature, were tested to determine whether significant amounts of Ca or Mg carbonate had precipitated during storage. Appendix VIII briefly outlines the experimental procedure. The results of this experiment, which are summarized in Table 14, reveal that for these water samples large quantities of Ca (up to 60% of the total) had precipitated, presumably as calcite, during the 3-month storage period. Only minor amounts of Mg (up to 1.6 ppm) had precipitated after the storage period. There is a direct correlation between the Ca and Mg results; the samples which indicated the greatest losses of Ca also indicated the greatest losses of Mg. Clearly, standard EDTA complexometric analysis of these samples would yield underestimates for Ca concentrations. Sekerka and Lechner (1974) have also observed Cu, Ag, and Hg losses owing to precipitation in unacidified aqueous samples.

Chemical Equilibria

Calculations of inorganic equilibria and ionic speciation for individual water analyses were done using a Fortran IV version of the computer program WATEQ (Truesdell and Jones, 1974; Plummer, 1972) and a revised version of the program WATEQF (Plummer, 1975). WATEQF was designed for treating water samples from low-temperature aqueous environments (0-50°C); if equilibria at higher temperatures are to be considered (up to 350°C), the computer program SOLMNEQ should be employed for the calculations (Kharaka and Barnes, 1973).

For any given chemical reaction

$$aA + bB \rightleftarrows cC + dD + ne^-$$

where a, b, c, and d are the stoichiometric coefficients of the chemical species A, B, C, and D respectively and n is the

Table 14. Summary of Sample Bottle – Sample Solution Analysis, Unacidified Groundwater Samples.

Sample No.	Sample bottle*	Filter paper,† 0.45 μm	Sample solution‡	Total§
Distribution of Ca				
FW1-1	0.92 (37)	0.01 (0.4)	2.32 (93)	3.24 (130)
FW1-2	1.40 (56)	0.01 (0.4)	2.15 (86)	3.54 (142)
FW1-3	0.72 (29)	0.08 (3.2)	2.42 (97)	3.24 (130)
FW2-1	1.37 (55)	0.03 (1.3)	0.97 (39)	2.37 (95)
FW2-2	0.70 (28)	0.01 (0.6)	2.02 (81)	2.74 (110)
FW2-3	0.27 (11)	0.01 (0.6)	2.10 (84)	2.40 (96)
Distribution of Mg				
FW1-1	0.05 (1.3)	0.05 (1.1)	2.18 (53)	2.28 (55)
FW1-2	0.07 (1.6)	0.03 (0.8)	2.34 (57)	2.44 (59)
FW1-3	0.04 (0.9)	0.50 (1.1)	2.30 (56)	2.40 (58)
FW2-1	0.05 (1.2)	0.01 (0.2)	0.95 (23)	1.01 (24)
FW2-2	0.02 (0.4)	0.01 (0.2)	0.99 (24)	1.02 (25)
FW2-3	0.01 (0.3)	0.01 (0.2)	1.07 (26)	1.09 (27)

NOTE: All concentrations expressed as millimoles per litre, within parentheses as parts per million.
*Sample solution removed; bottle rinsed with double-distilled H_2O and precipitate dissolved with conc. HNO_3.
†Sample solution filtered through 0.45 μm; filter paper washed in conc. HNO_3.
‡Sample solution <0.45 μm.
§Sample bottle + filter paper + sample solution = total.

number of electrons, e^-, involved in redox reactions, there is a corresponding mass-action equation given by

$$K = \frac{[C]^c\ [D]^d\ [e^-]^n}{[A]^a\ [B]^b}$$

K is termed the mass balance constant or "equilibrium constant" of the reaction and the square brackets indicate activities of the chemical species (Garrels and Christ, 1965).

The values and sources of the equilibrium constant used in the WATEQF calculations are listed in a report by Davison (1976). When data for the equilibrium constant of a given chemical reaction are available at more than one temperature, the equilibrium constant may be expressed either by a power function of the absolute temperature, T,

$$\log K = A + BT + C/T + D \log T$$

where A, B, C, and D are constants; or by the van't Hoff equation,

$$\log K = \log k_{Tr} - \frac{H_{Tr}}{2.3}\left(\frac{1}{T} - \frac{1}{Tr}\right)$$

in which Tr is the reference temperature (Truesdell and Jones, 1974). The latter expression is used when experimental equilibrium constants are known over a wide range of temperature conditions. Davison (1976) lists the expressions of this form used in WATEQF. The van't Hoff relation is a linear interpolation used to estimate the equilibrium constant when its value at 25°C and $H_1°$ are known.

Solid Phase Equilibria

The degree of equilibrium of a particular solid mineral phase with an aqueous solution (i.e. $AX_{(s)} \rightarrow A^+_{(aq)} + X^-_{(aq)}$) can be expressed as a saturation index, denoted SI (Wigley, 1971):

$$SI_{mp} = \log \frac{IAP}{K_{sp}}$$

where mp denotes the particular mineral phase, IAP is the ion activity product in the solution (i.e. $[A^+]X\ [X^-]$), and k_{sp} is the equilibrium constant or "solubility product" of the particular mineral phase. An SI (saturation index) of 0.0 indicates that the solution is exactly saturated with respect to the mineral phase, mp; a positive SI implies that the solution is supersaturated with respect to the mineral phase; a negative SI indicates undersaturation. WATEQF is capable of calculating the degree of saturation for 99 different mineral phases.

Spatial Distribution of Major Constituents

In November, 1973, all the observation wells and flowing wells in the study area were sampled to determine the spatial distribution of the major chemical constituents in the aquifer. Temperature, pH, and specific conductance were measured in the field at the time of sampling using the techniques outlined previously. The water samples were shipped in tightly capped 2-litre polyethylene bottles to the Western Laboratory, Water Quality Branch, in Calgary for subsequent chemical analysis. The laboratory analyses of the samples, recorded in Table 15, were completed within one month of sampling.

Table 15. Major Ion Analyses for November 1973 Groundwater Samples.

Well No.	Ca	Mg	Na	K	SO_4	HCO_3	Cl	pH*	-log pCO_2	Spec. cond. (μmhos/cm)
OWE_s	4.9	2.4	2.5	0.23	3.3	9.4	0.3	6.9	1.28	1360
OWC_s	5.1	2.0	3.8	0.23	4.0	9.5	0.5	7.0	1.38	1540
OWG_s	5.2	2.5	3.4	0.23	3.5	9.1	0.5	7.0	1.39	1500
OWF_d	5.1	2.9	11.2	0.26	7.1	11.8	1.4	7.1	1.39	2280
FWI_s	4.8	2.8	3.7	0.23	4.6	9.5	0.4	6.9	1.28	1480
OWD_s	4.9	2.7	2.5	0.23	3.3	9.4	0.3	7.0	1.38	1540
Uncertainty†	±0.7	±0.6	±0.4	±0.04	±0.6	±1.2	±0.2	–	–	–
OWB_s	4.8	2.9	3.4	0.23	3.9	9.4	0.5	6.8	1.18	1520
OWC_s	5.1	2.8	3.8	0.23	3.9	9.5	0.5	7.0	1.38	1540
OWA_s	5.5	3.0	3.9	0.24	3.5	9.8	1.2	6.8	1.17	1790
$FW2_d$	3.4	1.0	20.4	0.18	10.8	6.6	1.7	7.5	2.04	2640
Uncertainty†	±0.4	±0.6	±2.1	±0.01	±1.0	±0.7	±0.1	–	–	–
$FW3_i$	5.4	3.1	5.8	0.25	5.9	10.8	0.7	7.0	1.33	1930

NOTE: All concentrations expressed as millimoles per litre.
*pH and specific conductivity measured in the field.
†Uncertainty expressed as 2-S of laboratory analyses for 1973 and 1974 sampling periods.
s = shallow
d = deep
i = intermediate

The water samples from the wells in the shallow portion of the aquifer were chemically similar: pH = 6.8-7.0, specific conductance = 1350-1790 μmhos/cm, Ca = 4.8-5.5 mmoles/l, Mg = 2.0-3.0 mmoles/l, Na = 2.5-3.9 mmoles/l, K = 0.23-0.24 mmoles/l, HCO_3 = 9.1-9.8 mmoles/l, SO_4 = 3.3-4.6 mmoles/l, and Cl = 0.3-1.2 mmoles/l.

Compared with the samples from the shallow wells, the samples collected from the two deep wells (OWF and FW2) contained much higher concentrations of Na, SO_4 and Cl. Water from FW2 had a lower concentration of Ca, Mg, and HCO_3 than the shallow wells. The HCO_3 content of the sample from OWF was significantly higher than that in the samples from any of the other wells. FW3 is completed at an intermediate depth in the aquifer. The ionic concentration of the water of this well is higher than that of the shallow wells, but lower than that of the deep ones. Both Na and SO_4 show a higher concentration compared with the shallow wells.

Speciation and Mineral Equilibria

Calculations of the species distribution and degree of saturation with respect to stoichiometric mineral phases were carried out for all of the wells sampled during November, 1973, using a modified version of WATEQF. The effects of ion pairing and complexing were accounted for in all of the calculations. The species distribution for each sample based on the major ion analyses is presented by Davison (1976). Table 16 contains a summary of the mineral saturation results.

Almost all of the samples were saturated with respect to calcite ($CaCO_3$), dolomite ($CaMg(CO_3)_2$), silica gel (SiO_2 — amorphous). All of the samples were undersaturated with respect to gypsum ($CaSO_4$). The samples taken from the wells in the deeper portions of the aquifer were nearer to gypsum saturation than the samples from the shallow wells (Table 16).

Table 16. Summary of Chemical Saturation, November 1973 Groundwater Samples, from WATEQF (No Fe, Mn, or Eh data).

Piezometer	$^*SI_C$	SI_D	SI_G	SI_{SILG}
OWE	0.0	-0.4	-0.9	-0.10
OWC	0.1	-0.1	-0.8	-0.07
OWG	0.1	-0.2	-0.8	-0.07
OWF	0.2	0.1	-0.6	-1.10
FW1	-0.1	-0.4	-0.8	-0.04
OWD	0.1	-0.1	-0.9	-0.10
Uncertainty†	±0.10	±0.30	±0.10	–
OWB	-0.1	-0.5	-0.8	-0.10
OWC	9.1	-0.1	-0.8	-0.07
OWA	-0.1	-0.4	-0.9	-0.07
FW2	0.1	-0.3	-0.7	-0.07
FW3	0.1	0.0	-0.7	-0.10

$^*SI_{mp} = \log \frac{IAP}{K_{sp}}$

$SI_{mp} = 0 (\pm \text{uncertainty}) \rightarrow$ saturation

$SI_{mp} > 0 \rightarrow$ supersaturation

$SI_{mp} < 0 \rightarrow$ undersaturated

C = calcite, $CaCO_3$

D = dolomite, $CaMg(CO_3)_2$

G = gypsum, $CaSO_4$

SILG = silica gel, SiO_2 (amorphous)

†Uncertainty based on analytical and storage variation in determinations of Ca, Mg, HCO_3 and SO_4.

Chemical Processes Occurring within the Aquifer

The main spatial chemical characteristics of the groundwater in the aquifer are illustrated in Figures 64, 65, and 66. The concentrations of the total dissolved constituents, Na, SO_4, and Cl, increased with increasing depth in the aquifer and increasing distance along the groundwater flow path. Figure 66, which is a modified Piper plot of the data (after Edmunds, 1970), suggests a linear trend from Ca–Mg–HCO_3 type water in the shallow portion of the aquifer to more concentrated Na–SO_4 type water at depth. This trend in water chemistry with depth has been observed in many other groundwater flow systems in southeastern Saskatchewan and southwestern Manitoba. A number of concurrent chemical reactions have been suggested to account for the chemical evolution of such groundwaters (Rutherford, 1966; Cherry, 1972). These are:

1. Sequential dissolution of calcite and dolomite under high pCO_2 conditions encountered in the soil zone during groundwater recharge. This could generate a Ca-HCO_3 dominated water with minor amounts of Mg.
2. Dissolution of minor amounts of halite NaCl as a source of Cl present in the groundwaters.
3. Dissolution of minor amounts of highly soluble sulphate minerals such as gypsum, epsomite ($MgSO_4 \cdot 7H_2O$), mirabilite ($Na_2SO_4 \cdot 10H_2O$), or thenardite (Na_2SO_4) to yield Mg, Ca, Na, and SO_4 ions.
4. Exchange of Ca and Mg for exchangeable Na or K on montmorillonite clays.

To test whether these mechanisms could generate the chemical pattern observed in the described groundwater flow systems, various solutions to the defining mineral dissolution, cation exchange, and mass balance equations were attempted. The results indicated that the chemistry of the groundwater at all the sampling locations except for OWA could be generated by:

1. Dissolution of halite
2. Dissolution of gypsum
3. Exchange of Mg and Ca for exchangeable Na and K on montmorillonite clays
4. Dissolution of calcite and/or dolomite.

The following example illustrates the computations involved.

The water analysis for the sample from OWE is:

Ca_A	= 4.9 mmoles/l	HCO_{3A}*	= 9.4 mmoles/l
Mg_A	= 2.4 mmoles/l	SO_{4A}	= 3.3 mmoles/l
Na_A	= 2.5 mmoles/l	Cl_A	= 0.3 mmoles/l
K_A	= 0.2 mmoles/l	pH	= 6.9

*Subscript A denotes water analysis.

Step I Assume that all the chloride comes from halite (H) dissolution,

$$NaCl_{(halite)} \rightleftarrows Na_H + Cl_H$$
$$Cl_A = Cl_H$$
$$\therefore Na_H = Cl_H$$
$$\text{i.e. } 0.3\ NaCl \rightleftarrows 0.3\ Na_H + 0.3\ Cl_H$$

Step II Assume that the remaining sodium and potassium come from cation exchange (CE) for calcium and magnesium on montmorillonite clays,

Sodium and potassium available from CE is:

$$Na_A + K_A - Na_H = (Na + K)_{CE}$$
$$\text{i.e. } 2.5\ Na_A + 0.2\ K_A - 0.3\ Na_H = 2.4\ (Na + K)_{CE}$$

Step III Assume that all sulphate comes from gypsum (GYP) dissolution,

$$CaSO_{4\,(gypsum)} \rightleftarrows Ca_{GYP} + SO_{4\ GYP}$$
$$SO_{4A} + SO_{4GYP}$$
$$\therefore Ca_{GYP} = SO_{4A}$$
$$\text{i.e. } 3.3\ CaSO_4 \rightleftarrows 3.3\ Ca_{GYP} + 3.3\ SO_{4GYP}$$

Step IV Calcium and magnesium available from calcite/dolomite (CAL/DOL) dissolution is equal to the total calcium plus magnesium before cation exchange minus the calcium contributed by gypsum dissolution,

$$(Ca + Mg)_{CAL/DOL} = Ca_A + Mg_A + (Ca + Mg)_{CE} - Ca_{GYP}$$
$$\text{i.e. } 4.9\ Ca_A + 2.4\ Mg_A + 1.2\ (Ca + Mg)_{CE} - 3.3\ Ca_{GYP} = 5.2\ (Ca + Mg)_{CAL/DOL}$$

Step V In order to maintain a near-neutral pH during calcite/dolomite dissolution,

$$2(Ca + Mg)_{CAL/DOL} = HCO_{3\,CAL/DOL}$$
$$\text{i.e. } 2 \times 5.2\ (Ca + Mg)_{CAL/DOL} = 10.4\ HCO_{3\,CAL/DOL}$$

Step VI Compare $HCO_{3\,CAL/DOL}$ with HCO_{3A}

$$\text{i.e. } HCO_{3\,CAL/DOL} = 10.4 \text{ mmoles/l}$$
$$HCO_{3A} = 9.2 \text{ mmoles/l}$$

Within the uncertainties of the analyses the calculated $HCO_{3\,CAL/DOL}$ equals HCO_{3A} for OWE.

Similar calculations for the other sample localities in the aquifer yield $HCO_{3\,CAL/DOL}$ values approximately equal to the HCO_{3A} measured in the sample (Table 17). It is very likely that an even better correlation would have been obtained if the bicarbonate concentrations had been measured in the field.

Table 17. Comparison of Calculated Bicarbonate ($HCO_{3CAL/DOL}$) and Analyzed Bicarbonate (HCO_{3A}) Concentrations for November 1973 Groundwater Samples.

Sample location	OWA	OWB	OWC	OWD	OWE	OWG	FW1	FW3	OWF	FW2
$HCO_{3CAL/DOL}$	13.0	10.8	11.1	11.1	10.4	11.5	10.6	10.6	12.4	6.0
HCO_{3A}	9.8	9.4	9.5	9.4	9.4	9.1	9.5	10.8	11.8	6.6

NOTE: Concentrations expressed in millimoles per litre.

$HCO_{3CAL/DOL}$ = bicarbonate concentration predicted assuming the excess Ca + Mg (after stoichiometric gypsum dissolution and cation exchange) is contributed from calcite/dolomite dissolution.

HCO_{3A} = analyzed bicarbonate concentration.

A prerequisite to this hypothesis is the availability of gypsum and halite in the till and/or aquifer materials. Cherry (1972) has postulated that if such minerals exist in the tills of the prairies, they could have been emplaced by the mobilization of deep-seated brines during the excessive loading of Pleistocene glaciation.

Although this theory offers a possible source for the gypsum and halite, a much simpler explanation can be reached if the sediments in the area (and for that matter in most of the Western Plains) are considered in combination with the setting of the aquifers in the hydrogeological environment. It is a well-known fact that the bulk of the till material is locally derived and the till composition reflects the underlying or nearby strata (Pawluk and Bayrock, 1969). It is also well known that the bedrock sediments in most of southern Saskatchewan were deposited in a marine and/or brackish water environment. These sediments comprise mainly clays and silts and have a varying organic matter and sulphide mineral content. Examination of drill cuttings and cores of these sediments from various parts of the province showed the presence of sulphide minerals and their weathering product: gypsum. It would therefore be logical to assume that since the bulk of the sediment in the till is derived from the bedrock, the sulphate ions were derived from dissolution of dispersed gypsum and/or from the weathering of sulphide minerals. Furthermore, oxidation of organic sulphides would also add to the sulphate ion content. A similar origin for the sulphate ions in groundwater is also proposed by Wallick and Krouse (1977). In addition, many buried valley aquifers straddle the contact between the bedrock and the overlying Pleistocene deposits as is, for example, the case in the study area. In such instances there is a direct contribution to the groundwater from the bedrock.

The existence of gypsum in tills and soils has been documented by several authors, for example, Rozkowski (1967), Pawluk and Bayrock (1969), Maclean and Pawluk (1975), and Christiansen (1968b).

As was pointed out before, the groundwater chemistry in OWA differs from that of the other shallow wells in that the Cl content is higher (Fig. 65). Because of the proximity of OWA to the brine pond it was originally thought that this indicated subsurface brine migration, especially since a small brine seep is present in the dyke just north of OWA. However, the results of subsequent sampling programs show much lower Cl values, similar to the other shallow wells. It is therefore likely that the higher Cl value in the November 1973 sample is external in origin (analytical error, bottle contamination, etc.).

The linear trend apparent on the modified Piper plot of the major ion content of the groundwaters in the study area suggests that the mixing of groundwaters of differing composition in the aquifer could also be responsible for the observed chemical pattern (Fig. 66). Included on this diagram are some chemical analyses from shallow wells in the till in the vicinity of the study area (Rutherford, 1966). It seems likely that older concentrated $Na-SO_4-Cl$ waters migrating from underlying formations may be mixing in the aquifer with younger dilute $Ca-HCO_3$ waters produced by the sequential dissolution of calcite and dolomite during vertical recharge through the overlying till. Meneley (1970) has observed a similar mixing of chemically distinct waters in the Tyner Valley buried aquifer system near Saskatoon, Saskatchewan. Here, younger $Ca-Mg-HCO_3$ water, which is recharged through the overlying glacial till, appears to be mixing in the aquifer with older $Na-SO_4-Cl$ water entering horizontally from another formation.

Temporal Distribution of Dissolved Constituents

A preliminary appraisal of the chemical analyses of samples collected periodically from two flowing wells in the study area (FW1 and FW2) revealed significant chemical fluctuations with time. Several investigators have reported significant temporal variations in the water chemistry of various groundwater flow systems which can be related to (1) rapid groundwater transit after recharge in shallow flow systems (Jacobson, 1973; Hoag, 1975); (2) natural or artificial fluctuations of the water table into and out of weathering profiles (Bergstrom, 1974); and (3) mixing of waters of differing chemistries in highly pumped aquifers (Fritz *et al.*, 1974). To establish the significance of tem-

poral variations in the aqueous chemical constituents of the aquifer in this study, samples were collected daily from the two flowing wells FW1 and FW2 for a 2-week period in November, 1972, and daily from FW1 and FW2 for 3 months during the summer of 1973. Samples were taken at approximately the same time each day (within an hour) to eliminate the effects of diurnal chemical variations. FW1 is set into the top 5 ft of the aquifer and FW2 is set into the bottom 5 ft of the aquifer. Eh, pH, temperature, and specific conductance were measured immediately in the field, and Ca, Mg, Fe, and HCO_3 were determined in the field laboratory within ½ hr of sampling. Determinations were done in triplicate to achieve a maximum uncertainty of ±2% for these methods. Details of the sampling and analytical techniques have been outlined previously. The results are presented in Figures 67 and 68. Concurrent hydrographs and precipitation records are included with the chemical data for comparison.

(a) Flowing Well 1

Throughout the month of November, 1972, the pH, Eh, Ca, Mg, and HCO_3 levels varied in the groundwater issuing from FW1. Levels of Ca, pH, and HCO_3 gradually increased during the monitoring period, whereas Eh and Mg decreased during the same period (see Fig. 67). No systematic variations were observed in the specific conductance or the Fe levels for this period. The water levels in the observation wells in the aquifer declined continuously during the month of November ($\Delta H = 0.20$ ft).

A large storm occurred early in the sampling period of the summer of 1973 (June 2-4), which induced a distinctive peak in the well hydrographs of the study area. Although some of the chemical records are sparse for this early period (i.e. Eh and Mg), it is possible to relate a response in pH, Ca, Fe, and HCO_3 to this storm event. The pH of the water in FW1 rose sharply to a peak (from pH = 7.0 to pH = 7.3) 2 days after the well hydrograph had peaked. Levels of Ca and HCO_3 in the water rose gradually and both peaked approximately 10 days after the storm. The Fe content of the well water increased sharply 15 days after the storm (from 5.5 ppm to 7.0 ppm); these high iron levels were only observed for a period of 3 days, whereupon the iron content of the well water returned to its original level. Throughout the remainder of the summer of 1973 there were no further major variations in either the hydrograph record or the pH, Ca, Mg, Fe, or HCO_3 records. The pH declined until the latter part of June (pH = 6.9) and then began to increase gradually (except for some minor perturbations) during the rest of the summer (up to pH = 7.25). Ca and HCO_3 levels decreased slightly, Mg levels increased slightly, and the Fe content remained fairly constant during the rest of the summer monitoring period. Specific conductance measurements for FW1 showed no apparent response to the intense storm in early June. However, the specific conductance level gradually declined until mid-July (from 1400 μmhos/cm to 1250 μmhos/cm) and then rose sharply back to its original level, with no apparent relationship to any of the other measured constituents. This pattern is paralleled by the specific conductance record for FW2 during the same period (Fig. 68). Since continuous calibration of the conductivity probe during the monitoring period did not reveal any instrument problems, probe poisoning or power supply fluctuations can be ruled out as possible causes of these variations. Variations in Na, SO_4, and Cl (which were not analyzed for) may be responsible for the specific conductance variations observed in FW1.

Although the reliability and thermodynamic significance of Eh measurements in natural environments is a debated topic, some workers feel that meaningful Eh values can be obtained in certain well-poised environments (Langmuir, 1971; Whitfield, 1974). For instance, the presence of moderate quantities of Fe or Mn (i.e. Fe > 1 ppm) near neutral pH can induce stable and meaningful measurements (Langmuir, 1971). These requirements exist in the groundwater of this study.

The Eh values for FW1 describe a regular trend during the summer of 1973. Two distinctive maxima peaks occur: one in late June, and the other in mid-August. This temporal variation in Eh for FW1 does not seem to be related to variations of other constituents. One would expect fluctuations in the iron levels of the water in response to such dramatic Eh variations (up to 100 mV). If the Eh measurements actually represent natural redox conditions, it is possible that the observed variations were induced either by other organic or inorganic reactions.

(b) Flowing Well 2

Daily measurements of pH, Eh, specific conductance, Ca, Mg, Fe, and HCO_3 for water issuing from FW2 during the summer of 1973 are presented in Figure 68. The pH level remained fairly constant throughout the 3-month observation period (7.55 ± 0.5), although slightly higher values occurred early in June and in mid-July (7.70). The Ca content of the water from FW2 increased in early June (from 125 ppm to 145 ppm), gradually decreased until the beginning of July (120 ppm) and then increased again during the rest of the 1973 monitoring period (up to 130 ppm). The Mg content of the water was highest at the beginning of the monitoring period (40 ppm) and it gradually declined throughout the rest of the summer (down to 35 ppm). Levels of HCO_3 climbed slightly until early July (from 400 ppm to 410 ppm) and then gradually declined throughout July and August (down to 390 ppm).

The Ca in FW2 seemed to respond to the intense storm that occurred in early June, and the Ca peaked approximately 10 days after the well hydrograph peaked. None of the other measured constituents responded noticeably to the storm influence however.

The Fe level in FW2 rose sharply late in June (from 3.2 ppm to 5.5 ppm), remained high until the end of July, and then dropped sharply to the previous level. The Eh trend for FW2 seems to parallel the Fe trend closely for the greater part of the summer (with the exception of August), with low Eh levels corresponding to high Fe levels. During mid-July (starting July 15) the specific conductance, Eh, and Fe levels in FW2 responded suddenly and simultaneously. The hydrostatic pressure within the aquifer also began to increase at this time, suggesting that the aquifer was being recharged. Direct rainfall infiltration can be ruled out as a likely recharge mechanism, since the mid-summer months are characterized by sparse rainfall and high evapotranspiration. The fact that the changes in water chemistry of the deeper portion of the aquifer and this recharge event occurred simultaneously, whereas the chemistry of the shallow portion of the aquifer had no similar response to this hydrodynamic event, seems to suggest that the source of this recharge is a deeper groundwater flow system. This observation also lends support to the mixing hypothesis discussed earlier.

(c) Ferric Oxyhydroxide Stability

Maximum and minimum field values of Eh were used to calculate the effect of Eh variations on the ferric-oxyhydroxide stability relationships in the groundwaters under investigation. Ferric-oxyhydroxide stability was calculated manually by the pQ method (Langmuir and Whittemore, 1971) using measured Eh, pH, Fe, and SO_4 values for FW1 and FW2.

The pQ is given by

$$pQ = (E^\circ - Eh) / 1.9842 \times 10^{-4}\, T - \log Fe^{2+} - 3(\log K_w + pH)$$

where $E^\circ = -1.226 \times 10^{-3} + 4.147 \times 10^{-3}\, T - 5.111 \times 10^{-6}\, T^2$ volts,

K_w = solubility of water = $[H^+][OH^-]$, and
$T = {}^\circ K$.

At 7°C, $E^\circ = 0.7482$ volts and $K_w = 10^{-14.63}$. The calculated pQ is compared with the logarithm of the solubility product denoted pK_{sp}, for the reactions

$$Fe(OH)_3 \text{ (amorphous)} \rightleftarrows Fe^{3+} + 3OH^-;\ pK_{sp} = +36.0^* \text{ @7°C}$$

$$\text{a-FeOOH (goethite)} + H_2O \rightleftarrows Fe^{3+} + 3OH^-;\ pK_{sp} = +42.75^* \text{ @7°C}$$

*calculated from $pK_{sp} = pK_T + H^\circ_{298} + \dfrac{C^\circ P_{298}\,(T - 298.15)}{4.5757}\left[\dfrac{1}{298.15} - \dfrac{1}{T}\right]$

If the calculated pQ falls within the range 36.0 → 42.8, the concentration of iron in the groundwater and the Eh are likely controlled by the oxyhydroxide phase. Low pQ values in this range suggest control by an amorphous oxyhydroxide phase; higher pQ values suggest control by a more crystalline phase.

Table 18 lists the results of the pQ calculations for the range of Eh observed in samples from FW1 and FW2 during

Table 18. pQ Calculations for Eh Range Observed in Flowing Wells 1 and 2 during 1973-1974.

Date	Eh	pH	Fe_{TOT}	$[FeOH^+]$	$[FeSO_4^0]$	$[Fe^{2+}]$	pQ*
			Flowing well 1				
10-7-73	−30 mV	7.06	1.06	0.05	0.14	0.48	41.0
9-8-73	+40 mV	7.16	1.02	0.05	0.12	0.47	39.5
10-7-74	+60 mV	6.85	1.04	0.05	0.13	0.48	40.0
16-8-74	+18 mV	6.74	0.91	0.04	0.11	0.41	38.2
			Flowing well 2				
10-7-73	−74 mV	7.60	0.88	0.03	0.22	0.32	40.4
24-7-73	−30 mV	7.60	0.61	0.02	0.15	0.22	39.8
10-8-74	+129 mV	7.47	0.59	0.02	0.15	0.21	37.3
10-7-74	+20 mV	7.30	0.65	0.02	0.16	0.23	39.7

NOTE: All concentrations expressed as 10^{-4} mol/l.

Eh and pH measured immediately in the field.

Fe_{TOT} from chemical analyses.

$[FeOH^+]$, $[FeSO_4^0]$ and $[Fe^{2+}]$ from WATEQF calculations for complete chemical analyses.

*$36.0 \leq pQ \leq 42.5$ implies control by a ferric oxyhydroxide phase.

this study. $[FeOH^+]$, $[FeSO_4^0]$, and $[Fe^{2+}]$ were determined using activity coefficients for the species from WATEQF and

$Fe^{2+} + H_2O \leftrightarrows FeOH^+ + H^+; K_{eq} = 10^{-8.30}$ (Langmuir and Whittemore, 1971)

$Fe^{2+} + SO_4^{=} \leftrightarrows FeSO_4^0; K_{eq} = 10^{2.20}$ (Izatt *et al.*, 1969)

All the pQ values for FW1 and FW2 were observed to fall within the ferric-oxyhydroxide stability range ($36.0 \leq pQ \leq 42.8$) despite the large variation in Eh (and pH) values measured for these wells (Table 18).

ERROR ANALYSIS

Introduction

Sampling errors, inadequate sample storage and preservation techniques, analytical errors, inaccurate dissociation constants and inaccuracies in the calculation of activity coefficients can result in errors in the calculations of chemical equilibria and the distribution of chemical species. Sampling errors refer to those errors introduced either by the contamination of the sample at the time of sampling or the sampling of an inhomogeneous population. Wells and springs that intersect more than one chemical type of water, piezometers and wells that are inadequately flushed out prior to sampling, and sampling stations that are subject to temporal chemical variations can exhibit significant sampling error.

Groundwater samples are often particularly susceptible to changes in the pressures of O_2 and CO_2, and improper sample storage and preservation techniques can result in a chemical alteration of the sample as it adjusts to new equilibrium conditions. For instance, during this study, the pH levels in groundwater samples have been observed to increase up to 1.0 pH unit owing to CO_2 escape to the atmosphere during storage. This often results in supersaturation of the sample with respect to carbonate mineral phases; losses of dissolved species because of precipitation would therefore be expected in unpreserved samples. The preservation techniques should also be chosen to comply with the analytical techniques used. If, for example, the samples are to be analyzed by atomic absorption spectroscopy techniques, the sample matrix should closely approximate the matrix of the standards that are to be used. This can be accomplished by the normalization of both the samples and AAS standards with a predetermined volume of reagent grade acid (either HCl or HNO_3).

Among the remaining sources of error, analytical error is probably the most significant source of error in calculations of mineral solubilities and chemical speciation for the major chemical constituents in groundwater samples (Merino, 1975). Two factors can contribute to analytical errors: inaccuracy and analytical variability.

Analytical Inaccuracy

Analytical inaccuracy (constant error or bias) refers to those errors which have the same magnitude and sign throughout a series of observations. Analytical inaccuracy in the determination of the major chemical constituents in aqueous solutions is often the result of faulty standards or improper analytical technique. Interlaboratory quality control studies which have been carried out in the United States and Canada indicate that large inaccuracies can exist in the standard analysis of many major chemical constituents (Robertson *et al.*, 1963; Traversy and Wales, 1970; Skougstad, 1975; Carron and Aspila, 1978). Tables 19 and 20 summarize the results of these studies.

Table 19. U.S. Geological Survey Interlaboratory Quality Control Study (modified after Skougstad, 1975).

Determination	SRWS No. 31* (12/70) Mean	2 - S†
Ca	12.77 mg/l	1.68
Mg	2.22	0.64
Na	25.33	1.76
K	0.79	0.28
HCO_3	34.74	2.48
SO_4	29.70	2.94
Cl	27.10	2.74
F	0.35	0.14
SiO_2	7.14	1.26
Spec. cond.	217.55 μmhos	9.24
pH	7.68 units	0.52

*SRWS No. 31 was issued to 32 competing laboratories.
†S = Standard deviation of sample population.

Throughout the summer of 1974, during this particular investigation, Ca and Mg were analyzed in the field laboratory by EDTA complexometric titration and AAS methods. The EDTA methods indicated higher Ca and lower Mg levels than the AAS techniques (Figs. 69, 70). Some of the discrepancy was attributed to a faulty Ca standard which accounted for a 16% positive bias in the EDTA determinations of Ca. The remaining inaccuracy appeared to be related to the quantity of iron and/or manganese present in the samples. Those samples with the highest iron and manganese levels indicated the greatest AAS – EDTA discrepancy (Figs. 69, 70). It is probable that the EDTA titration procedure yielded overestimates for Ca and Mg owing to the formation of interfering Fe-Mn-EDTA complexes (Traversy, 1971). Skougstad (1975)

Table 20. Inland Waters Interlaboratory Quality Control Study.

(modified after Traversy and Wales, 1970)

Laboratory	Ca		Hardness		Na		K	
No.	Mean	2-S	Mean	2-S	Mean	2-S	Mean	2-S
101	13.3	1.82	52.5	4.72	11.5	0.79	6.8	0.39
102	13.8	1.18	54.2	3.90	11.9	0.13	6.3	0.08
103	13.2	0.77	52.2	0.68	11.4	0.14	6.4	0.14
104	13.5	0.52	50.5	0.90	11.4	0.43	5.9	0.16
105	13.1	0.26	52.5	0.00	12.0	0.40	5.9	0.21

NOTE: Concentrations expressed as mg/l.

S = Standard deviation of sample population.

(modified after Carron and Aspila, 1978)

Analytical parameter	Sample 1		Sample 2		Sample 3		Sample 4		Sample 5	
	Mean	2-S	Mean	2-S	Mean	2-S	Mean	2-S	Mean	2-S
Ca	43.53	3.92	39.73	2.84	16.26	1.44	35.90	2.20	30.55	2.02
Mg	11.25	1.54	10.38	1.02	3.79	0.62	8.34	0.80	6.72	0.72
Hardness	155	9.72	141.7	9.34	56.2	5.26	124.8	8.02	104.3	7.12
Na	8.08	0.96	79.67	10.61	4.72	1.12	55.91	9.96	8.39	0.88
K	1.54	0.28	6.20	1.42	1.18	0.26	10.30	1.30	1.07	0.32
Alkalinity	114	8.90	119	45.2	40.4	5.70	81.7	42.8	77.3	5.30
Cl	14.2	2.40	72.7	7.44	7.88	1.90	63.0	4.68	18.3	2.20
SO_4	37.3	7.08	41.6	5.64	14.5	4.02	32.3	7.42	20.5	3.66

A total of 35 laboratories participated.

observed a similar discrepancy between Ca determined by both EDTA titration and AAS techniques.

Failure to detect and correct for various interferences which can accompany the AAS determination of Ca, Mg, and K can also be a source of analytical inaccuracy in the major constituent analyses of groundwaters. Angino and Billings (1972) present a comprehensive treatment of interference problems encountered in AAS analyses.

Variability

The scatter or dispersion of a set of sample observations is referred to as the variability of the observations (Davis, 1973). The statistic generally used to express variability is the standard deviation (S). For a series of observations $X_1, X_2, X_3, \ldots$,

$$S = [\ \Sigma (X - \bar{x})^2 / n\text{-}1\ ]^{\frac{1}{2}}$$

where $\bar{x}$ is the sample mean. The variance, S^2, is linearly additive. Thus, for a system with $S_1^2, S_2^2, S_3^2, \ldots$ independent variances the total variance S_T^2 is

$$S_T^2 = S_1^2 + S_2^2 + S_3^2 + \ldots$$

In analysis of variance it is conventional to express variation in terms of a unitless coefficient of variation, V,

$$V = \frac{100S}{\bar{x}}$$

Since V^2 is directly related to S^2,

$$V_T^2 = V_1^2 + V_2^2 + V_3^2 + \ldots$$

For a given groundwater sample location, variations in the measured chemical constituents can be attributed to two broad independent sources: (a) sampling variation, V_S and (b) laboratory/storage variation, V_L. The total variation (V_T) of any individual constituent can thus be expressed,

$$V_T^2 = V_L^2 + V_S^2$$

During the three sampling periods of this particular hydrogeochemical investigation a total of over 300 groundwater samples were collected from wells FW1 and FW2. The variations of the measured chemical constituents for these samples were assessed using a modified version of the computer program NORMSTAT. NORMSTAT calculated

the sampling mean ($\bar{x}$) and the coefficient of total variation (V_T^2) of each chemical constituent. This was carried out individually for each well, each sampling period and each laboratory involved. The results are summarized in Tables 21, 22, and 23.

Sampling Variation

Sampling variation can arise from the sporadic contamination of samples at the time of collection, or the sampling of an inhomogeneous population. Inhomogeneity is the result of temporal and/or spatial variation. If sample contamination is minimized by using proper care in the field, the sampling variation can yield a meaningful estimate of the inhomogeneity of the sample population. The sampling variation determined for periodic samples collected from the same location is thus a measure of the temporal variation of the sample population at that locality.

Distribution of Variations

During the summer of 1973, samples were collected daily from the two flowing wells FW1 and FW2. Triplicate determinations yielded a maximum analytical variation of ±2% for the Ca, Mg, and Fe analyses performed in the field laboratory. Analyses of HCO_3 and specific conductance had maximum laboratory variations of ±1%. The coeffi-

Table 21. Mean, Standard Deviation, Total Coefficient of Variation for Major Ions in Field Determinations: Flowing Well 1, 1972-1974.

Chemical constituents	Nov. 1972 and Summer 1973 field analyses				Summer 1974 field analyses				Summer 1973 and 1974 Water Quality Lab.			
	n	$\bar{X}$	S	V_T^2	n	$\bar{X}$	S	V_T^2	n	$\bar{X}$	S	V_T^2
pH	92	7.11	0.11	2.4	34	6.91	0.20	8.4	–	–	–	–
Eh	72	−65	27	1725	34	+96	29	912	–	–	–	–
Conductance (μmhos/cm)	91	1375	55	16	34	1308	50	14.6	37	1540	93	36.5
Calcium (ppm)	84	157	6.5	17.1	34	154	5.0	10.5	37	187	14.5	60.1
Magnesium (ppm)	78	77	6.25	65.9	30	72	6.50	81.5	36	60	7.0	100
Sodium (ppm)	–	–	–	–	32	92	8.0	75.6	37	85	4.7	30.6
Potassium (ppm)	–	–	–	–	34	10.8	0.85	61.9	37	9.7	0.8	68.0
Manganese (ppm)	–	–	–	–	33	.275	0.04	211.6	33	.254	0.07	759.5
Iron (ppm)	77	5.8	0.35	36	34	5.7	0.50	76.9	33	5.3	2.3	1883
Bicarbonate (ppm)	85	625	13	4.3	27	571	12.0	4.4	36	592	37	39.1
Sulphate (ppm)	–	–	–	–	–	–	–	–	37	403	26.5	43.2
Chloride (ppm)	–	–	–	–	30	13.5	0.7	26.9	37	14.5	3.8	686.8

n = number of observations.

$\bar{X}$ = sample mean.

S = standard deviation of observation.

V_T^2 = total coefficient of variation = $\left(\frac{100S}{\bar{X}}\right)$.

Table 22. Mean, Standard Deviation, Total Coefficient of Variation for Major Ions in Field Determinations: Flowing Well 2, 1972-1974.

Chemical constituent	Nov. 1972 and Summer 1973 field analyses				Summer 1974 field analyses				Summer 1973 and 1974 Water Quality Lab.			
	n	$\bar{X}$	S	V_T^2	n	$\bar{X}$	S	V_T^2	n	$\bar{X}$	S	V_T^2
pH	84	7.63	0.06	0.62	34	7.36	0.07	0.9	–	–	–	–
Eh(mV)	67	−106	14	174.4	33	+33	20.5	3859	–	–	–	–
Conductance (μmhos/cm)	86	2304	48	4.3	34	2230	89	15.9	36	2597	70	7.3
Calcium (ppm)	79	106	1.75	2.7	34	110	2.1	3.6	36	135	3.5	6.7
Magnesium	74	34	1.7	25	32	30	2.7	81	35	26	3.8	213.6
Sodium	–	–	–	–	33	483	10	4.3	36	455	12	7.0
Potassium	–	–	–	–	34	10.6	1.2	128	36	7.3	0.11	2.3
Manganese	–	–	–	–	33	.126	.014	123	33	0.15	0.08	2844
Iron	59	3.8	0.45	140.5	34	3.7	0.26	49.4	32	3.3	0.95	828.7
Bicarbonate	79	403	5.25	1.7	27	382	12.5	10.7	35	407	11	7.3
Sulphate	–	–	–	–	–	–	–	–	36	988	25	6.4
Chloride	–	–	–	–	29	63.2	3.1	34.3	36	61.8	1.0	2.6

Table 23. Mean, Standard Deviation, Total Coefficient of Variation for Major Ions, Western Laboratory: Flowing Wells 1 and 2, 1973.

Constituent	Flowing well 1				Flowing well 2			
	n	$\bar{x}$	S	V_T^2	n	$\bar{x}$	S	V_T^2
Spec. Cond.	11	1548	111.3	51.7	11	2685	81	9.14
Ca (ppm)	11	186.9	21.6	133.0	11	130.9	7.9	36.8
Mg	11	55.0	4.5	67.8	11	25.8	11.2	891.5
Na	11	87.3	3.2	13.4	11	434	30	44.6
K	11	10	1.15	132.3	11	7.4	0.2	7.72
Fe	9	5.88	0.76	167.4	7	3.6	1.9	2840
Mn	8	0.24	0.01	4.95	9	0.25	0.29	13620
HCO_3	10	559.9	55.5	98.4	10	383	36	87.5
SO_4	11	384.4	22.1	33.0	11	954	26	7.53
Cl	11	13.6	1.6	140.4	11	61.7	1.2	3.72

Table 24. Distribution of Coefficients of Variation for 1973 Sampling Period: Flowing Wells 1 and 2 (field analyses only).

Constituent	Flowing well 1			Flowing well 2		
	V_L^2	V_S^2	V_T^2	V_L^2	V_S^2	V_T^2
pH	–	–	2.4	–	–	0.62
Eh	–	–	1725	–	–	174.4
Spec. Cond.	1*	15	16	1*	3.2	4.3
Ca	4	13.1	17.1	~†	~	2.7
Mg	4	61.9	65.9	4	21	25
Fe	4	32	36	4	136.2	140.2
HCO_3	1	3.3	4.3	1	0.7	1.7

*Maximum laboratory variability (spec. cond., ±1%; Ca, Mg, Fe, ±2%; HCO_3, ±1%).
†Laboratory variation not determined (≈ 2%).
V_L^2 = coefficient of laboratory variation.
V_S^2 = coefficient of sampling variation.
V_T^2 = coefficient of total variation = $V_L^2 + V_S^2$.

cients of total variation, sampling variation, and laboratory variation were calculated from these daily samples. Sampling variation (temporal variations) accounted for most of the total variation in Mg and Fe observations for both FW1 and FW2 (Table 24). Sampling variation was also a major component of the total variation for the Ca and HCO_3 observations from FW1 (Table 24). The total variation of Ca and HCO_3 observations from FW2 was extremely small and was entirely a result of laboratory variation (Table 24).

Once a week during the 1973 summer sampling period, bulk water samples were collected from FW1 and FW2, and subsequently split; one half of the split sample was sent to the Western Regional Laboratory for complete chemical analysis, and the other half was analyzed in the field-based laboratory. Appendix IX lists the results of the chemical analyses of these split samples. Total variation, sampling variation, and laboratory variation were computed for the Ca, Mg, Fe, and HCO_3 determinations from the field laboratory (Table 25). This sampling variation was used to compute the laboratory variation in the results from the Western Laboratory. This laboratory variation is the combination of laboratory analytical variation and an additional unknown variation introduced by the shipping and storage of unpreserved samples. Sampling variation was a minor component (i.e. < 10%) of the total variation in the Western Laboratory determinations of Ca, Mg, Fe, and HCO_3 for these samples (Table 25). This implies that the determinations done by the Western Laboratory could not be used to illustrate the temporal variations in the chemistry of the groundwaters of this study.

Uncertainty

There is always a degree of uncertainty associated with each discrete measurement of a system. Thus, it is probably most realistic to express each discrete measurement as a range of statistically probable values instead of a single value. The spread of two standard deviations (±2S) of the variations about the measured value is referred to as the uncertainty associated with the measured value. The uncertainty is the 95% likelihood that the observed value lies within these upper and lower confidence limits.

The analytical/storage uncertainties associated with the Western Laboratory determinations of Ca, Mg, Fe, and

Table 25. Comparison of Split Groundwater Samples, 1973, between Field Laboratory and Western Laboratory Analyses: Flowing Wells 1 and 2.

Constituents	Field lab			Western lab		
	V_L^2	V_S^2	V_T^2	V_L^2	V_S^2*	V_T^2
			Flowing well 1			
Ca	4.0	1.7	5.7	131.3	1.7	133.0
Mg	4.0	7.5	11.5	60.3	7.5	67.8
Na	–	–	–	–	–	13.4†
K	–	–	–	–	–	132.3†
Fe	8.2	4.2	8.2	163.2	4.2	167.4
Mn	–	–	–	–	–	4.95†
HCO_3	1.0	1.1	2.1	97.3	1.1	98.4
SO_4	–	–	–	–	–	33.0†
Cl	–	–	–	–	–	140.0†
Spec. Cond.	–	–	14.7	–	–	51.7†
			Flowing well 2			
Ca	4.0	7.6	11.6	29.2	7.6	36.8
Mg	4.0	73	77.0	818.5	73	891.5
Na	–	–	–	–	–	44.6†
K	–	–	–	–	–	7.72†
Fe	4.0	688	692	2152	688	2840
Mn	–	–	–	–	–	12621†
HCO_3	1.0	6.1	7.1	81.4	6.1	87.5
SO_4	–	–	–	–	–	7.5†
Cl	–	–	–	–	–	3.7†
Spec. Cond.	–	–	13.4	–	–	9.1†

*Constant for any given sample concentration, i.e., reflects inhomogeneity of sample population.
†No field analyses done to allow separation of V_L^2 and V_S^2.

HCO_3 were calculated for this particular study. These results were used to establish the resulting uncertainties in the saturation indices calculated for calcite (SI_C), dolomite (SI_D), gypsum (SI_G), magnesite (SI_{MAG}), and siderite (SI_{SID}). SI calculations were carried out using the computer program WATEQF for the ±2S range of Ca, Mg, Fe, and HCO_3 values reported by the Western Laboratory. Analytical/storage uncertainties resulted in large uncertainties in the calculation of SI_D and SI_{SID} for both wells and also in SI_{MAG} for flowing well 2 (Table 26).

Table 26. Saturation Index Uncertainty Arising from Analytical/Storage Uncertainties of the Chemical Species: Flowing Wells 1 and 2.

	Flowing well 1	Flowing well 2
SI_C	0.42 ± 0.10	−0.01 ± 0.10
SI_D	0.60 ± 0.22	−0.50 ± 0.30
SI_G	−0.85 ± 0.10	−0.70 ± 0.05
SI_{MAG}	−0.22 ± 0.14	−0.85 ± 0.30
SI_{SID}	0.79 ± 0.30	0.38 ± 0.30

SI = saturation index = $\log \frac{IAP}{K_{sp}}$

C = calcite
D = dolomite
G = gypsum
MAG = magnesite
SID = siderite

Table 27. Summary of Analytical/Storage Uncertainty in the Western Laboratory Determination of Ca, Mg, Fe, and HCO_3 during this Study: Flowing Wells 1and 2.

Constituent	Flowing well 1 $\bar{X}$ ± Uncertainty	Flowing well 2 $\bar{X}$ ± Uncertainty
Ca	187 ± 42 ppm	131 ± 14 ppm
Mg	55 ± 8.8 ppm	26 ± 15 ppm
Fe	5.9 ± 1.5 ppm	3.6 ± 3.0 ppm
HCO_3	560 ± 110 ppm	383 ± 70 ppm

During this particular hydrogeochemical study, significant analytical/storage uncertainties were observed in the standard Western Laboratory determinations of Ca, Mg, Fe, and HCO_3 (Table 27). These uncertainties resulted in significant uncertainties in subsequent mineral equilibria calculations for the groundwater samples. The analytical/storage uncertainties were also found to be many times greater in magnitude than observed temporal variations of these species in the groundwaters. This implies that the results of the Western Laboratory chemical analyses could not be used to illustrate temporal chemical variations affecting the groundwaters of this study. Chemical analyses that were performed in replicate in the field laboratory reduced the analytical and storage uncertainties to a level that allowed temporal chemical variations in the groundwaters to be distinguished.

SATURATION INDEX CALCULATIONS

In addition to the calculation of the saturation indices for calcite, dolomite, and gypsum in the WATEQF II program, similar calculations were performed on a number of samples using a WANG MODEL 700 C programmable calculator. Because of limited storage capability, the program does not include ion pairing and complexing. The program for the Wang calculator was developed by van Everdingen (pers. comm.). The saturation index was calculated by using the expression,

$$SI = \log \frac{IAP}{Ksp}$$

The value of log IAP was obtained from the Wang printout and log Ksp (logarithm of solubility constant for a specific mineral species at a certain temperature) was obtained from the literature (Garrels and Christ, 1965; Blount, 1965). A comparison of the results on the saturation indices obtained from both programs is shown in Figures 71, 72, and 73. Two sets of values are illustrated in the figures:

- saturation index values based on the results of the analyses of the Western Laboratory
- saturation index values based on the results of field analyses of split sample.

An examination of Figures 71, 72, and 73 shows that the saturation index values obtained by the Wang program in comparison to the WATEQF II program are (a) essentially the same for calcite; (b) the same or slightly lower for dolomite; and (c) slightly lower (more negative) for gypsum. If the uncertainty in the value of the saturation index is considered (Table 26), then the values obtained by both programs can be considered similar. This implies that ion pairing and complexing over the range of ionic concentration (Table 28) both in the surface water and the groundwater is negligible.

Table 28. Range of Ionic Concentration in Surface and Groundwater

	Groundwater		Surface water	
Parameter	FW1	FW2	North of K1	Plant runoff K2
Ca	174-191	118-130	76-102	74-200
Mg	65-75	26-33	37-52	26-103
Na	80-97	389-480	22-34	88-1340
K	90-13.0	7.0-7.6	3.0-6.0	92-390
CO_3	-	-	-	0-11
HCO_3	612-642	390-431	337-436	261-317
SO_4	332-410	900-1000	77-194	130-940
Cl	2.5-14	60-64	3.5-10.5	180-2200
pH	7.01-7.20	7.53-7.70	7.91-8.30	8.08-8.56

Figures 71 and 72 also show that the degree of saturation with respect to calcite and dolomite increases drastically during storage. Furthermore, a slight decrease in the degree of saturation with respect to gypsum (or systematically low SO_4 and/or Ca values in the water quality analyses) can be noted. Figure 73 shows a similar pattern for the surface water in Cutarm Creek north of the K1 plant, whereas the plant runoff from the K2 plant shows exactly the opposite pattern with respect to the saturation index of calcite and dolomite. It was noted during sampling that these samples contained considerable amounts of algae and other aquatic biota and it is therefore most likely that continuing respiration by the organisms during storage and transport increased the CO_2 content, which suppressed the saturation index. This contention is further supported by the considerable decrease in the pH that can be noted between the field value and the laboratory value, from 8.4 to 8.00 respectively.

The differences in the saturation index which occur between the field and the laboratory for both groundwater and surface water indicate that great care has to be exercised if the data from the laboratory are to be used in the calculation of solid phase equilibria.

SUMMARY

The chemistry of the groundwater in the aquifer studied exhibits significant spatial variation. Generally, there is an increase in TDS and pH with depth and an attendant chemical evolution of the water with depth and distance along the groundwater flow path. The shallow portion of the aquifer is characterized by dilute Ca–HCO_3 water, whereas the deep portion of the aquifer is characterized by more concentrated Na–SO_4 water. This spatial variation can be explained by:

- calcite and/or dolomite dissolution during groundwater recharge through the soil zone; continuous halite and gypsum dissolution in the aquifer along the groundwater flow path; and continuous cation exchange of Ca and Mg for Na in the aquifer along the groundwater flow path.
- the mixing of chemically distinct groundwaters within the aquifer. Dilute Ca–HCO_3 water could be entering the upper portion of the aquifer as recharge through the till and mixing with more concentrated Na–SO_4 water entering the aquifer at depth from deeper flow systems.

During this study, temporal variations were observed to affect the chemistry of the water in the aquifer. The shallow groundwater (FW1) responded chemically to a distinctive recharge event which occurred early in June,

1973. Ca, Mg, HCO_3, Fe (?), and pH levels increased in the shallow well after this recharge event. These variations could result from the recharge of Ca–Mg–HCO_3 water through fractures in the overlying till. Throughout the rest of the summer HCO_3, Ca, Mg, and pH levels in FW1 showed little variation. Variations in the specific conductance and Eh of FW1 water occurred throughout the summer, but these did not appear to be related to any of the other chemical constituents which were measured. The variations in the specific conductance of FW1 water paralleled those for the deep well (FW2) water and seemed to be related to a mid-summer rise in the hydrostatic pressure in the aquifer. The specific conductance variations had a larger magnitude in FW2 than in FW1.

The chemistry of the water in the deep well (FW2) did not respond as dramatically as that in FW1 to the spring recharge event. Only Ca (and possibly Mg (?)) increased noticeably in FW2 water after this event.

The Fe, Eh, and specific conductance levels in FW2 varied simultaneously during the middle of the summer observation period. These variations appeared to be related to a mid-summer hydrostatic pressure increase in the aquifer. Probably, this chemical response in the deep well was caused by groundwater entering the deep portion of the aquifer from deeper flow systems.

Freezing of water samples, both acidified and non-acidified, introduces considerable uncertainty in the analytical results for these samples. The effect of freezing on the ionic concentration of most ions is such that the analytical results should be disregarded.

To guard against possible misinterpretation of hydrogeochemical data the analytical/storage uncertainties associated with discrete chemical measurements of a system should be assessed. It is obvious from this study that sole reliance upon the analytical results of laboratory analyses would introduce significant uncertainties in mineral equilibrium calculations for groundwater samples. Furthermore, the analytical/storage uncertainties associated with the laboratory analyses were found to be of such magnitude that they would mask temporal variations in the ionic species in groundwaters. The results of a comparative study of field and laboratory analyses of surface water show that similar caution has to be exercised in the interpretation of laboratory analyses.

In order to determine whether the laboratory analysis for a particular ionic species in a water sample is adequate for monitoring purposes, both the range of the temporal variation and the analytical/storage uncertainty of the species should be determined.

Sequential Sampling of Observation Well Network and Monitoring

The observation wells were sampled sequentially over the period 1971-1975 to determine whether any changes in the water chemistry were caused by the presence of the brine pond. The results of the analyses are shown in Table 29. Examination of Table 29 shows that no significant changes have taken place in the water chemistry of the aquifer at the points of sampling. The small variations in the concentrations of the various ionic species are well within the variability of the groundwater chemistry as shown in Tables 21, 22, and 23. This would suggest that no contamination of the aquifer by the brine has taken place. However, this statement requires further elaboration. To detect contaminant movement in the shallow subsurface by monitoring of the water chemistry in a few widely spaced observation wells the completion zones of the wells must be located within the travel paths of the contaminant. The patterns of contamination zones in the shallow subsurface vary widely and are a function of, for example, the behaviour of the contaminant in the soil, water, and rock environment; ranges in geologic and hydrologic conditions in space; and ranges in hydrologic conditions in time (Legrand, 1965). If the geologic conditions which are present are further examined, then the following comments can be made. The main aquifer in the area is glacio-fluvial in origin. This type of fluvial deposit is characterized by a heterogeneous distribution of the various types of sediment, both in a lateral and vertical sense. This is well illustrated, for example, in the geological cross sections (Plate 3), which show that even with a short distance between the testholes, it is next to impossible to correlate individual beds. The transmissivity of an unconsolidated sediment is a function of the type of sediment; the lack of continuity of the individual beds will therefore strongly affect the distribution of the transmissivity in the subsurface. This in turn will strongly influence the migration of any contaminant. Another factor which will further complicate the travel path of the contaminant once it has reached the aquifer is the difference in density between the brine and the fresh water, which will affect the flow path of the brine. To assume therefore that the completion zone of the observation well intersects the flow path of the contaminant or that sufficient dispersion and diffusion of the contaminant take place so that it will be detected by sequential sampling of the observation wells is folly. To improve the usefulness of the observation wells in detecting possible contamination the wells should be pumped for several days at the highest rate possible before taking the water samples. If there is contamination in the vicinity of the well, it may then be possible to draw some of the contaminated water into the wells. However, it should always be realized that even with extended pumping times, only a limited portion of the subsurface environment can be sampled. Furthermore, it should be kept in mind that in six of the seven wells used in this study the completion interval is located in the upper portion of the aquifer. Although this distribution appears to be sufficient to define the gradient distribution in the aquifer, it is completely inadequate to monitor the water chemistry, especially if the effect of the different density of the brine on the flow aspect of an advancing brine front is considered. To improve this situation would require the installation of several observation wells and/or piezometers with completion zones at different depths in the aquifer. This means a considerable investment in new structures, as well as high operating costs in terms of well maintenance, sampling, and chemical analyses. Even with an expanded observation well network, however, there is still the problem that each sampling site is only a point source in a much larger environment. Alternatives to an expanded observation well network would be sequential testdrilling and/or geophysical methods. Depending on the drilling method, the testholes should be electric logged or water samples for analysis should be taken over several intervals. This method has the advantage that additional stratigraphic information is obtained to delineate the areas where additional observation wells or piezometers would be needed for further monitoring. However, this method is cost intensive and has the same disadvantage as an observation well network in that each sampling site is a point source only.

The geophysical methods which are of particular interest are the resistivity methods. The advantage of surface resistivity surveys is that the method is nondestructive and it provides a much more continuous coverage between adjacent points. One of the main drawbacks of this method is that because of salt accumulation in the soil (spillage, spray, dust) a highly conductive layer is generally present at the surface in the vicinity of the brine pond, which would concentrate any applied current in this layer and thereby mask resistivity contrasts at depth. To overcome this problem it is suggested that electrodes be installed permanently at different depths and locations in the aquifer. Once the back-

Table 29. Sequential analyses of observation wells A - G.

	WELL A					WELL B			WELL C		
DATE	24/03/71	26/11/73	08/06/74	21/07/74	20/11/75	11/03/71	23/11/73	19/11/75	10/03/71	23/11/73	19/11/75
pH	7.7	6.8	7.5	6.9	6.9	7.5	7.0	6.8	7.5	7.0	6.8
Cond.	1470	1810	1600	1450	1460	1440	1510	1480	1560	1550	1540
Ca	183*	223	143	191	170	167	195	198	193*	203	185
Mg	62*	77	66	61	72	61*	63	73	74*	69	80
Na	70	92	71	74	78	72	80	77	78	88	85
K	9.3	9.7	9.1	9.2	9.4	8.8	8.9	8.8	8.8	8.9	8.8
HCO_3	590*	597	228	594	603	517*	572	576	623*	577	612
SO_4	370*	396	370	370	450	394*	363	472	425*	376	505
Cl	11.0	42	19	11	11	12	18	12	11	19	10

	WELL D		WELL E			WELL F			WELL G		
DATE	15/03/71	26/11/73	18/03/71	26/11/73	17/11/75	20/03/71	21/11/73	18/11/75	23/03/71	23/11/73	20/11/75
pH	7.8	6.9	7.5	6.8	6.9	8.0	7.1	6.9	7.9	7.0	6.8
Cond.	1330	1540	925	1370	1355	2010	2280	2230	1520	1490	1504
Ca	168*	184	143*	191	165	205*	204	192	168*	197	182
Mg	63*	68	67*	55	67	75*	69	80	65*	67	74
Na	83	88	55	62	59	255	266	260	71	80	80
K	9.4	9.3	9.6	9.0	9.4	8.5	10	11	9.1	9.1	9.4
HCO_3	514*	602	490*	579	594	721*	708	703	528*	573	604
SO_4	436*	390	338*	279	380	691*	683	710	389*	355	493
Cl	14	17	8.3	12	8.6	51	51	49	12	15	12

* Values incorrect (determined on water samples that were frozen).

ground resistivity values are determined for the various electrode configurations, sequential surveys should detect any changes caused by brine movement and aid in the delineation of contaminated areas and the rate of movement of the contaminant. Although a considerable cost will be associated with the initial installation, it will be significantly less than, for example, the expansion of the observation well network. Furthermore, operating and maintenance costs in comparison with the other methods are relatively low. Excellent results were obtained by Banner and van Everdingen (1979) in a study of the propagation of the freezing front in unsaturated and saturated soils by using multi-electrode systems installed in the subsurface. Although the objective of similar installations near brine ponds is to detect brine and monitor its rate of movement, the problem is analogous to that studied by Banner and van Everdingen (1979) because in both cases it is the significant change in the resistivity of the medium, caused either by freezing of the soil or by the presence of brine, which is measured.

In summary, the sequential analyses of samples from the observation wells show that no contamination of the aquifer underlying the brine has occurred in the location where the wells are completed. However, the spatial distribution of the sampling points (i.e. completion intervals) in the hydrogeological environment is inadequate to monitor contamination of the aquifer. It is therefore suggested that the existing observation well network be greatly expanded or that alternative methods of monitoring be adopted. Of the latter, the permanent installation of electrodes at various depths and places appears to be most promising, both in terms of cost (capital, maintenance and operation) and continuity of surveillance.

Conclusions

Thick deposits of fluvial sediments are present in the buried valley that underlies the northern part of the waste disposal basin. The fluvial deposits are overlain by approximately 35 ft (11 m) of fractured and oxidized tills under the basin.

A major facies change occurs in the fill of the buried valley between the waste disposal basin and Cutarm Creek which will retard brine movement in the buried valley towards Cutarm Creek.

The hydrographs of the observation wells show that the response of the wells to natural and manmade input is essentially the same. For long-term monitoring of the water levels in the wells, continuous monitoring of a few wells (where the number is determined by the quality of the recording equipment) supplemented by spot measurements in the other wells would be sufficient. A significant saving in the operating and maintenance cost of the monitoring program can thus be realized.

Extensive studies of hydrodynamic response tests in the observation wells show that minor well development occurs during consecutive tests, and that the magnitude of the transmissivity is affected to a minor degree by the size of the slug.

An evaluation of the long-term hydrograph record of the observation wells and an extensive study of the barometric efficiency of the wells show that the aquifer is semiconfined at best. This conclusion corroborates the findings of the geological investigation.

Steady state electric analog simulations of the hydrogeological environment in the vicinity of the waste disposal basin show that once brine has reached the buried valley (a) brine pollution by groundwater discharge directly into Cutarm Creek does not appear to be a major pollution hazard; (b) extensive pollution of the aquifer west of the brine pond would occur; (c) an area of several hundred acres immediately east of the waste disposal basin would eventually be polluted. The time period over which the latter pollution would occur is, according to the simulations, thirty years. However, in the time calculations, the effect of the density of the brine on its potential flow path in the subsurface was not considered, nor were the physicochemical processes induced by the brine in the sediments which affect the permeability taken into account. The stated time period appears therefore to represent a minimum rather than a maximum value.

The lack of data on the effect of brine on the permeability of the sediments and the rate of progress of the physicochemical processes warrants further study. Without a proper definition of these processes predictive models of contaminant movement in the vicinity of brine waste disposal basins become a theoretical exercise.

Transient state electric analog model simulations show that if the hydraulic gradient is to be reversed to limit the spread of pollutants, injection rates between 350 and 600 lgpm would be required on a continuous basis. Injection rates of this magnitude would put a considerable strain on the freshwater resources in the area, and alternative methods such as grout and slurry curtains might have to be considered.

The various hydrochemical surveys and studies conducted in the area show that

- freezing of water samples, both acidified and nonacidified, introduces considerable uncertainty in the analytical results
- the chemistry of the groundwater in the aquifer exhibits considerable spatial variation. The shallow portion of the aquifer is characterized by dilute Ca–HCO_3 type water, whereas the deep portion shows a more concentrated Na–SO_4 type water.
- daily analyses for several ions in a field laboratory show that considerable temporal variation occurs in the chemistry of the groundwater. The chemistry of the water in the shallow portion of the aquifer responded distinctively to a major recharge event which occurred in June 1973.
- the analytical/storage uncertainties associated with the Western Laboratory analyses of groundwater samples are of such magnitude that they mask the temporal variations in the chemical environment in the aquifer. Furthermore, they introduce significant uncertainties in the mineral equilibrium calculations.

– to determine whether the laboratory analysis for a particular ionic species in a water sample is adequate for monitoring purposes, the range of the temporal variation and the analytical/storage uncertainty of the species should be determined.

The sequential water sampling program of the observation wells shows that no brine contamination has occurred in the aquifer at the points of sampling. However, if the various aspects of the flow of brine in this hydrogeological environment are considered, then the distribution of the completion zones of the observation wells is inadequate to monitor contaminant movement and additional data points will be required. Rather than increasing the number of observation wells drastically, it is suggested that geophysical surveillance be considered. The type of system that is envisaged for monitoring purposes, both in terms of cost and continuity of surveillance, would consist of electrodes permanently installed at different depths and locations in the aquifer.

References

Acton, D.F., Clayton, J.S., Ellis, J.G., Christiansen, E.A., and Kupsch, W.O. 1960. Physiographic Divisions of Saskatchewan. Sask. Res. Council, Map 1.

Angino, E.E., and Billings, G.K. 1972. Atomic absorption spectrometry in geology. Modern Methods in Geochem. and Geophys., No. 7, 191 pp.

Anonymous, 1964-1967. Record of wells. Water Rights Branch, Sask. Water Resources Comm., Regina.

Anonymous, 1965. Potash in Saskatchewan. Sask. Dept. Miner. Resour. 24 pp.

Anonymous, 1966. Groundwater and wells. Edw. E. Johnson, Inc., St. Paul, Minn.

Anonymous, 1968-1975. Record of wells. Water Rights Branch, Sask. Dept. Environment, Regina.

Anonymous, 1970. Areal evaporation for five years, 1964-1969. Dept. of Energy, Mines, and Resources, Surveys & Mapping Branch, Ottawa.

Baar, C.A., 1972. Actual geological problems in Saskatchewan potash mines. Sask. Res. Council Rep. E 72-18, 98 pp.

Back, W., and Barnes, I. 1965. Equipment for field measurement of electrochemical potentials. U.S. Geol. Surv. Res. Notes C: 366-368.

Bailey, A.D., 1953. Devonian system of the Williston Basin area: Manit. Dept. Mines Nat. Resources, Mines Branch, Publ. 52-5.

Banner, J.A., and van Everdingen, R.O. 1979. Frost gauges and freezing gauges. NHRI Paper No. 3, Inland Waters Directorate, Environment Canada, 17 pp.

Baver, L.D. 1959. Soil Physics. John Wiley & Sons Inc., N.Y., 3rd ed., 489 pp.

Bear, J. 1972. Dynamics of fluids in porous media. American Elsevier Publishing Co. Ltd., N.Y., p. 732.

Beckie, V.G., and Balzer, J.E. 1970. Industrial groundwater investigation at Welby, Saskatchewan: G.A.C. meeting, Winnipeg, Aug. 30-Sept. 2, 1970. Unpublished report.

Bergstrom, J. 1974. Seasonal variations and distribution of dissolved iron in an aquifer. Nordic Hydrology, 5:1-31.

Blount, C.W. 1965. The solubility of anhydrite in the systems $CaSO_4$-H_2O and $CaSO_4$-NaCl-H_2O and its geologic significance. Ph.D. thesis, Univ. of California, L.A., Univ. Microfilms, Inc., Ann Arbor, Mich.

Bourne, D.R. 1976. An electric analog simulation of groundwater flow patterns at a potash waste disposal pond located near Esterhazy, Saskatchewan. Unpubl. M.Sc. thesis, Univ. British Columbia, Vancouver, B.C. 123 pp.

Bredehoeft, J.D., Cooper, H.H. Jr., and Papadopulos, I.S. 1966. Inertial and storage effects in well-aquifer systems: an analog investigation. Water Resour. Res. 2 (4): 697-707.

Carron, J.M., and Aspila, K.I. 1978. Interlaboratory quality control study No. 14. Inland Waters Directorate, Ontario Region, Water Quality Branch, Environment Canada. Rep. Ser. 51.

Cherry, J.A. 1972. Geochemical processes in shallow groundwater flow systems in five areas in southern Manitoba, Canada. 24th International Geological Congress, sec. 11, pp. 208-221.

Cherry, J.A., and Whitaker, S.H. 1969. Geology and groundwater resources of Yorkton area (62 M), Saskatchewan. Sask. Res. Council, Map 9.

Christiansen, E.A. 1967. Collapse structures near Saskatoon, Saskatchewan, Canada. Can. J. Earth Sci. 5:757-767.

Christiansen, E.A. 1968a. A thin till in west central Saskatchewan, Canada. Can. J. Earth Sci. 5:329-336.

Christiansen, E.A. 1968b. Pleistocene stratigraphy of the Saskatoon area, Saskatchewan, Canada. Can. J. Earth Sci. 5:1167-1173.

Christiansen, E.A. 1969. Pleistocene stratigraphy of the Swift Current Creek, Prelate Ferry, Empress, and Medicine Hat sections. Unpubl. mimeo prepared for Mid-West Friends of the Pleistocene Fieldtrip 1969, Sask. Res. Council.

Christiansen, E.A. 1970. Sinkholes in eastern Saskatchewan. Sask. Res. Council 24th Annu. Rep., pp. 32-34.

Christiansen, E.A. 1971a. Geology and groundwater resources of the Melville area (62 K,L), Saskatchewan. Sask. Res. Council, Map 12.

Christiansen, E.A. 1971b. Geology of the Crater Lake collapse structure in southeastern Saskatchewan, Canada. Can. J. Earth Sci. 8: 1505-1513.

Christiansen, E.A. (ed.) 1972. Guidebook on Geology and Its Application to Engineering Practice in the Qu'Appelle Valley Area. Regina, Geotech. Group and Sask. Geol. Soc.

Christiansen, E.A., and Whitaker, S.H. 1976. Glacial thrusting of drift and bedrock. *In* Glacial Till, an Inter-disciplinary Study. Edited by R.F. Legget. Royal Soc. Can. Spec. Publ. 12, pp. 121-132.

Clark, W.E. 1967. Computing the barometric efficiency of a well. J. Hydraulics Div., Am. Soc. Civil Eng. 93 (HY4, July 1967): 93-98.

Clayton, L., and Moran, S.R. 1974. A glacial process form model. *In* Glacial Geomorphology. Edited by D.R. Coates. Publ. Geomorphol. State Univ. New York, Binghampton, N.Y., 398 pp.

Clister, W.E. 1973. Hydrogeology of a subsurface radioactive waste management site in a shallow groundwater flow system. M.Sc. thesis, Univ. of Manitoba. 139 pp.

Cooper, Jr., H.H., Bredehoeft, J.D., and Papadopulos, I.S. 1967. Response of a finite-diameter well to an instantaneous charge of water. Water Resour. Res. 3(1): 263-269.

Davis, J.C. 1973. Statistics and data analysis in geology. John Wiley & Sons Inc., Toronto.

Davison, C.C. 1974. Preliminary study of the chemical changes occurring in water samples during storage prior to laboratory chemical analysis. Unpubl. B.Sc. thesis, Earth Sci. Dept., Univ. Waterloo, Waterloo, Ont.

Davison, C.C. 1976. A hydrochemical investigation of a brine disposal lagoon-aquifer system, Esterhazy, Saskatchewan. Unpubl. M.Sc. thesis Univ. Waterloo, Waterloo, Ont.

Demayo, A., Davis, A.R., and Forbes, M.A. 1978. Forms of metals in water. Inland Waters Directorate, Water Quality Branch, Environment Canada, Sci. Ser. No. 87.

Dennison, E.G., and Simpson, F. 1973. Hydrogeologic and economic factors in decision making under uncertainty for normative sub-surface disposal of fluid waste, northern Williston Basin, Saskatchewan, Canada. Symp. underground waste management and artificial recharge, Amer. Assoc. Petrol. Geol., Vol. 2, pp. 879-927.

Domenico, P.A. 1972. Concepts and models in groundwater hydrology. McGraw-Hill Book Co., Toronto, 403 pp.

Dunk, R., Mostyn, R.A., and Hoare, H.C. 1969. The determination of sulphate by indirect atomic absorption spectrometry. Atomic Absorption Newsletter, 8(4):79-81.

Edmunds, W.M. 1970. Trace element variations across an oxidation reduction barrier in a limestone aquifer. Proc. Symp. Hydrogeochem. Biogeochem., Tokyo, Japan, Sept. 1970, pp. 500-526.

Ferris, J.C., and Knowles, D.B. 1954. The slug test for estimating transmissibility. U.S. Geol. Surv. Groundwater Note 26.

Ferris, J.C., Knowles, D.B., Brown, R.H., and Stallman, R.W. 1962. Theory of aquifer tests. U.S. Geol. Surv. Water Supply Paper 1536-E, 174 pp.

Fishman, M.J. 1966. The use of atomic absorption for analysis of natural waters. Atomic Absorption Newsletter, 5, (5): 102-106.

Freeze, R.A. 1969a. Hydrogeology and groundwater resources of the Gravelbourg aquifer, Saskatchewan. Dept. Energy, Mines and Resources, Inland Waters Branch, Sci. Ser. No. 6, 60 pp.

Freeze, R.A. 1969b. Hydrology of the Good Spirit Lake Drainage Basin, Saskatchewan. Dept. Energy, Mines and Resources, Inland Waters Branch, Tech Bull. No. 14.

Freeze, R.A. 1969c. Regional groundwater flow—Old Wives Lake drainage basin, Saskatchewan. Inland Waters Branch, Dept. Energy, Mines and Resources, Sci. Ser. No. 5, 245 pp.

Freeze, R.A., and Witherspoon, P.A. 1966. Theoretical analysis of regional groundwater flow: (1) analytical and numerical solutions to the mathematical model. Water Resour. Res. 2:641-656.

Freeze, R.A., and Witherspoon, P.A. 1967. Theoretical analysis of regional groundwater flow: (2) effect of water-table configuration and subsurface permeability variation. Water Resour. Res. 3:623-634.

Fritz, P., Drimmie, R.J., and Render, F.W. 1974. Stable isotope contents of a major prairie aquifer in central Manitoba, Canada. Reprint Isotope Techniques in Groundwater Hydrology 1974, IAEA-SM-182/22, pp. 379-398.

Fritz, P., Cherry, J.A., Weyer, K.U., and Sklash, M. 1976. Storm runoff analyses using environmental isotopes and major ions. *In* Interpretation of Environmental Isotope and Hydrochemical Data in Groundwater Hydrology, IAEA, Vienna, Austria, pp. 111-130.

Garrels, R.M., and Christ, C.L. 1965. Solutions, minerals, and equilibria. Freeman, Cooper & Co., San Francisco, 450 pp.

Gendzwill, D.J., and Hajnal, Z. 1971. Seismic investigation of the Crater Lake structure in southeastern Saskatchewan. Can. J. Earth Sci. 8: 1514-1524.

Gilliland, J.A. 1969. A rigid plate model of the barometric effect. J. Hydrol. 7:233-245.

Grayston, L.D., Sherwin, D.F., and Allan, J.F. 1966. Chapter 5, middle Devonian. *In* Geological History of Western Canada. Edited by R.G. McCrossam and R.P. Glaister. Alberta Soc. Petr. Geol., pp. 49-59.

Grisak, G.E., and Cherry, J.A. 1975. Hydrologic characteristics and response of a fractured till and clay confining a shallow aquifer. Can. Geotech. J. 12:23-43.

Grisak, G.E., Cherry, J.A., Vonhof, J.A., and Blumele, J.P. 1975. Hydrogeologic and hydrochemical properties of fractured till in the Interior Plains region. *In* Glacial Till. Edited by R.F. Legget. Roy. Soc. Can. Spec. Publ. 12. pp. 304-335.

Hem, J.D. 1970. Study and interpretation of the chemical characteristics of natural water. U.S. Geol. Surv. Water Supply Paper 1473, 2nd ed., 363 pp.

Hoag, R.B. 1975. Periodical variations of dissolved constituents in groundwaters of Eustis Mine area, Sherbrooke, Quebec. Unpubl. Ph.D. thesis, McGill Univ., Montreal, Que., Chapter 3.

Holter, M.E. 1969. The middle Devonian prairie evaporite of Saskatchewan. Sask. Dept. Miner. Resour. Rep. 123.

Hvorslev, M.J. 1951. Time lag and soil-permeability in groundwater observations. Waterways Expt. Sta. Bull. No. 36, Corps Eng., Vicksburg, Miss., 51 pp.

Izatt, R.M., Ebough, D., Christensen, J.J., and Barthdomev, C.H. 1969. Calorimetrically determined Log K, H°, and S° values for the interaction of SO_4 ion with several bi- and tri-valent metal ions. Chem. Soc. London J., Sec. A, Pt. 1, pp. 47-53.

Jacobson, R.L. 1973. Controls on the quality of some carbonate groundwaters: dissociation constants of calcite and $CaHCO_3^+$ from 0°C to 50°C. Unpubl. Ph.D. thesis, Penn. State Univ.

Kahn, H.L. 1968. Principles and practice of atomic absorption. Adv. Chem. Ser. 73:183.

Karplus, W.J. 1958. Analog simulation. McGraw-Hill Book Co., Inc., New York, 434 pp.

Keys, D.A., and Wright, J.Y. 1966. Geology of the I.M.C. potash deposit, Esterhazy, Saskatchewan. Northern Ohio Geol. Soc., 2nd Symp. on Salt, Vol. 1, pp. 95-101.

Kharaka, Y.K., and Barnes, Ivan. 1973. SOLMNEQ: Solution-mineral equilibrium computations. U.S. Dept. Int. Geol. Surv. Computer Distribution, No. G204, 82 pp.

Klassen, R.W. 1972. Wisconsin events and the Assiniboine and Qu'Appelle valleys of Manitoba and Saskatchewan. Can. J. Earth Sci. 9:544-560.

Kruseman, G.P., and de Ridder, N.A. 1970. Analysis and evaluation of pumping test data. Int. Inst. Land Reclam. Improv. Wageningen, The Netherlands, Bull. 11.

Kupsch, W.O. 1962. Ice-thrust ridges in western Canada. J. Geol., 70:582-594.

Lane, D.M. 1959. Dawson Bay Formation in the Quill Lakes–Qu'Appelle area, Saskatchewan. Sask. Dept. Miner. Resour. Rep. 38.

Langmuir, D. 1971. Eh-pH determination. *In* Procedures in Sedimentary Petrology. Edited by R.E. Carver. John Wiley & Sons. Chapter 3, pp. 597-634.

Langmuir, D., and Whittemore, D.O. 1971. Variations in stability of precipitated ferric oxyhydroxide, nonequilibrium systems in natural water chemistry. Adv. Chem. Ser. 106: 209-234.

Law, J. 1955. Geology of northwestern Alberta and adjacent areas. Am. Assoc. Petr. Geol. Bull. 39: 1927-1975.

Legrand, H.E. 1965. Patterns of contaminated zones of water in the ground. Water Resour. Res. 1:83-95.

Lissey, A. 1962. Groundwater resources of the Regina area, Saskatchewan. City of Regina, City Engineering Dept., Hydrology Div. Rep. No. 1.

Maclean, A.H., and Pawluk, S. 1975. Soil genesis in relation to groundwater and soil moisture regimes near Vegreville, Alberta. J. Soil Sci. 26 (3):278-293.

Masch, F.D., and Denny, K.J. 1966. Grain size distribution and its effect on the permeability of unconsolidated sands. Water Resour. Res. 2(4):665-677.

McNaughton, D.W. 1975. A hydrogeological, geochemical, and isotopic study of an uncontaminated flow system, Perch Lake basin, Ontario. M.Sc. thesis, Univ. Waterloo, Waterloo, Ont.

Mawson, C.E. 1964. Survey of hydrologic applications of tracers in Canada. Atomic Energy of Canada Ltd., AECL-2005, 14 pp.

Maybank, J., and Calvert, J.G. 1970. Comparison of brine and water evaporation from standard evaporation pans. Sask. Res. Council Rep. 70-6, 17 pp.

Mensley, W.A. 1965. Geohydrologic aspects of salt disposal in Saskatchewan. Sask. Dept. Industry & Commerce, Regina, Sask., pp. 223-226.

Meneley, W.A. 1970. Geotechnology. *In* Physical Environment of Saskatoon. Edited by E.A. Christiansen. Nat. Res. Council Canada, Ottawa, Ont.

Merino, E. 1975. Diagenesis in Tertiary sandstones from Kettleman North Dome, California. II. Interstadial solutions: distribution of aqueous species at 100°C and chemical relation to the diagenetic mineralogy. Geochim. Cosmochim. Acta, 39:1629-1647.

Meyboom, P. 1963. Patterns of groundwater flow in the prairie profile. Proc. Hydrol. Symp. No. 3, Nat. Res. Council Canada, pp. 5-20.

Meyboom, P. 1966a. Groundwater studies in the Assiniboine River Drainage Basin, Part I: The evaluation of a flow system in south-central Saskatchewan. Geol. Surv. Can. Bull, 139. 62 pp.

Meyboom, P. 1966b. Unsteady groundwater flow near a willow ring in hummocky moraine. J. Hydrol. 4:38-62.

Norris, S.E. 1962. Permeability of glacial till. U.S. Geol. Surv. Prof. Paper 450-E: 150-151.

Patten, E.P. Jr. 1965. Design, construction, and use of electric analog models. *In* Analog model study of ground water in the Houston district, Texas. Texas Water Comm. Bull. 6508.

Pawluk, S., and Bayrock, L.A. 1969. Some characteristics and physical properties of Alberta tills. Res. Council Alberta Bull. 26.

Peterson, R. 1954. Studies of Bearpaw shale at a dam site in Saskatchewan. Proc. Am. Soc. Civil Eng., Vol. 80, separate no. 476.

Plummer, L.N. 1972. Program WATEQ–Fortran IV version. U.S. Geol. Surv., Reston, Virginia.

Plummer, L.N. 1975. Program WATEQF–a Fortran IV version of WATEQ. U.S. Geol. Surv., Reston. Virginia.

Poschke, K. 1965. Praktische Erfahrungen beim Betrieb der Laugenversenkanlagen im Kalikombinat "Werra". Freiberg. Forschungsh. A 354 Aufbereitung, pp. 7-22.

Richards, J.H., and Fung, K.I. 1969. Atlas of Saskatchewan. Univ. Saskatchewan, Saskatoon, Sask.

Robertson, C.E., Feth, J.H., Sachner, P.R., and Anderson, P. 1963. Differences between field and laboratory determinations of pH, alkalinity, and specific conductance of natural water. U.S. Geol. Surv. Prof. Paper 475-C, C212-C215.

Rozkowski, A. 1967. The origin of hydrochemical patterns in hummocky moraine. Can. J. Earth Sci. 4:1065-1092.

Rutherford, A.A. 1966. Water quality survey of Saskatchewan groundwaters. ARDA Project C-66-1, Chem. Div., Sask. Res. Council.

Sekerka, Ivan, and Lechner, J.F. 1974. Influence of container material on the loss of silver, mercuric and cupric ions from water solutions. Inland Waters Directorate, Environment Canada, Tech. Bull. No. 69.

Skibitzke, H.E. 1961. The use of analog computers for studies in groundwater hydrology. Geol. Soc. London, Inst. Water Eng., Vol. 17, No. 3.

Skougstad, M.W. 1975. Reliability of water-quality data. Int. Symp. Geochem. Natural Waters, Canada Centre for Inland Waters, Burlington, Ontario.

Sloan, C.E. 1972. Groundwater hydrology of prairie potholes in North Dakota. U.S. Geol. Surv. Prof. Paper 585-C.

Smoak, W.G., Wong, C.M., Savage, W.F., Rinne, W.W., and Gransee, Col. 1969. Spray systems–a method of increasing water evaporation rates to facilitate brine disposal from desalting plants. U.S. Dept. Interior, Bur. Reclamation, Res. & Development Prog. Rep. no. 480 (contract 14-01-0001-1306).

Streeton, D.H. 1967. The geology of the Prairie Evaporite Formation of the Yorkton area, Saskatchewan. Unpubl. M.A. thesis, Univ. Saskatchewan, Saskatoon, Sask.

Todd, D.K. 1959. Groundwater Hydrology. John Wiley & Sons, New York, 336 pp.

Topilka, J.D. 1967. Farm water wells. Water Stud. Inst., Saskatoon, Sask., Rep. no. 3, pp. 36-40.

Toth, J. 1963. A theoretical analysis of groundwater flow in small drainage basin J. Geophys. Res. 68(16):4795-4811.

Traversy, W.J. 1971. Methods for chemical analyses of waters and wastewaters. Water Quality Div., Inland Waters Branch, Dept. Fisheries and Forestry, Ottawa, Canada.

Traversy, W.J., and Wales, R.W. 1970. Interlaboratory quality control study no. 1: calcium, total hardness, sodium, and potassium. Rep. Ser. No. 12, Inland Waters Branch, Dept. Energy, Mines and Resources, Ottawa, Canada.

Truesdell, A.H., and Jones, B.F. 1974. WATEQ, a computer program for calculating mineral equilibria of natural waters. J. Res., U.S. Geol. Surv. 2(2):233-248.

Vandenberg, A. 1978. An unusual pumptest near Esterhazy, Saskatchewan. Inland Waters Directorate, Environment Canada, Sci. Ser. No. 102.

Van der Kamp, G. 1976. Determining aquifer transmissivity by means of well response tests: the underdamped case. Water Resour. Res. 12:71-77.

van Everdingen, R.O. 1968. The influence of the South Saskatchewan reservoir on the local groundwater regime–a prognosis. Geol. Surv. Can. Paper 65-39.

van Everdingen, R.O. 1971. Surface-water composition in southern Manitoba reflecting discharge of saline subsurface waters and subsurface solution of evaporites. Geol. Assoc. Canada Spec. Paper No. 9:343-352.

Vonhof, J.A. 1970. Waste disposal at International Minerals and Chemical Corporation (Canada) Ltd. K2 Plant, Gerald, Saskatchewan. Internal report.

Vonhof, J.A. 1975a. Waste disposal problems near potash mines in Saskatchewan, Canada. Moscow Symp. Groundwater Pollution, Int. Assoc. Sci. Hydrol., IASH-AIHS Publ. no. 103, pp. 191-215.

Vonhof, J.A. 1975b. Hydrodynamic response–or slug tests as a means to monitor the progress of well development. Can. Geotech. J. 12:1-12.

Wainerdi, R.E., and Uken, E.A. (ed.) 1971. Modern Methods of Geochemical Analysis. Plenum Press, New York.

Wallick, E.I., and Krouse, H.R. 1977. Sulphur isotope geochemistry of a groundwater generated Na_2SO_4/Na_2CO_3 deposit and the associated drainage basin of Horseshoe Lake, Metiskow, east central Alberta, Canada. Proc. 2nd Int. Symp. Water-Rock Interaction, Strasbourg, August 17-25, 1977.

Walton, W.C., and Prickett, T.A. 1963. Hydrogeologic electric analog computers. Proc. Amer. Soc. Civil Eng. 89 (HY 6): 67-90.

Wardlaw, N.C. 1968. Carnallite-sylvite relationship in the Middle Devonian Prairie Evaporite Formation, Saskatchewan. Geol. Soc. Am. Bull. 49:331-342.

Wartena, L. 1974. Basic difficulties in predicting evaporation. J. Hydrol. 23:159-177.

Weyer, K.U. 1972. Conceptual models for evaluation of the subterranean water cycle in Paleozoic highlands. Proc. 24th Int. Geol. Congr., section 11, Montreal, Canada, pp. 107-117.

Weyer, K.U. 1973. Modelvorstellungen zur Untersuchung der unterirdischen Wasserzirkulation im Mittelgebirgen mit anstehenden Festgestein. Deutsch. Gewaesserkd. Mitt. 17 (4): 106-112.

Weyer, K.U., and Feder, G.L. 1978. Suggested field procedures for collection of groundwater samples for inorganic analysis. Guide prepared for Groundwater Quantity and Quality Control Committee, Int. Poplar River Water Quality Board, Int. Joint Comm., 12 pp.

Whitfield, M. 1974. Thermodynamic limitations on the use of the platimum electrode in Eh measurements. Limnol. Oceanogr. 19(5):857-865.

Wickenden, R.T.D. 1945. Mesozoic stratigraphy of the eastern Plains, Manitoba and Saskatchewan. Geol. Surv. Canada Man. 239, 87 pp.

Wigley, T.M.L. 1971. Ion pairing and water quality measurements. Can. J. Earth Sci. 8(4):468-476.

Wright, C.E. 1972. Bedrock geology of the Qu'Appelle Valley south of Esterhazy. *In* Guidebook on Geology and Its Application to Engineering Practice in the Qu'Appelle Valley Area. Edited by E.A. Christiansen. Regina Geotech. Group and Sask. Geol. Soc., pp. 35-39.

Illustrations

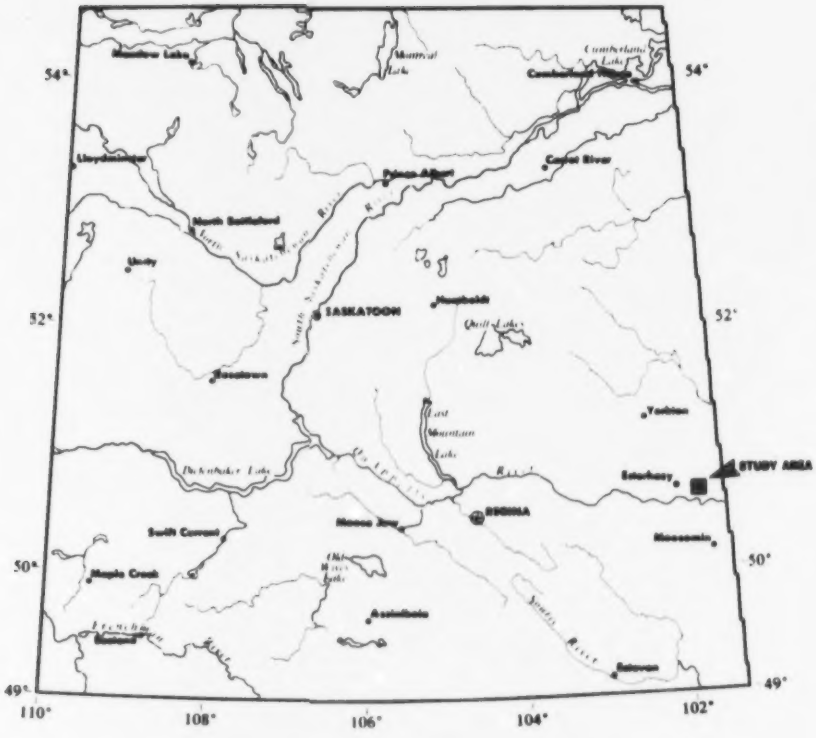

Figure 1. Location of area under investigation.

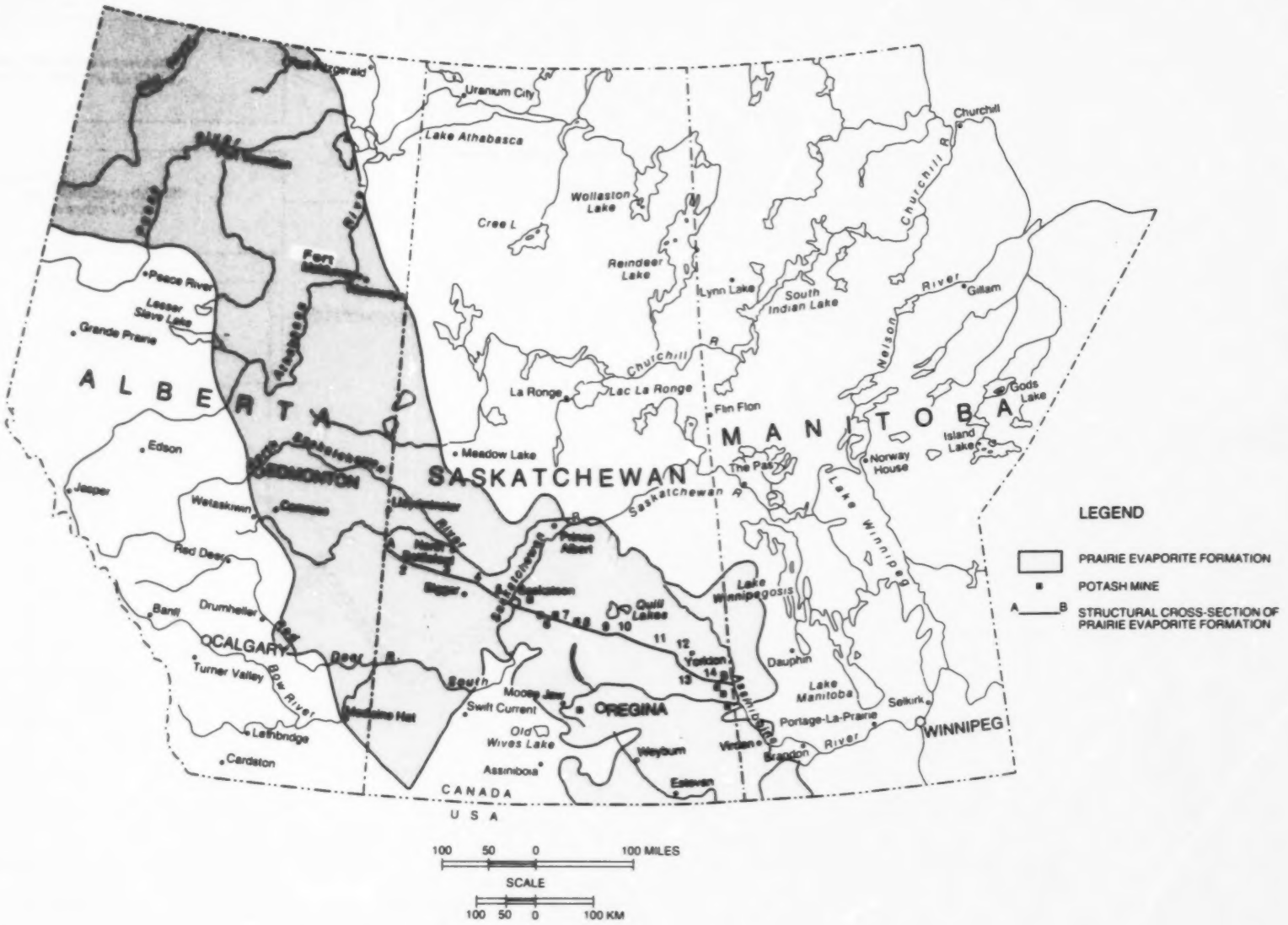

Figure 2. Distribution of Prairie Evaporite Formation in Prairie Provinces.

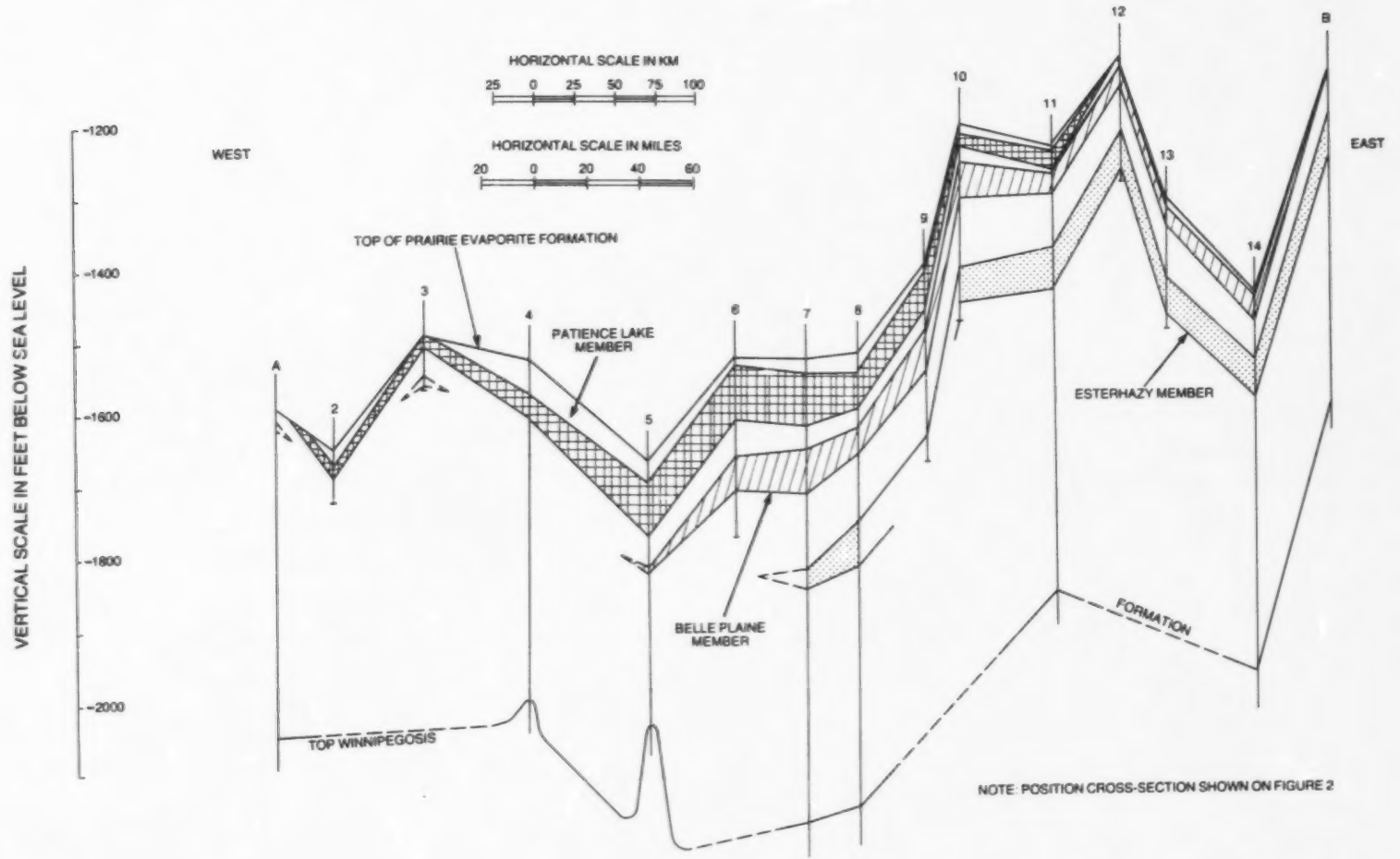

Figure 3. Structural cross section of Prairie Evaporite Formation, Saskatchewan.

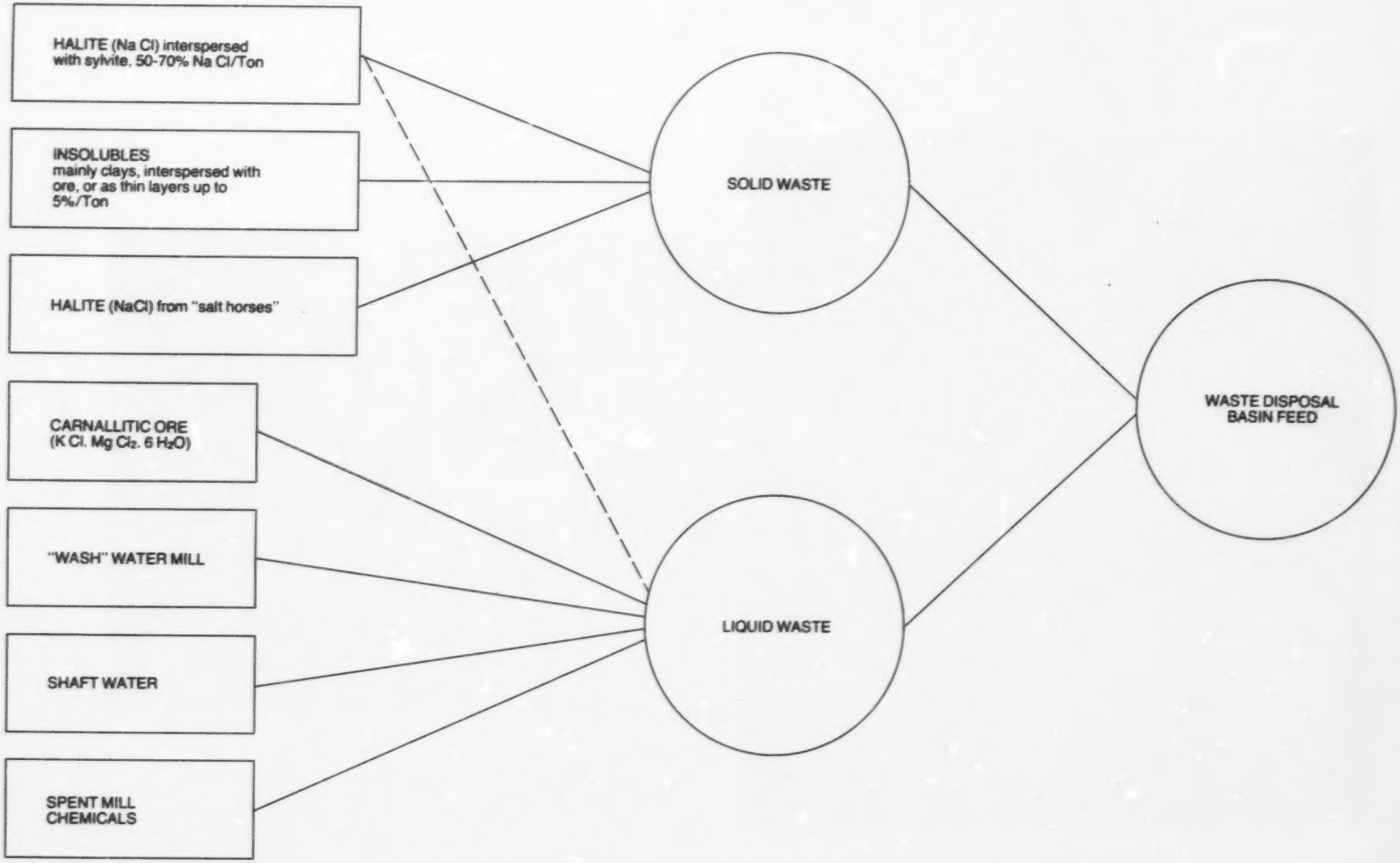
HALITE (Na Cl) interspersed with sylvite, 50-70% Na Cl/Ton
INSOLUBLES mainly clays, interspersed with ore, or as thin layers up to 5%/Ton
HALITE (NaCl) from "salt horses"
CARNALLITIC ORE (K Cl. Mg Cl2. 6 H2O)
"WASH" WATER MILL
SHAFT WATER
SPENT MILL CHEMICALS
SOLID WASTE
LIQUID WASTE
WASTE DISPOSAL BASIN FEED

Figure 4. Kind and origin of wastes in the Saskatchewan potash industry.

Figure 5. Waste disposal basin, I.M.C.C. K2 potash plant, Esterhazy, Saskatchewan

Figure 6. Dyke erosion.

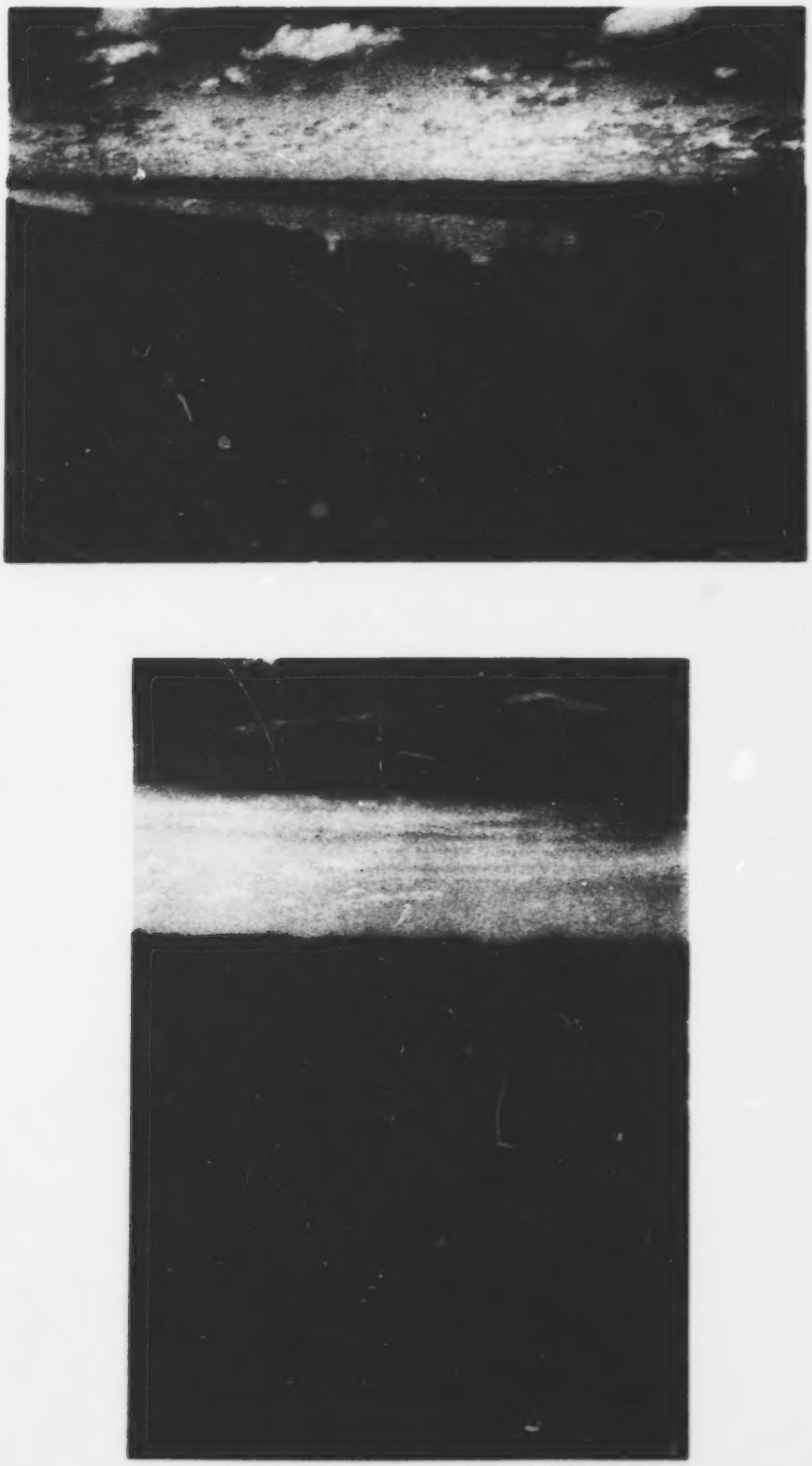

Figure 7. Dyke protection (upper) straw bale boom (lower) conveyor belt.

Figure 7. (cont'd) Dyke protection (upper) car wrecks (lower) waste salt covers.

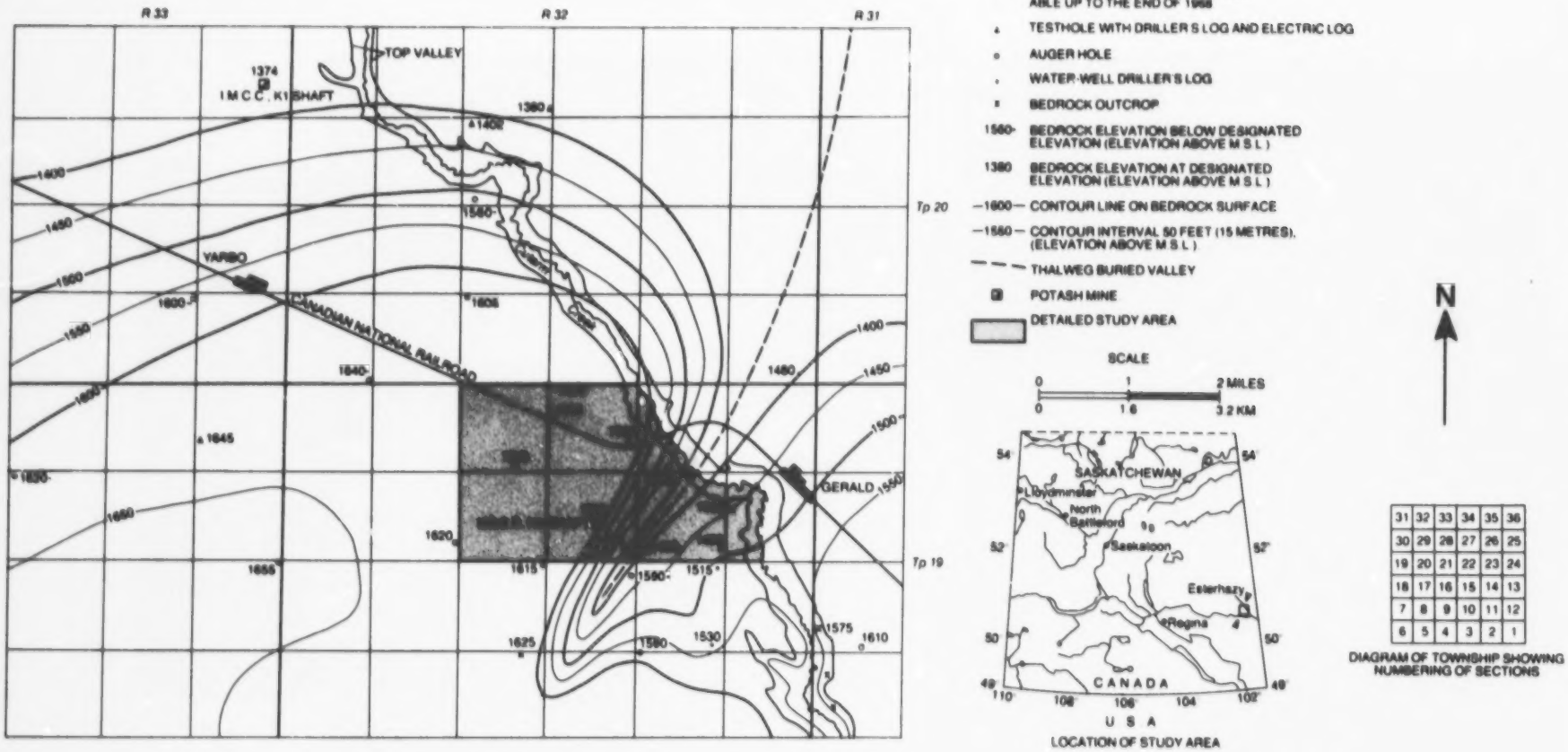

Figure 8. Pre-1969 bedrock topography.

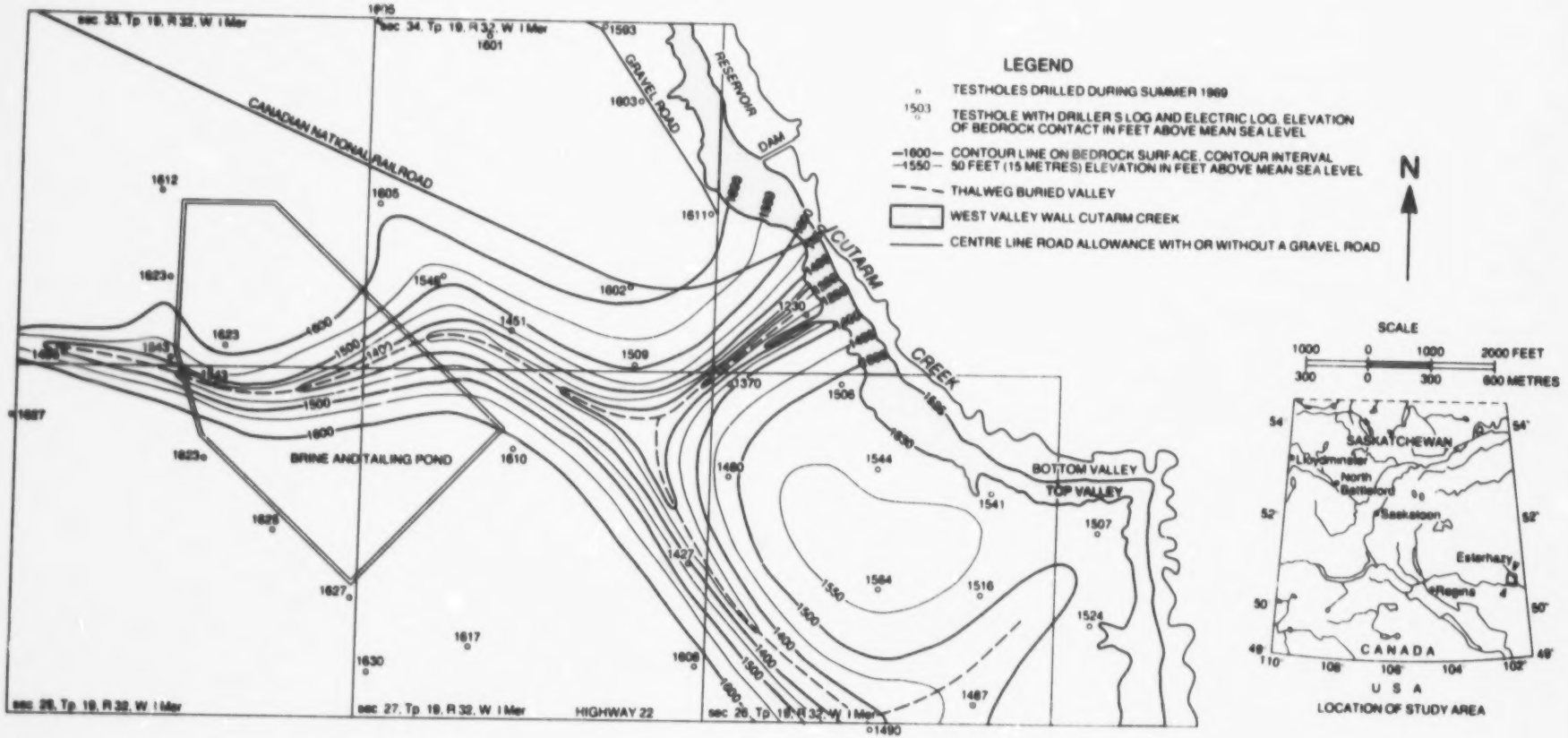
LEGEND
TESTHOLES DRILLED DURING SUMMER 1969
1503 TESTHOLE WITH DRILLER'S LOG AND ELECTRIC LOG, ELEVATION OF BEDROCK CONTACT IN FEET ABOVE MEAN SEA LEVEL
—1600— CONTOUR LINE ON BEDROCK SURFACE, CONTOUR INTERVAL —1550— 50 FEET (15 METRES) ELEVATION IN FEET ABOVE MEAN SEA LEVEL
THALWEG BURIED VALLEY
WEST VALLEY WALL CUTARM CREEK
CENTRE LINE ROAD ALLOWANCE WITH OR WITHOUT A GRAVEL ROAD
N
SCALE
1000 0 1000 2000 FEET
300 0 300 600 METRES
CANADIAN NATIONAL RAILROAD
GRAVEL ROAD
RESERVOIR DAM
CUTARM CREEK
BRINE AND TAILING POND
BOTTOM VALLEY
TOP VALLEY
HIGHWAY 22
sec 33, Tp 19, R 32, W 1 Mer
sec 34, Tp 19, R 32, W 1 Mer
sec 28, Tp 19, R 32, W 1 Mer
sec 27, Tp 19, R 32, W 1 Mer
sec 26, Tp 19, R 32, W 1 Mer
SASKATCHEWAN
Lloydminster
North Battleford
Saskatoon
Estevan
Regina
CANADA
U S A
LOCATION OF STUDY AREA

Figure 9. Bedrock topography after 1969 drilling program.

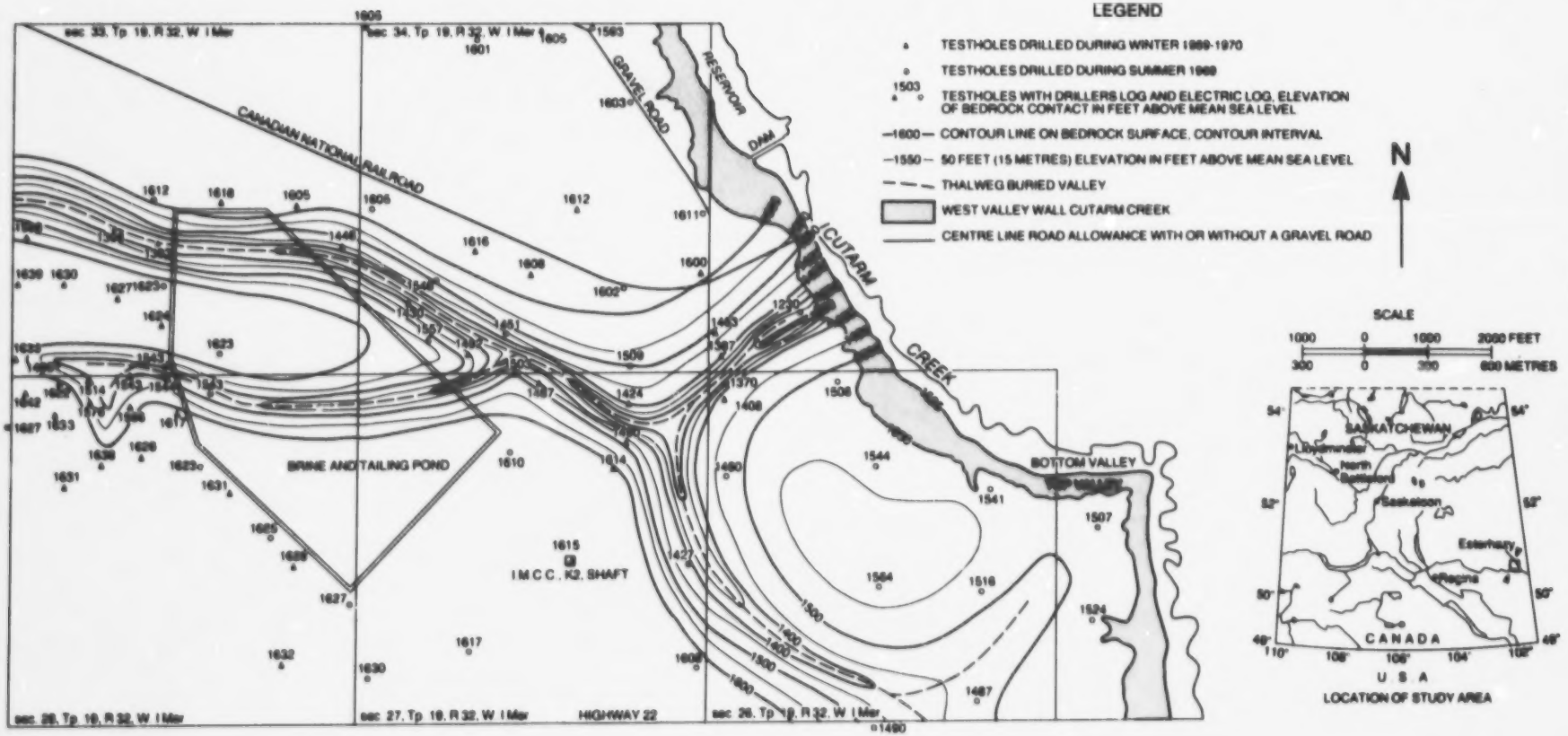
LEGEND
TESTHOLES DRILLED DURING WINTER 1969-1970
TESTHOLES DRILLED DURING SUMMER 1969
1503
TESTHOLES WITH DRILLERS LOG AND ELECTRIC LOG, ELEVATION OF BEDROCK CONTACT IN FEET ABOVE MEAN SEA LEVEL
—1600— CONTOUR LINE ON BEDROCK SURFACE, CONTOUR INTERVAL
—1550— 50 FEET (15 METRES) ELEVATION IN FEET ABOVE MEAN SEA LEVEL
THALWEG BURIED VALLEY
WEST VALLEY WALL CUTARM CREEK
CENTRE LINE ROAD ALLOWANCE WITH OR WITHOUT A GRAVEL ROAD
N
SCALE
1000 0 1000 2000 FEET
300 0 300 600 METRES
CANADIAN NATIONAL RAILROAD
GRAVEL ROAD
RESERVOIR
DAM
CUTARM CREEK
BRINE AND TAILING POND
IMCC K2 SHAFT
BOTTOM VALLEY
HIGHWAY 22
sec 33, Tp 19, R 32, W I Mer
sec 34, Tp 19, R 32, W I Mer
sec 28, Tp 19, R 32, W I Mer
sec 27, Tp 19, R 32, W I Mer
sec 26, Tp 19, R 32, W I Mer
SASKATCHEWAN
Lloydminster
North Battleford
Saskatoon
Estevan
Regina
CANADA
U S A
LOCATION OF STUDY AREA

Figure 10. Bedrock topography after 1969-1970 drilling program.

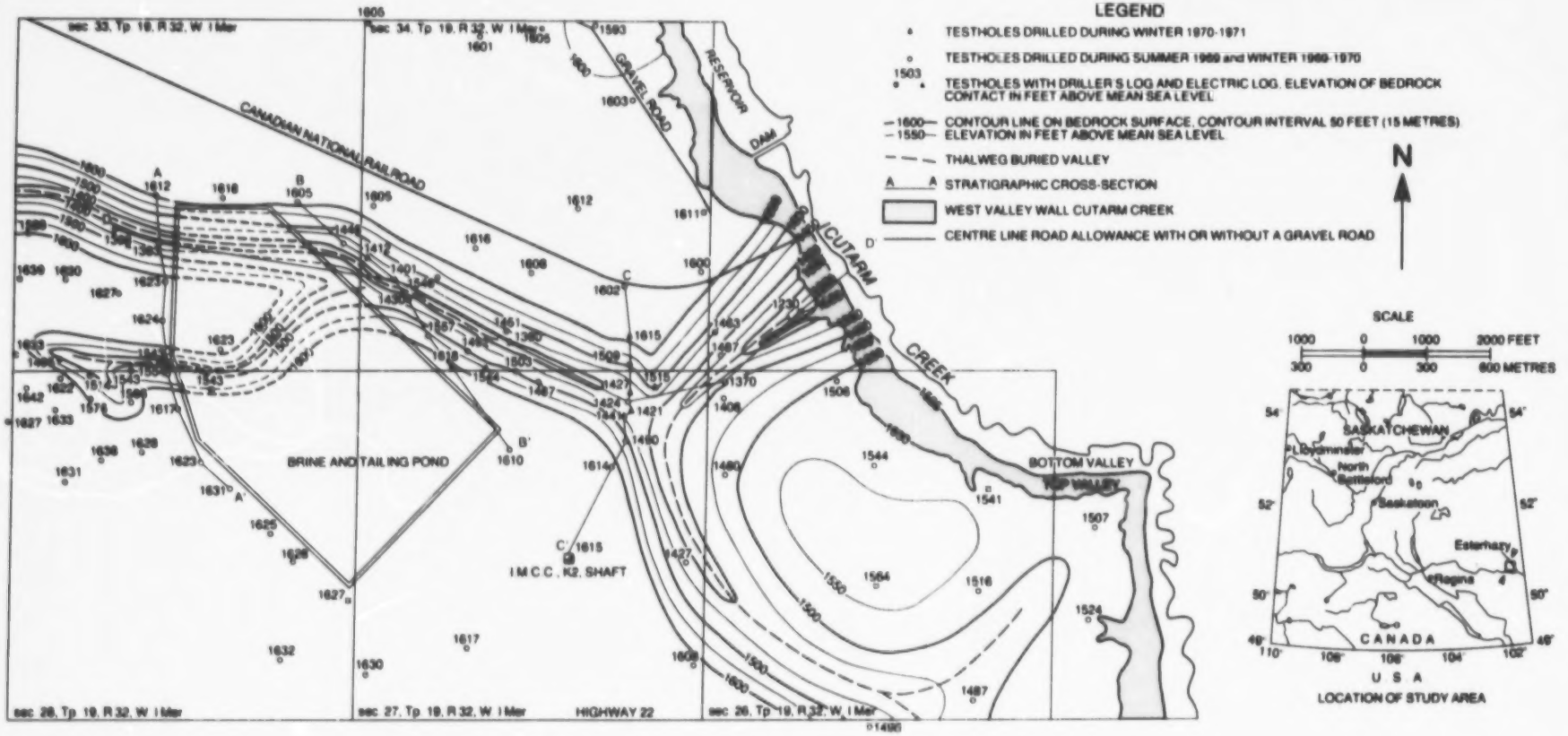
LEGEND
TESTHOLES DRILLED DURING WINTER 1970-1971
TESTHOLES DRILLED DURING SUMMER 1969 and WINTER 1969-1970
1503 TESTHOLES WITH DRILLER S LOG AND ELECTRIC LOG. ELEVATION OF BEDROCK CONTACT IN FEET ABOVE MEAN SEA LEVEL
1600 CONTOUR LINE ON BEDROCK SURFACE. CONTOUR INTERVAL 50 FEET (15 METRES)
1550 ELEVATION IN FEET ABOVE MEAN SEA LEVEL
THALWEG BURIED VALLEY
A A STRATIGRAPHIC CROSS-SECTION
WEST VALLEY WALL CUTARM CREEK
CENTRE LINE ROAD ALLOWANCE WITH OR WITHOUT A GRAVEL ROAD
N
SCALE
1000 0 1000 2000 FEET
300 0 300 600 METRES
sec 33, Tp 19, R 32, W 1 Mer
sec 34, Tp 19, R 32, W 1 Mer
sec 28, Tp 19, R 32, W 1 Mer
sec 27, Tp 19, R 32, W 1 Mer
sec 26, Tp 19, R 32, W 1 Mer
CANADIAN NATIONAL RAILROAD
GRAVEL ROAD
RESERVOIR
DAM
CUTARM CREEK
BRINE AND TAILING POND
BOTTOM VALLEY
TOP VALLEY
I M C C . K2. SHAFT
HIGHWAY 22
SASKATCHEWAN
Lloydminster
North Battleford
Saskatoon
Estevan
Regina
CANADA
U S A
LOCATION OF STUDY AREA

Figure 11. Bedrock topography after 1970-1971 and 1972-1973 drilling program.

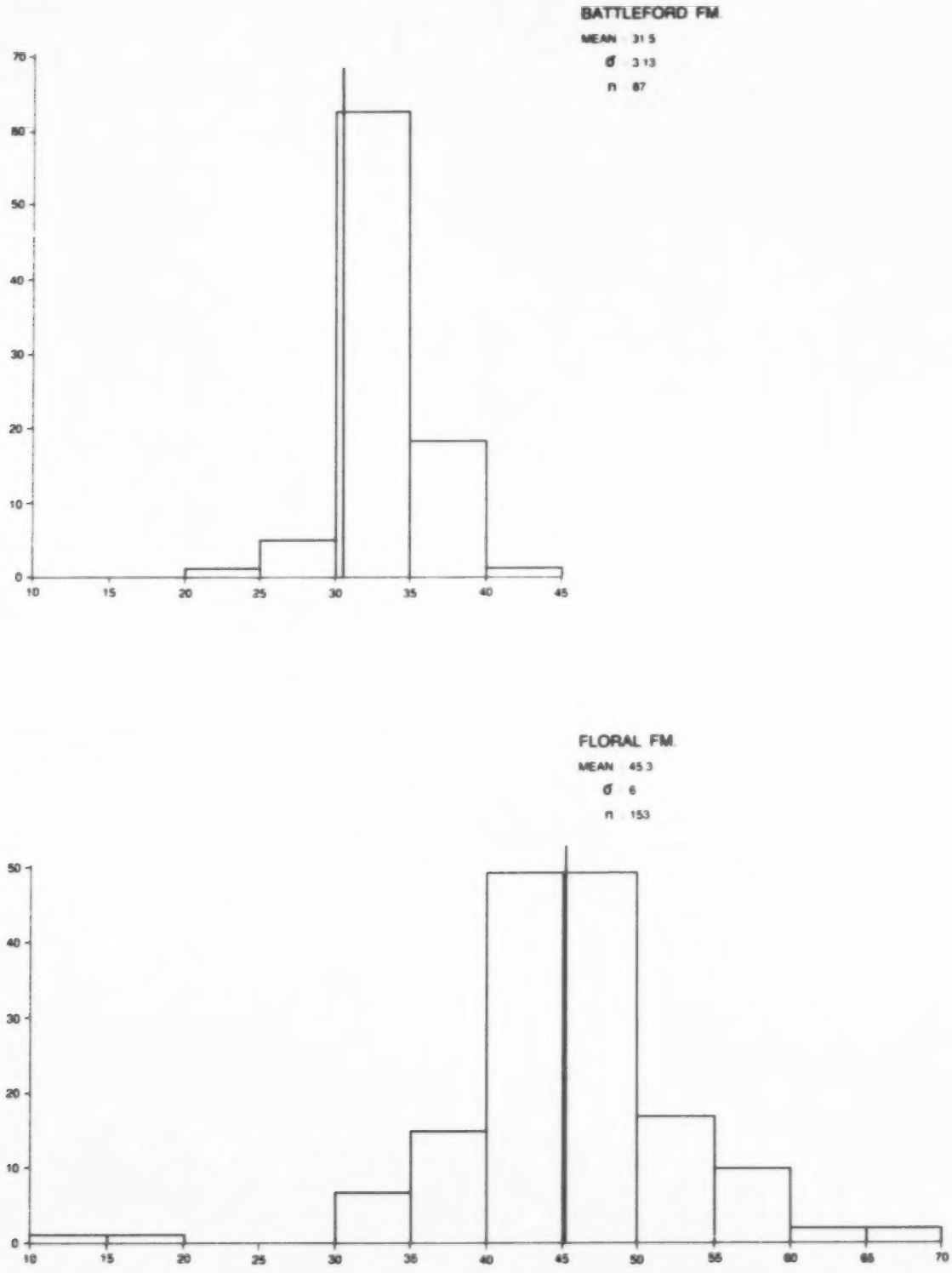

Figure 12. Total carbonate content in Battleford and Floral Formations.

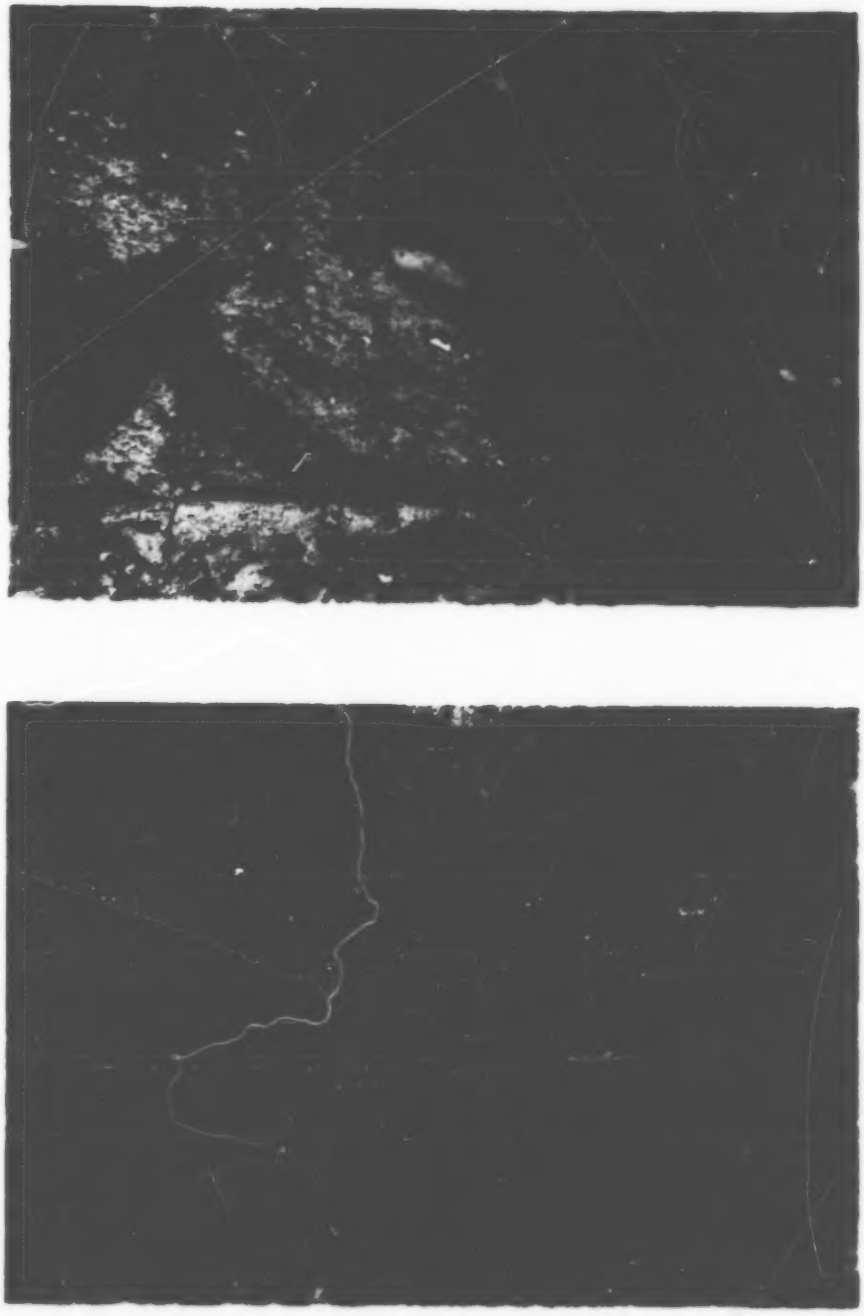

Figure 13. Oxidized fractures in till (Floral Formation).

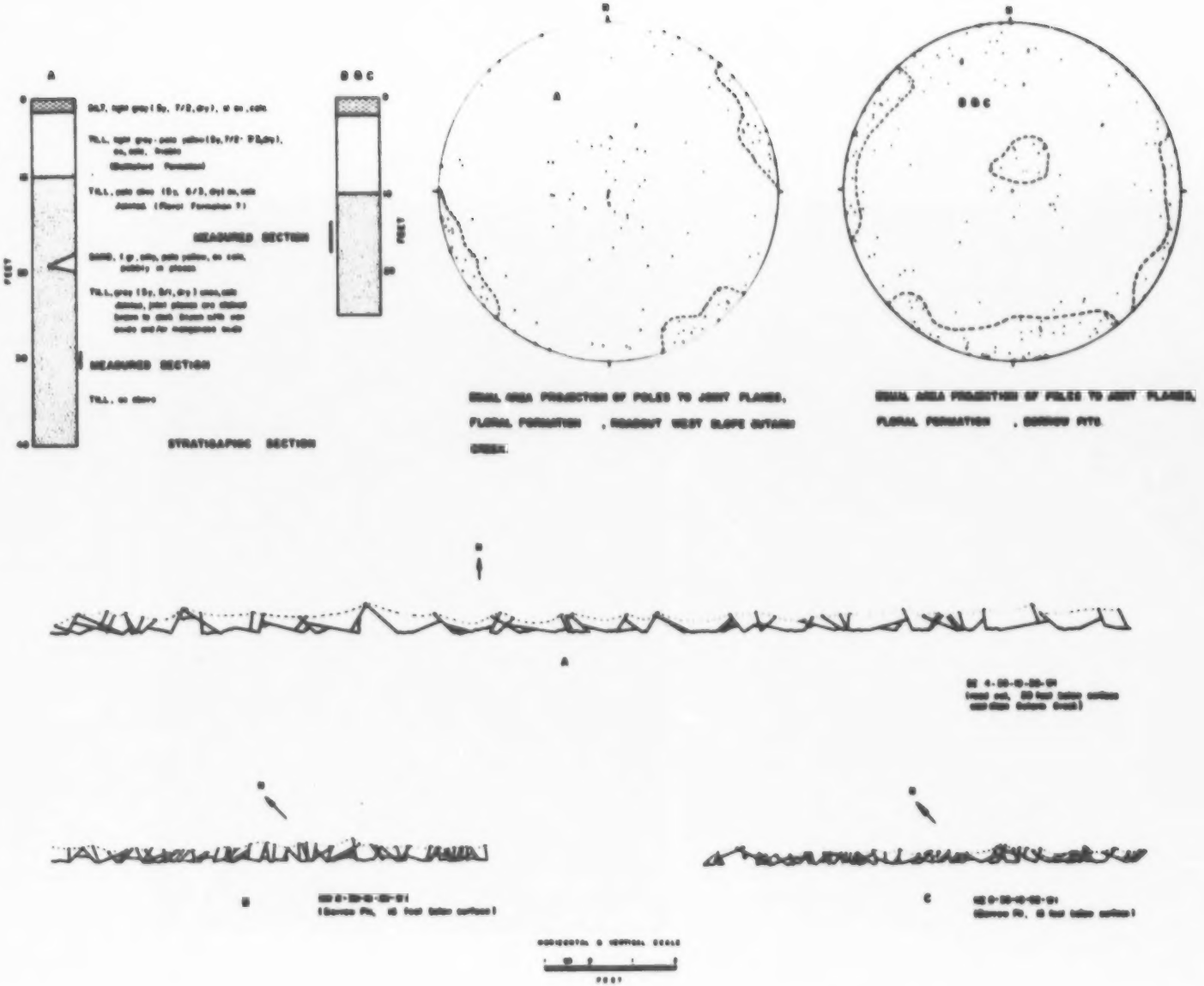

Figure 14. Plan view and polar projection of fracture pattern in Floral Formation.

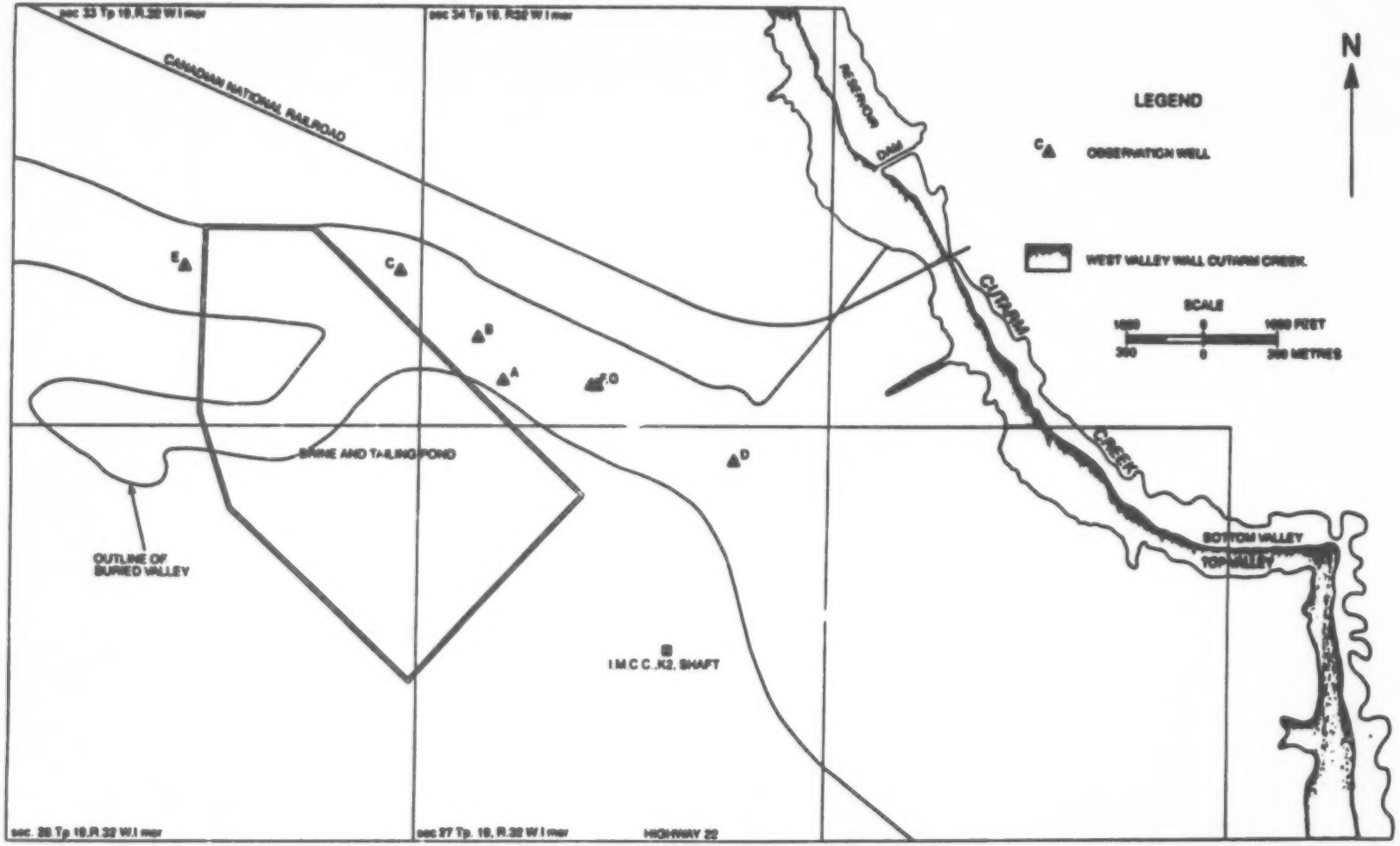

Figure 15. Location of observation wells.

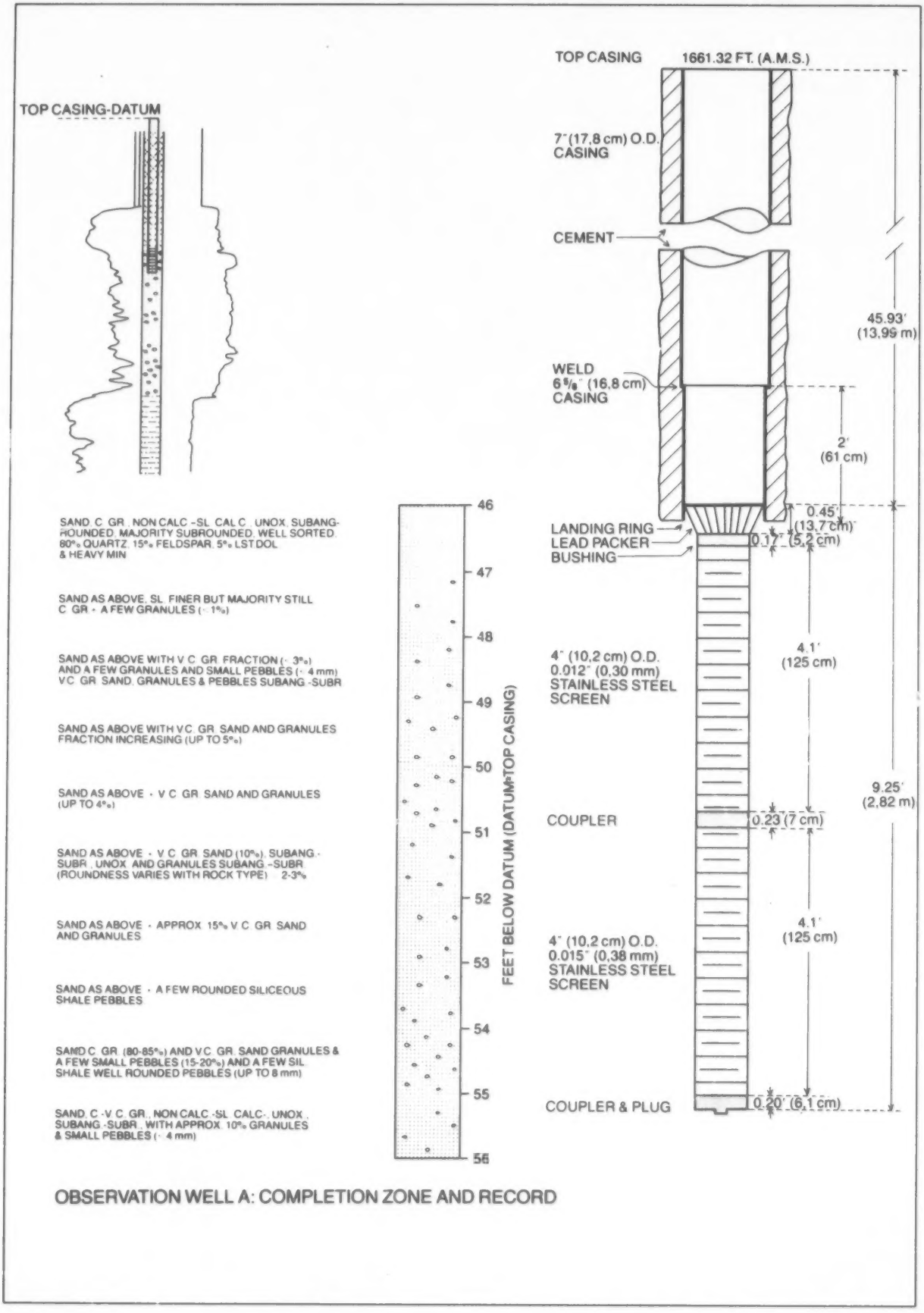
TOP CASING-DATUM
SAND, C, GR., NON CALC -SL. CAL C., UNOX, SUBANG-ROUNDED, MAJORITY SUBROUNDED, WELL SORTED, 80% QUARTZ, 15% FELDSPAR, 5% LST.DOL & HEAVY MIN
SAND AS ABOVE, SL. FINER BUT MAJORITY STILL C. GR. - A FEW GRANULES (< 1%)
SAND AS ABOVE WITH V.C. GR. FRACTION (< 3%) AND A FEW GRANULES AND SMALL PEBBLES (< 4 mm) V.C. GR. SAND, GRANULES & PEBBLES SUBANG.-SUBR
SAND AS ABOVE WITH V.C. GR. SAND AND GRANULES FRACTION INCREASING (UP TO 5%)
SAND AS ABOVE - V.C. GR. SAND AND GRANULES (UP TO 4%)
SAND AS ABOVE - V.C. GR. SAND (10%), SUBANG.-SUBR., UNOX. AND GRANULES SUBANG.-SUBR. (ROUNDNESS VARIES WITH ROCK TYPE) 2-3%
SAND AS ABOVE - APPROX. 15% V.C. GR. SAND AND GRANULES
SAND AS ABOVE - A FEW ROUNDED SILICEOUS SHALE PEBBLES
SAND, C. GR. (80-85%) AND V.C. GR. SAND GRANULES & A FEW SMALL PEBBLES (15-20%) AND A FEW SIL. SHALE WELL ROUNDED PEBBLES (UP TO 8 mm)
SAND, C.-V.C. GR., NON CALC.-SL. CALC., UNOX., SUBANG.-SUBR., WITH APPROX. 10% GRANULES & SMALL PEBBLES (< 4 mm)
46
47
48
49
50
51
52
53
54
55
56
FEET BELOW DATUM (DATUM=TOP CASING)
TOP CASING
1661.32 FT. (A.M.S.)
7" (17,8 cm) O.D. CASING
CEMENT
45.93' (13,99 m)
WELD
6 5/8" (16,8 cm) CASING
2' (61 cm)
0.45' (13,7 cm)
LANDING RING
LEAD PACKER
BUSHING
0.17' (5,2 cm)
4" (10,2 cm) O.D. 0.012" (0,30 mm) STAINLESS STEEL SCREEN
4.1' (125 cm)
9.25' (2,82 m)
COUPLER
0.23' (7 cm)
4" (10,2 cm) O.D. 0.015" (0,38 mm) STAINLESS STEEL SCREEN
4.1' (125 cm)
COUPLER & PLUG
0.20' (6,1 cm)

OBSERVATION WELL A: COMPLETION ZONE AND RECORD

Figure 16. Observation well A: completion zone and record.

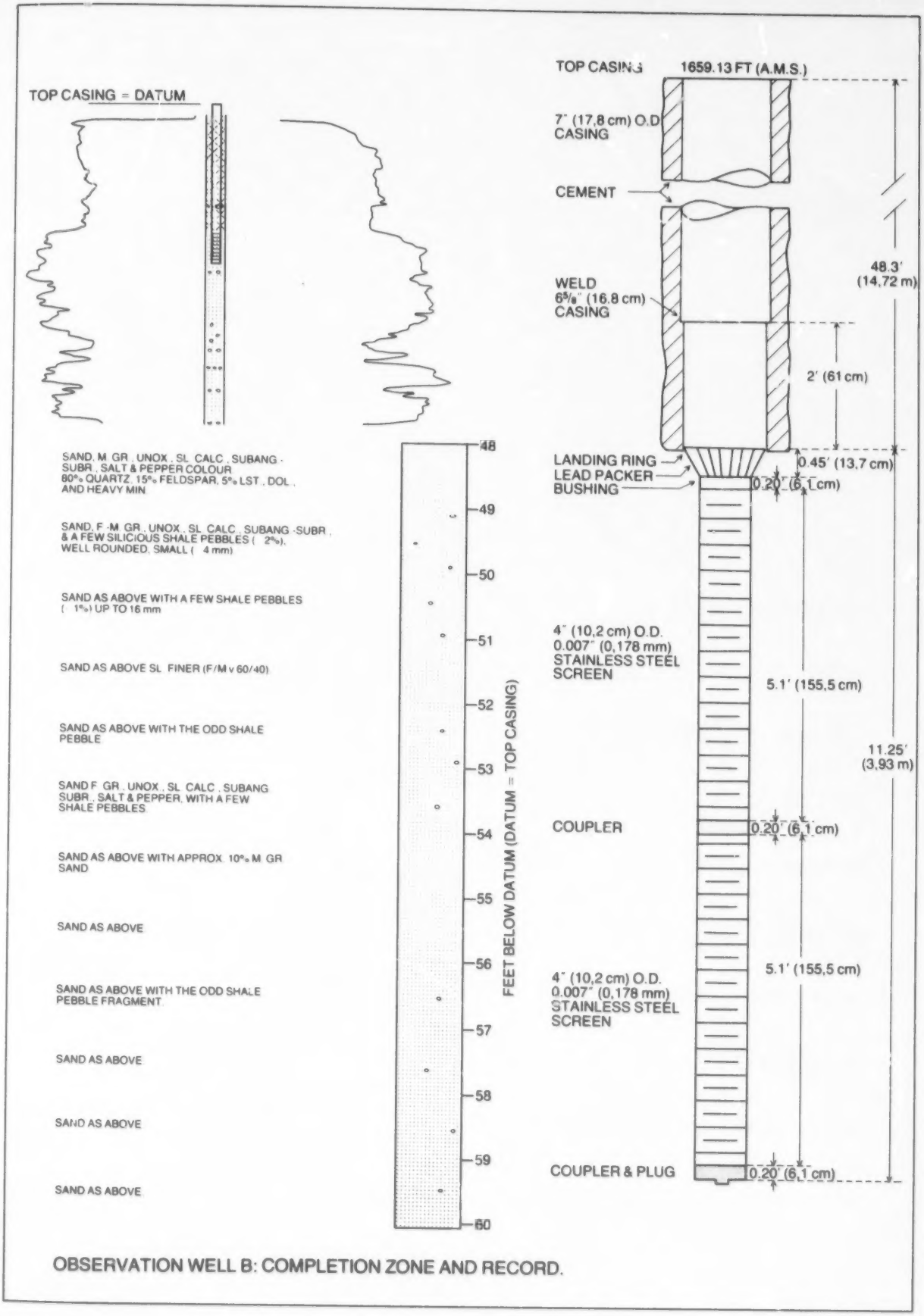
TOP CASING = DATUM
SAND, M. GR., UNOX., SL. CALC., SUBANG - SUBR., SALT & PEPPER COLOUR 80% QUARTZ, 15% FELDSPAR, 5% LST., DOL., AND HEAVY MIN.
SAND, F.-M. GR., UNOX., SL. CALC., SUBANG.-SUBR., & A FEW SILICIOUS SHALE PEBBLES (2%), WELL ROUNDED, SMALL (4 mm)
SAND AS ABOVE WITH A FEW SHALE PEBBLES (1%) UP TO 16 mm
SAND AS ABOVE SL. FINER (F/M v 60/40)
SAND AS ABOVE WITH THE ODD SHALE PEBBLE
SAND F. GR., UNOX., SL. CALC., SUBANG SUBR., SALT & PEPPER, WITH A FEW SHALE PEBBLES
SAND AS ABOVE WITH APPROX. 10% M. GR. SAND
SAND AS ABOVE
SAND AS ABOVE WITH THE ODD SHALE PEBBLE FRAGMENT
SAND AS ABOVE
SAND AS ABOVE
SAND AS ABOVE
48
49
50
51
52
53
54
55
56
57
58
59
60
FEET BELOW DATUM (DATUM = TOP CASING)
TOP CASING 1659.13 FT (A.M.S.)
7" (17,8 cm) O.D. CASING
CEMENT
WELD
6⅝" (16.8 cm) CASING
48.3' (14,72 m)
2' (61 cm)
LANDING RING
LEAD PACKER
BUSHING
0.45' (13,7 cm)
0.20' (6,1 cm)
4" (10,2 cm) O.D. 0.007" (0,178 mm) STAINLESS STEEL SCREEN
5.1' (155,5 cm)
11.25' (3,93 m)
COUPLER
0.20' (6,1 cm)
5.1' (155,5 cm)
4" (10,2 cm) O.D. 0.007" (0,178 mm) STAINLESS STEEL SCREEN
COUPLER & PLUG
0.20' (6,1 cm)
OBSERVATION WELL B: COMPLETION ZONE AND RECORD.

Figure 17. Observation well B: completion zone and record.

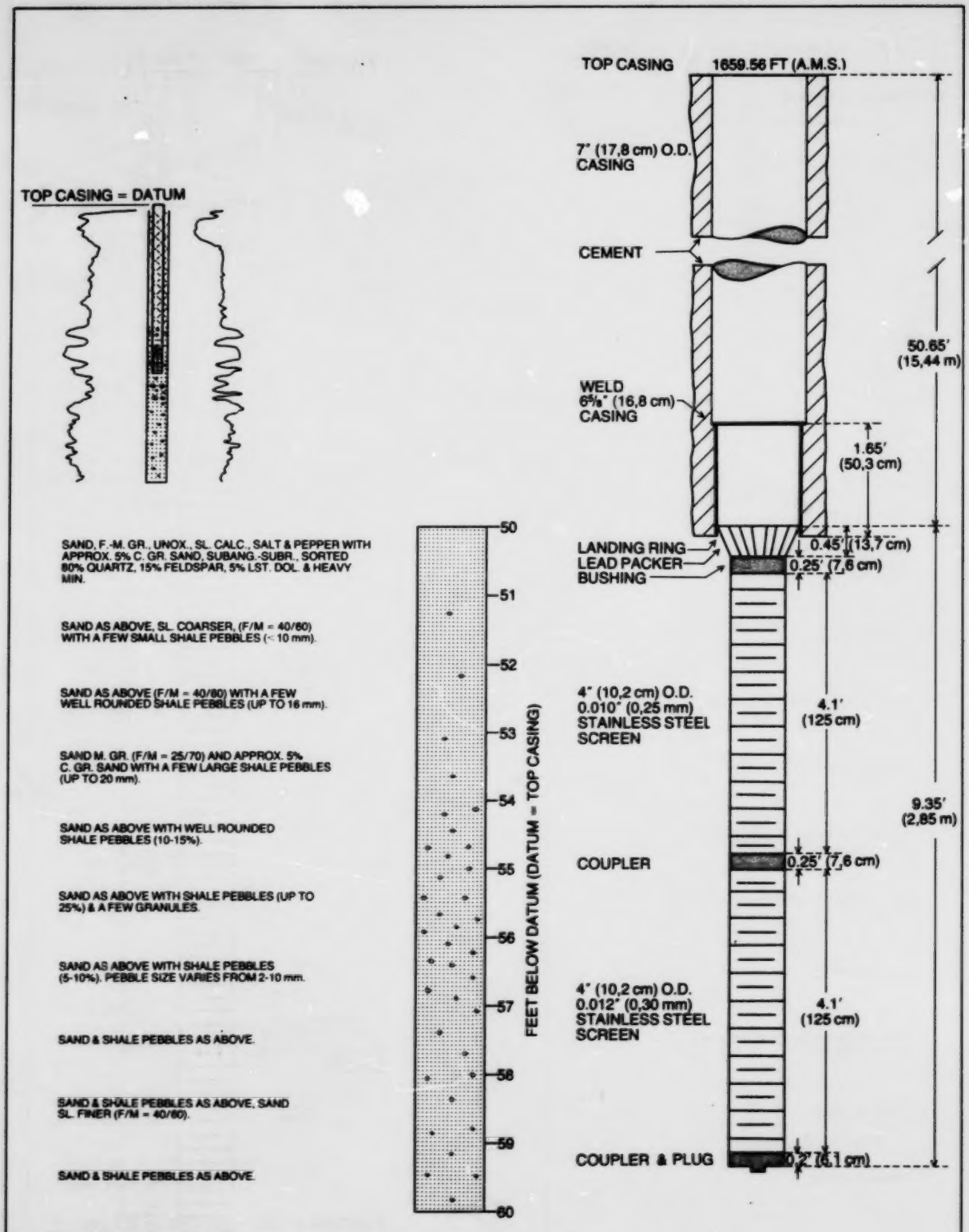
TOP CASING = DATUM
SAND, F.-M. GR., UNOX., SL. CALC., SALT & PEPPER WITH APPROX. 5% C. GR. SAND, SUBANG.-SUBR., SORTED 80% QUARTZ, 15% FELDSPAR, 5% LST. DOL. & HEAVY MIN.
SAND AS ABOVE, SL. COARSER, (F/M = 40/80) WITH A FEW SMALL SHALE PEBBLES (< 10 mm).
SAND AS ABOVE (F/M = 40/80) WITH A FEW WELL ROUNDED SHALE PEBBLES (UP TO 16 mm).
SAND M. GR. (F/M = 25/70) AND APPROX. 5% C. GR. SAND WITH A FEW LARGE SHALE PEBBLES (UP TO 20 mm).
SAND AS ABOVE WITH WELL ROUNDED SHALE PEBBLES (10-15%).
SAND AS ABOVE WITH SHALE PEBBLES (UP TO 25%) & A FEW GRANULES.
SAND AS ABOVE WITH SHALE PEBBLES (5-10%). PEBBLE SIZE VARIES FROM 2-10 mm.
SAND & SHALE PEBBLES AS ABOVE.
SAND & SHALE PEBBLES AS ABOVE, SAND SL. FINER (F/M = 40/80).
SAND & SHALE PEBBLES AS ABOVE.
50
51
52
53
54
55
56
57
58
59
60
FEET BELOW DATUM (DATUM = TOP CASING)
TOP CASING
1659.56 FT (A.M.S.)
7" (17,8 cm) O.D. CASING
CEMENT
WELD
6⅝" (16,8 cm) CASING
50.65' (15,44 m)
1.65' (50,3 cm)
LANDING RING
LEAD PACKER
BUSHING
0.45' (13,7 cm)
0.25' (7,6 cm)
4" (10,2 cm) O.D. 0.010" (0,25 mm) STAINLESS STEEL SCREEN
4.1' (125 cm)
9.35' (2,85 m)
COUPLER
0.25' (7,6 cm)
4" (10,2 cm) O.D. 0.012" (0,30 mm) STAINLESS STEEL SCREEN
4.1' (125 cm)
COUPLER & PLUG
0.27' (8,1 cm)

OBSERVATION WELL C: COMPLETION ZONE AND RECORD

Figure 18. Observation well C: completion zone and record.

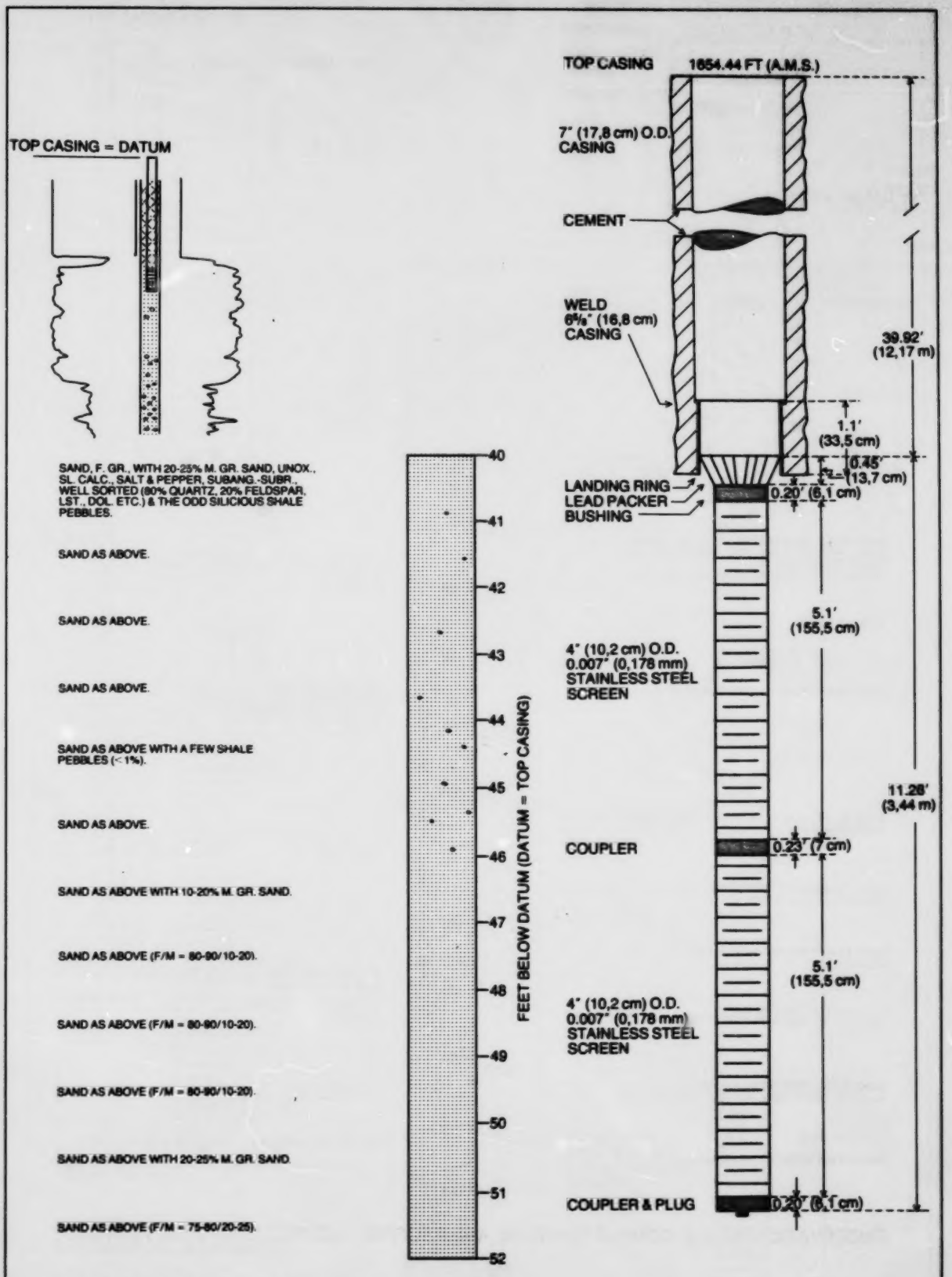

OBSERVATION WELL D: COMPLETION ZONE AND RECORD

Figure 19. Observation well D: completion zone and record.

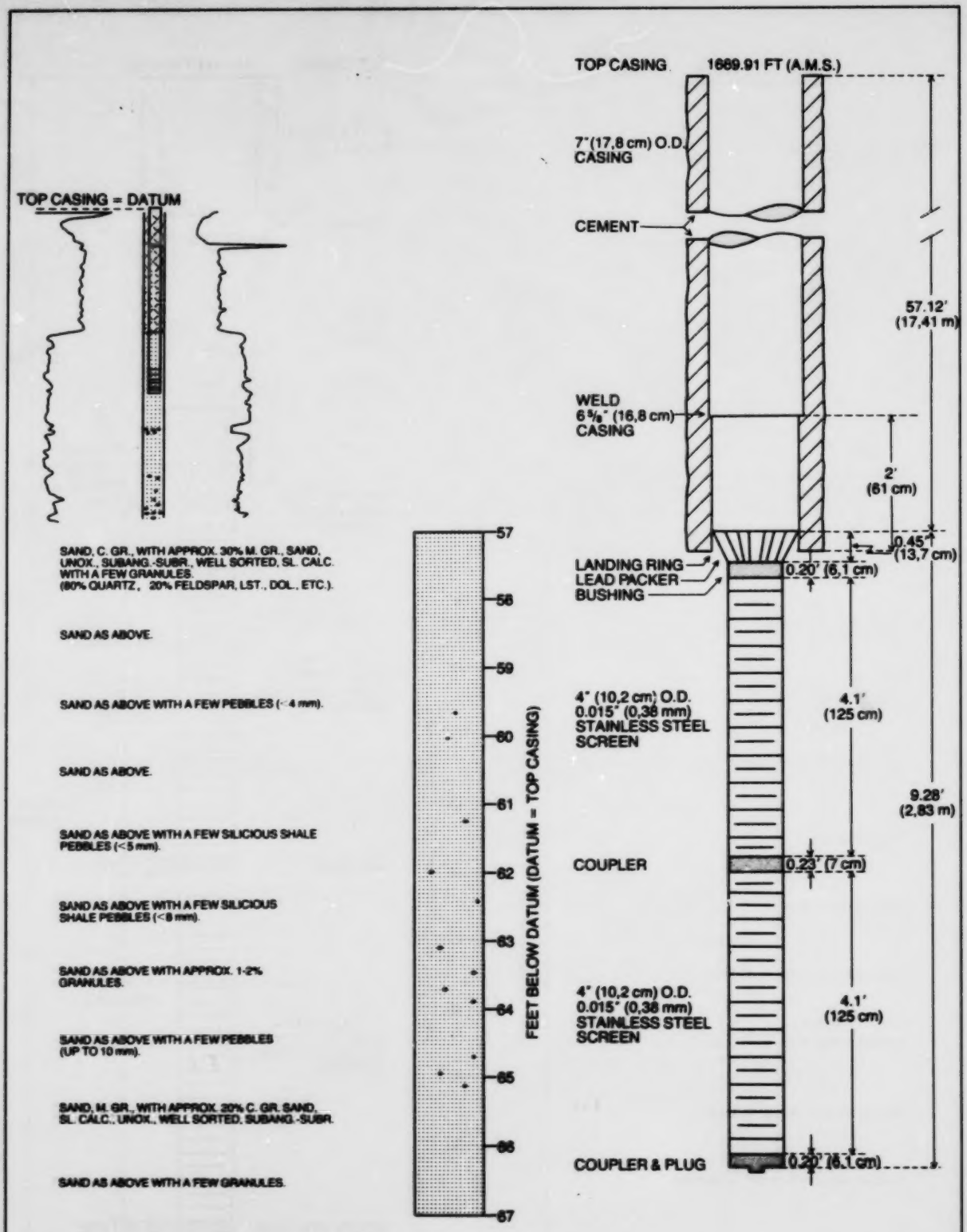
TOP CASING = DATUM
SAND, C. GR., WITH APPROX. 30% M. GR., SAND, UNOX., SUBANG.-SUBR., WELL SORTED, SL. CALC. WITH A FEW GRANULES. (80% QUARTZ, 20% FELDSPAR, LST., DOL., ETC.).
SAND AS ABOVE.
SAND AS ABOVE WITH A FEW PEBBLES (< 4 mm).
SAND AS ABOVE.
SAND AS ABOVE WITH A FEW SILICIOUS SHALE PEBBLES (< 5 mm).
SAND AS ABOVE WITH A FEW SILICIOUS SHALE PEBBLES (< 8 mm).
SAND AS ABOVE WITH APPROX. 1-2% GRANULES.
SAND AS ABOVE WITH A FEW PEBBLES (UP TO 10 mm).
SAND, M. GR., WITH APPROX. 20% C. GR. SAND, SL. CALC., UNOX., WELL SORTED, SUBANG.-SUBR.
SAND AS ABOVE WITH A FEW GRANULES.
57
58
59
60
61
62
63
64
65
66
67
FEET BELOW DATUM (DATUM = TOP CASING)
TOP CASING 1669.91 FT (A.M.S.)
7" (17,8 cm) O.D. CASING
CEMENT
57.12' (17,41 m)
WELD
6 5/8" (16,8 cm) CASING
2' (61 cm)
0.45' (13,7 cm)
LANDING RING
LEAD PACKER
BUSHING
0.20' (6,1 cm)
4" (10,2 cm) O.D. 0.015" (0,38 mm) STAINLESS STEEL SCREEN
4.1' (125 cm)
9.28' (2,83 m)
COUPLER
0.23' (7 cm)
4" (10,2 cm) O.D. 0.015" (0,38 mm) STAINLESS STEEL SCREEN
4.1' (125 cm)
COUPLER & PLUG
0.20' (6,1 cm)

OBSERVATION WELL E: COMPLETION ZONE AND RECORD

Figure 20. Observation well E: completion zone and record.

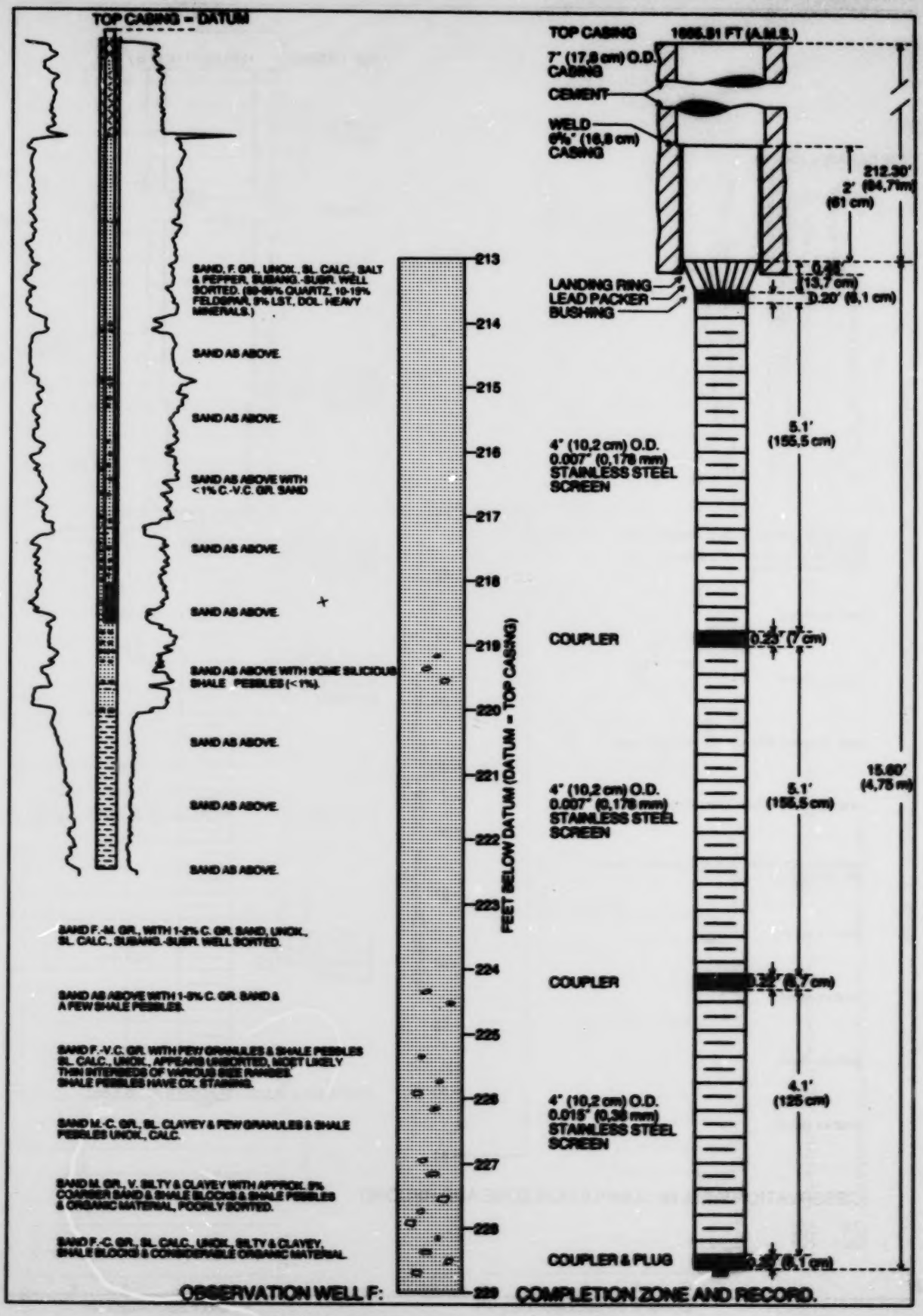
TOP CASING = DATUM
SAND, F. GR., UNIOX., SL. CALC., SALT & PEPPER, SUBANG.-SUBR. WELL SORTED. (60-65% QUARTZ, 10-15% FELDSPAR, 5% LST., DOL. HEAVY MINERALS.)
SAND AS ABOVE.
SAND AS ABOVE.
SAND AS ABOVE WITH <1% C.-V.C. GR. SAND
SAND AS ABOVE.
SAND AS ABOVE.
SAND AS ABOVE WITH SOME SILICIOUS SHALE PEBBLES (<1%).
SAND AS ABOVE.
SAND AS ABOVE.
SAND AS ABOVE.
SAND F.-M. GR., WITH 1-2% C. GR. SAND, UNIOX., SL. CALC., SUBANG.-SUBR. WELL SORTED.
SAND AS ABOVE WITH 1-2% C. GR. SAND & A FEW SHALE PEBBLES.
SAND F.-V.C. GR. WITH FEW GRANULES & SHALE PEBBLES SL. CALC., UNIOX., APPEARS UNSORTED, MOST LIKELY THIN INTERBEDS OF VARIOUS SIZE RANGES. SHALE PEBBLES HAVE OX. STAINING.
SAND M.-C. GR., SL. CLAYEY & FEW GRANULES & SHALE PEBBLES UNOX., CALC.
SAND M. GR., V. SILTY & CLAYEY WITH APPROX. 5% COARSER SAND & SHALE BLOCKS & SHALE PEBBLES & ORGANIC MATERIAL, POORLY SORTED.
SAND F.-C. GR., SL. CALC., UNOX., SILTY & CLAYEY, SHALE BLOCKS & CONSIDERABLE ORGANIC MATERIAL
213
214
215
216
217
218
219
220
221
222
223
224
225
226
227
228
229
FEET BELOW DATUM (DATUM = TOP CASING)
OBSERVATION WELL F:
TOP CASING 1695.91 FT (A.M.S.)
7" (17,8 cm) O.D. CASING
CEMENT
WELD
6⅝" (16,8 cm) CASING
212.30'
2' (64,7 m)
(61 cm)
0.45'
(13,7 cm)
LANDING RING
LEAD PACKER
BUSHING
0.20' (6,1 cm)
4" (10,2 cm) O.D. 0.007" (0,178 mm) STAINLESS STEEL SCREEN
5.1'
(155,5 cm)
COUPLER
0.25' (7 cm)
4" (10,2 cm) O.D. 0.007" (0,178 mm) STAINLESS STEEL SCREEN
5.1'
(155,5 cm)
15.60'
(4,75 m)
COUPLER
0.22' (6,7 cm)
4" (10,2 cm) O.D. 0.015" (0,38 mm) STAINLESS STEEL SCREEN
4.1'
(125 cm)
COUPLER & PLUG
0.20' (6,1 cm)
COMPLETION ZONE AND RECORD.

Figure 21. Observation well F: completion zone and record.

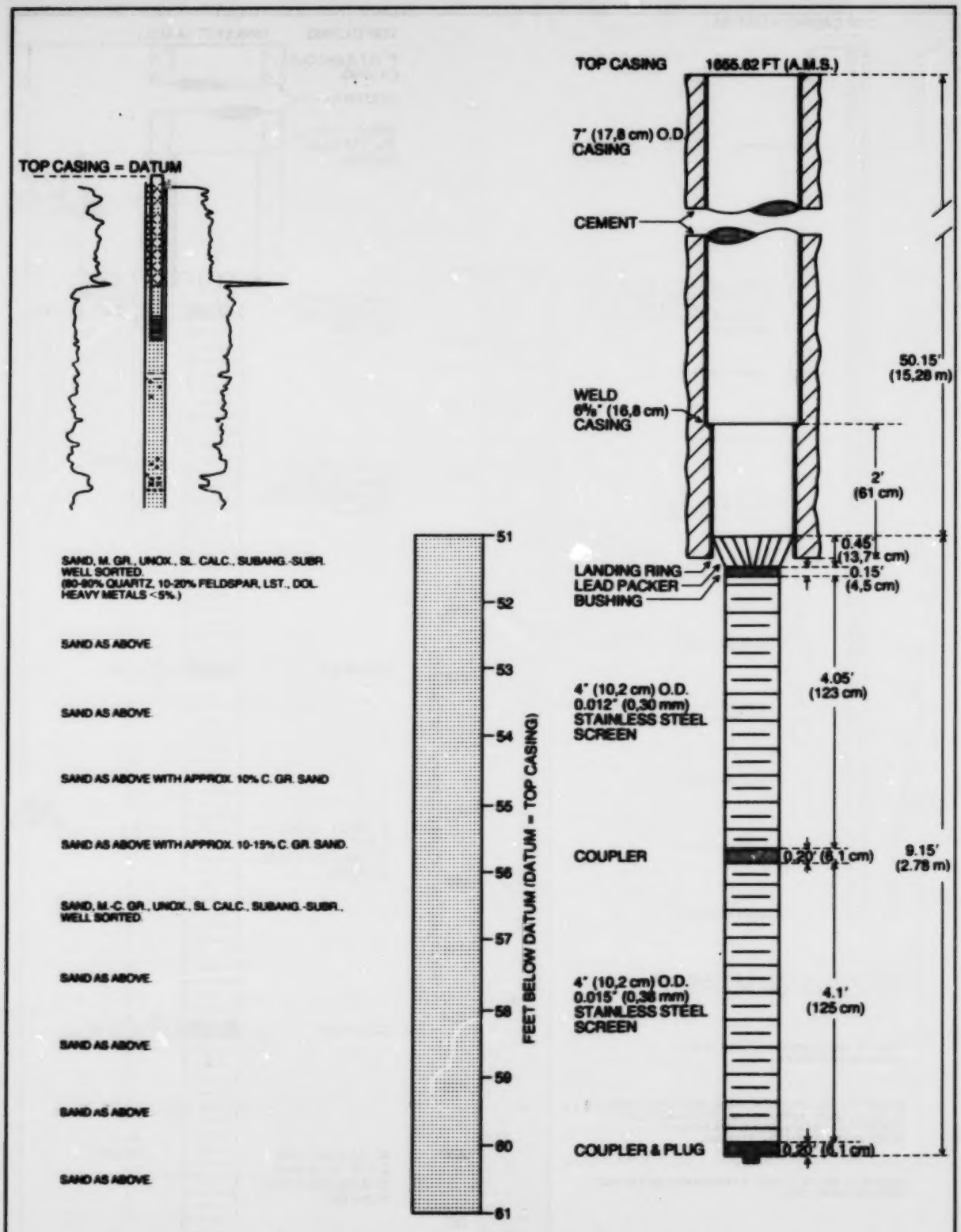

OBSERVATION WELL G: COMPLETION ZONE AND RECORD

Figure 22. Observation well G: completion zone and record.

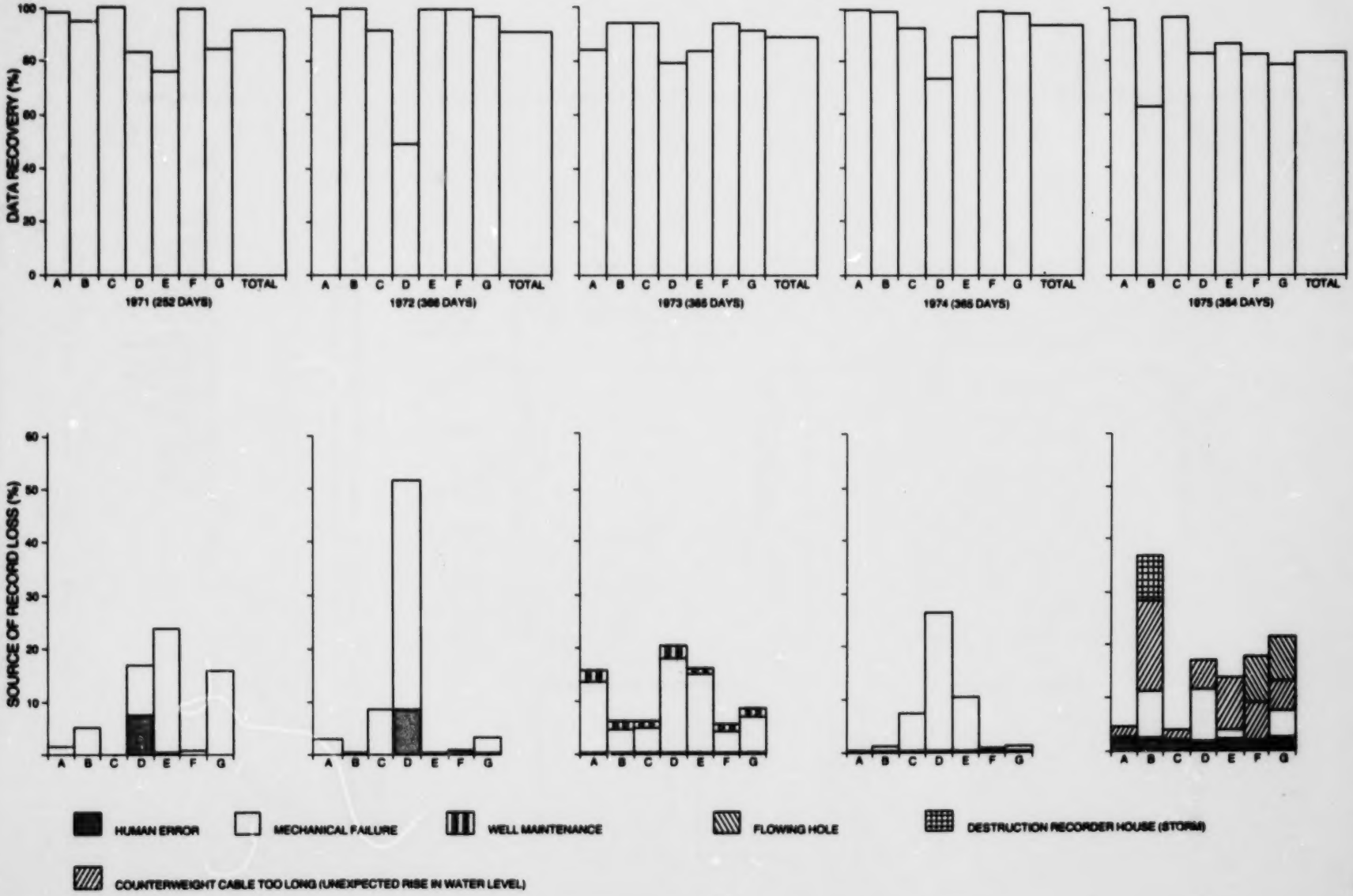

Figure 23. Hydrograph data recovery for each observation well and cause of record loss.

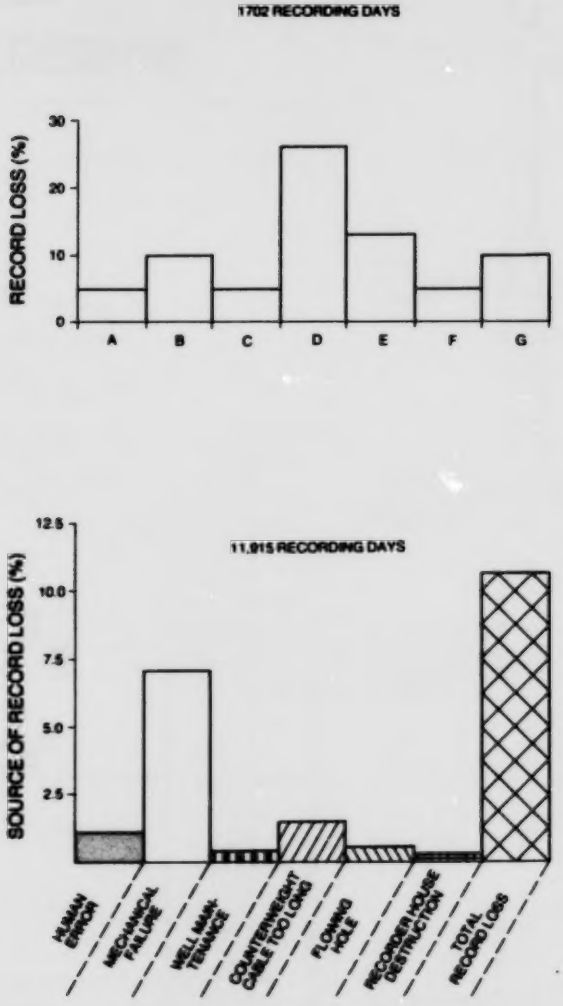

Figure 24. Summary of record loss for each observation well over total recording period and source of record loss.

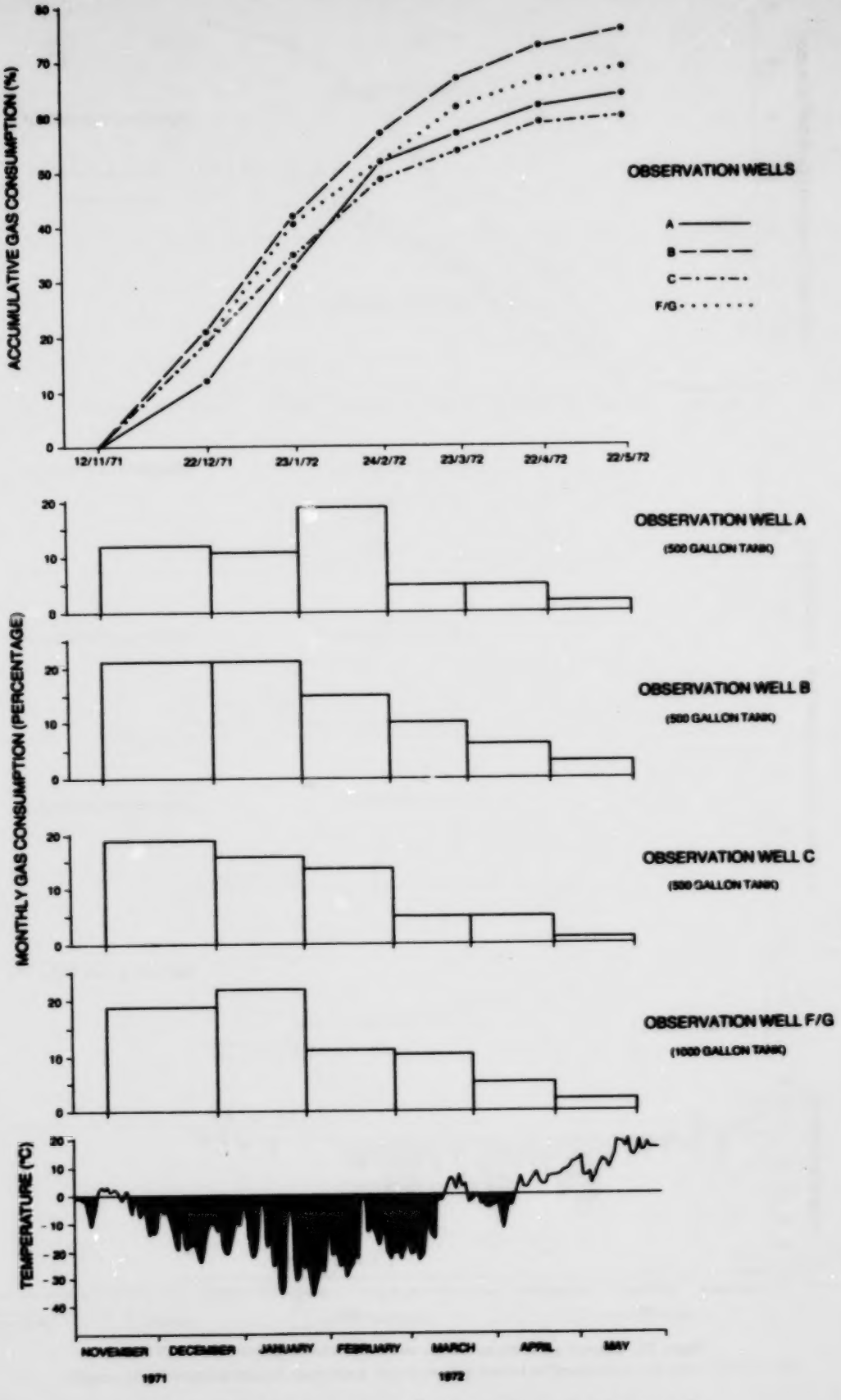

Figure 25. Propane gas consumption for each observation well: winter 1971-1972.

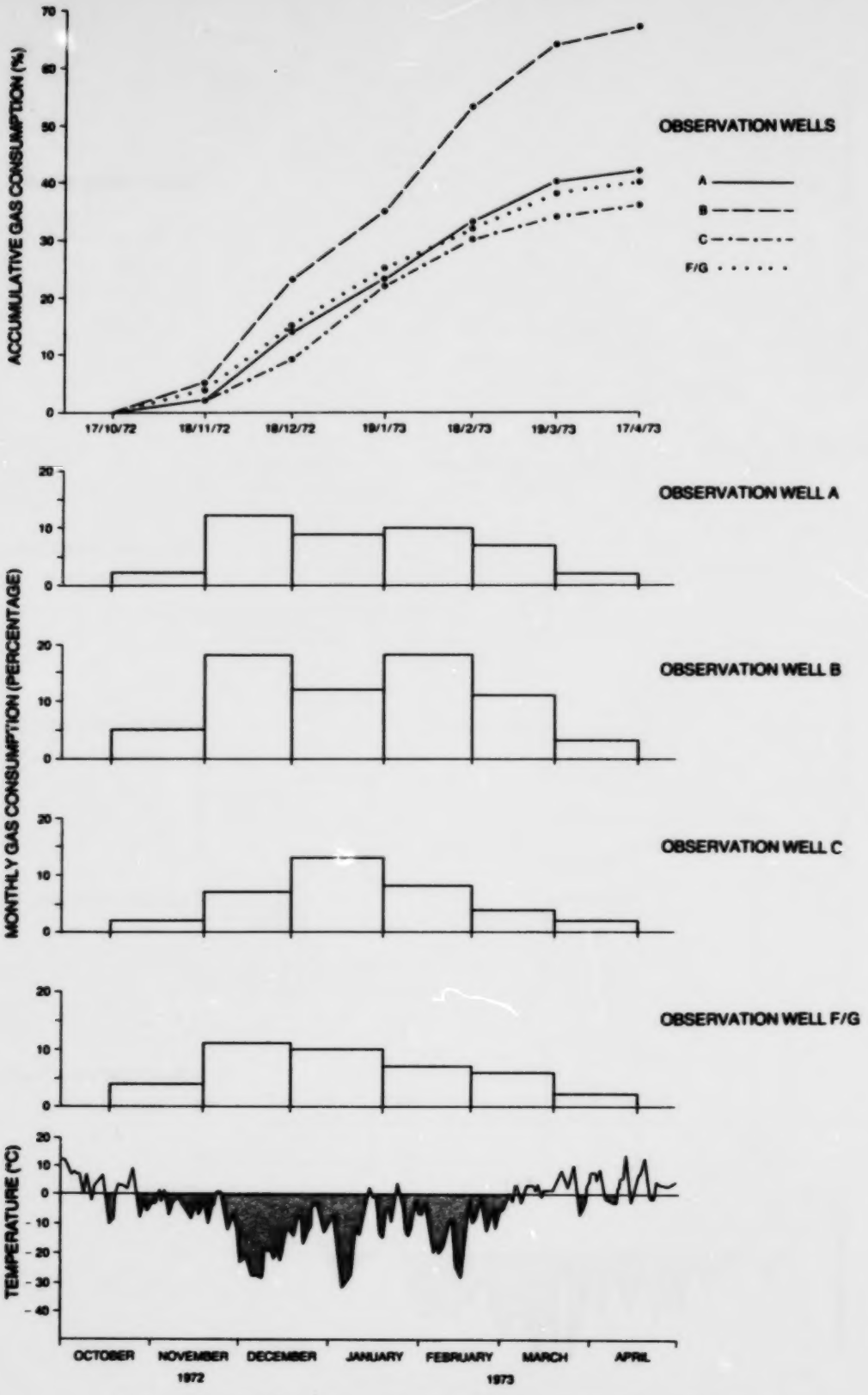

Figure 26. Propane gas consumption for each observation well: winter 1972-1973.

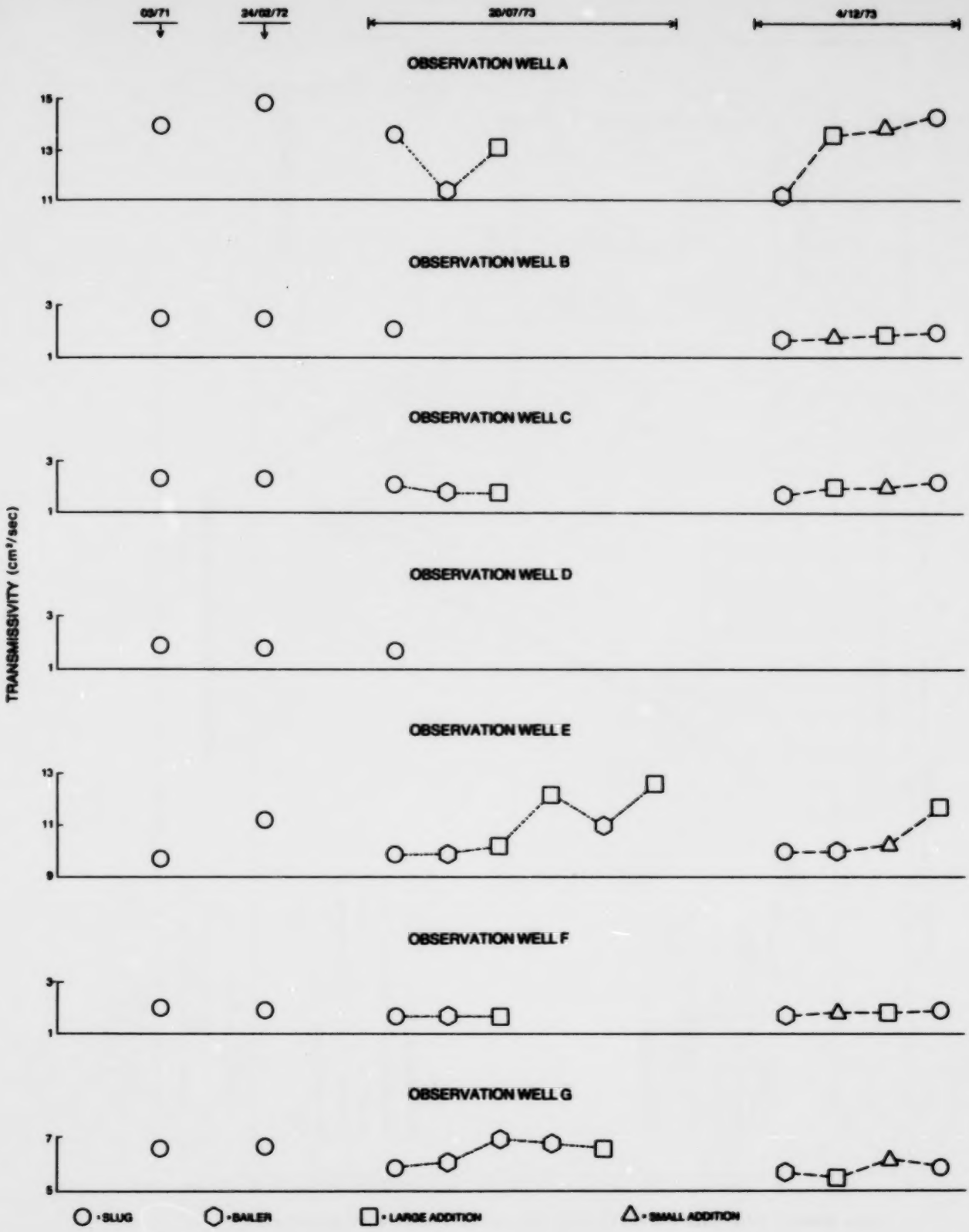

Figure 27. Transmissivities of observation wells from slug tests at different times over period 1971-1974.

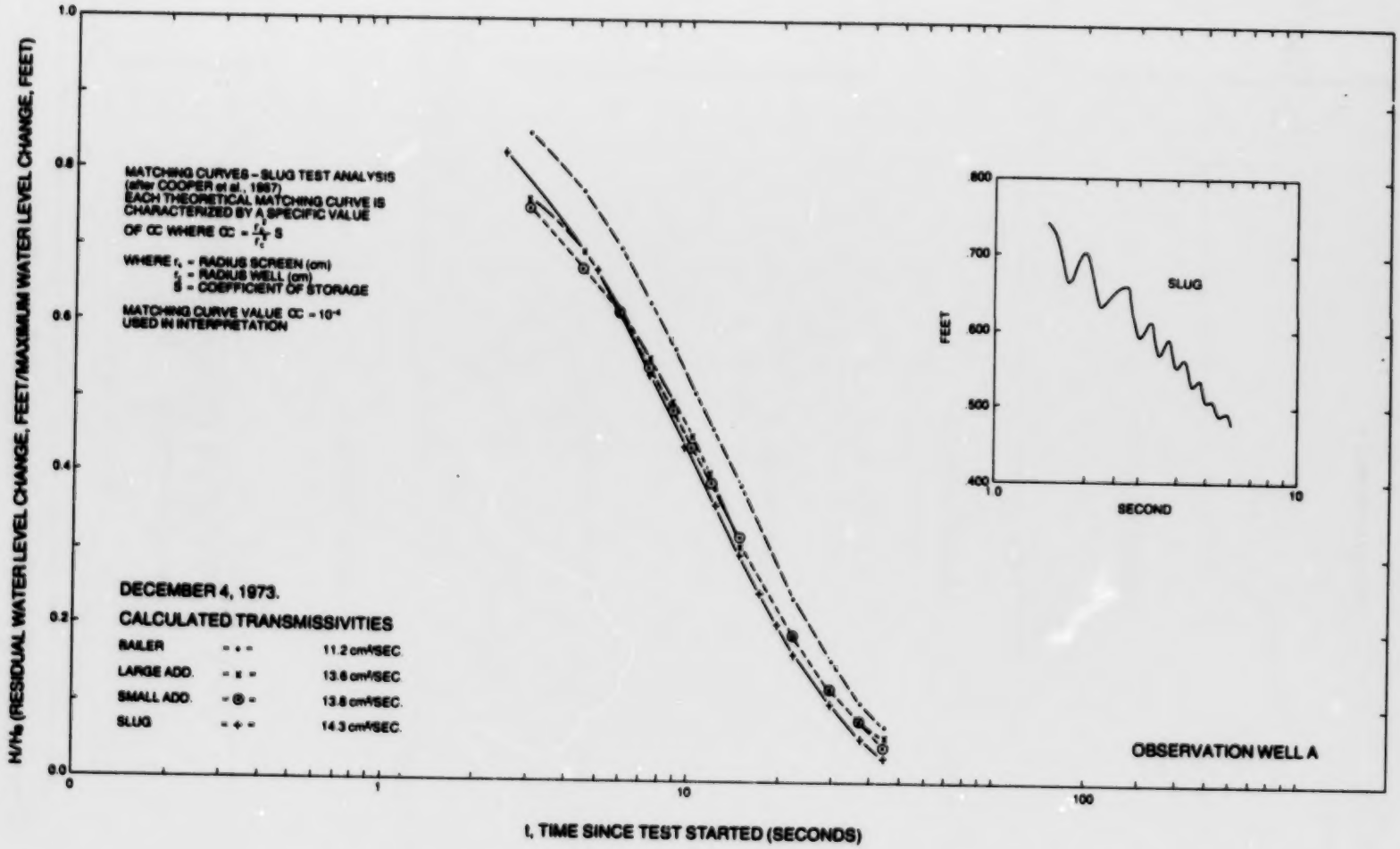
H/Ho (RESIDUAL WATER LEVEL CHANGE, FEET/MAXIMUM WATER LEVEL CHANGE, FEET)
t, TIME SINCE TEST STARTED (SECONDS)
MATCHING CURVES – SLUG TEST ANALYSIS
(after COOPER et al., 1967)
EACH THEORETICAL MATCHING CURVE IS CHARACTERIZED BY A SPECIFIC VALUE OF CC WHERE CC = $\frac{r_s^2}{r_c^2}$ S
WHERE r_s = RADIUS SCREEN (cm)
r_c = RADIUS WELL (cm)
S = COEFFICIENT OF STORAGE
MATCHING CURVE VALUE CC = 10^{-4}
USED IN INTERPRETATION
DECEMBER 4, 1973.
CALCULATED TRANSMISSIVITIES
BAILER - + - 11.2 cm²/SEC.
LARGE ADD. - x - 13.6 cm²/SEC.
SMALL ADD. - ⊙ - 13.8 cm²/SEC.
SLUG - + - 14.3 cm²/SEC.
OBSERVATION WELL A
SLUG
FEET
SECOND

Figure 28. Consecutive slug tests with different size slug in observation well A and damped oscillation.

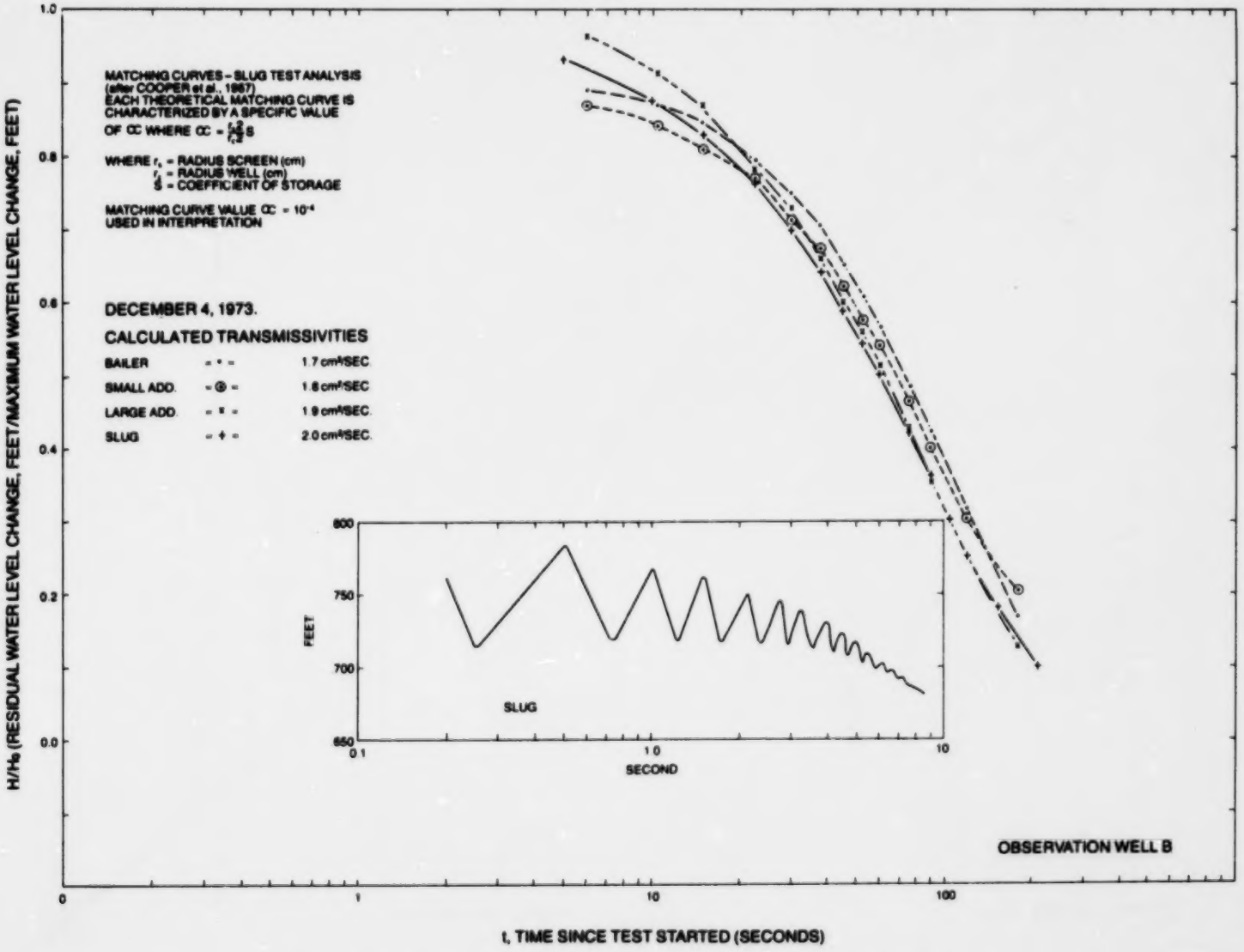
MATCHING CURVES - SLUG TEST ANALYSIS
(after COOPER et al., 1967)
EACH THEORETICAL MATCHING CURVE IS
CHARACTERIZED BY A SPECIFIC VALUE
OF α WHERE α = $\frac{r_c^2}{r_w^2} S$
WHERE r_c = RADIUS SCREEN (cm)
r_w = RADIUS WELL (cm)
S = COEFFICIENT OF STORAGE
MATCHING CURVE VALUE α = 10^{-4}
USED IN INTERPRETATION
DECEMBER 4, 1973.
CALCULATED TRANSMISSIVITIES
BAILER - • - 1.7 cm²/SEC.
SMALL ADD. - ⊛ - 1.8 cm²/SEC.
LARGE ADD. - ⁑ - 1.9 cm²/SEC.
SLUG - + - 2.0 cm²/SEC.
FEET
SLUG
SECOND
OBSERVATION WELL B
H/Ho (RESIDUAL WATER LEVEL CHANGE, FEET/MAXIMUM WATER LEVEL CHANGE, FEET)
t, TIME SINCE TEST STARTED (SECONDS)

Figure 29. Consecutive slug tests with different size slug in observation well B and damped oscillation.

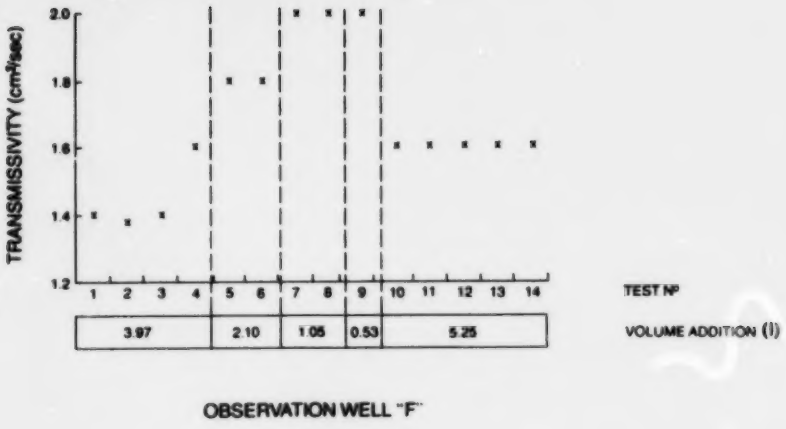

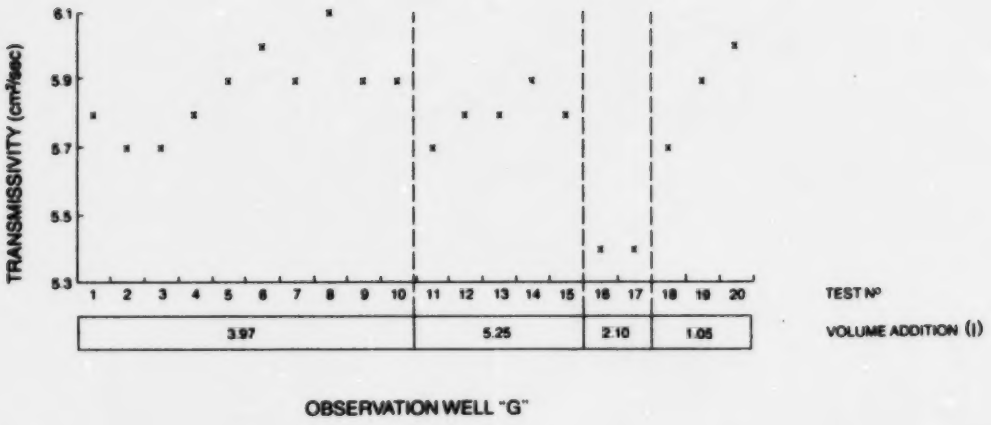

Figure 30. Sequential hydrodynamic response tests with different volumes added in observation wells F and G, December 10 and 11, 1974.

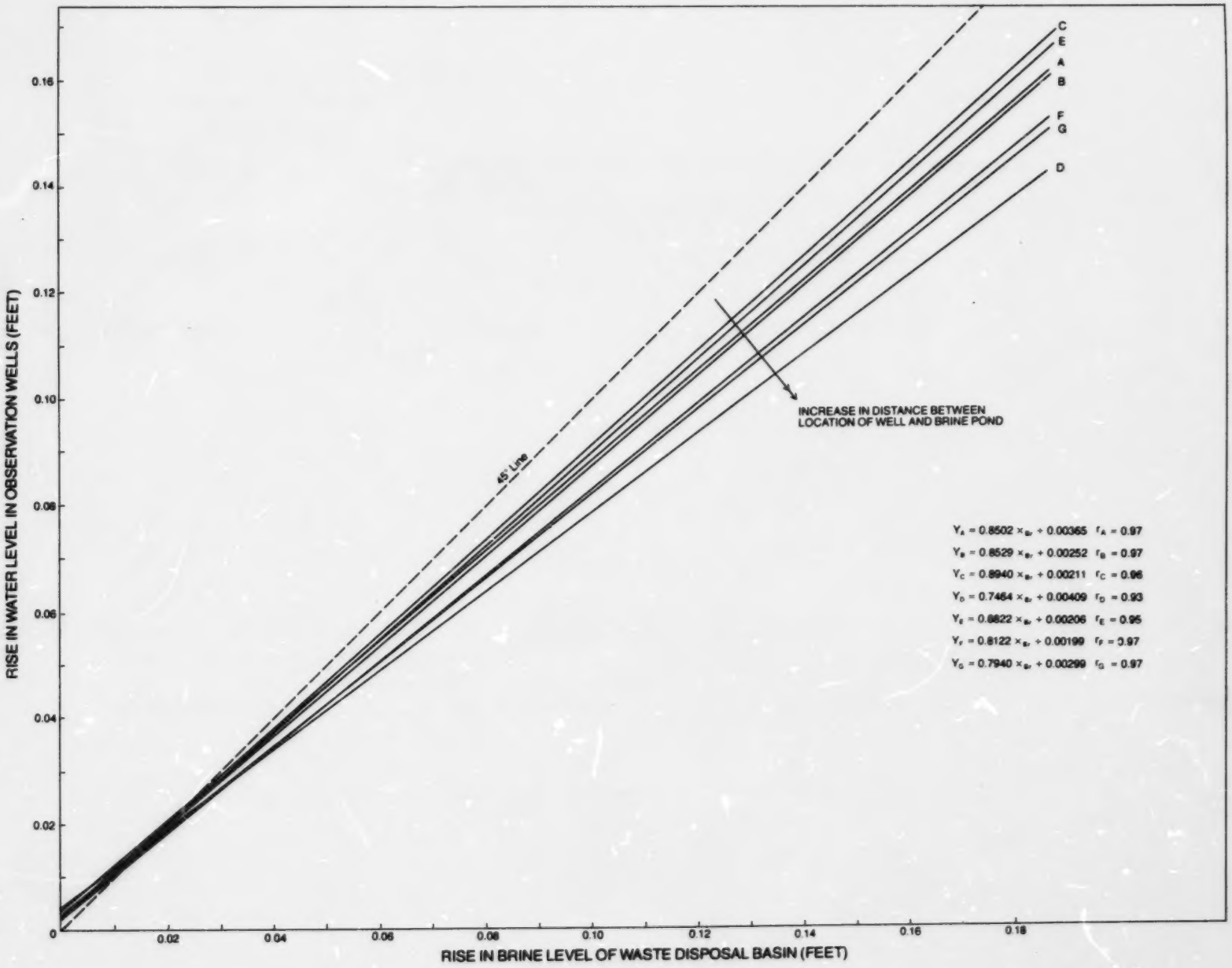

Figure 31. Instantaneous rise in brine level versus rise in water level in each well.

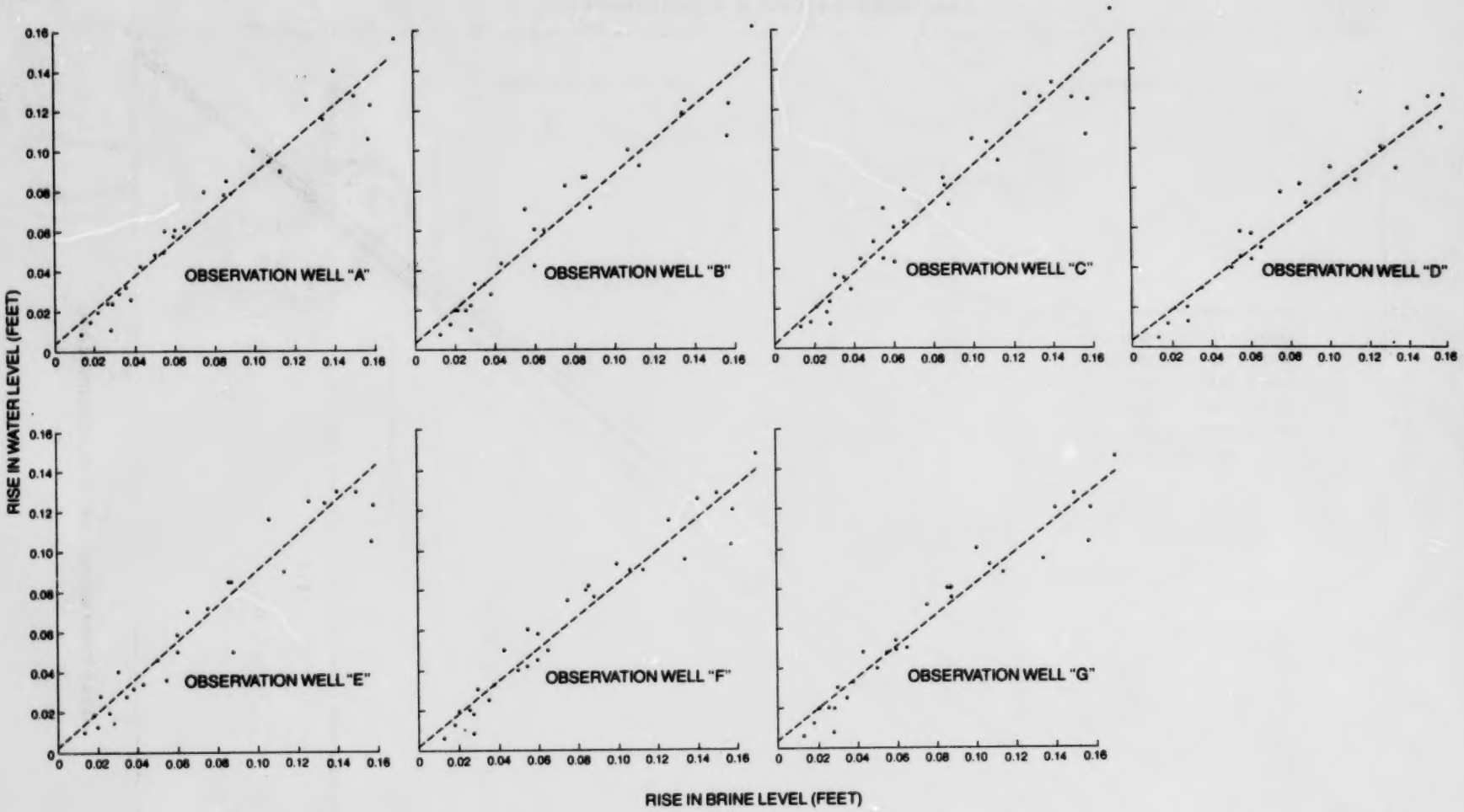

Figure 32. Lines of best fit of instantaneous rise in brine level versus water level in each well and correlation factors.

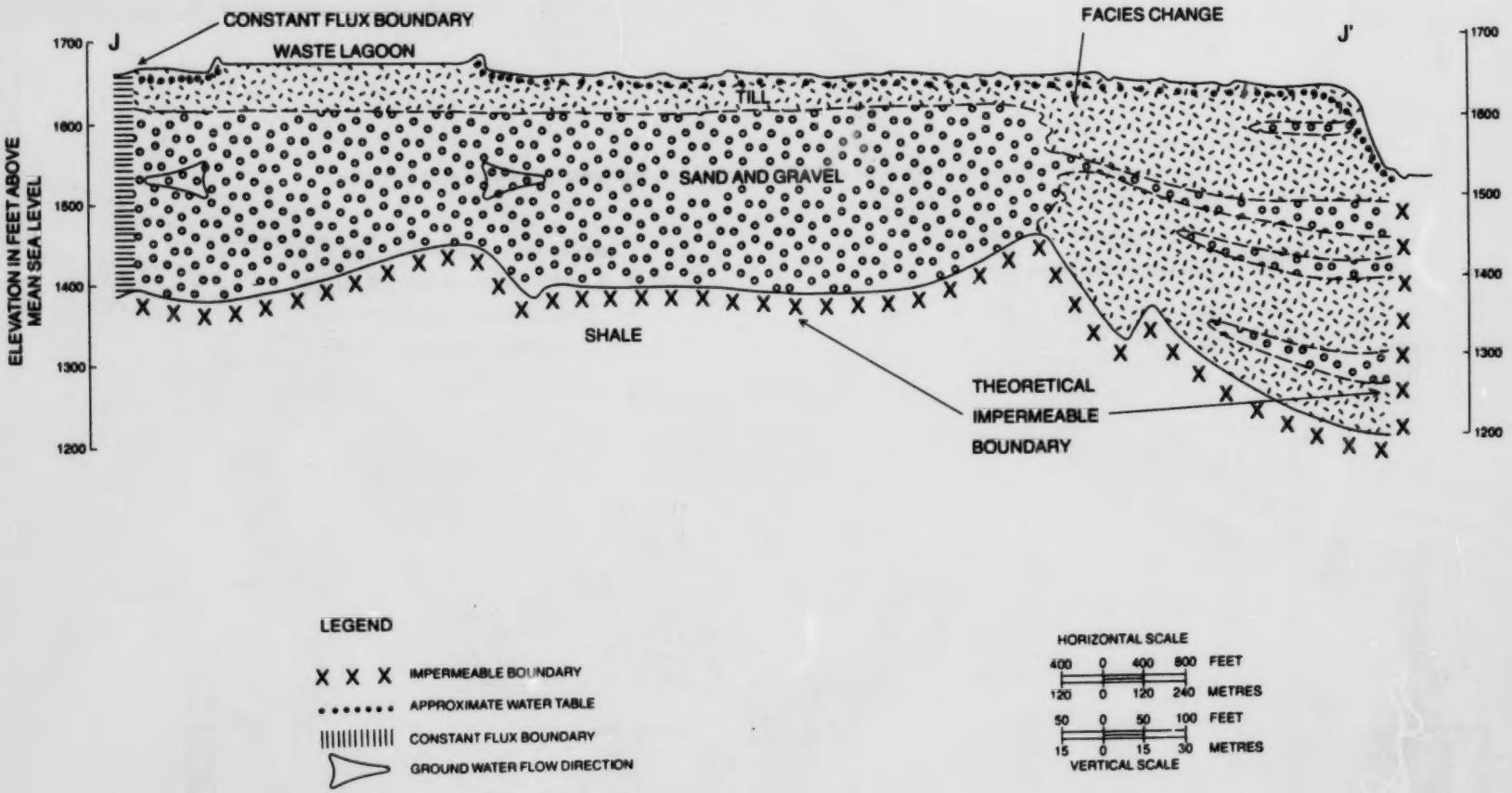

Figure 33. Cross section J-J' illustrating the essential components of the study site boundary value problem.

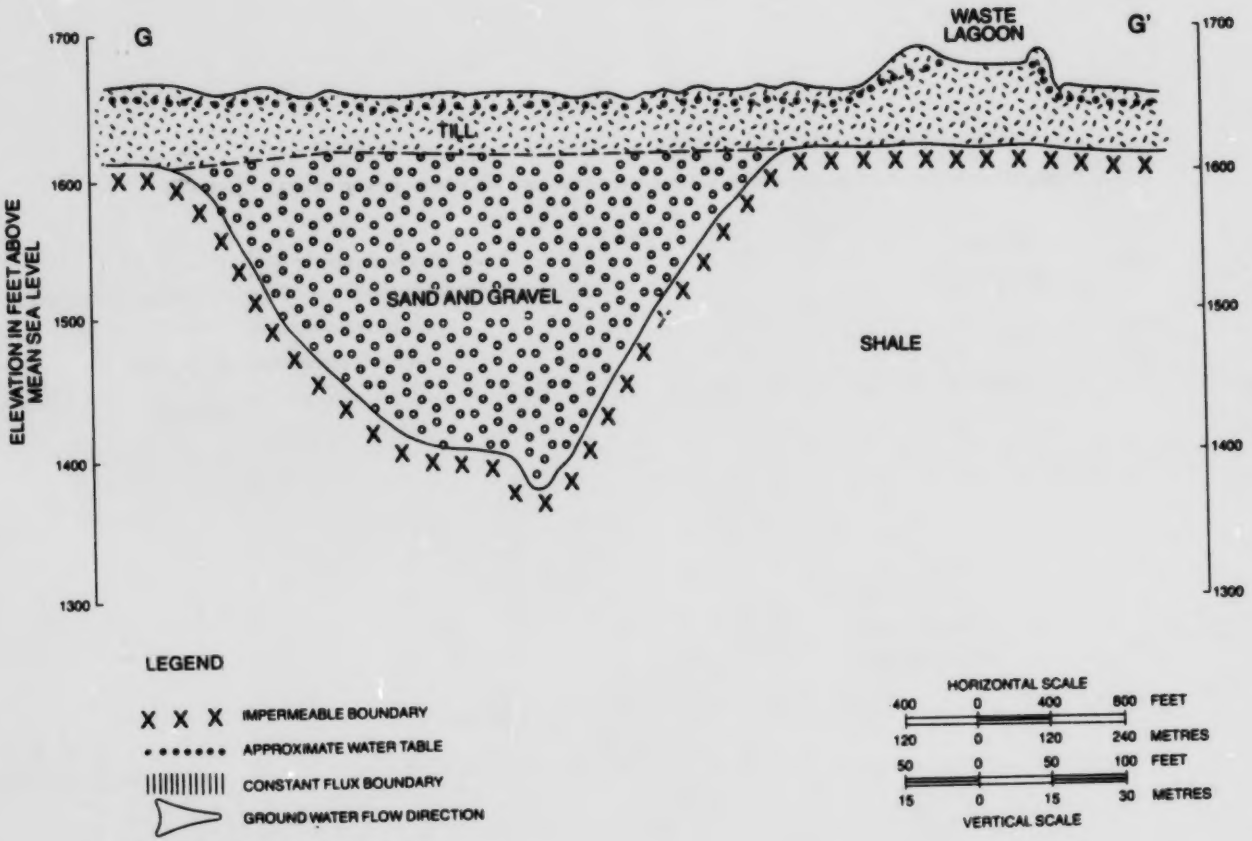

Figure 34. Cross section G-G′ illustrating the essential components of the study site boundary value problem.

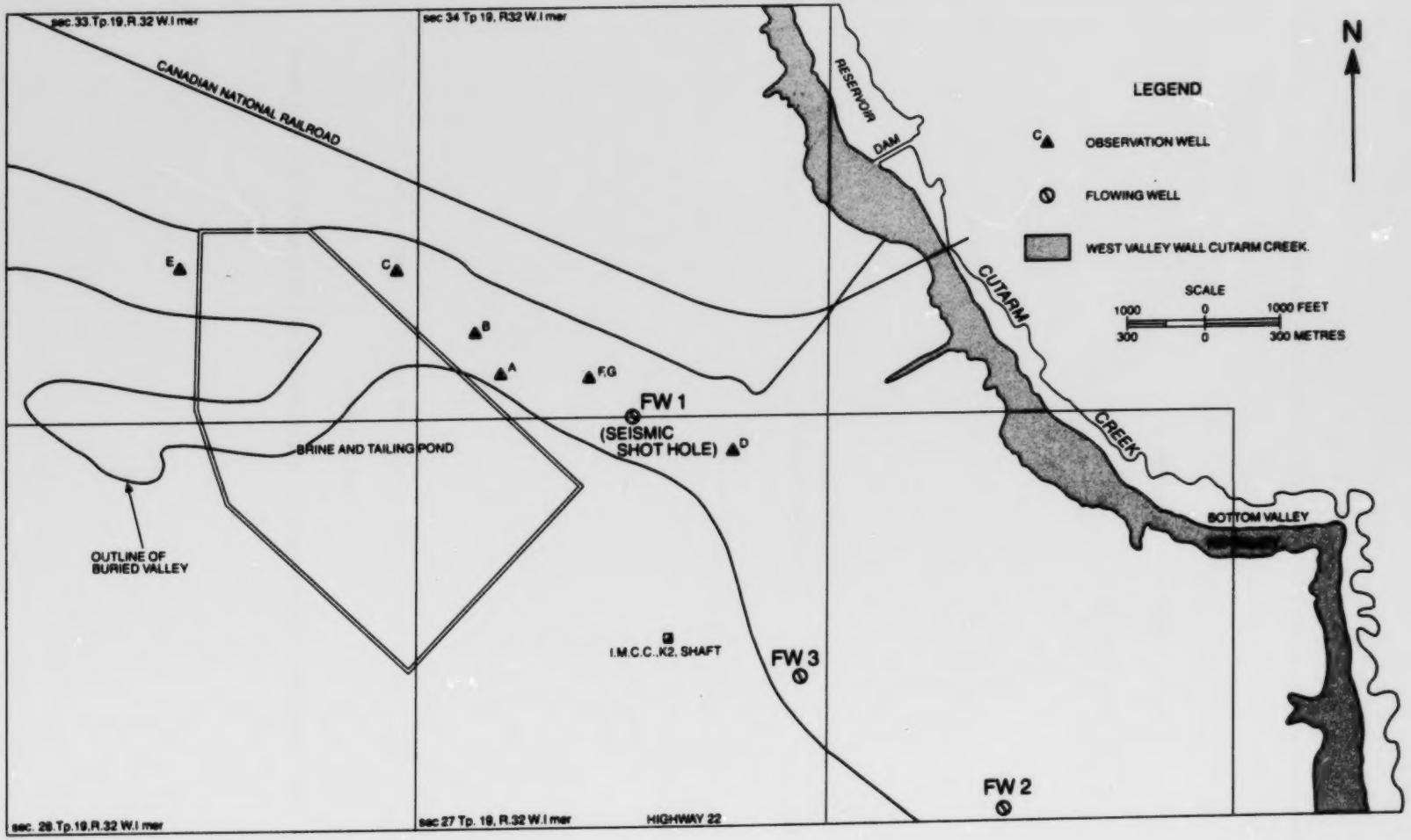

Figure 35. Location of observation wells and flowing holes.

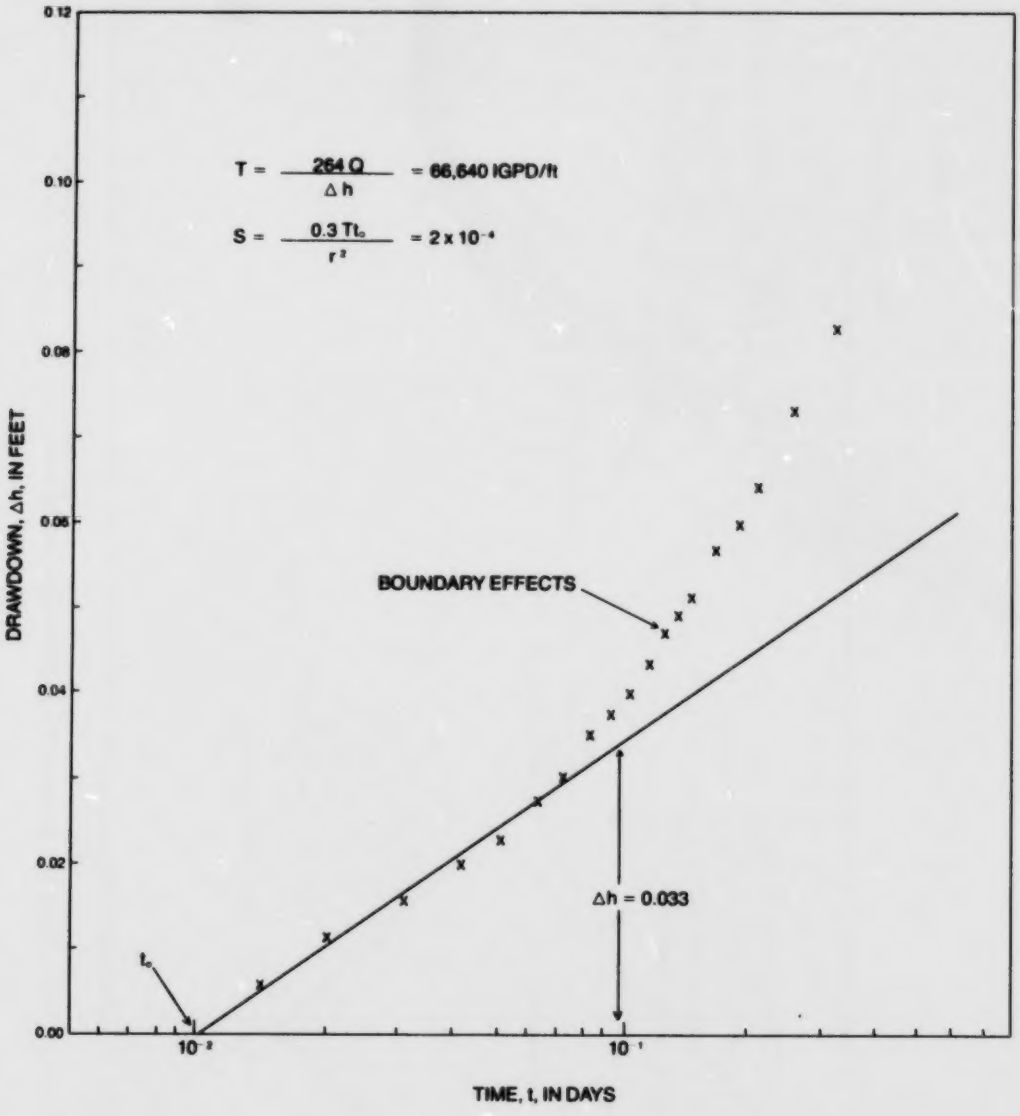

Figure 36. Jacob method applied to observation well A with observation well B pumping at 8.3 lgpm (37.7 l/min).

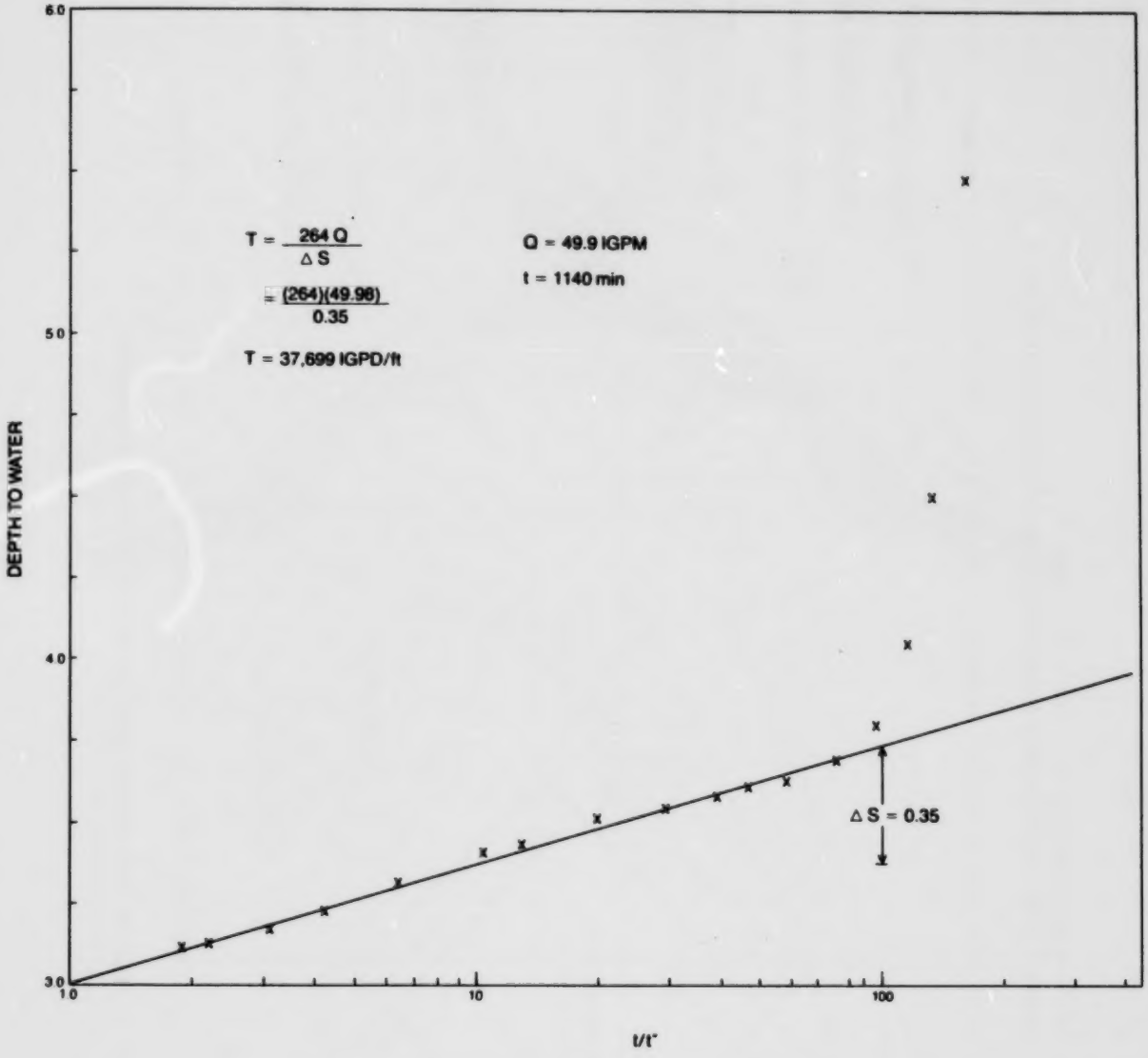

Figure 37. Theis recovery method applied to observation well F.

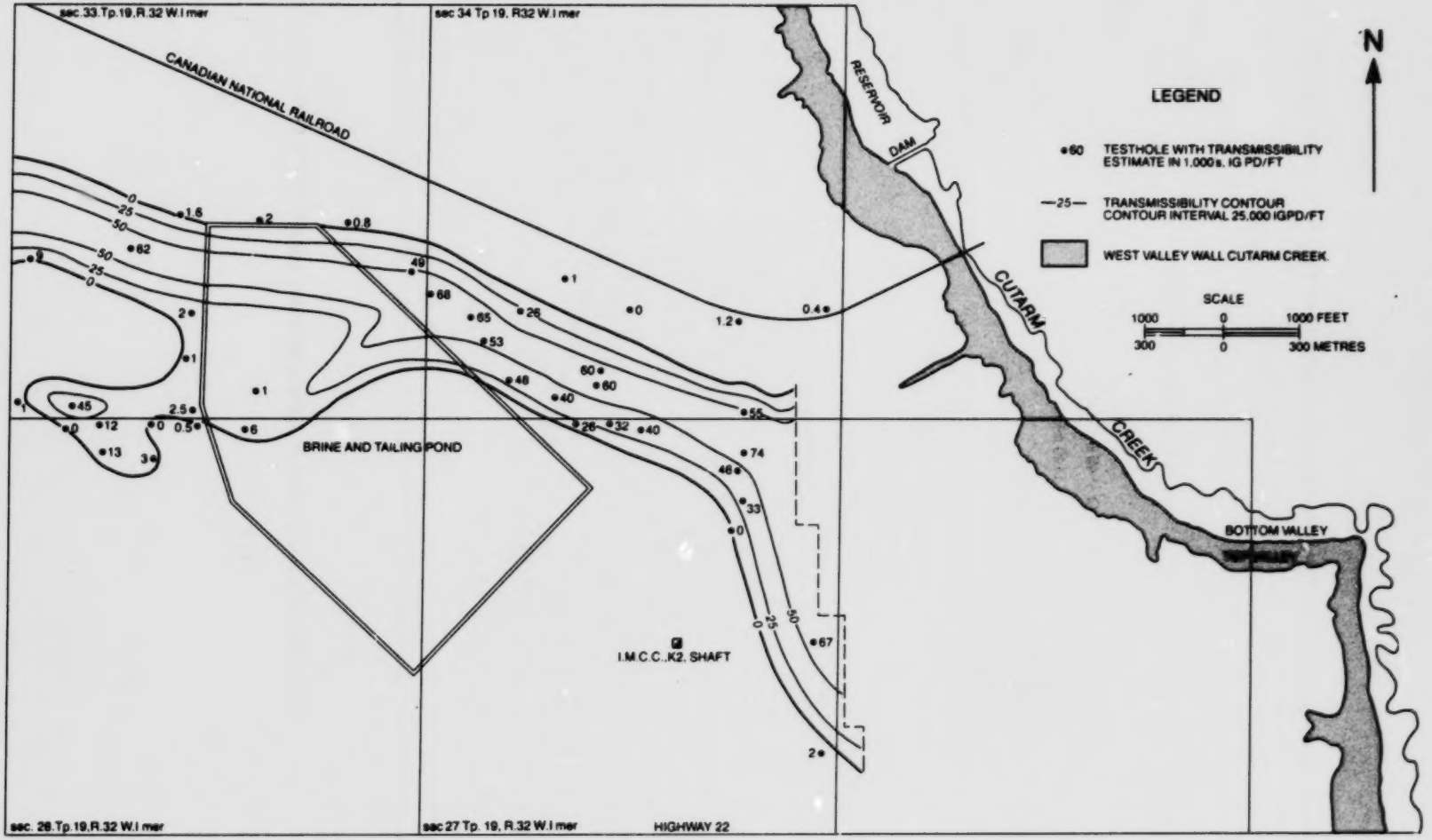

Figure 38. Transmissibility estimate (Igpd/ft) in the buried valley fluvial deposits.

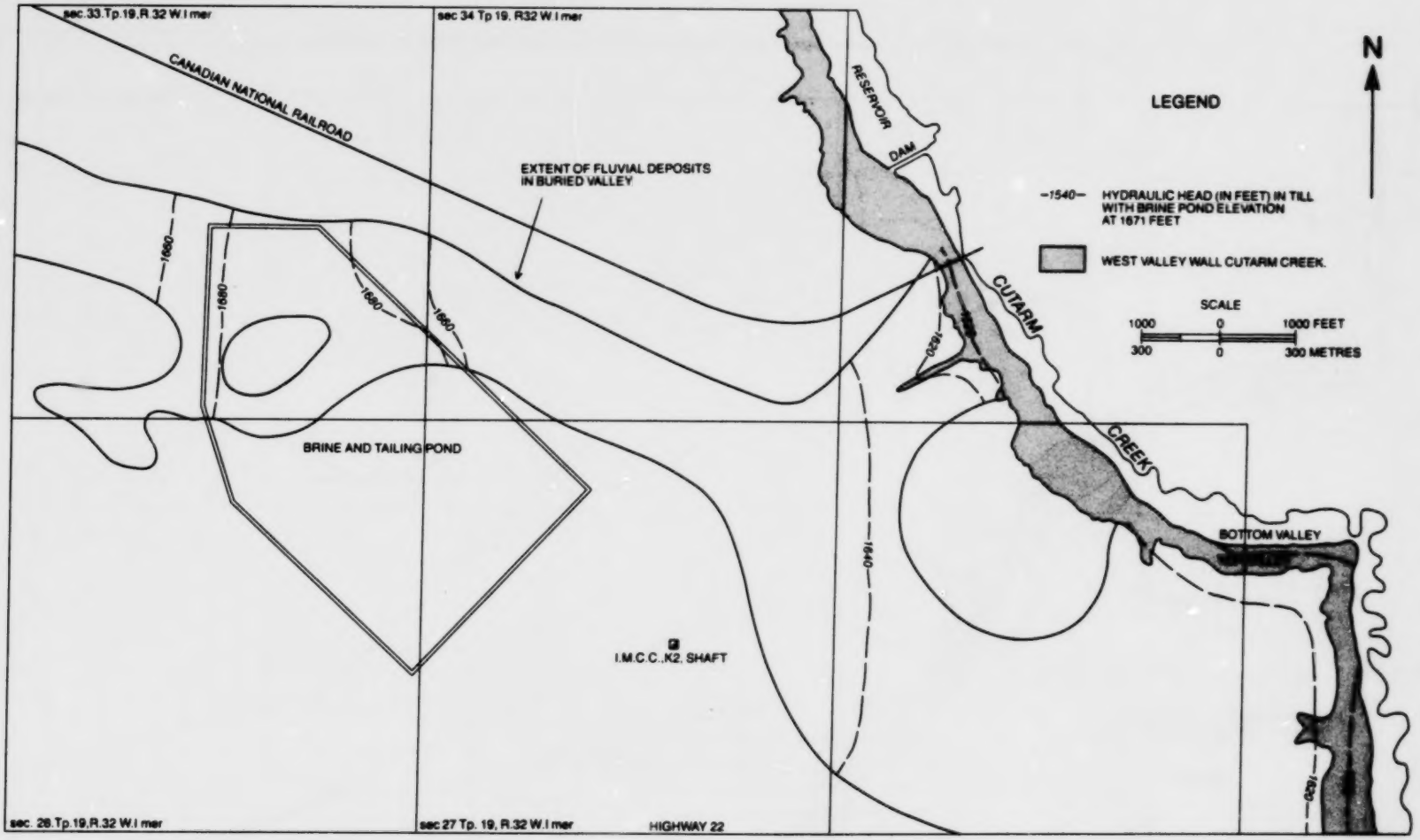

Figure 39. Steady state groundwater flow pattern in the till layer for a brine elevation of 1671 ft.

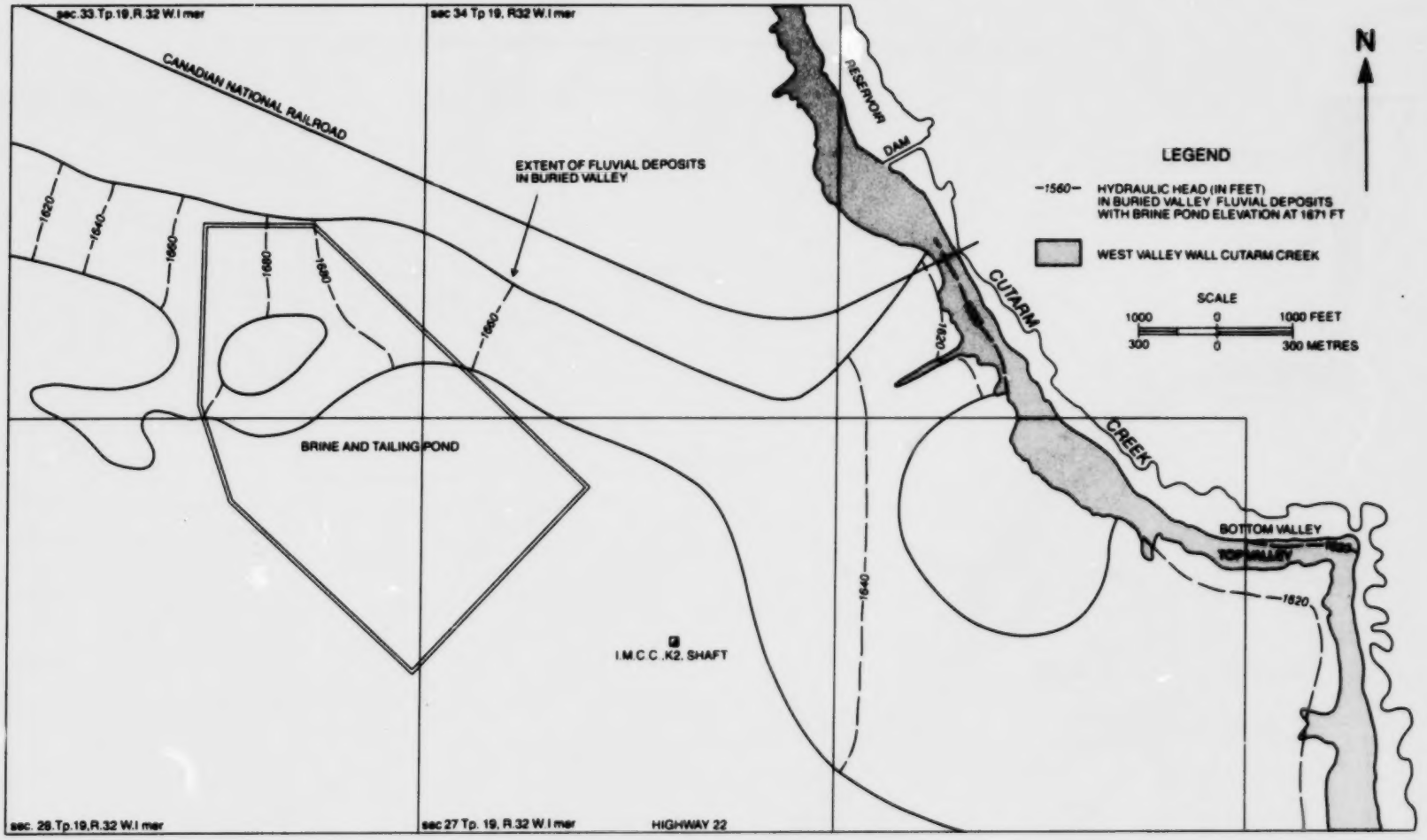

Figure 40. Steady state groundwater flow pattern in the buried valley aquifer for a brine elevation of 1671 ft.

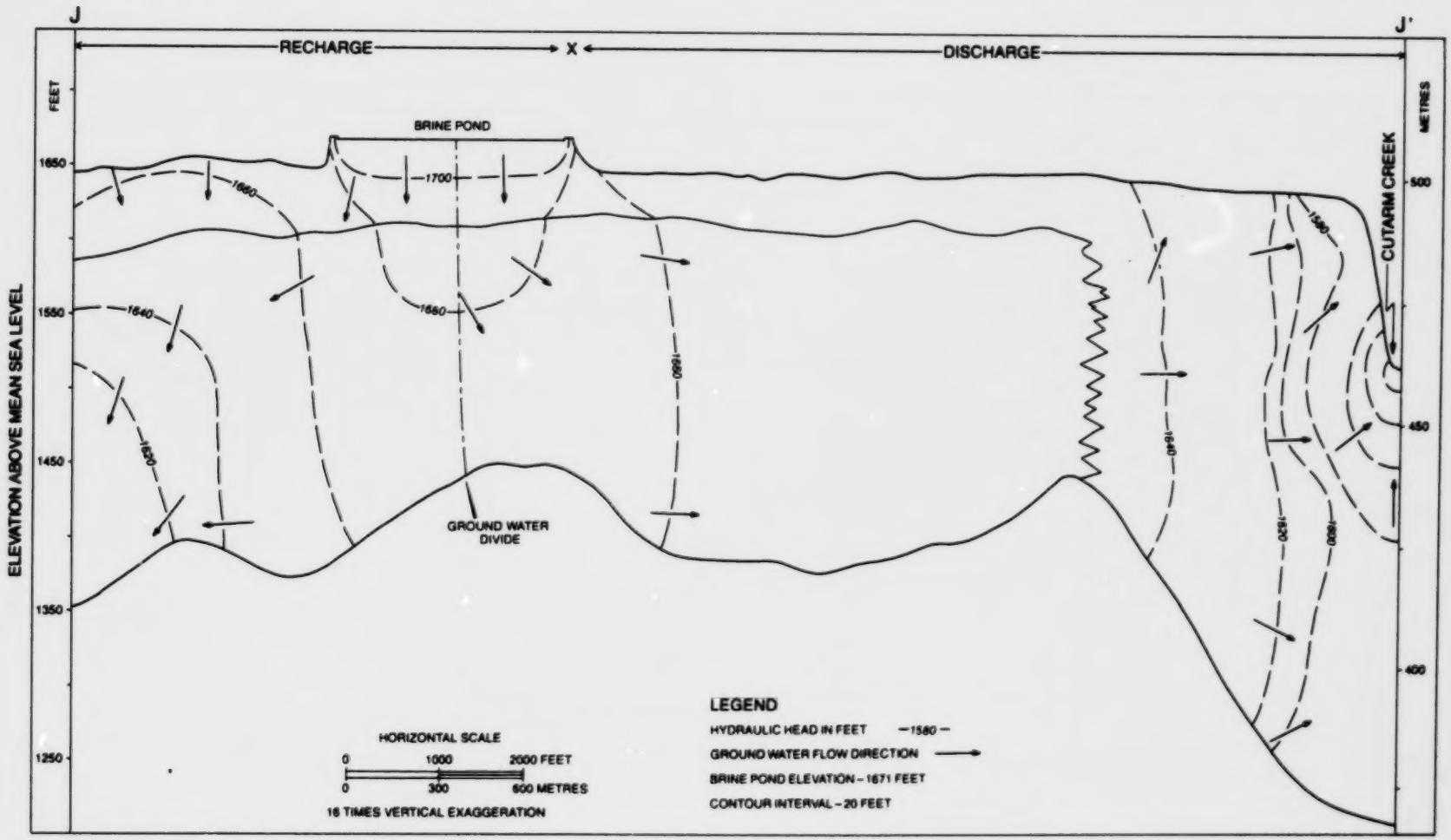

Figure 41. *Steady state groundwater flow pattern along cross section J-J' for a brine elevation of 1671 ft.*

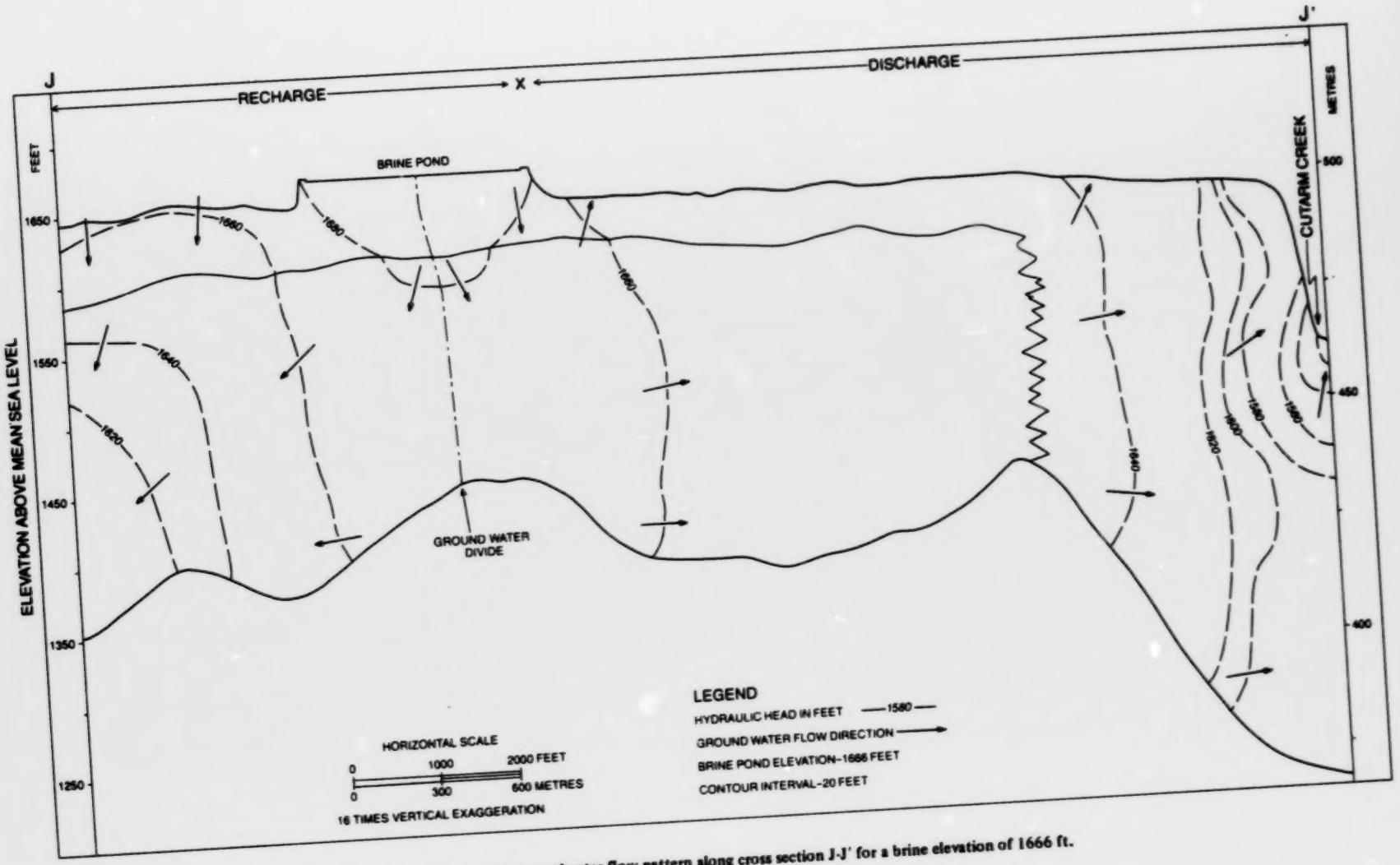

Figure 42. Steady state groundwater flow pattern along cross section J-J' for a brine elevation of 1666 ft.

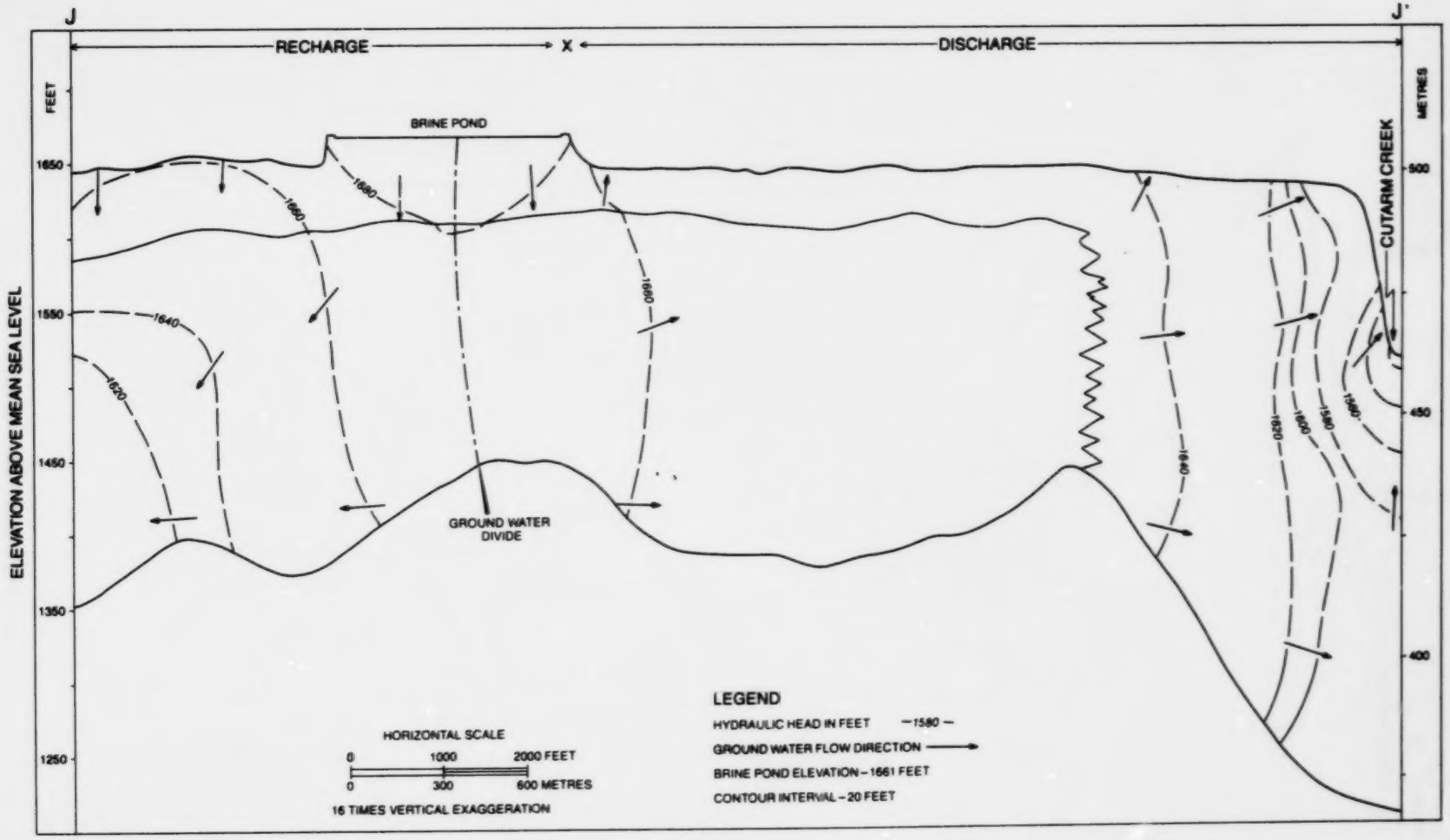

Figure 43. Steady state groundwater flow pattern along cross section J-J' for a brine elevation of 1661 ft.

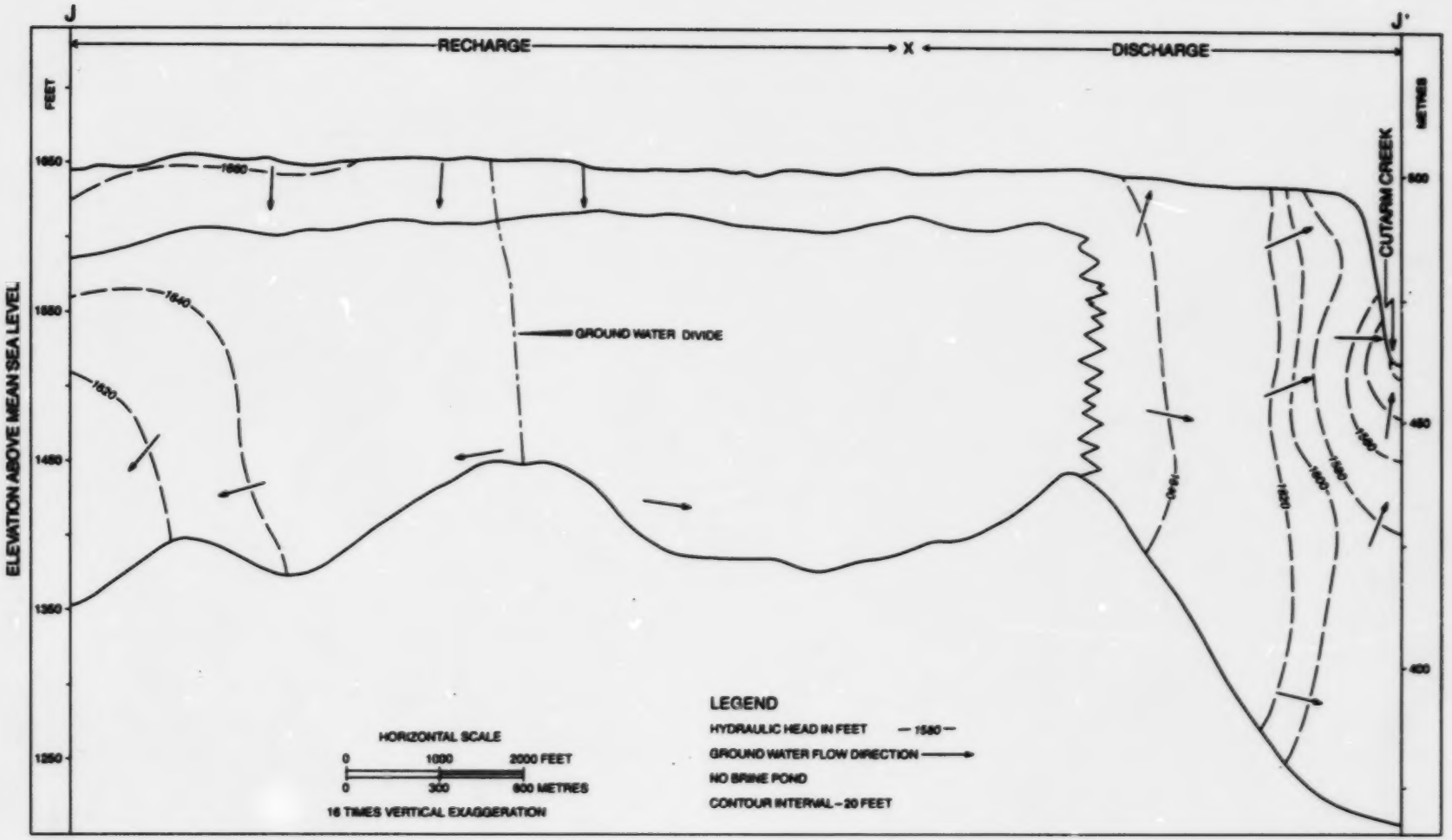

Figure 44. Steady state groundwater flow pattern along cross section J-J' with no brine pond present.

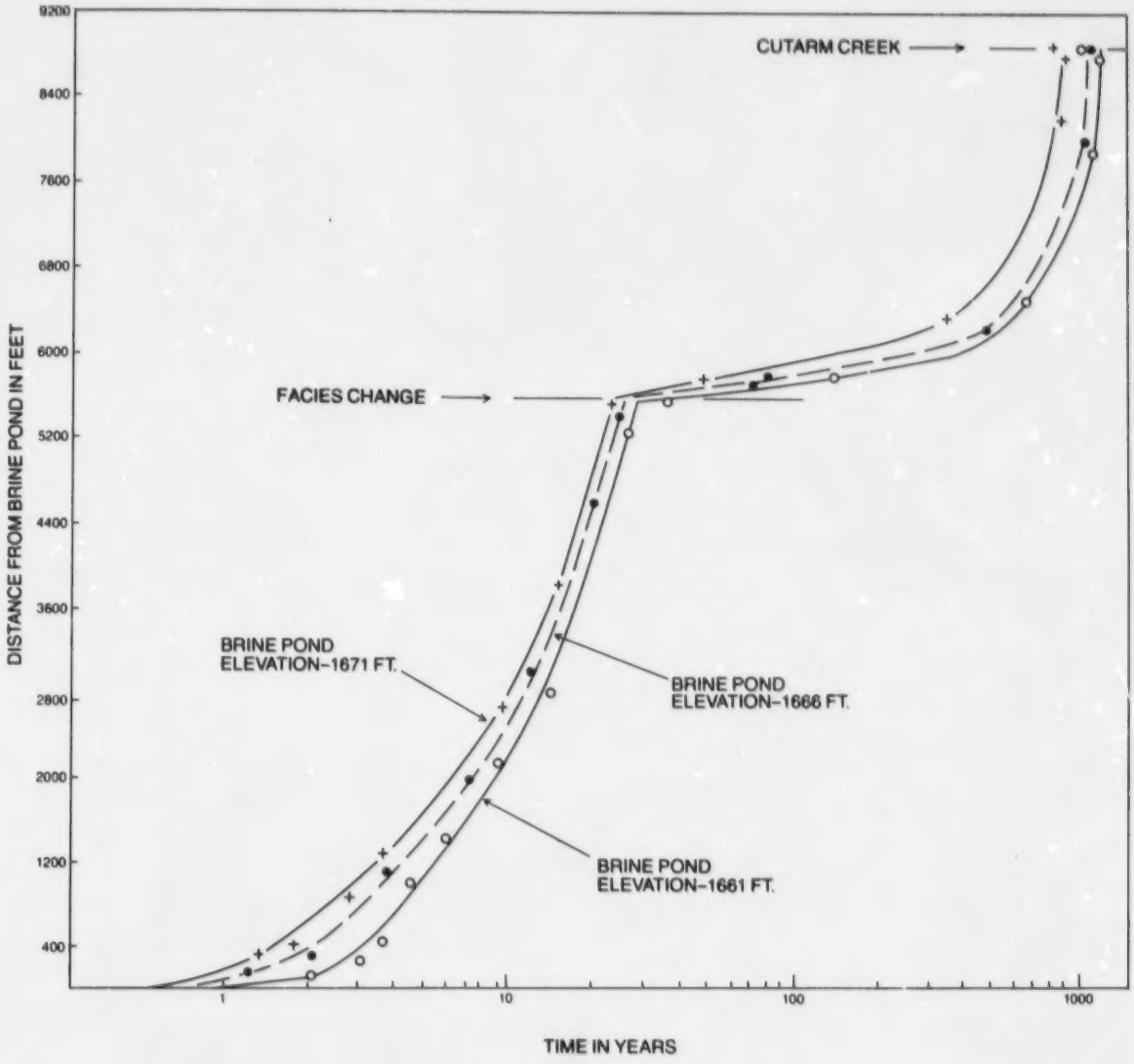

Figure 45. Graph of the travel time of brine moving from the brine pond plotted against distance from the eastern dyke of the brine pond.

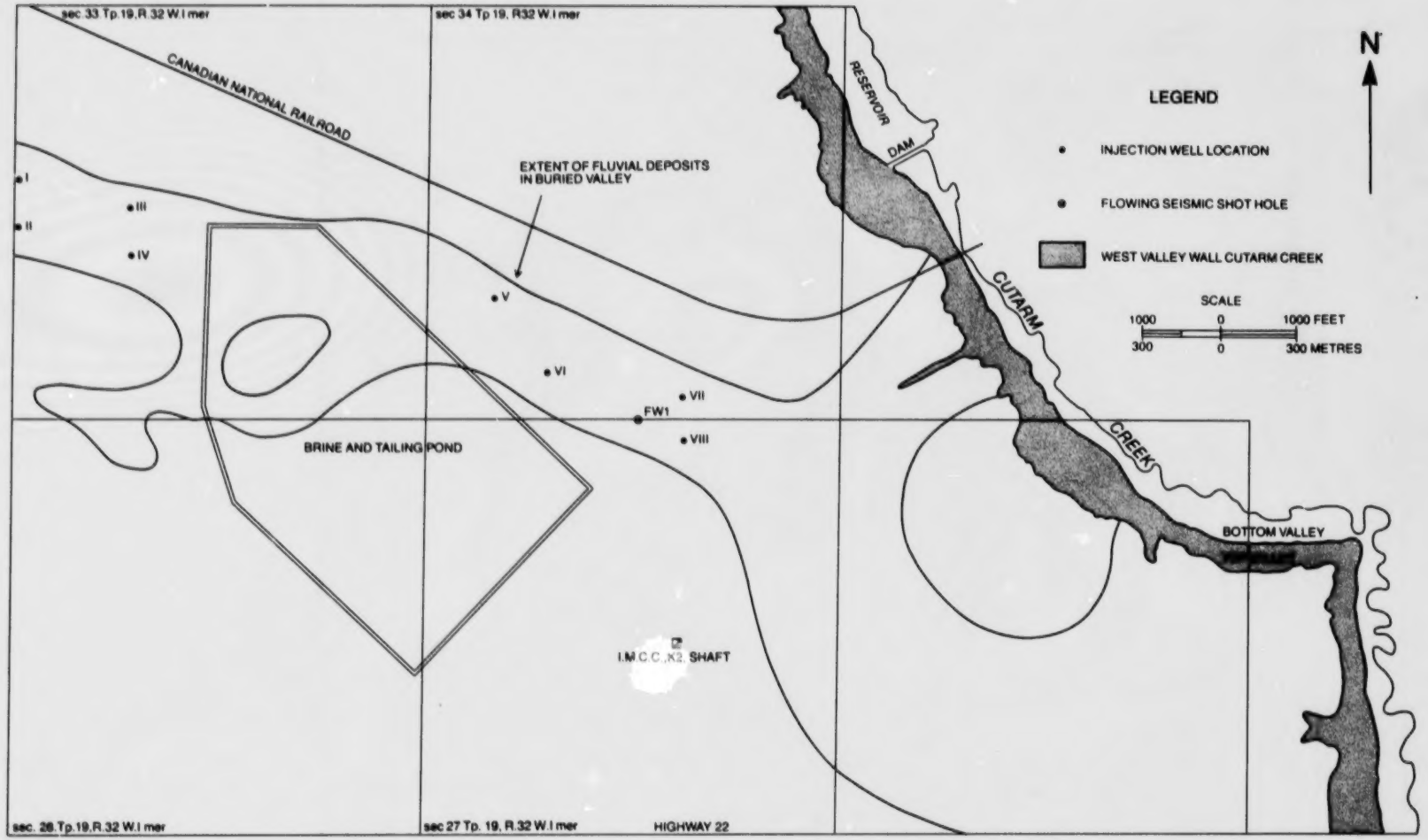

Figure 46. Location of injection wells and flowing seismic shothole (FW1).

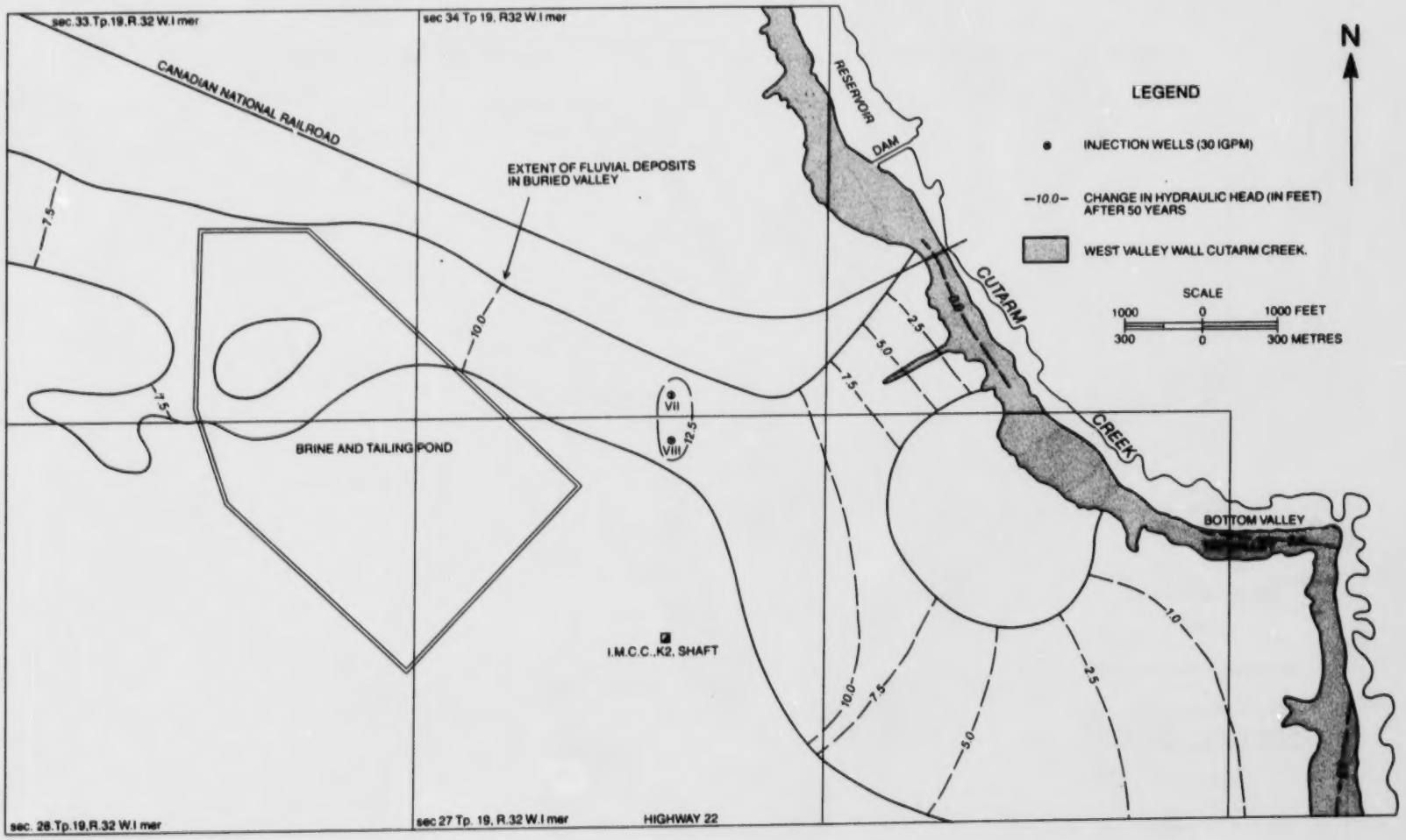

Figure 47. Change in hydraulic head in the buried valley aquifer after 50 years of injection at 30 Igpm (136 l/min) per well.

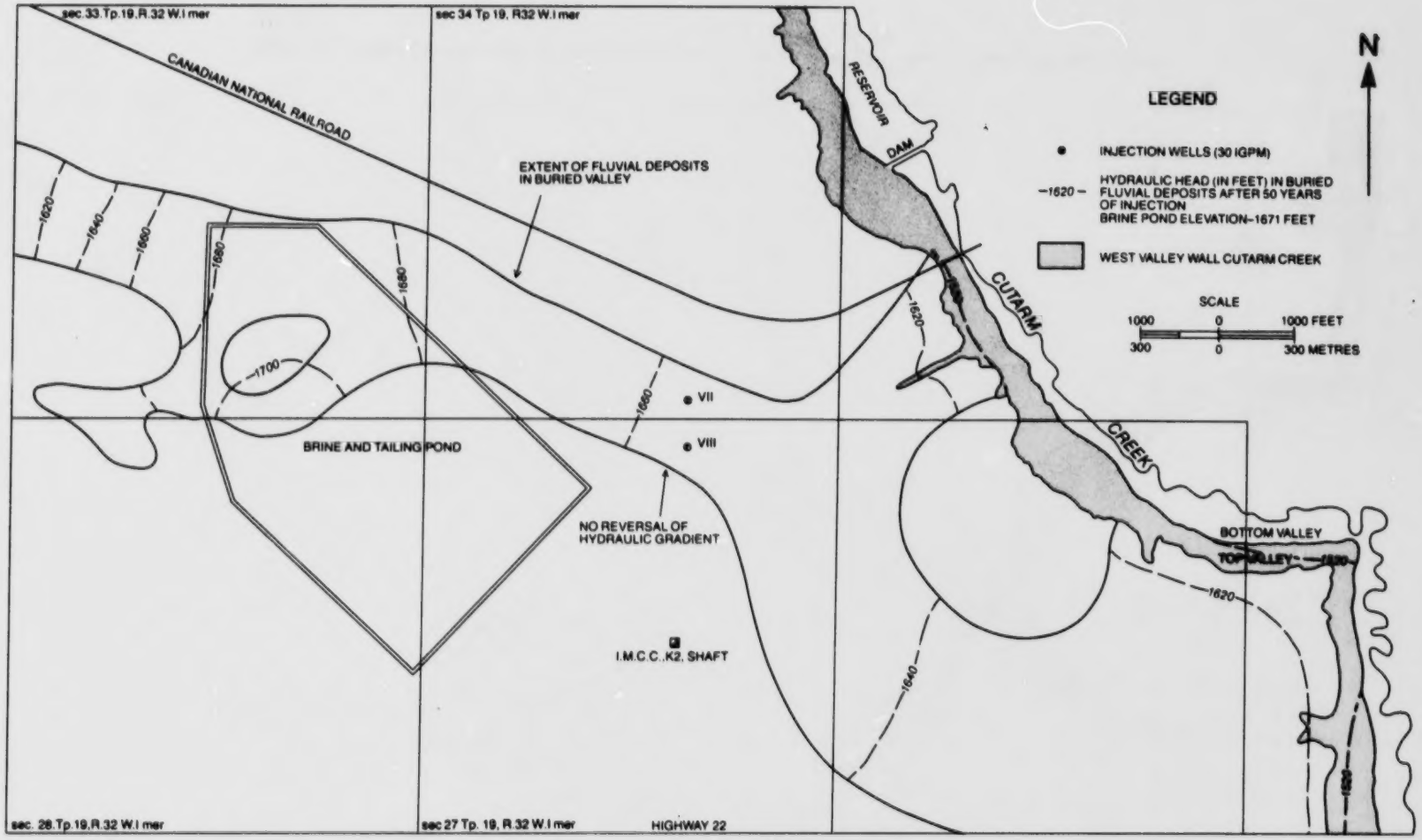

Figure 48. Resultant hydraulic head distribution in the buried valley aquifer after 50 years of injection at 30 Igpm (136 l/min) per well.

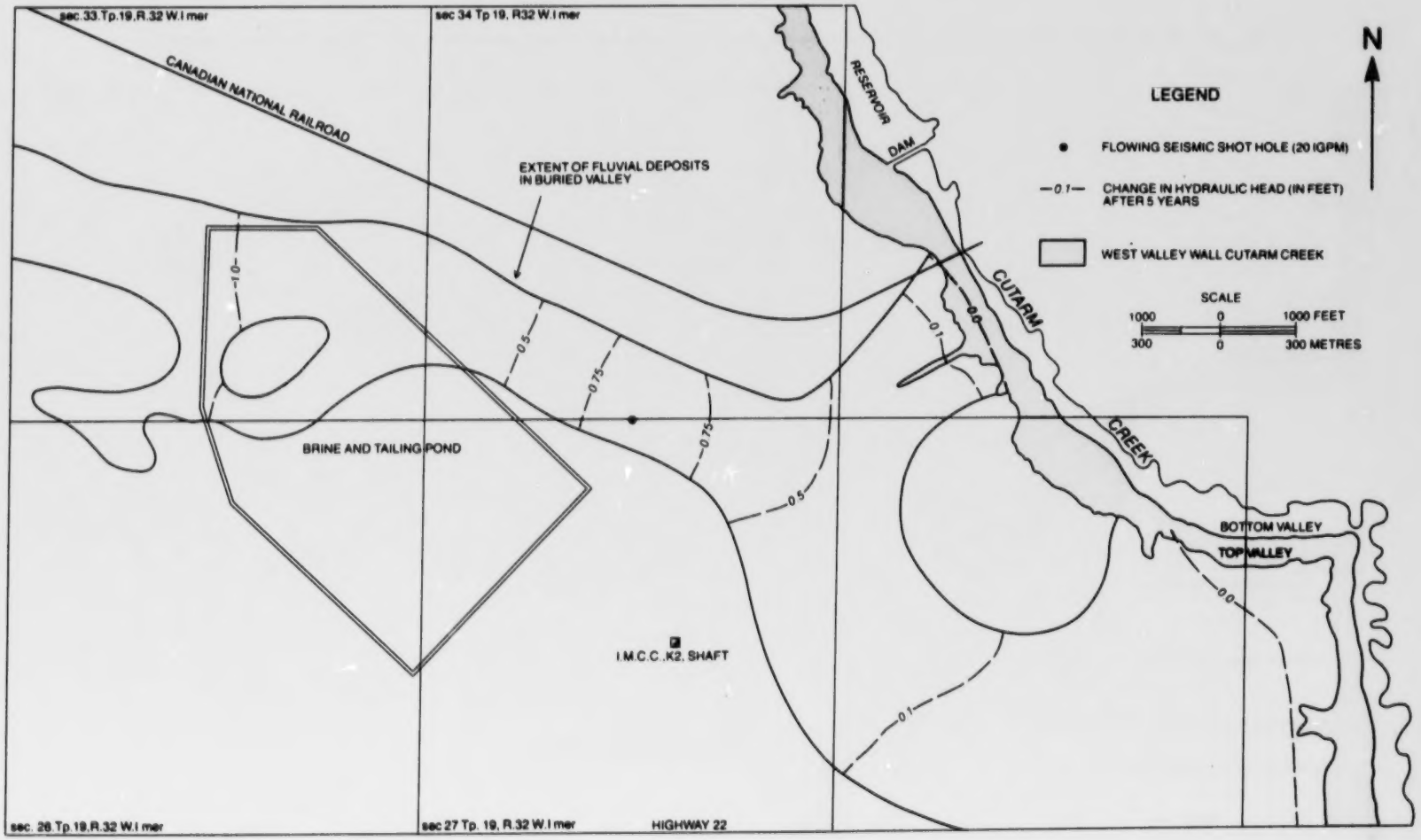

Figure 49. Change in hydraulic head in the buried valley aquifer after 5 years for the seismic shothole (FW1) discharging at a rate of 20 Igpm (91 l/min).

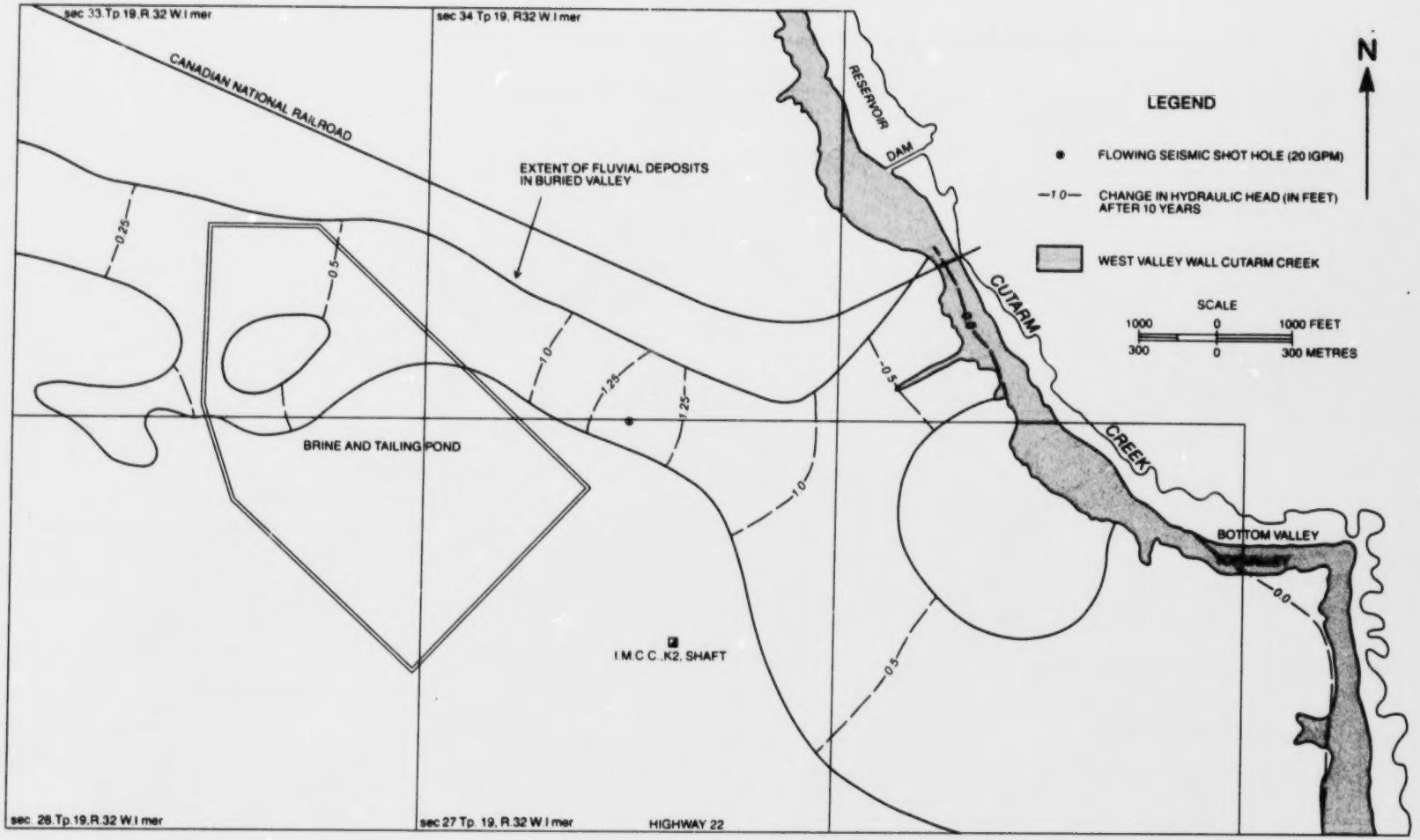
sec 33 Tp 19, R 32 W I mer
sec 34 Tp 19, R32 W I mer
CANADIAN NATIONAL RAILROAD
EXTENT OF FLUVIAL DEPOSITS IN BURIED VALLEY
RESERVOIR DAM
CUTARM CREEK
BRINE AND TAILING POND
I.M.C.C. K2. SHAFT
BOTTOM VALLEY
sec 28 Tp 19, R 32 W I mer
sec 27 Tp 19, R 32 W I mer
HIGHWAY 22
N
LEGEND
FLOWING SEISMIC SHOT HOLE (20 IGPM)
—10— CHANGE IN HYDRAULIC HEAD (IN FEET) AFTER 10 YEARS
WEST VALLEY WALL CUTARM CREEK
SCALE
1000 0 1000 FEET
300 0 300 METRES

Figure 50. Change in hydraulic head in the buried valley aquifer after 10 years for the seismic shothole (FW1) discharging at a rate of 20 Igpm (91 l/min).

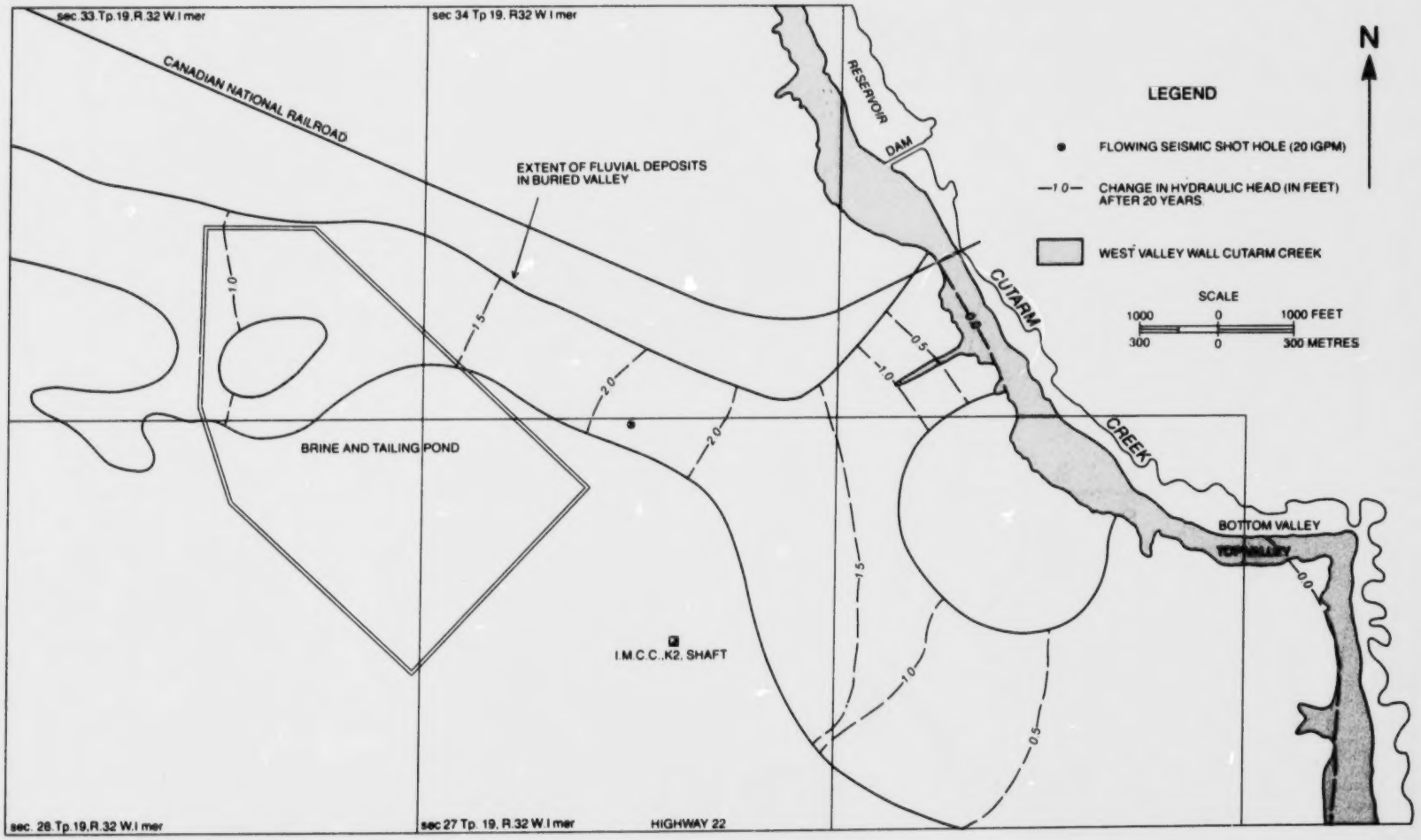
sec 33 Tp 19 R 32 W I mer
sec 34 Tp 19 R32 W I mer
CANADIAN NATIONAL RAILROAD
EXTENT OF FLUVIAL DEPOSITS IN BURIED VALLEY
RESERVOIR DAM
CUTARM CREEK
BRINE AND TAILING POND
I.M.C.C. K2. SHAFT
BOTTOM VALLEY
sec 26 Tp 19 R 32 W I mer
sec 27 Tp 19 R 32 W I mer
HIGHWAY 22
N
LEGEND
FLOWING SEISMIC SHOT HOLE (20 IGPM)
—10— CHANGE IN HYDRAULIC HEAD (IN FEET) AFTER 20 YEARS
WEST VALLEY WALL CUTARM CREEK
SCALE
1000 0 1000 FEET
300 0 300 METRES

Figure 51. Change in hydraulic head in the buried valley aquifer after 20 years for the seismic shothole (FW1) discharging at a rate of 20 Igpm (91 l/min).

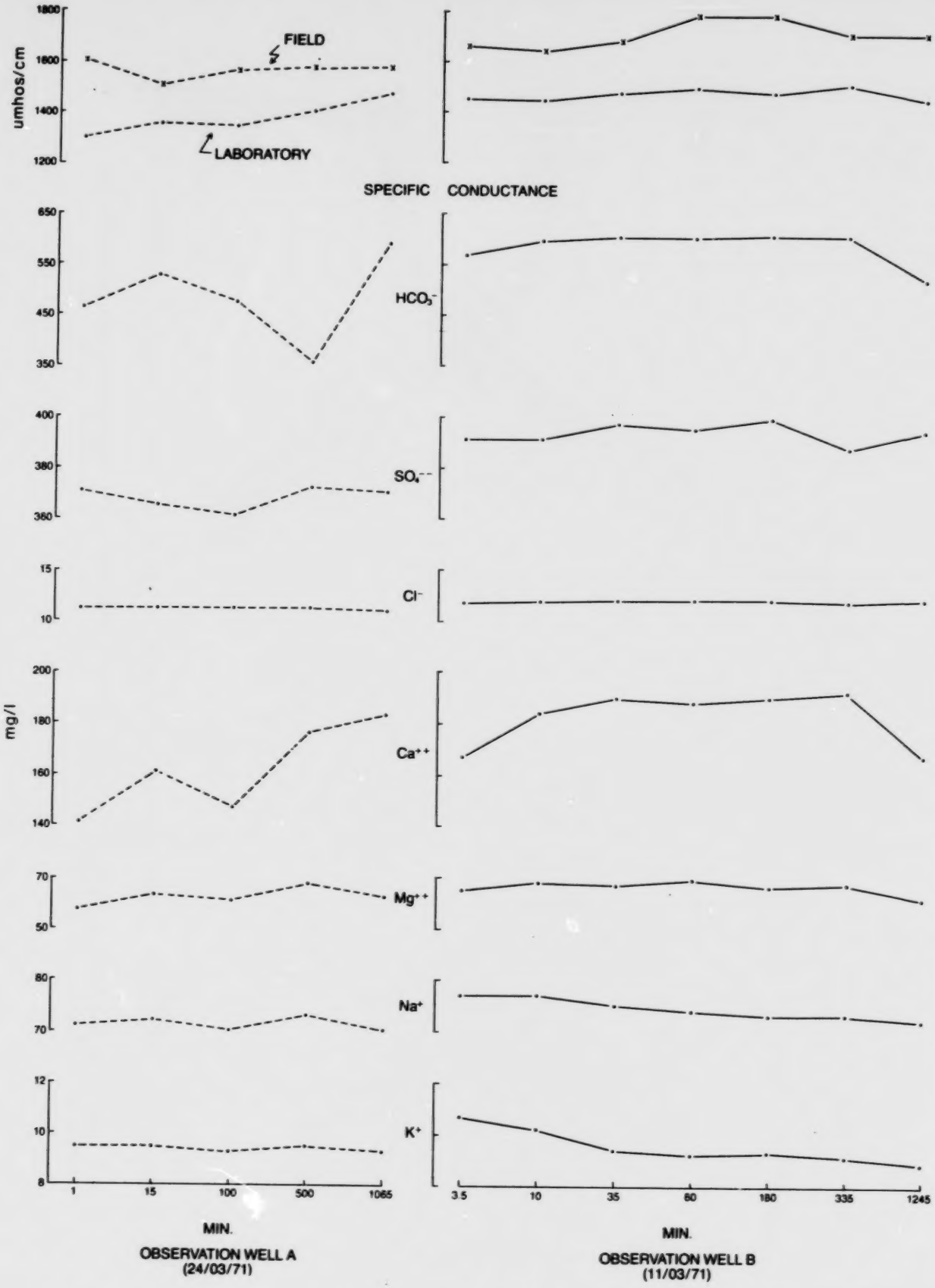

Figure 52. Analytical results of water samples taken during the pump test at observation wells A and B, which froze prior to analysis.

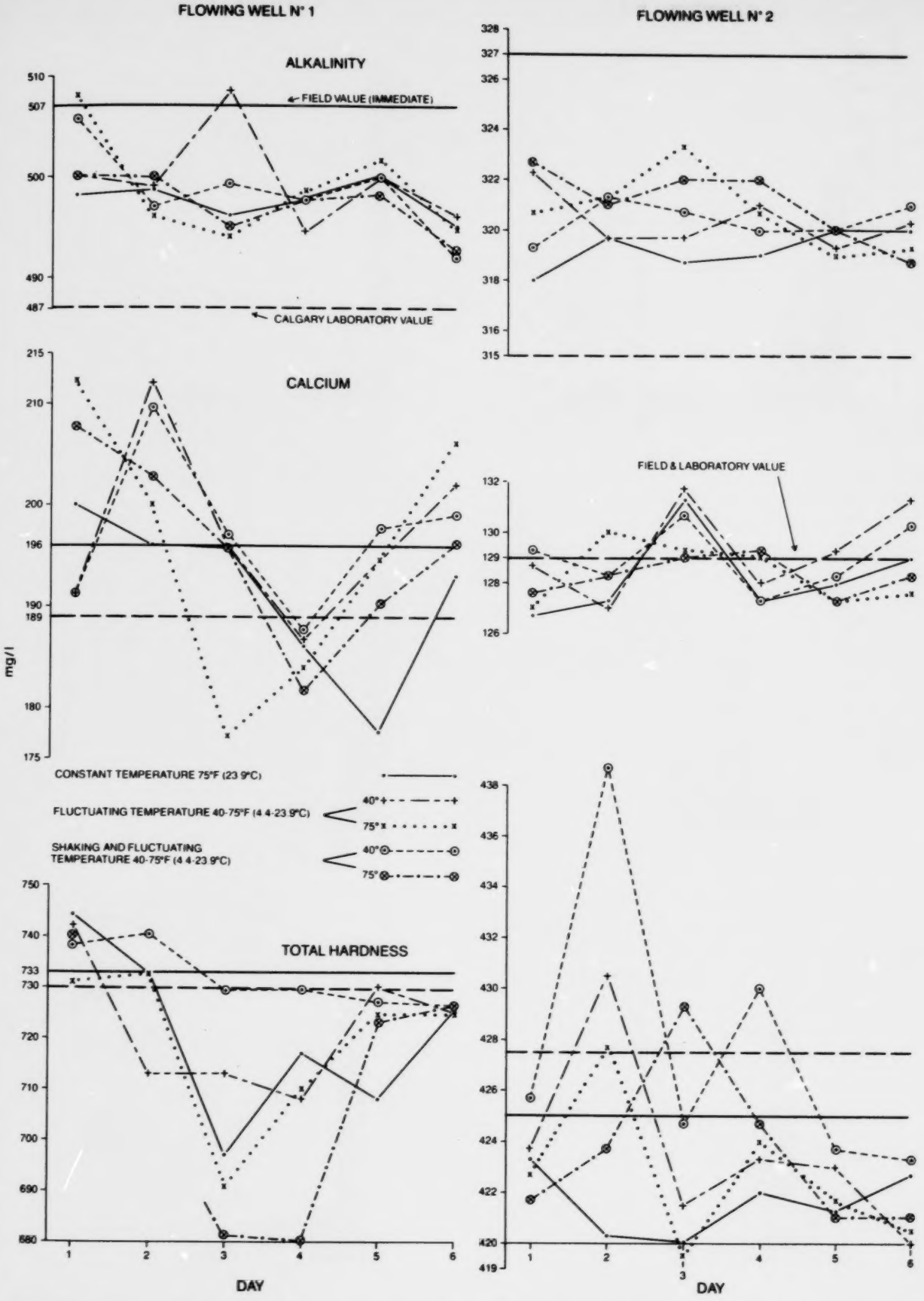

Figure 53. Daily analyses of alkalinity, calcium, and total hardness of samples from flowing wells 1 and 2 subjected to temperature cycles and shaking.

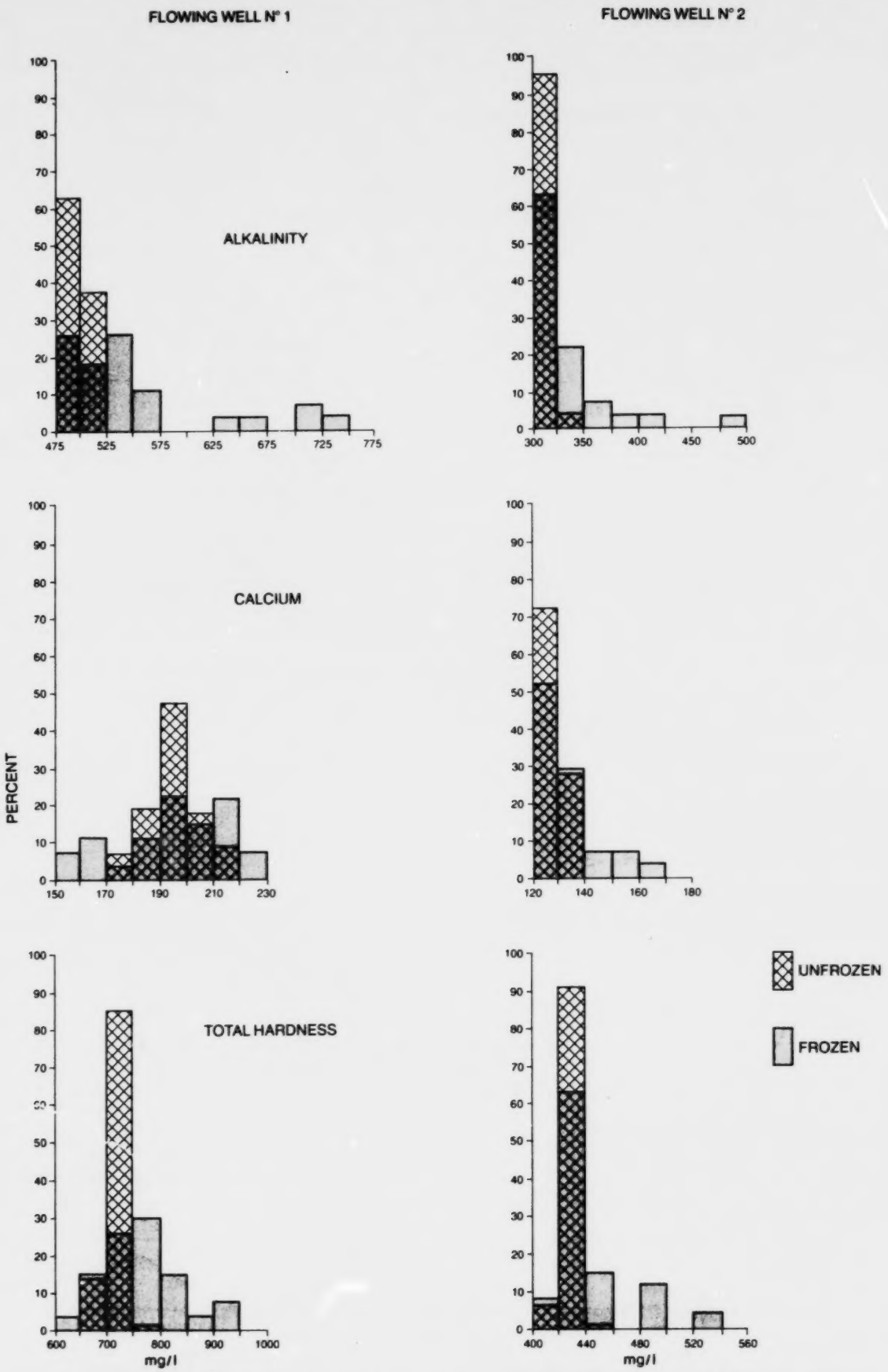

Figure 54. Histogram of concentration of alkalinity, calcium, and total hardness of frozen versus unfrozen samples.

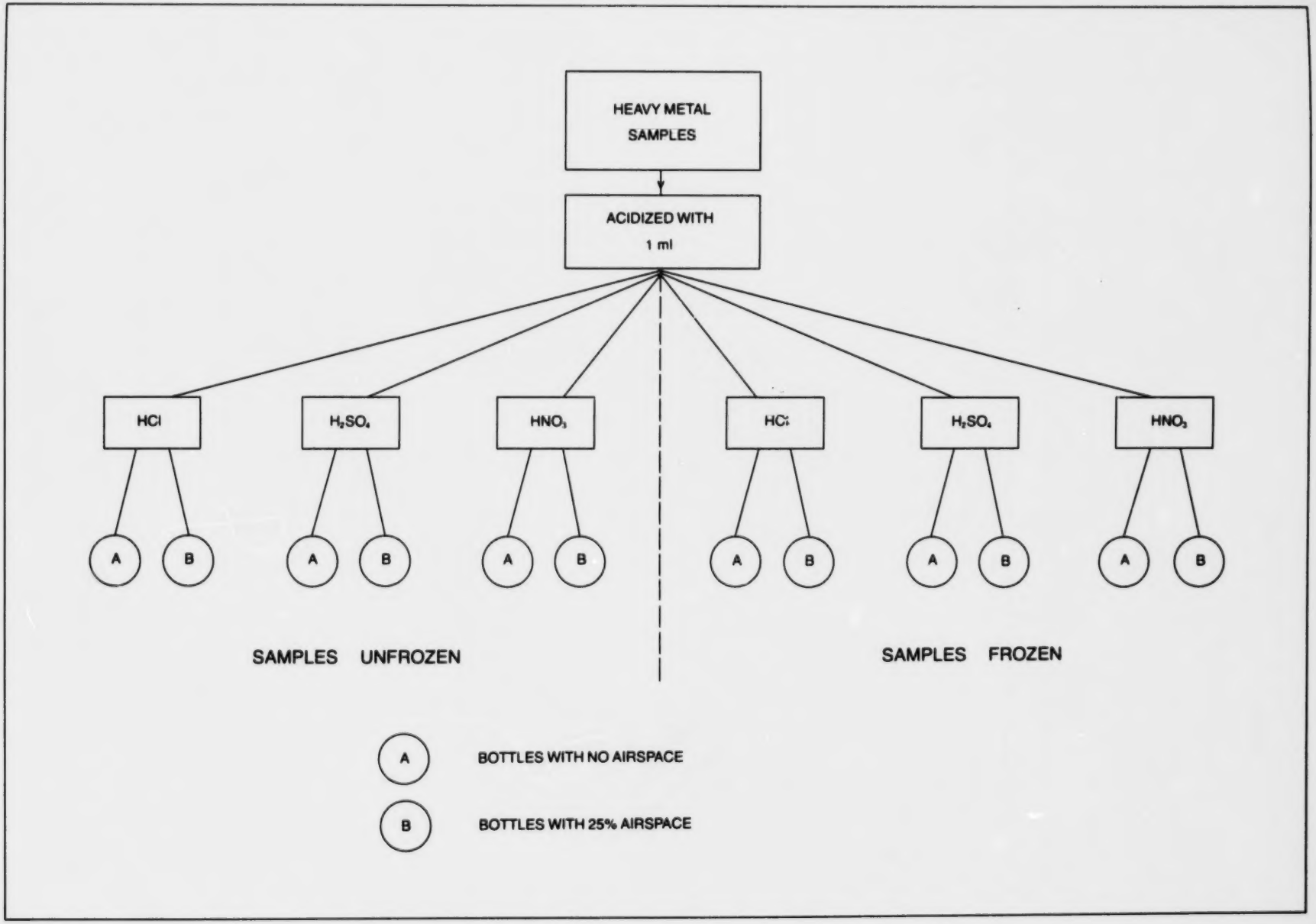

Figure 55. Sampling flow sheet for heavy metal preservation study.

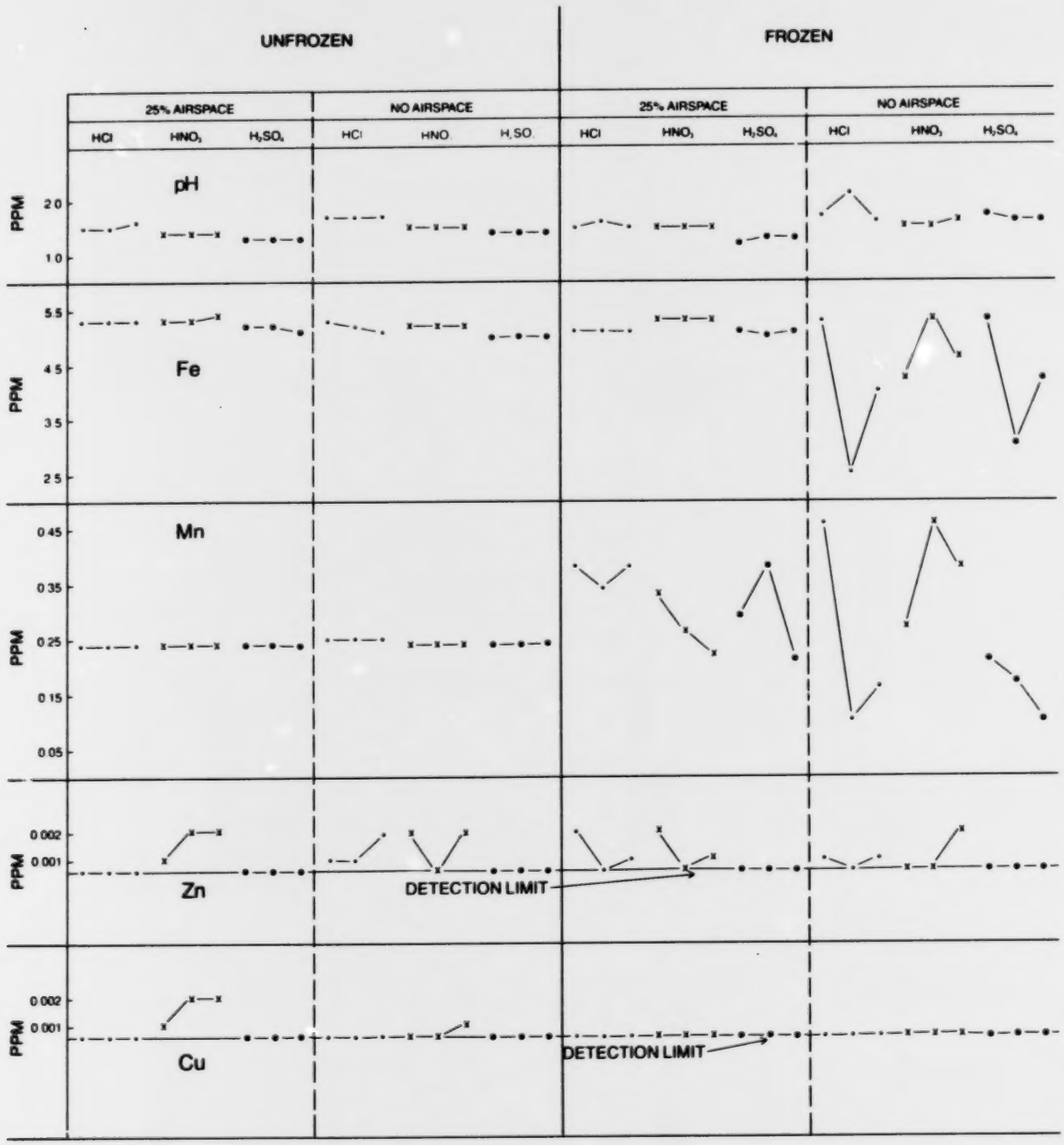

NOTE:
BOTH Pb & Cd BELOW DETECTION LIMIT FOR ALL SAMPLES

WELL N° 1 (SW.2-34-19-32-W1)

SAMPLES COLLECTED 18/12/72
SAMPLES ANALYZED 27/12/72

Figure 56. Analytical results, heavy metal samples, flowing well 1.

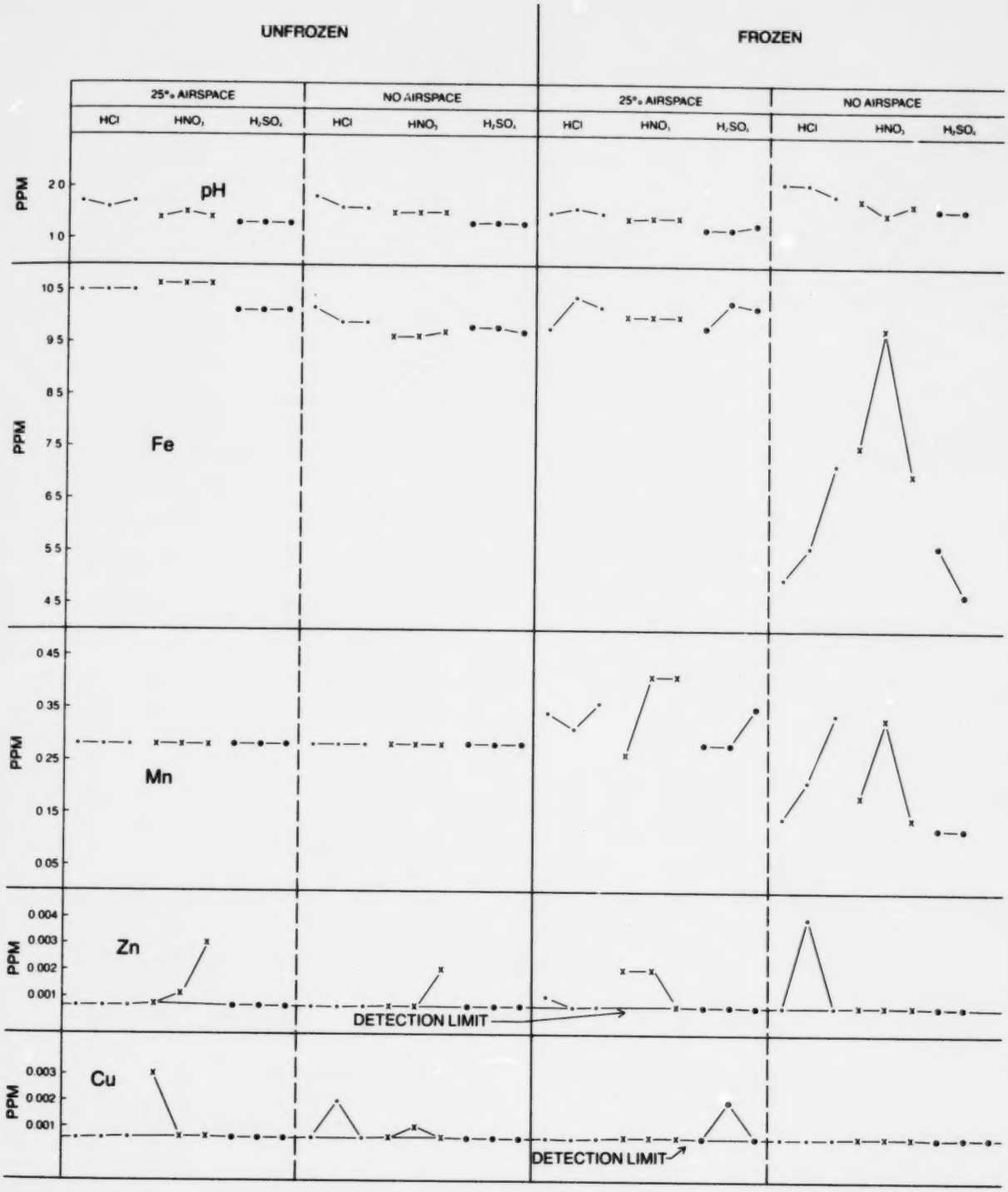

NOTE:
BOTH Pb & Cd BELOW DETECTION LIMIT FOR ALL SAMPLES

WELL N° 3 (N.E. 1-27-19-32-W 1)

SAMPLES COLLECTED 18/12/72
SAMPLES ANALYZED 27/12/72

Figure 57. Analytical results, heavy metal samples, flowing well 3.

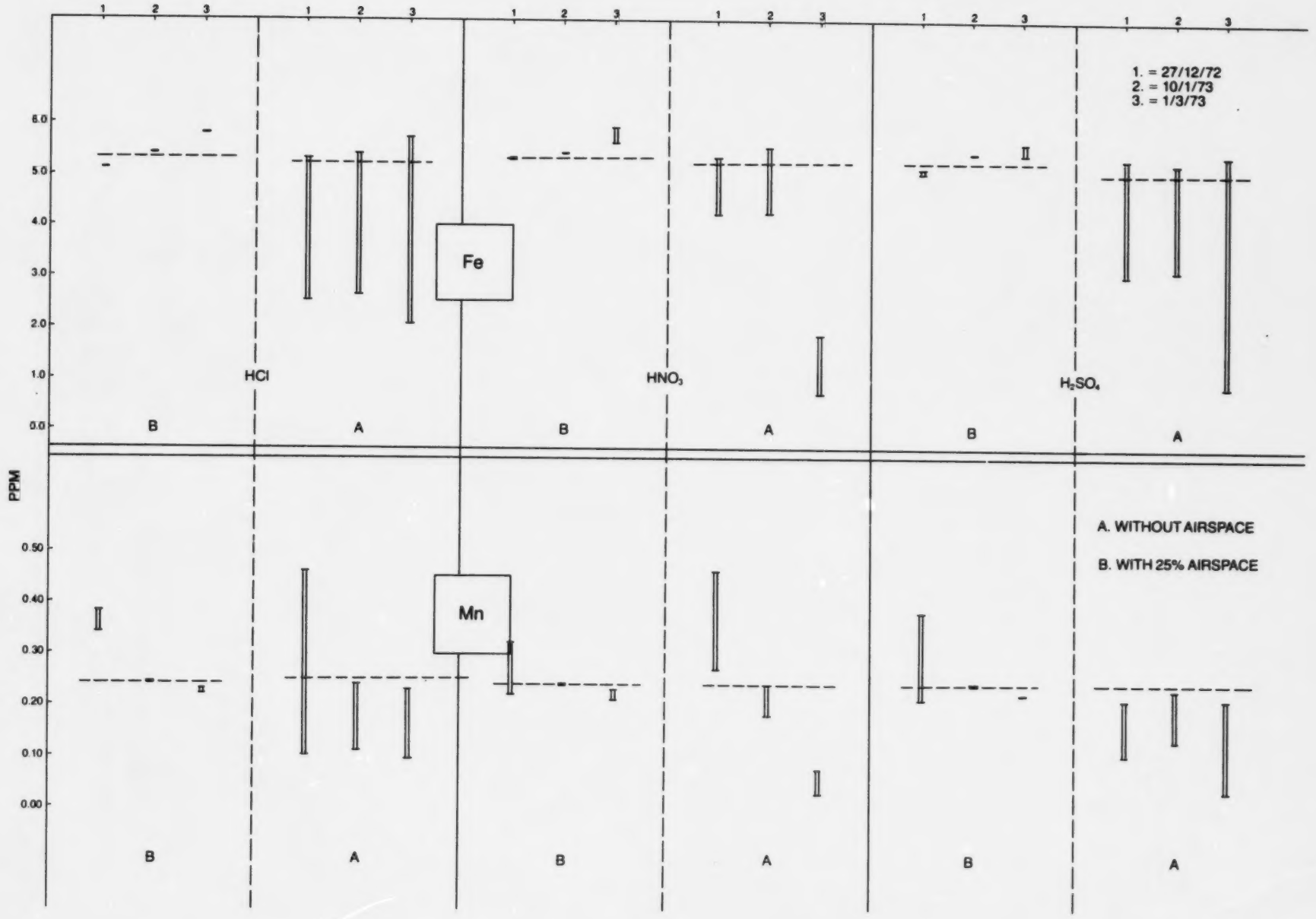

Figure 58. Successive analyses, frozen heavy metal samples, flowing well 1.

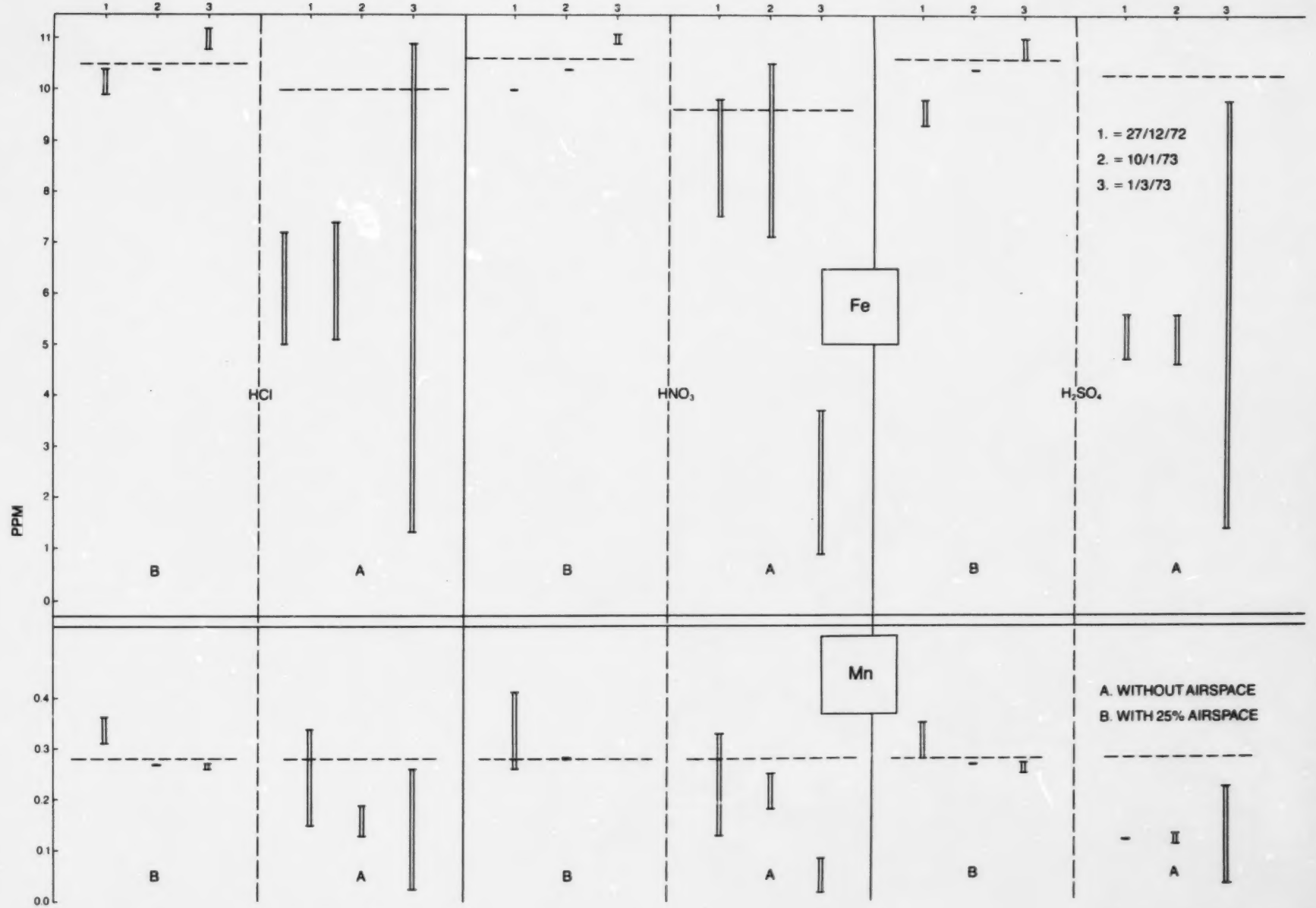

Figure 59. Successive analyses, frozen heavy metal samples, flowing well 3.

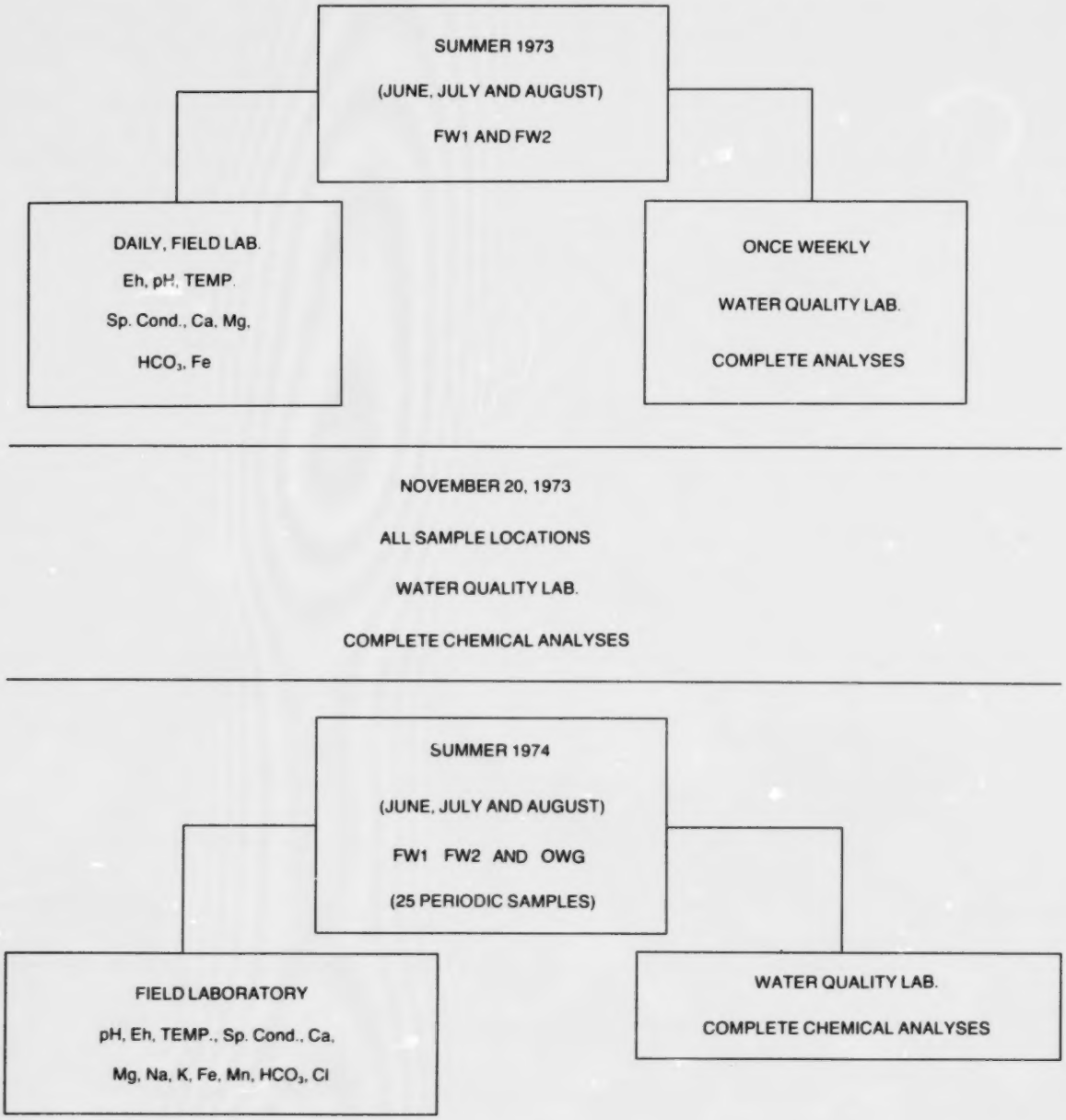

Figure 60. Summary of hydrochemical sampling schedule, 1973 and 1974.

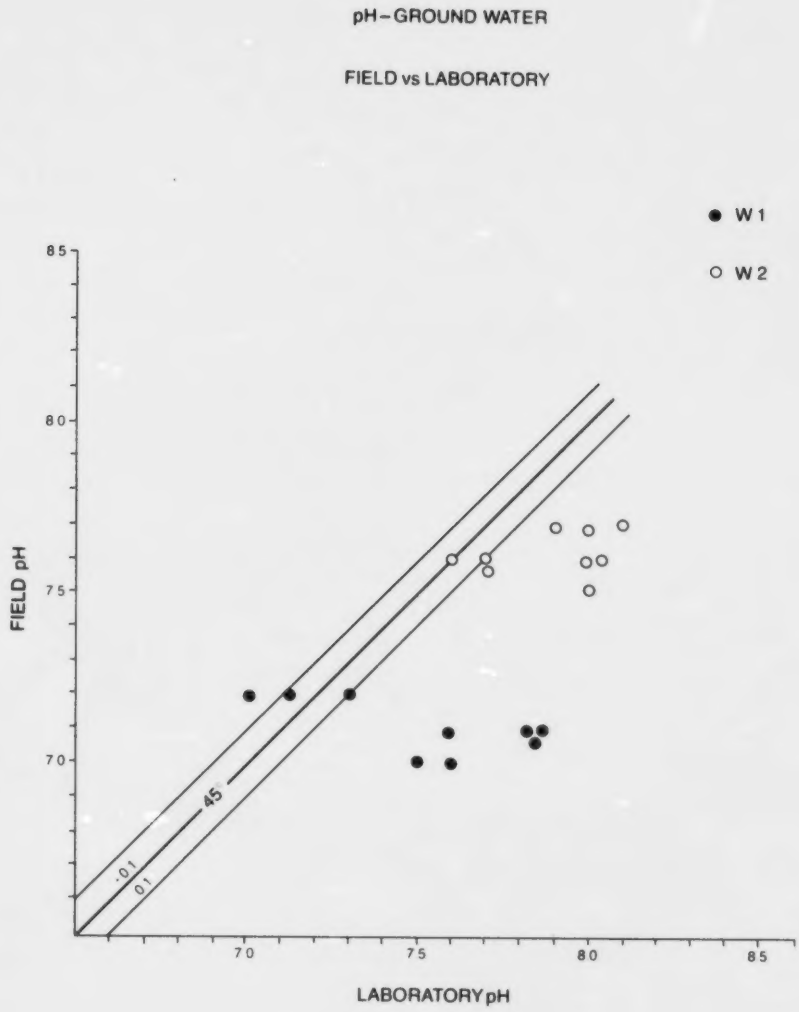

Figure 61. Comparison of field and laboratory measured pH values of groundwater samples (after Davison, 1974).

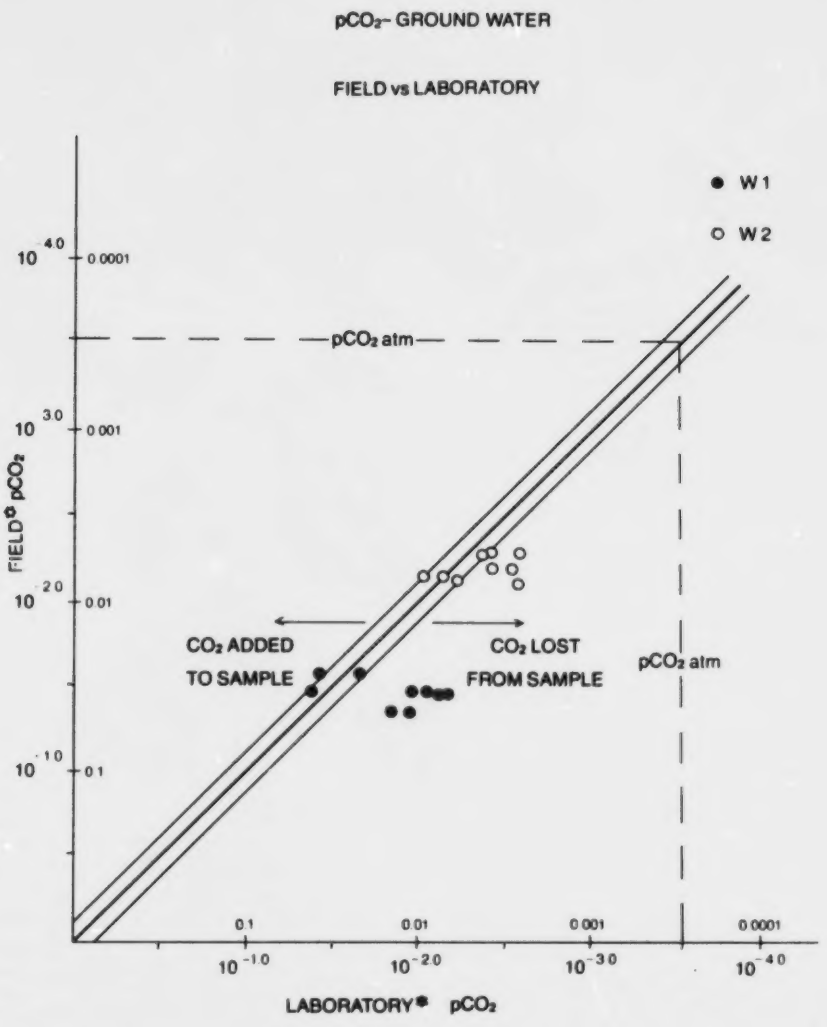

Figure 62. Comparison of field and laboratory pCO_2 values of groundwater samples (after Davison, 1974).

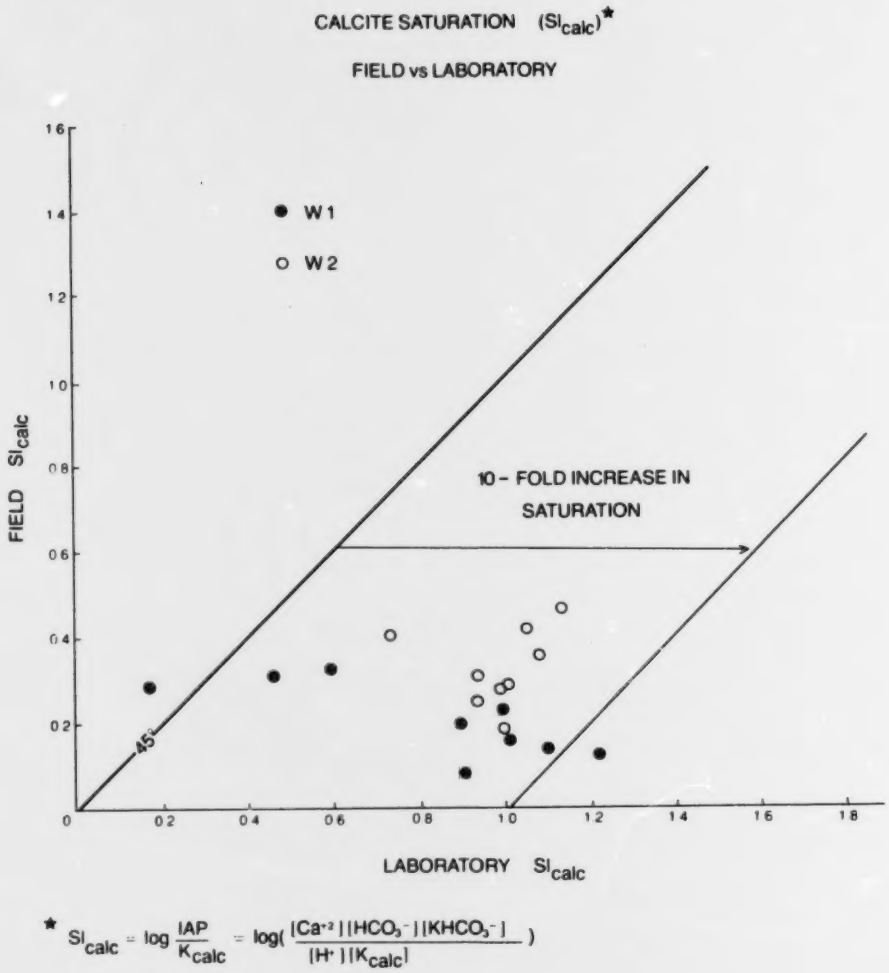

$$* \; SI_{calc} = \log \frac{IAP}{K_{calc}} = \log\left(\frac{[Ca^{+2}][HCO_3^-][KHCO_3^-]}{[H^+][K_{calc}]}\right)$$

Figure 63. Calcite saturation in stored groundwater samples (after Davison, 1974).

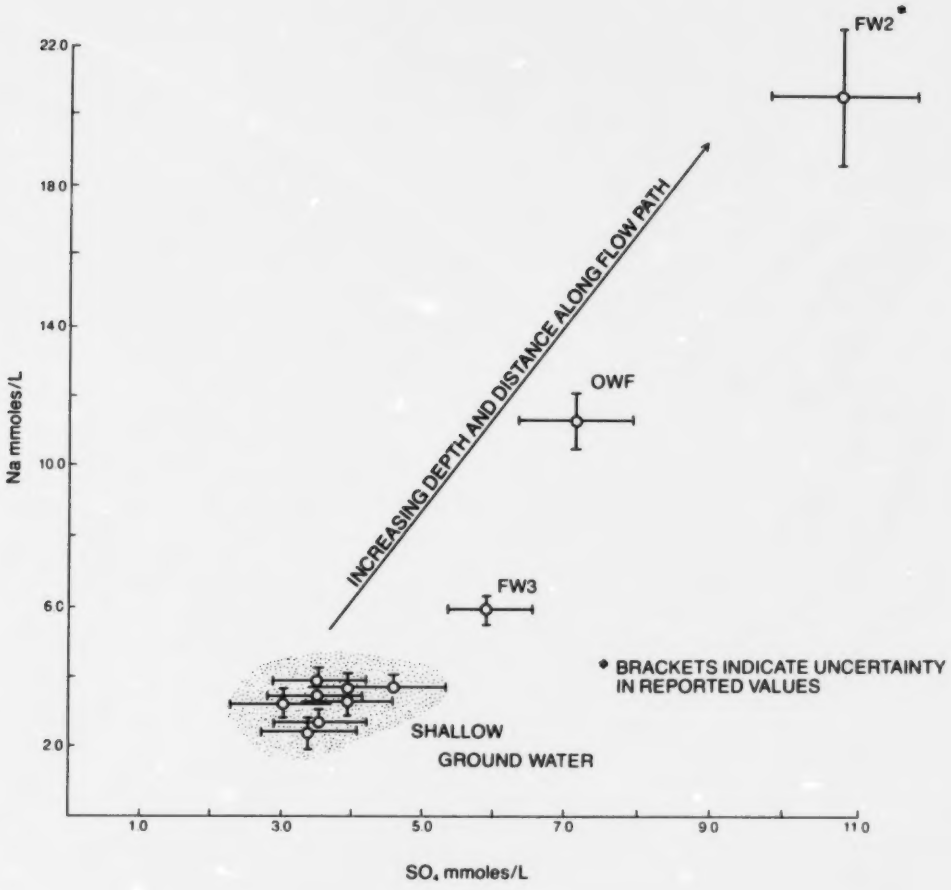

Figure 64. Na-SO_4 ion plot of aquifer water samples.

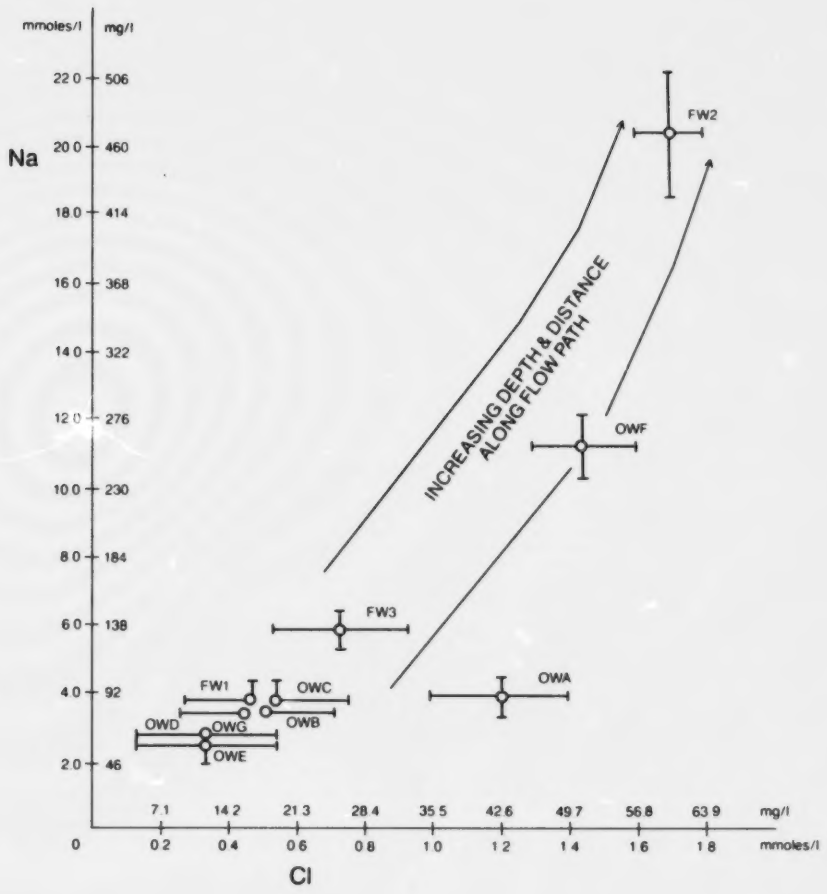

Figure 65. Na-Cl plot of aquifer water samples.

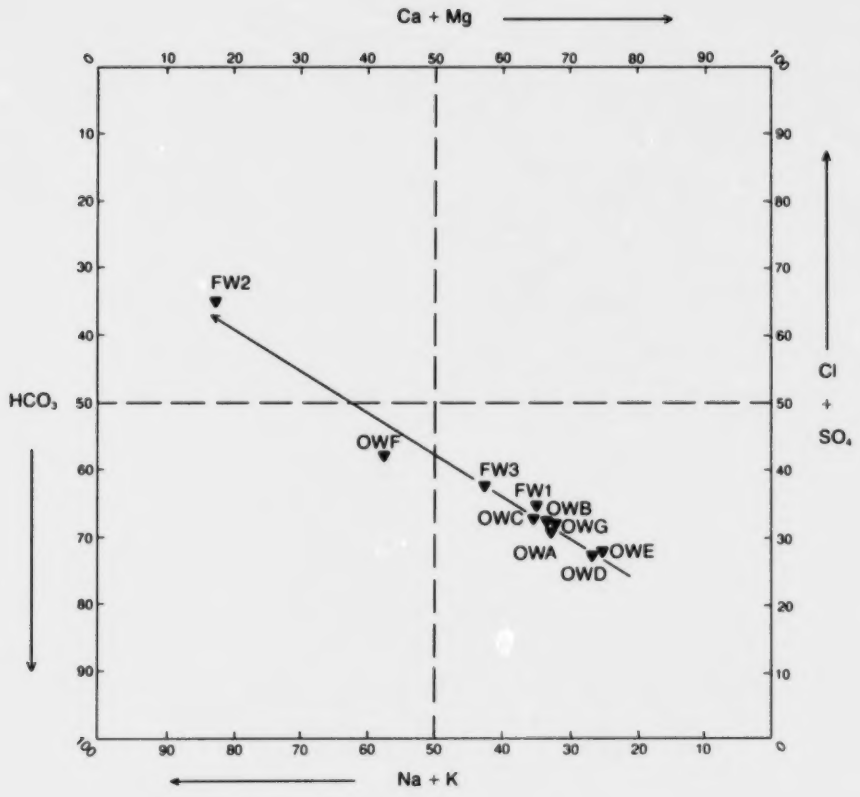

Figure 66. Modified Piper ion plot of aquifer water samples.

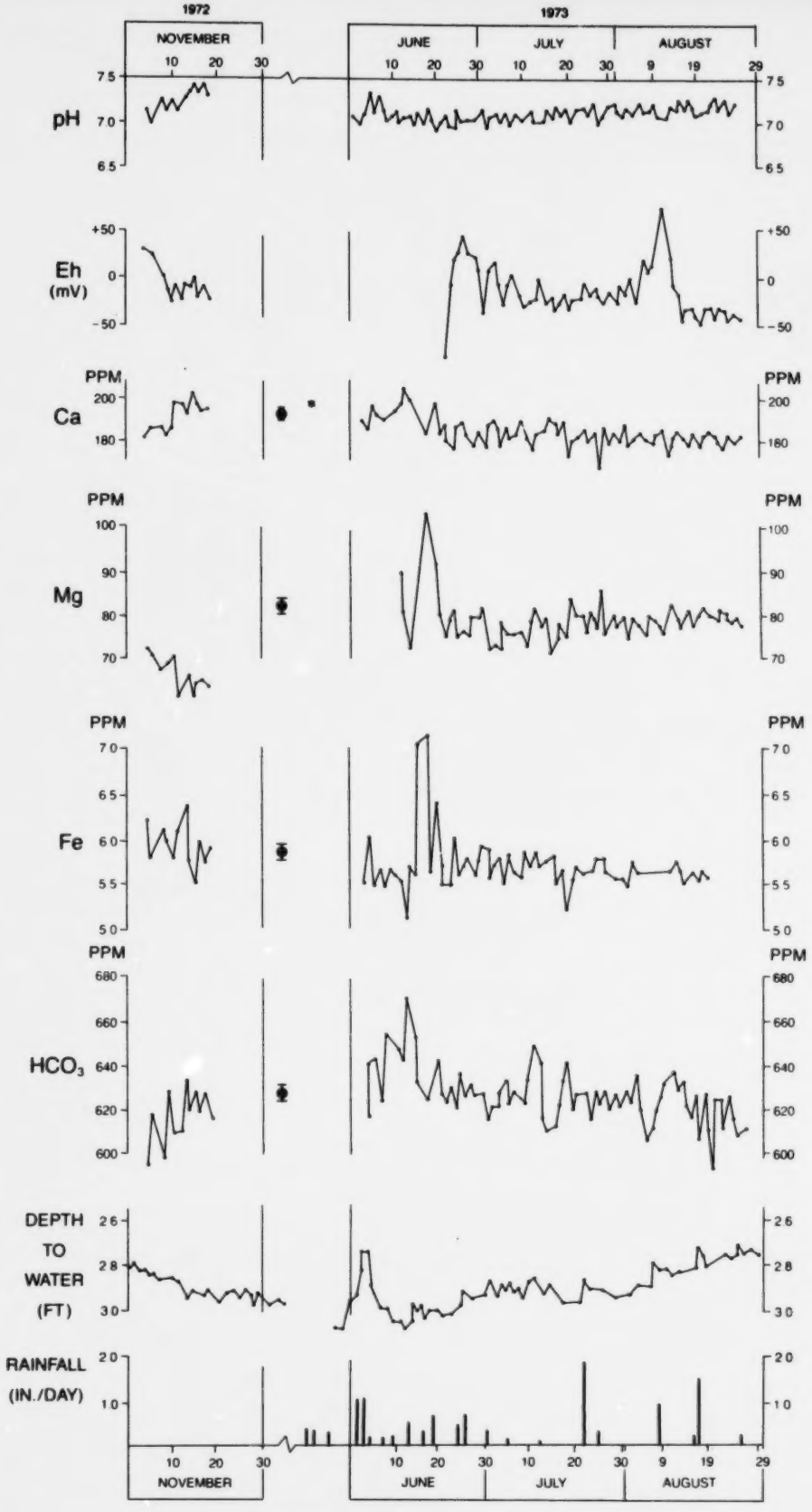

• ANALYTICAL UNCERTAINTY (DAVISON, 1976)

Figure 67. Temporal ion plots for water samples collected from flowing well 1 during November 1972 and June, July, and August 1973.

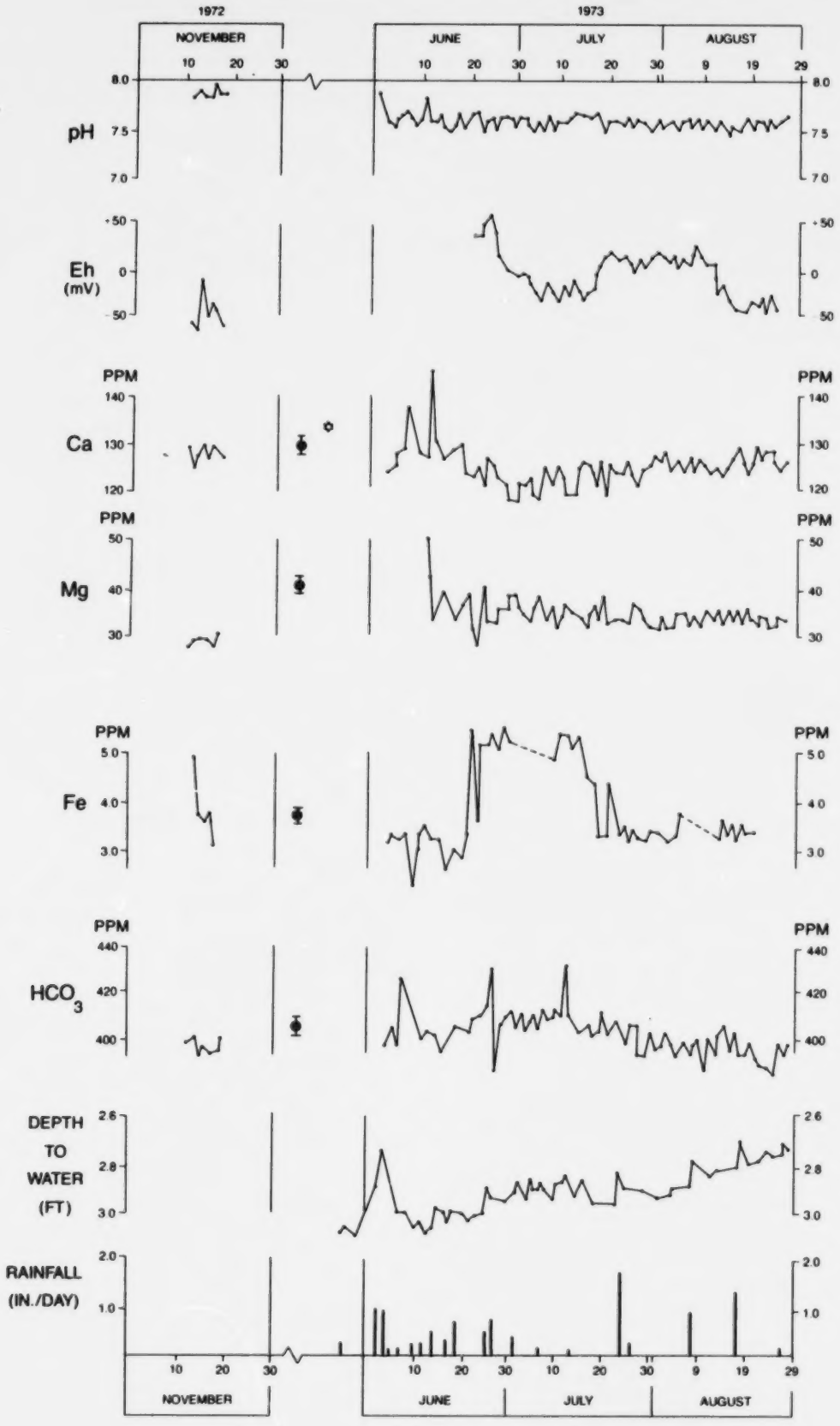

✡ ANALYTICAL UNCERTAINTY (DAVISON 1976)

Figure 68. Temporal ion plots for water samples collected from flowing well 2 during November 1972 and June, July, and August 1973.

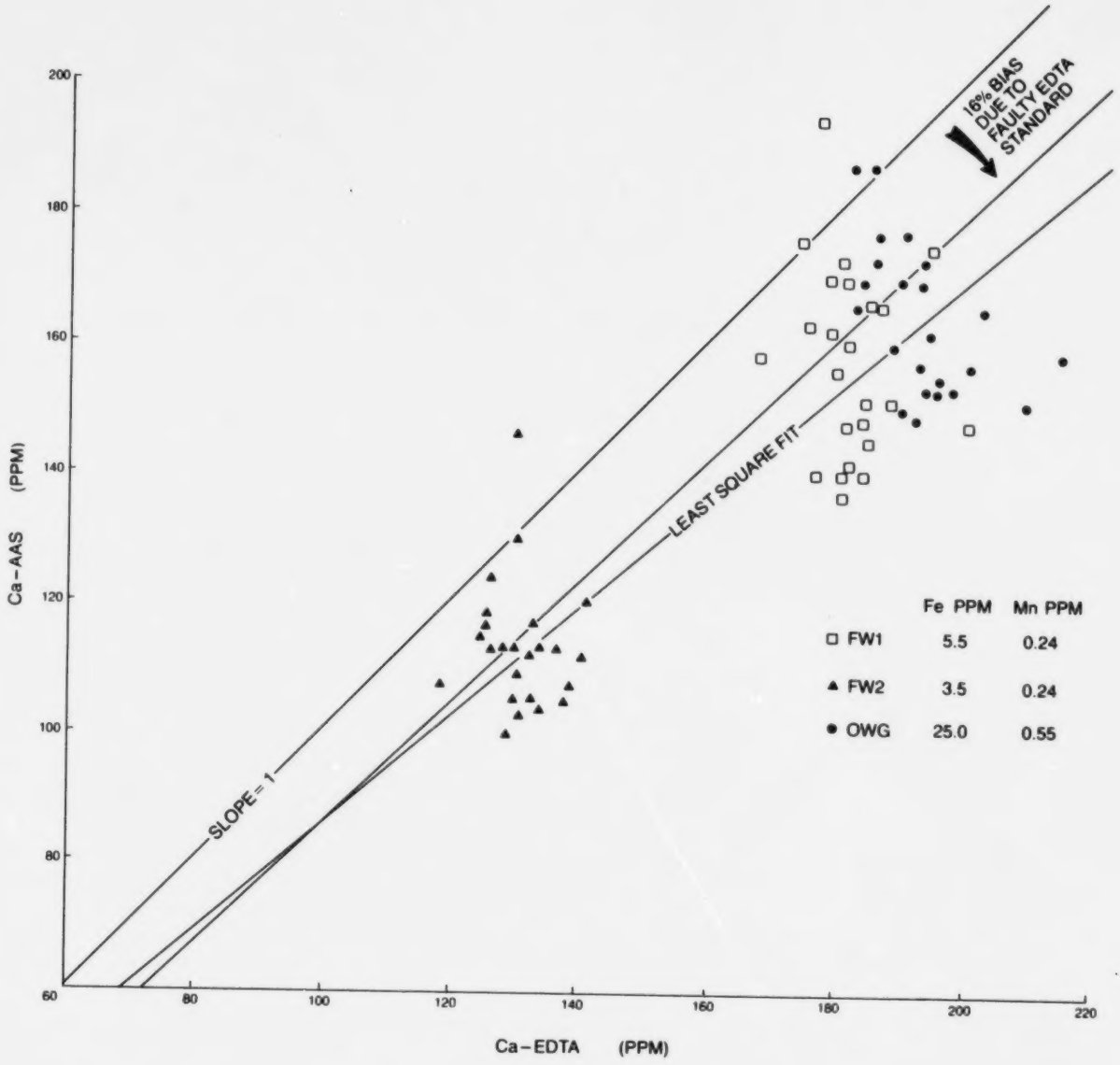

Figure 69. Comparison of AAS-EDTA determination of Ca in groundwater samples.

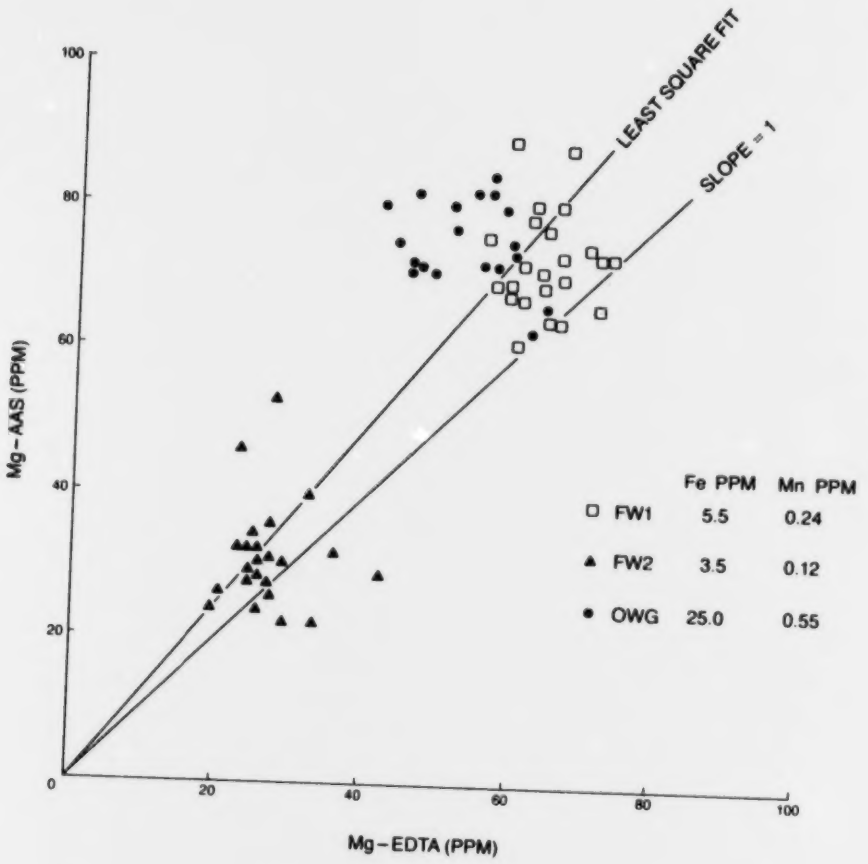

Figure 70. Comparison of AAS-EDTA determination of Mg in groundwater samples.

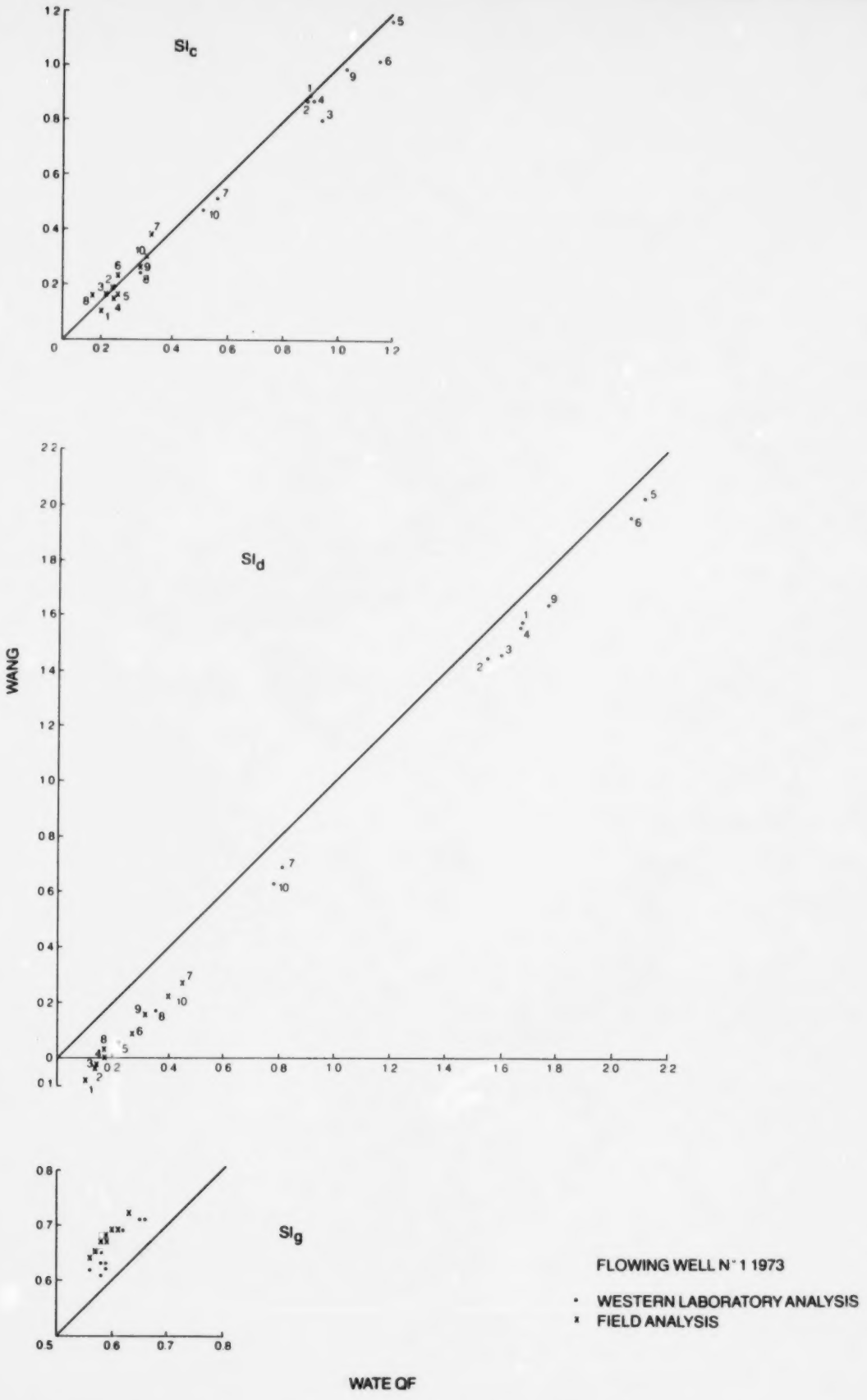

Figure 71. Comparison of saturation indices obtained from WATEQF II program and Wang computer: flowing well 1.

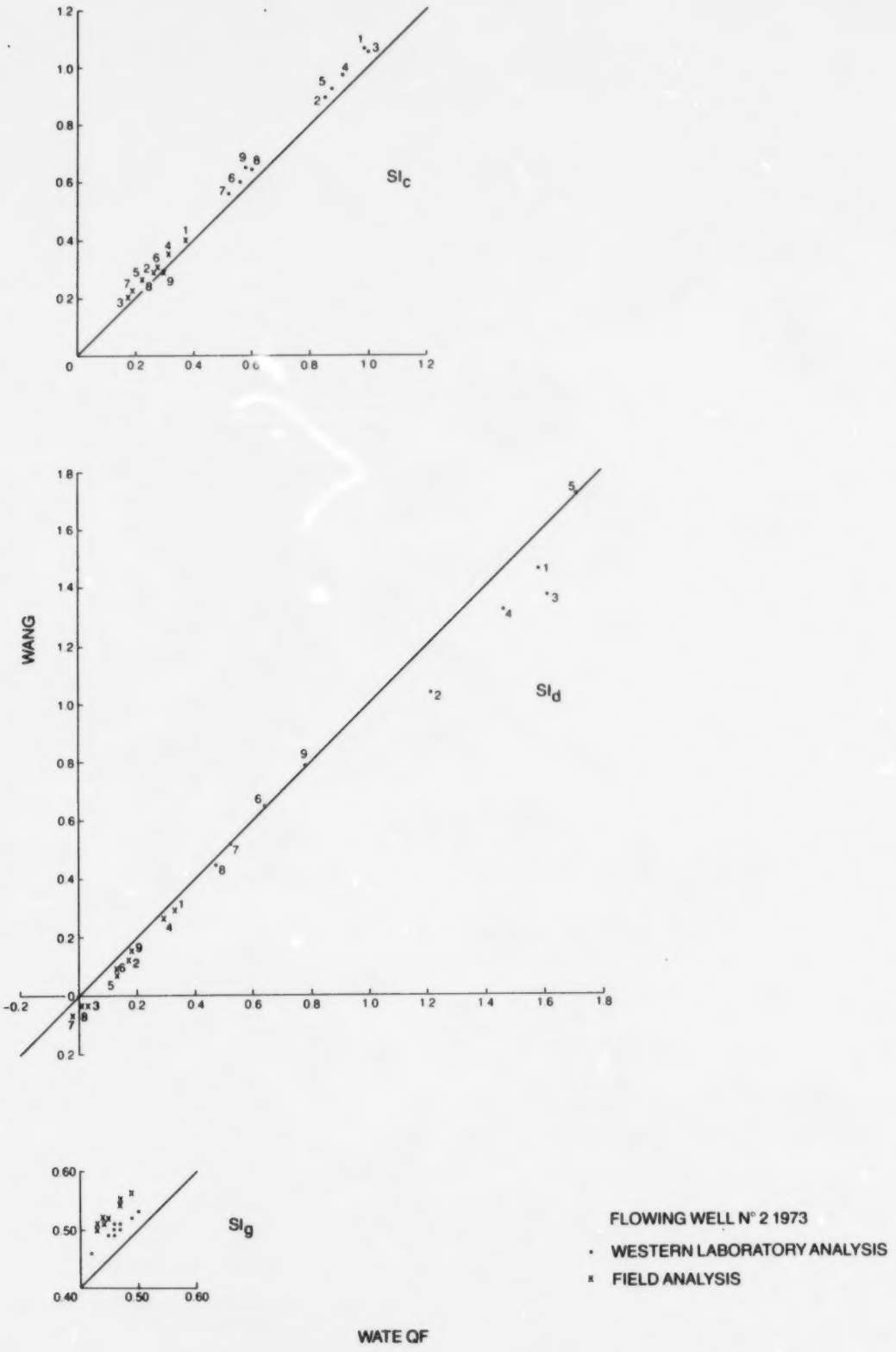

Figure 72. Comparison of saturation indices obtained from WATEQF II program and Wang computer: flowing well 2.

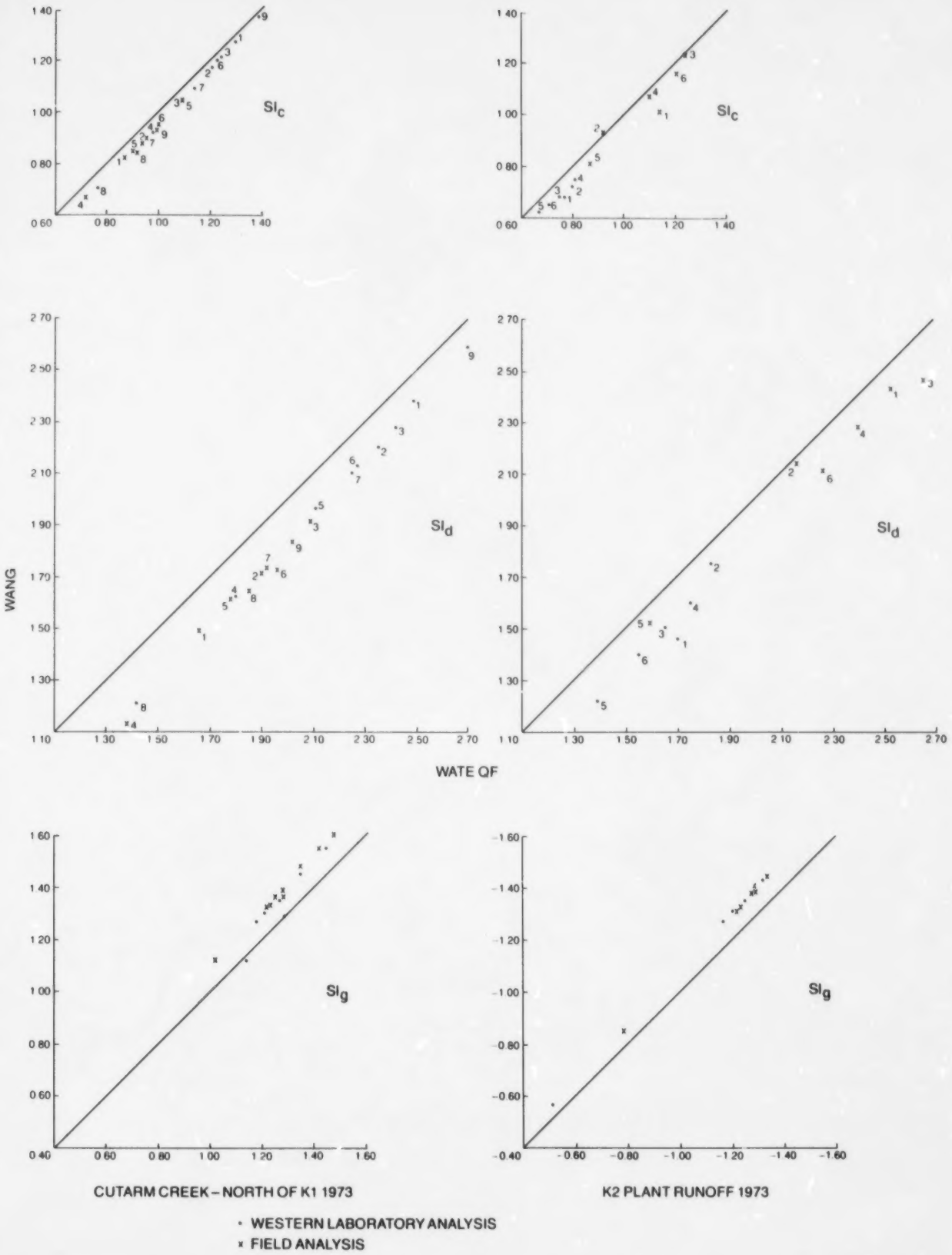

Figure 73. Comparison of saturation indices obtaind from WATEQF II program and Wang computer: Cutarm Creek north of K1 mine and plant runoff K2 mine site.

APPENDIX I

Hydrodynamic Response or Slug-Testing Equipment (J. A. Banner and J. A. Vonhof)

Hydrodynamic Response or Slug-Testing Equipment (J. A. Banner and J. A. Vonhof)

The slug-testing apparatus consisted of two main parts: tools to quickly introduce or extract a quantity of water into or from the well being tested and a mechanism to continuously record the water level in the well.

The "arrow tube" was developed for this project as a means of quickly introducing water from a point just above the water surface to raise the water level in the well a controlled amount in a minimum of time and with a minimum of disturbance by impact. The arrow tube used for this project consisted of a 3-ft (90 cm) length of 4-in. (101.6 mm) outside diameter aluminum tubing, open top and bottom, and fitted with brass spiders to guide the arrow. The arrow consisted of a 3/8-in. (9.5 mm) diameter brass shaft, 3 ft (90 cm) long, fitted with a 3 ¾-in. (9.5 cm) four-bladed head fabricated from 1/16-in. (1.6 mm) brass plate. The arrow was normally held up inside the aluminum tube by the spring-loaded plunger of an electric solenoid, but was free to fall to a point where the head protruded from the bottom of the tube when the solenoid plunger was electrically retracted. The arrow tube was prepared for use by stretching a double layer of Saran Wrap across the bottom of the tube and holding it in place with rubber bands. The tube was then filled with the desired amount of water and lowered down into the well by means of an electric cable which both supported the tube and provided a connection to the solenoid. The tube was positioned close to the water surface but far enough above it so that when the surface was raised by the additional water, the bottom of the tube was still out of the water. At the appropriate time, the solenoid cable was connected via a push button to a battery, the solenoid was tripped, the arrow was dropped through the Saran Wrap, and the water was released.

Water was extracted from the well, when required, by means of a bailer consisting of a 3-ft (90 cm) length of 3-in. (76 mm) copper pipe fitted at one end with a 1-in. (27 mm) foot valve and at the other end with a lifting ring. The bailer was lowered into the well by means of a rope tied to the lifting ring. The foot valve allowed the bailer to fill gently without excessive displacement of the water surface. At the appropriate time, the bailer was quickly withdrawn, lowering the water level in the well.

The water level in the well was measured by means of a pressure transducer and a transducer indicator and recorded by a strip-chart recorder. The pressure transducer, a Celesco model P1D variable reluctance transducer with full scale range of ± 1 psid, was installed in an aluminum protective case. To prevent problems associated with compression of entrapped air in the cavity of the transducer, the case was fitted with a porous cup, and the transducer cavity, porous cup and connecting tubing were filled with water. The reference side of the transducer was connected to the atmosphere via 2 mm internal diameter nylon tubing taped to the connecting cable. The response time of this system was faster than the response of the recorder used to record it.

The transducer was connected via the cable to a Pace model CD25 transducer indicator. This unit provided not only an indicating meter with expanded ranges but also controls for calibrating the transducer, a calibrated variable offset to suppress any desired percentage of the transducer range and an output to drive a recorder. This output was recorded by a Hewlett Packard Mosley 680 strip-chart servo-recorder which provided a wide choice of chart speeds and allowed range expansion independent of the transducer indicator. The transducer indicator and the recorder were powered by a Terado model 50-201 reed-controlled constant-frequency 150-W power converter operated from a 12-V automobile battery.

In use, the transducer was filled with water and calibrated in a column of water of known height, usually one foot (305 mm), until a two-point calibration was achieved. This gave an accuracy (combined hysteresis and non-linearity) of ± ¼% of the calibrated range. Then, with the recorder running, the transducer was lowered into the water in the well. If water was to be added, the transducer was placed about 10% of its range below the water surface; if water was to be removed, it was placed at about 90%. The arrow tube or bailer was then positioned. When the effects of introducing the transducer into the water had dissipated, the arrow tube was tripped or the bailer withdrawn. Recording was continued until the water level ceased falling or rising.

Few problems were encountered with this equipment. At some sites, induced 60-H_z currents caused noise in the recording system. This was eliminated by grounding the equipment to a short ground rod driven into the ground.

At other sites, grounding the system had to be avoided to prevent noise. Filling the transducer with water was a nuisance and the porous cups were easily broken. These problems were eliminated in a modification (not used on this project) which made use of Statham model PL 131C-XX-350 miniature flush-diaphragm strain-gauge transducers mounted in cases with radial holes at the height of the diaphragms.

APPENDIX II

Pump-Test Data for Observation Wells A to G

PUMPING TEST DATA - DRAWDOWN TEST

OBSERVATION WELL A — Nearest testhole(s) IWB 44

Elevation 1661.32 ft. — Depth 45.5 ft.

TIME SINCE START OF PUMPING		Pumping Well B Radius(r) 860 Pumping rate (Q) 8.33		C 1915 16.66		F 1305 49.98		G 1305 49.98	
minutes	days	Dwdn.	$t/r^2\ 10^{-8}$	Dwdn.	$t/r^2\ 10^{-7}$	Dwdn.	$t/r^2\ 10^{-8}$	Dwdn.	$t/r^2\ 10^{-8}$
15	0.0142	0.006	1.92			0.014	0.83	0.021	
30	0.0208	0.0115	2.81			0.039	1.22	0.057	
45	0.0312	0.016	4.23			0.062	1.83	0.09	
60	0.0416	0.02	5.63	0.0166	0.1136	0.088	2.45	0.123	
75	0.052	0.023	7.03	0.0249	0.1418	0.11	3.05	0.15	
90	0.0625	0.0275	8.45			0.129	3.67	0.18	
105	0.0729	0.0301	9.86			0.148	4.28	0.202	
120	0.0833	0.035	11.26			0.166	4.89	0.23	
135	0.0937	0.0375	12.68	0.0498	0.2556	0.183	5.50	0.25	
150	0.104	0.04	14.06			0.20	6.11	0.27	
165	0.114	0.0435	15.49						
180	0.125	0.047	16.90			0.2275	7.34	0.31	
195	0.135	0.049	18.31	0.0747	0.368				
210	0.145	0.051	19.71			0.252	8.56	0.342	
240	0.167	0.057	22.58	0.0913	0.4554	0.277	9.81	0.374	
270	0.187	0.060	25.35			0.301	1.10	0.402	
300	0.208	0.064	28.16			0.321	1.22	0.43	
360	0.250	0.0725	33.80			0.36	1.47	0.478	
450	0.312	0.083	42.25			0.41	1.83	0.533	
600	0.417			0.1826	1.137	0.476	2.45	0.611	
750	0.520								
900	0.625			0.2407	1.704				

PUMPING TEST DATA - DRAWDOWN TEST

OBSERVATION WELL B — Nearest testhole(s) IWB 43

Elevation 1659.13 ft. — Depth 47.3 ft.

TIME SINCE START OF PUMPING		Pumping Well A Radius(r) 860 Pumping rate (Q) 49.9		C 1085 16.6		F 1935 49.9		G 1935 49.9	
minutes	days	Dwdn.	t/r^2 (10^{-8})	Dwdn.	t/r^2 10^{-7}	Dwdn.	t/r^2 10^{-8}	Dwdn.	t/r^2 10^{-8}
15	0.0142	0.05	1.919						
30	0.0208	0.10	2.812	0.01	0.177	0.0015	0.556	0.0015	0.556
45	0.0312	0.14	4.225	0.025	0.266	0.007	0.835	0.007	0.835
60	0.0416	0.18	5.634	0.034	0.355	0.017	1.113	0.02	1.113
75	0.052	0.22	7.03			0.026	1.388	0.0345	1.388
90	0.0625	0.24	8.45	0.056	0.5319	0.038	1.669	0.05	1.669
105	0.0729	0.265	9.856			0.05	1.947	0.075	1.947
120	0.0833	0.295	11.26	0.077	0.709	0.06	2.225	0.08	2.225
135	0.0937	0.32	12.67			0.071	2.504	0.096	2.504
150	0.104	0.34	14.06			0.081	2.777	0.111	2.777
180	0.125	0.385	16.90	0.11	1.064	0.103	3.338	0.141	3.338
210	0.145	0.43	19.71	0.125	1.24	0.123	3.898	0.17	3.898
240	0.167	0.455	22.579	0.137	1.42	0.141	4.46	0.195	4.46
270	0.187	0.485	25.35	0.15	1.59	0.16	5.01	0.22	5.01
300	0.208	0.515	28.16			0.179	5.56	0.245	5.56
330	0.229	0.54	30.98						
360	0.250					0.21	6.68	0.29	6.68
390	0.270	0.587	36.61	0.193	2.30				
450	0.312	0.63	42.25	0.21	2.66	0.251	8.34	0.344	8.34
510	0.354	0.665	47.88						

PUMPING TEST DATA - DRAWDOWN TEST

OBSERVATION WELL C — Nearest testhole(s) IWB 49

Elevation 1659.56 ft. — Depth 50.6 ft.

TIME SINCE START OF PUMPING		Pumping Well	A	B		F		G	
		Radius(r)	1915	1085		3000		3000	
		Pumping rate (Q)	49.9	8.33		49.9		49.9	
minutes	days	Dwdn.	$t/r^2\ 10^{-8}$	Dwdn.	$t/r^2\ 10^{-7}$	Dwdn.	$t/r^2\ 10^{-8}$	Dwdn.	t/r^2
30	0.0208	0.0085	0.567						
45	0.0312	0.02	0.852	0.001	0.266				
60	0.0416	0.035	1.136	0.004	0.355				
75	0.052	0.05	1.418	0.008	0.443	0.003	0.577	0.001	0.577
90	0.0625	0.069	1.704	0.01	0.5319	0.0085	0.694	0.004	0.694
105	0.0729	0.087	1.988	0.013	0.620				
120	0.0833	0.104	2.272	0.0175	0.709	0.016	0.925	0.028	0.925
135	0.0937	0.1225	2.556	0.02	0.798				
150	0.104	0.14	2.836	0.023	0.885	0.026	1.155	0.045	1.155
180	0.125	0.17	3.408	0.029	1.064				
210	0.145	0.193	3.976	0.034	1.24	0.049	1.62	0.078	1.620
240	0.167	0.22	4.554	0.04	1.42	0.06	1.855	0.095	1.855
270	0.187	0.258	5.113	0.044	1.59	0.072	2.083	0.111	2.083
300	0.208	0.281	5.680	0.0485	1.77	0.084	2.314	0.128	2.314
330	0.229			0.0525	1.95				
360	0.250	0.325	6.817	0.056	2.13				
390	0.270	0.347	7.385			0.116	3.009		
450	0.312	0.385	8.522	0.068	2.66	0.138	3.472		
510	0.345	0.42	9.413						
600	0.417	0.468	11.372	0.0835	3.55	0.185	4.633		
750	0.520			0.092	4.43				
900	0.625			0.105	5.32				

PUMPING TEST DATA - DRAWDOWN TEST

OBSERVATION WELL D — Nearest testhole(s) IWB 56

Elevation 1654.44 ft. — Depth 33.8 ft.

TIME SINCE START OF PUMPING		Pumping Well Radius(r) F: 2035; Pumping rate (Q): 49.9		G: 2035; 49.9					
minutes	days	Dwdn.	$t/r^2\ 10^{-8}$	Dwdn.	$t/r^2\ 10^{-8}$	Dwdn.	t/r^2	Dwdn.	t/r^2
15	0.0142	0.01	0.343	0.005	0.34				
30	0.0208	0.02	0.502	0.017	0.50				
45	0.0312	0.03	0.754	0.025	0.75				
60	0.0416	0.043	1.00	0.036	1.00				
75	0.052	0.06	1.255	0.05	1.26				
90	0.0625	0.071	1.51	0.065	1.51				
105	0.0729	0.084	1.76	0.08	1.76				
120	0.0833	0.10	2.01	0.095	2.01				
135	0.0937	0.112	2.26	0.11	2.26				
150	0.104	0.126	2.51	0.125	2.51				
180	0.125	0.15	3.02	0.152	3.02				
210	0.145	0.171	3.52	0.178	3.52				
240	0.167	0.192	4.03	0.204	4.03				
270	0.187	0.215	4.53	0.226	4.54				
300	0.208	0.235	5.03	0.25	5.03				
360	0.273	0.250	6.04	0.29	6.04				
450	0.326	0.3125	7.55	0.347	7.55				
600	0.407	0.417	10.07	0.431	10.07				

PUMPING TEST DATA - DRAWDOWN TEST

OBSERVATION WELL E

Nearest testhole(s) IWB 59

Elevation 1669.91 ft.

Depth 56.0 ft.

TIME SINCE START OF PUMPING		Pumping Well B Radius(r) 3715 Pumping rate (Q) 8.33							
minutes	days	Dwdn.	t/r^2 10^{-8}	Dwdn.	t/r^2	Dwdn.	t/r^2	Dwdn.	t/r^2
240	0.167	0.001	1.2101						
255	0.177	0.003	1.283						
270	0.187	0.0045	1.358						
285	0.197	0.0065	1.434						
300	0.208	0.007	1.509						
330	0.229	0.01	1.661						
360	0.250	0.0145	1.812						
390	0.270	0.0185	1.962						
420	0.291	0.021	2.114						
450	0.312	0.025	2.264						
480	0.333	0.027	2.413						
510	0.354	0.03	2.566						
540	0.375	0.034	2.717						
570	0.395	0.039	2.868						
600	0.417	0.041	3.022						

PUMPING TEST DATA - DRAWDOWN TEST

OBSERVATION WELL F

Elevation 1655.51 ft.

Nearest testhole(s) IWB 70

Depth 212.3 ft.

TIME SINCE START OF PUMPING		Pumping Well A		B		C		D	
		Radius(r) 1305		1935		3000		3035	
		Pumping rate (Q) 49.9		8.33		16.6		16.6	
minutes	days	Dwdn.	$t/r^2\ 10^{-8}$	Dwdn.	$t/r^2\ 10^{-7}$	Dwdn.	$t/r^2\ 10^{-8}$	Dwdn.	$t/r^2\ 10^{-8}$
15	0.0142	0.011	0.833					0.0015	0.343
30	0.0208	0.04	1.22					0.005	0.502
45	0.0312	0.062	1.83	0.0035	0.835			0.009	0.754
60	0.0416	0.105	2.45	0.005	1.113			0.013	1.00
75	0.052	0.135	3.05	0.0065	1.388	0.005	0.57	0.018	1.255
90	0.0625	0.165	3.67	0.0095	1.669	0.007	0.69	0.024	1.51
105	0.0729	0.185	4.28	0.0105	1.947			0.029	1.76
120	0.0833	0.21	4.89	0.013	2,225	0.011	0.925	0.034	2.01
135	0.0937	0.235	5.50	0.015	2.504			0.039	2.26
150	0.104	0.255	6.11	0.0185	2.777	0.017	1.15	0.045	2.51
180	0.125	0.30	7.34	0.022	3.338			0.054	3.02
210	0.145	0.325	8.56	0.027	3.898	0.03	1.62	0.063	3.52
240	0.167	0.355	9.81	0.0305	4.46	0.036	1.85	0.073	4.03
270	0.187	0.371	1.10	0.032	5.01	0.043	2.08	0.082	4.53
300	0.208	0.405	1.22	0.0355	5.56	0.051	2.31	0.09	5.03
360	0.250	0.45	1.47	0.0425	6.68			0.104	6.04
450	0.312	0.52	1.83	0.0525	8.34	0.08	3.47	0.125	7.55
510	0.345	0.54	2.03						
600	0.417	0.583	2.45	0.062	11.137	0.104	4.63	0.157	10.07
750	0.520					0.127	5.78		
900	0.625					0.15	6.94		

PUMPING TEST DATA - DRAWDOWN TEST

OBSERVATION WELL F — Nearest testhole(s) IWB 70

Elevation 1655.51 ft. — Depth 212.3 ft.

TIME SINCE START OF PUMPING		Pumping Well G Radius(r) Pumping rate (Q) 49.9							
minutes	days	Dwdn.	t/r^2 10^{-6}	Dwdn.	t/r^2	Dwdn.	t/r^2	Dwdn.	t/r^2
15	0.0142	0.155	0.604						
30	0.0208	0.235	0.885						
45	0.0312	0.29	1.33						
60	0.0416	0.335	1.77						
75	0.052	0.38	2.21						
90	0.0625	0.415	2.66						
105	0.0729	0.45	3.10						
135	0.0937	0.50	3.99						
150	0.104	0.527	4.43						
180	0.125	0.57	5.32						
210	0.145	0.61	6.20						
240	0.167	0.647	7.11						
300	0.208	0.71	8.86						
360	0.250	0.76	10.64						
450	0.312	0.82	13.29						
600	0.417	0.91	17.75						

PUMPING TEST DATA - DRAWDOWN TEST

OBSERVATION WELL G — Nearest testhole(s) IWB 70

Elevation 1655.62 ft. — Depth 57.0 ft.

TIME SINCE START OF PUMPING		Pumping Well Radius(r) / Pumping rate (Q)	A 1305 49.9	B 1935 8.33		C 3000 16.6		D 2035 16.6	
minutes	days	Dwdn.	$t/r^2\ 10^{-8}$	Dwdn.	$t/r^2\ 10^{-8}$	Dwdn.	$t/r^2\ 10^{-8}$	Dwdn.	t/r^2
15	0.0312	0.005	0.83						
30	0.0416	0.037	1.22						
45	0.0312	0.07	1.83	0.0015	0.835			0.0035	0.754
60	0.0416	0.105	2.45	0.0035	1.113	0.0025	0.46	0.008	1.00
75	0.052	0.13	3.05	0.005	1.388	0.004	0.57	0.011	1.255
90	0.0625	0.162	3.67	0.006	1.669	0.006	0.69	0.0175	1.51
105	0.0729	0.185	4.28	0.0075	1.947	0.0085	0.81	0.021	1.76
120	0.0833	0.21	4.89	0.011	2.225	0.0105	0.93	0.0275	2.01
135	0.0937	0.235	5.50	0.0125	2.504	0.013	1.04	0.033	2.26
150	0.104	0.26	6.11	0.016	2.777	0.0175	1.15	0.0385	2.51
180	0.125	0.30	7.34	0.021	3.338	0.0245	1.38	0.049	3.02
210	0.145	0.335	8.56	0.025	3.898	0.03	1.62	0.0585	3.52
240	0.167	0.37	9.81	0.030	4.46	0.0385	1.85	0.068	4.03
270	0.187	0.398	$1.10^{(10^{-7})}$	0.032	5.01	0.045	2.08	0.077	4.53
300	0.208	0.424	1.22	0.036	5.56	0.052	2.31	0.084	5.03
360	0.250	0.467	1.47	0.042	6.68	0.065	2.78	0.099	6.04
450	0.312	0.526	1.83	0.053	8.34	0.0825	3.47	0.12	7.55
510	0.354	0.559	2.03						
600	0.417	0.603	2.45	0.064	11.137	0.106	4.63	0.1535	10.07
750	0.520					0.128	5.78		
900	0.625					0.150	6.94		

PUMPING TEST DATA - DRAWDOWN TEST

OBSERVATION WELL G — Nearest testhole(s) IWB 70

Elevation 1655.62 ft. — Depth 51.0 ft.

TIME SINCE START OF PUMPING		Pumping Well F Radius(r) - Pumping rate (Q) 49.9							
minutes	days	Dwdn.	$t/r^2\ 10^{-6}$	Dwdn.	t/r^2	Dwdn.	t/r^2	Dwdn.	t/r^2
15	0.0312	0.11	0.60						
30	0.0416	0.177	0.88						
45	0.0312	0.22	1.33						
60	0.0416	0.254	1.77						
75	0.052	0.287	2.21						
90	0.0625	0.313	2.66						
105	0.0729	0.337	3.10						
120	0.0833	0.36	3.54						
135	0.0937	0.38	3.99						
150	0.104	0.40	4.43						
180	0.125	0.444	5.32						
210	0.145	0.464	6.20						
240	0.167	0.50	7.11						
300	0.208	0.555	8.86						
360	0.250	0.599	10.64						
450	0.312	0.654	13.29						
600	0.417	0.728	17.75						

APPENDIX III

Theis Recovery Method Data Sheets for Observation Wells A to G

THEIS RECOVERY METHOD DATA SHEET

Well - A

Elevation - 1661.32 ft.

Depth - 46.55 ft. Diameter - 6.5" ID

Length - well screen - 8 ft. Size - .012/.015

Pumping Started - 24/3/71 - 16:45

Pumping Stopped (Recovery Starts) - 25/3/71 - 10:30

Total Pumping Time - 1065 min.

Pumping Rate (Q) - 49.98 Imp.-gal./min.

Remarks:

Completion Zone: 46.55 - 54.98 ft.

Pump Setting - 40 ft.

Radius - 5 in.

Date	Time	t	t''	t/t''	Depth to Water
25/3/71	10:30	1065.0	0.0		19.30 ft.
		1065.1	0.1	10651.0	14.77
		1065.2	0.2	5326.0	12.20
		1065.3	0.3	3551.0	11.14
		1065.4	0.4	2663.5	10.53
		1065.5	0.5	2131.0	10.11
		1065.6	0.6	1776.0	9.87
		1065.7	0.7	1522.4	9.69
		1065.8	0.8	1332.2	9.57
		1065.9	0.9	1184.3	9.48
		1066.0	1.0	1066.0	9.41
		1066.5	1.5	711.0	9.28
		1067.0	2.0	533.5	9.21
		1067.5	2.5	427.0	9.18
		1068.0	3.0	356.0	9.15
		1068.5	3.5	305.3	9.13
		1069.0	4.0	267.2	9.12
		1069.5	4.5	237.7	9.11
		1070.0	5.0	214.0	9.10
		1070.5	5.5	194.6	9.09
		1071.0	6.0	178.5	9.08

THEIS RECOVERY METHOD DATA SHEET

Well - A

Elevation -

Depth - 46.55 ft. Diameter - 6.5" ID

Length - well screen - Size - .012/.015

Pumping Started -

Pumping Stopped (Recovery Starts) -

Total Pumping Time -

Pumping Rate (Q) -

Remarks:

Completion Zone: 46.55 - 54.98 ft.

Pump Setting - 40 ft.

Radius - 5 in.

Date	Time	t	t''	t/t''	Depth to Water
25/3/71		1071.5	6.5	164.8	9.07
		1072.0	7.0	153.1	9.06
		1072.5	7.5	143.0	9.06
	10:38	1073.0	8.0	134.1	9.06
		1073.5	8.5	126.3	9.05
		1074.0	9.0	119.3	9.04
		1074.5	9.5	113.1	9.03
		1075.0	10.0	107.5	9.03
		1077.0	12.0	89.7	9.02
		1080.0	15.0	72.0	9.00
		1085.0	20.0	54.2	8.96
		1095.0	30.0	36.5	8.93
		1105.0	40.0	27.6	8.89
	11:30	1125.0	60.0	18.7	8.83
	13:45	1260.0	195.0	6.5	8.60

THEIS RECOVERY METHOD DATA SHEET

Well - B

Elevation - 1659.13 ft.

Depth - 48.95 ft. Diameter-6.5" ID

Length-well screen- 10 ft. Size-0.007

Remarks:

Pumping Started - 11/3/71 - 17:25

Pumping Stopped (Recovery Starts)-12/3/71 14:10

Total Pumping Time - 1245 mins.

Pumping Rate (Q) - 8.33 Imp.-gal./min.

Completion Zone: 48.95-59.35 ft.

Pump Setting - 40 ft.

Radius - 4 in.

Date	Time	t	t''	t/t''	Depth to Water
12/3/71	14:10	1245.0	0.0		10.85
		1245.1	0.1	12451.0	10.44
		1245.2	0.2	6226.0	10.05
		1245.3	0.3	4151.0	9.67
		1245.4	0.4	3113.5	9.33
		1245.5	0.5	2491.0	9.02
		1245.6	0.6	2076.0	8.73
		1245.7	0.7	1779.6	8.44
		1245.8	0.8	1557.3	8.22
		1245.9	0.9	1384.3	7.98
		1246.0	1.0	1246.0	7.74
		1246.5	1.5	831.0	6.87
		1247.0	2.0	623.5	6.28
		1247.5	2.5	499.0	5.87
		1248.0	3.0	416.0	5.57
		1248.5	3.5	356.7	5.37
		1249.0	4.0	312.2	5.23
		1249.5	4.5	277.7	5.14
		1250.0	5.0	250.0	5.08
		1251.0	6.0	208.5	5.01

THEIS RECOVERY METHOD DATA SHEET

Well - B

Elevation -

Depth - 48.95 ft. Diameter - 6.5" ID

Length - well screen - 10 ft. Size - 0.007

Remarks:

Pumping Started -

Pumping Stopped (Recovery Starts) -

Total Pumping Time -

Pumping Rate (Q) -

Completion Zone: 48.95-59.35 ft.

Pump Setting - 40 ft.

Radius - 4 in.

Date	Time	t	t^{II}	t/t^{II}	Depth to Water
12/3/71		1252.0	7.0	178.6	4.95
		1253.0	8.0	156.6	4.92
		1254.0	9.0	139.3	4.90
		1255.0	10.0	125.5	4.90
	14:22	1257.0	12.0	104.7	4.90
		1258.0	13.0	96.7	4.89
		1260.0	15.0	84.0	4.89
		1265.0	20.0	63.2	4.89
		1270.0	25.0	50.8	4.89
	14:40	1275.0	30.0	42.5	4.89
		1280.0	35.5	36.6	4.89
		1290.0	45.0	28.7	4.89
	15:15	1305.0	60.0	21.7	4.86

THEIS RECOVERY METHOD DATA SHEET

Well - C

Elevation - 1659.56 ft.

Depth - 51.35 ft. Diameter - 6.5" ID

Length - well screen - 8 ft. Size - .010/.012

Pumping Started - 9/3/71 17:30

Pumping Stopped (Recovery Starts) - 10/3/71 14:05

Total Pumping Time - 1235 mins.

Pumping Rate (Q) - 16.66 Imp.-gals./min.

Remarks:

Completion Zone: 51.35 - 59.80 ft.

Pump Setting - 40 ft.

Radius - 4 in.

Date	Time	t	t''	t/t''	Depth to Water
10/3/71	14:04	1235.0	0.0		23.11
		1235.1	0.1	12351.0	21.86
		1235.2	0.2	6176.0	20.64
		1235.3	0.3	4117.7	19.52
		1235.4	0.4	3088.5	18.48
		1235.5	0.5	2471.0	17.52
		1235.6	0.6	2059.3	16.64
		1235.7	0.7	1765.3	15.80
		1235.8	0.8	1544.7	15.05
		1235.9	0.9	1373.2	14.45
		1236.0	1.0	1236.0	13.71
		1236.5	1.5	824.3	11.13
		1237.0	2.0	618.5	9.31
		1238.0	3.0	412.7	7.18
		1239.0	4.0	309.7	6.12
		1240.0	5.0	248.0	5.58
		1241.0	6.0	206.8	5.31
		1242.0	7.0	177.4	5.17
		1243.0	8.0	155.4	5.09
		1244.0	9.0	138.2	5.05
		1245.0	10.0	124.5	5.02

THEIS RECOVERY METHOD DATA SHEET

Well - C

Elevation -

Depth - 51.35 ft. Diameter - 6.5" ID

Length - well screen - Size - .010/.012

Pumping Started -

Pumping Stopped (Recovery Starts) -

Total Pumping Time -

Pumping Rate (Q) -

Remarks:

Completion Zone: 51.35 - 59.80 ft.

Pump Setting - 40 ft.

Radius - 4 in.

Date	Time	t	t''	t/t''	Depth to Water
10/3/71		1247.0	12.0	103.9	4.98
		1250.0	15.0	83.3	4.96
		1255.0	20.0	62.7	4.95
		1265.0	30.0	42.2	4.91
		1275.0	40.0	31.9	4.87
		1285.0	50.0	25.7	4.87
		1295.0	60.0	21.6	4.85
		1315.0	80.0	16.4	4.82
		1335.0	100.0	13.3	4.80
		1353.0	118.0	11.5	4.80

THEIS RECOVERY METHOD DATA SHEET

Well - D

Elevation - 1654.44 ft.

Depth - 40.57 ft. Diameter - 6·5" ID

Length - well screen - 10 ft. Size - 0·007

Pumping Started - 15/3/71 17:20

Pumping Stopped (Recovery Starts) - 16/3/71 10:50

Total Pumping Time - 1110 mins.

Pumping Rate (Q) - 16.66 Imp.-gal./min.

Remarks:

Completion Zone: 40.57 - 51.00 ft.

Pump Setting - 40 ft.

Radius - 4 in.

Date	Time	t	t^{II}	t/t^{II}	Depth to Water
16/3/71	10:50	1110.0	0.0		27.22
		1110.1	0.1	11101.0	26.00
		1110.2	0.2	5551.0	24.74
		1110.3	0.3	3701.0	23.60
		1110.4	0.4	2776.0	22.50
		1110.5	0.5	2221.0	21.44
		1110.6	0.6	1851.0	20.44
		1110.7	0.7	1586.7	19.52
		1110.8	0.8	1388.5	18.65
		1110.9	0.9	1234.3	17.86
		1111.0	1.0	1111.0	17.08
		1111.5	1.5	741.0	13.37
		1112.0	2.0	556.0	11.36
		1112.5	2.5	445.0	9.44
		1113.0	3.0	371.0	7.92
		1113.5	3.5	318.1	6.85
		1114.0	4.0	278.5	6.04
		1114.5	4.5	247.7	5.42
		1115.0	5.0	223.0	4.95
		1116.5	6.5	171.8	4.08
		1117.0	7.0	159.6	3.91

THEIS RECOVERY METHOD DATA SHEET

Well - D

Elevation - 1654.44 ft.

Depth - 40.57 ft. Diameter - 6.5" I.D

Length - well screen - Size - 0.007

Remarks:

Pumping Started -

Pumping Stopped (Recovery Starts) -

Total Pumping Time -

Pumping Rate (Q) -

Completion Zone: 40.57 - 51.00 ft.

Pump Setting - 40 ft.

Radius - 4 in.

Date	Time	t	t^{II}	t/t^{II}	Depth to Water
16/3/71		1118.0	8.0	139.7	3.70
		1119.0	9.0	124.3	3.57
		1120.0	10.0	112.0	3.49
		1122.0	12.0	93.5	3.42
		1125.0	15.0	75.0	3.40
		1127.5	17.5	64.4	3.40
		1130.0	20.0	56.5	3.37
		1135.0	25.0	45.4	3.35
		1140.0	30.0	38.0	3.34
		1150.0	40.0	28.7	3.34
		1160.0	50.0	23.2	3.33
		1200.0	90.0	13.3	3.32
		1280.0	170.0	7.53	3.29
	14:10	1330.0	220.0	6.1	3.29

THEIS RECOVERY METHOD DATA SHEET

Well - E

Elevation - 1669.91 ft.

Depth - 57.77 ft. Diameter - 6.5" ID

Length-well screen- 8 ft. Size-0.015

Pumping Started - 18/3/71 17:00

Pumping Stopped (Recovery Starts)- 19/3/71 14:55

Total Pumping Time - 1315 mins.

Pumping Rate (Q) - 49.98 Imp.-gal./min.

Remarks:

Completion Zone: 57.77 - 66.20 ft.

Pump Setting - 40 ft.

Radius - 5 in.

Date	Time	t	t''	t/t''	Depth to Water
19/3/71	14:55	1315.0	0.0		26.64
		1315.1	0.1	13151.0	22.50
		1315.2	0.2	6576.0	19.52
		1315.3	0.3	4384.3	17.94
		1315.4	0.4	3288.5	17.24
		1315.5	0.5	2631.0	16.83
		1315.6	0.6	2192.7	16.49
		1315.7	0.7	1879.6	16.27
		1315.8	0.8	1644.7	16.06
		1315.9	0.9	1462.1	15.88
		1316.0	1.0	1316.0	15.81
		1316.5	1.5	877.7	15.66
		1317.0	2.0	658.5	15.61
		1317.5	2.5	527.0	15.60
		1318.0	3.0	439.3	15.59
		1319.0	4.0	329.7	15.58
		1320.0	5.0	264.0	15.57
		1321.0	6.0	220.2	15.56
		1322.0	7.0	188.9	15.55
		1323.0	8.0	165.4	15.54
		1324.0	9.0	147.1	15.54

THEIS RECOVERY METHOD DATA SHEET

Well - E

Elevation -

Depth - 57.77 ft. Diameter - 6 5" ID

Length - well screen - Size - 0.015

Remarks:

Pumping Started -

Pumping Stopped (Recovery Starts) -

Total Pumping Time -

Pumping Rate (Q) -

Completion Zone: 57.77 - 66.20 ft.

Pump Setting - 40 ft.

Radius - 5 in.

Date	Time	t	t''	t/t''	Depth to Water
19/3/71		1325.0	10.0	132.5	15.53
		1327.0	12.0	110.6	15.52
		1330.0	15.0	88.7	15.51
	15:15	1335.0	20.0	66.7	15.50
		1340.0	25.0	53.6	15.48
		1365.0	50.0	27.3	15.43
		1390.0	75.0	18.5	15.40
		1420.0	105.0	13.5	15.36
		1470.0	155.0	9.5	15.31
		1615.0	300.0	5.4	15.22
	21:45	1725.0	410.0	4.2	15.17
20/3/71	01:00	1920.0	605.0	3.2	15:10
	10:25	2340.0	1025.0	2.3	14.98

THEIS RECOVERY METHOD DATA SHEET

Well - F

Elevation - 1655.51 ft.

Depth - 212.95 ft. Diameter - 6.5" ID

Length - well screen - 14 ft. Size - .007/.015

Remarks:

Pumping Started - 20/3/71 16:00

Pumping Stopped (Recovery Starts) - 21/3/71 11:00

Total Pumping Time - 1140 mins.

Pumping Rate (Q) - 49.98 Imp.-gal./min.

Completion Zone: 212.95 - 227.70 ft.

Pump Setting - 100 ft.

Radius - 5 in.

Date	Time	t	t^{II}	t/t^{II}	Depth to Water
21/3/71	11:00	1140.0	0.00		68.1
		1140.48	0.48	2376.0	48.00
		1141.0	1.0	1141.0	37.70
		1141.5	1.5	761.0	30.30
		1142.0	2.0	571.0	24.30
		1142.5	2.5	457.0	19.79
		1143.0	3.0	381.0	16.27
		1143.5	3.5	326.7	13.50
		1144.0	4.0	286.0	11.35
		1144.5	4.5	254.3	9.65
		1145.0	5.0	229.0	8.35
		1146.0	6.0	191.0	6.53
		1147.0	7.0	163.9	5.48
		1148.5	8.5	135.1	4.50
		1150.0	10.0	115.0	4.05
		1152.0	12.0	96.0	3.80
		1155.0	15.0	77.0	3.70
		1160.0	20.0	58.0	3.63
		1165.0	25.0	46.6	3.61
		1170.0	30.0	39.0	3.59
		1180.0	40.0	29.5	3.55

THEIS RECOVERY METHOD DATA SHEET

Well - P

Elevation -

Depth - 212.95 ft. Diameter - 6 5" ID

Length - well screen - Size - .007/.015

Remarks:

Pumping Started -

Pumping Stopped (Recovery Starts) -

Total Pumping Time -

Pumping Rate (Q) -

Completion Zone: 212.95 - 227.70 ft.

Pump Setting - 100 ft.

Radius - 5 in.

Date	Time	t	t''	t/t''	Depth to Water
21/3/71		1200.0	60.0	20.0	3.51
		1235.0	95.0	13.0	3.44
		1260.0	120.0	10.5	3.41
		1350.0	210.0	6.4	3.32
		1500.0	360.0	4.2	3.23
	20:00	1680.0	540.0	3.1	3.18
22/3/71	0:15	1935.0	795.0	2.4	3.13
	8:15	2415.0	1275.0	1.9	3.12

THEIS RECOVERY METHOD DATA SHEET

Well - C

Elevation - 1655.62 ft.

Depth - 50.65 ft Diameter - 6·5" ID

Length - well screen - 8 ft. Size - .012/.015

Remarks:

Pumping Started - 22/3/71 16:05

Pumping Stopped (Recovery Starts) - 23/3/71 10:30

Total Pumping Time - 1105 mins.

Pumping Rate (Q) - 49.98 Imp.-gal./min.

Completion Zone: 50.65 - 59.00 ft.

Pump Setting - 40 ft.

Radius - 5 in.

Date	Time	t	t''	t/t''	Depth to Water
23/3/71	10:30	1105.0	0.0		23.39
		1105.1	0.1	11051.0	17.93
		1105.2	0.2	5526.0	14.46
		1105.3	0.3	3684.3	13.10
		1105.4	0.4	2763.5	10.89
		1105.5	0.5	2211.0	9.63
		1105.6	0.6	1842.7	8.69
		1105.7	0.7	1579.6	7.83
		1105.8	0.8	1382.2	7.20
		1105.9	0.9	1228.8	6.60
		1106.0	1.0	1106.0	6.12
		1106.5	1.5	737.7	4.75
		1107.0	2.0	553.5	4.32
		1107.5	2.5	443.0	4.20
		1108.0	3.0	369.3	4.13
		1108.5	3.5	316.7	4.08
		1109.0	4.0	277.2	4.07
		1110.0	5.0	222.0	4.03
		1111.0	6.0	185.2	4.02
		1112.0	7.0	158.9	3.99
		1113.0	8.0	139.1	3.98

THEIS RECOVERY METHOD DATA SHEET

Well - C

Elevation -

Depth - 50.65 ft. Diameter - 6-5" ID

Length - well screen - Size - .012/.015

Remarks:

Pumping Started -

Pumping Stopped (Recovery Starts) -

Total Pumping Time -

Pumping Rate (Q) -

Completion Zone: 50.65 - 59.00 ft.

Pump Setting - 40 ft.

Radius - 5 in.

Date	Time	t	t''	t/t''	Depth to Water
23/3/71	10:39	1114.0	9.0	123.8	3.97
		1115.0	10.0	111.5	3.96
		1117.0	12.0	93.1	3.95
		1120.0	15.0	74.7	3.93
		1125.0	20.0	56.2	3.90
		1130.0	25.0	45.2	3.88
		1135.0	30.0	37.8	3.85
		1145.0	40.0	28.6	3.81
		1165.0	60.0	19.4	3.73
		1180.0	75.0	15.7	3.69
		1195.0	90.0	13.3	3.66
		1255.0	150.0	8.4	3.56
		1305.0	200.0	6.5	3.50
		1375.0	270.0	5.1	3.43
		1445.0	340.0	4.2	3.40
		1465.0	360.0	4.1	3.38
		1555.0	450.0	3.5	3.33
		1780.0	675.0	2.6	3.23
	22:45	1840.0	735.0	2.5	3.23
24/3/71	8:25	2420.0	1315.0	1.8	3.11

APPENDIX IV

Electric Analog Modeling (R. A. Bourne and J. A. Vonhof)

Electric Analog Modeling (R. A. Bourne and J. A. Vonhof)

THEORY

Two systems are analogous if there is a one-to-one correspondence between the characteristic equations that govern each system (i.e. every element in the investigated system must be present in the analog system). In the electrical analogy to groundwater flow, the flow of water through a porous medium is analogous to the flow of electricity through a resistor-capacitor (R-C) network. The resistors simulate resistance to flow of water, while capacitors represent the storage of water.

The analogy may be established either by a physical approach or a more conventional mathematical treatment. The following mathematical derivation is modified from Karplus (1958), Skibitzke (1961), Walton and Prickett (1963), and Patten (1965).

The first step in the mathematical approach is the replacement of the continuous porous medium by a discretized coordinate grid. Errors in the potential field are negligible if the distances between the nodes in the coordinate grid are small enough (Karplus, 1958). Figure IV-I illustrates one cell of the coordinate grid with the appropriate hydraulic heads and distances.

The second step involves approximating the 2nd-order partial differential equation of groundwater flow by finite difference expressions. Since we are dealing with two equations, the steady state and transient, it is best at this point to carry out the remainder of the presentation separately.

(i) Steady State

As stated previously, the nonlinear, heterogeneous, anisotropic, partial differential equation that describes three-dimensional steady state groundwater flow is:

$$\frac{\partial}{\partial x}\left[K(x, y, z)\frac{\partial \phi}{\partial x}\right]+\frac{\partial}{\partial y}\left[K(x, y, z)\frac{\partial \phi}{\partial y}\right]+\frac{\partial}{\partial z}\left[K(x, y, z)\frac{\partial \phi}{\partial z}\right]=0 \qquad (1)$$

Finite difference equations for the first space derivatives of this equation are approximated between nodes as their potential difference divided by the distance between them (Karplus, 1958)

$$\frac{\partial \phi}{\partial x_{(1-0)}} \simeq \frac{\phi_1 - \phi_0}{\Delta X} \qquad (2a)$$

$$\frac{\partial \phi}{\partial X_{(0-2)}} \simeq \frac{\phi_0 - \phi_2}{\Delta X} \qquad (2b)$$

$$\frac{\partial \phi}{\partial y_{(3-0)}} \simeq \frac{\phi_3 - \phi_0}{\Delta Y} \qquad (2c)$$

$$\frac{\partial \phi}{\partial y_{(0-4)}} \simeq \frac{\phi_0 - \phi_4}{\Delta Y} \qquad (2d)$$

$$\frac{\partial \phi}{\partial Z_{(5-0)}} \simeq \frac{\phi_5 - \phi_0}{\Delta Z} \qquad (2e)$$

$$\frac{\partial \phi}{\partial z_{(0-6)}} \simeq \frac{\phi_0 - \phi_6}{\Delta Z} \qquad (2f)$$

where the subscripts refer to the nodal points in Figure IV-1.

The hydraulic conductivity between any two nodes is assumed to be an average of the two nodal values. For example, between nodes 1 and 0, the hydraulic conductivity is:

$$K_{1-0} = \frac{K_1 + K_0}{2} \qquad (3)$$

Similarly, the average hydraulic conductivities for nodes 0 to 2, 3 to 0, 0 to 4, 5 to 0, and 0 to 6 are K_{0-2}, K_{3-0}, K_{0-4}, K_{5-0}, and K_{0-6}, respectively.

The second derivative of the space variable is obtained by subtracting the forward from the backward finite difference approximations:

$$\left(\frac{\partial^2 \phi}{\partial X^2}\right)_0 = \frac{\dfrac{\partial \phi}{\partial X_{(1-0)}} - \dfrac{\partial \phi}{\partial X_{(0-2)}}}{\Delta X} \qquad (4)$$

Substituting equations 2a and 2b, and inserting the corresponding average hydraulic conductivity values into

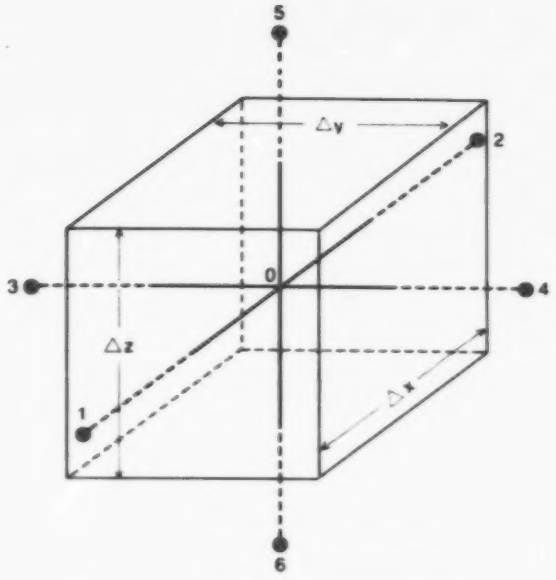

(A) ELEMENTAL CUBE OF POROUS MEDIUM

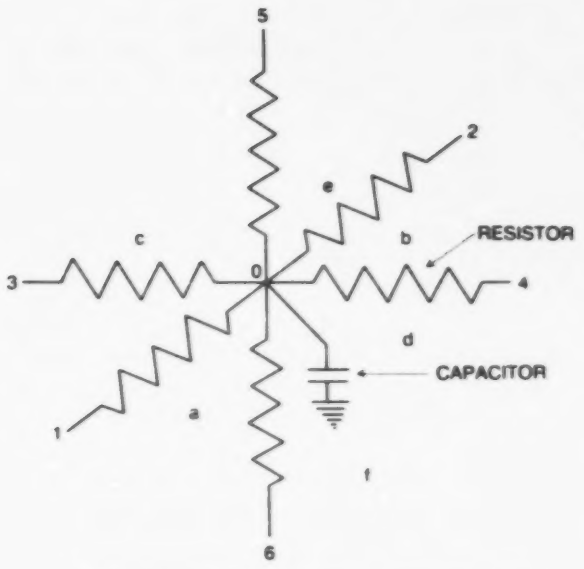

(B) RESISTOR-CAPACITOR ANALOG TO A CUBE OF POROUS MEDIUM

Figure IV-1. Schematic representation of current flow in a three-dimensional analog of a cube of porous medium (modified after Patten, 1965).

equation 4:

$$\left(\frac{\partial^2\phi}{\partial X^2}\right)_0 = \frac{K_{1-0}\dfrac{\phi_1-\phi_0}{\Delta X} - K_{0-2}\dfrac{\phi_0-\phi_2}{\Delta X}}{\Delta X} \qquad (5)$$

$$\left(\frac{\partial^2\phi}{\partial X^2}\right)_0 = \frac{K_{1-0}(\phi_1-\phi_0)}{\Delta X^2} + \frac{K_{0-2}(\phi_2-\phi_0)}{\Delta X^2} \qquad (6a)$$

Similarly, the second space derivatives of y and z are:

$$\left(\frac{\partial^2\phi}{\partial Y^2}\right)_0 = \frac{K_{3-0}(\phi_3-\phi_0)}{\Delta Y^2} + \frac{K_{0-4}(\phi_4-\phi_0)}{\Delta Y^2} \qquad (6b)$$

$$\left(\frac{\partial^2\phi}{\partial Z^2}\right)_0 = \frac{K_{5-0}(\phi_5-\phi_0)}{\Delta Z^2} + \frac{K_{0-6}(\phi_6-\phi_0)}{\Delta Z^2} \qquad (6c)$$

Combining equations 6a, 6b, and 6c, assuming $\Delta X = \Delta Y = \Delta Z = a$, and multiplying by a^2, one obtains:

$$K_{1-0}(\phi_1-\phi_0) + K_{0-2}(\phi_2-\phi_0) + K_{3-0}(\phi_3-\phi_0) + K_{0-4}(\phi_4-\phi_0) + K_{5-0}(\phi_5-\phi_0) + K_{0-6}(\phi_6-\phi_0) = 0 \qquad (7)$$

The equation for the nodal network, which is analogous to the volume of porous medium (Fig. IV-1), is obtained by applying Kirchoff's current law. The total current entering the node 0 equals zero, therefore:

$$\sum_{i=1}^{6} I_{i-0} = I_{1-0} + I_{2-0} + I_{3-0} + I_{4-0} + I_{5-0} + I_{6-0} = 0 \qquad (8)$$

Substituting Ohm's law ($I = V/R$) into equation 8:

$$\frac{1}{Ra}(V_1-V_0) + \frac{1}{Rb}(V_2-V_0) + \frac{1}{Rc}(V_3-V_0) + \frac{1}{Rd}(V_4-V_0) + \frac{1}{Re}(V_5-V_0) + \frac{1}{Rf}(V_6-V_0) = 0 \qquad (9)$$

The formal analogy becomes apparent by comparing equations 7 and 9. The analogous quantities are:

Hydraulic	*Electric*
Potential, head in feet ϕ-V	Voltage, in volts
Hydraulic conductivity, in lgpd/ft^2 K-1/R	Resistance, in ohms
Length, in feet $l_w - l_c$	Model length, in feet

(ii) Transient

The nonlinear partial differential equation that describes transient groundwater flow in three dimensions in a heterogeneous, anisotropic porous medium is:

$$\frac{\partial}{\partial x}\left[K(x, y, z)\frac{\partial \phi}{\partial x}\right] + \frac{\partial}{\partial y}\left[K(x, y, z)\frac{\partial \phi}{\partial y}\right] + \frac{\partial \phi}{\partial z}\left[K(x, y, z)\frac{\partial \phi}{\partial z}\right] = \gamma\left[\alpha(x, y, z) + n(x, y, z)\beta\right]\frac{\partial \phi}{\partial t} \quad (10)$$

The first and second space derivatives are exactly the same as in the steady state equation; therefore, substituting equations 2a, 2b, and 2c, rearranging; assuming $\Delta X = \Delta Y = \Delta Z = a$; and multiplying by a^2; equation 10 becomes:

$$K_{1-0}(\phi_1 - \phi_0) + K_{0-2}(\phi_2 - \phi_0) + K_{3-0}(\phi_3 - \phi_0) + K_{0-4}(\phi_4 - \phi_0) + K_{5-0}(\phi_5 - \phi_0) + K_{0-6}(\phi_6 - \phi_0) = a^2\gamma(\alpha_0 + n_0\beta)\cdot\frac{\partial \phi}{\partial t} \quad (11)$$

Again, the hydraulic conductivity between any two nodes is assumed to be an average of the two nodal values.

The equation for the nodal network (Fig. IV-1) is obtained by applying Kirchoff's current law. This time, however, the total current entering the node 0 equals the current flow from the node to the capacitor:

$$I_{1-0} + I_{2-0} + I_{3-0} + I_{4-0} + I_{5-0} + I_{6-0} = -\epsilon \quad (12)$$

Substituting Ohm's law into equation 12:

$$\frac{1}{Ra}(V_1 - V_0) + \frac{1}{Rb}(V_2 - V_0) + \frac{1}{Rc}(V_3 - V_0) + \frac{1}{Rd}(V_4 - V_0) + \frac{1}{Re}(V_5 - V_0) + \frac{1}{Rf}(V_6 - V_0) = -\epsilon \quad (13)$$

The rate at which the capacitor will store energy is proportional to the rate of change with time of the applied voltage:

$$-\epsilon = C\frac{\partial V}{\partial t} \quad (14)$$

Combining equations 13 and 14:

$$\frac{1}{Ra}(V_1 - V_0) + \frac{1}{Rb}(V_2 - V_0) + \frac{1}{Rc}(V_3 - V_0) + \frac{1}{Rd}(V_4 - V_0) + \frac{1}{Re}(V_5 - V_0) + \frac{1}{Rf}(V_6 - V_0) = C\frac{\partial V}{\partial t} \quad (15)$$

The formal analogy becomes apparent by comparing equations 11 and 15. Analogous quantities in the transient system are:

Hydraulic	*Electric*
Potential, head in feet ϕ - V	Voltage, in volts
Hydraulic conductivity, in lgpd/ft^2 K - 1/R	Resistance, in ohms
Storage coefficient a^2S_s - C	Capacitance, in farads
Discharge, in lgpd q_w - q_e	Current, in amperes
Volume (or mass), in Imp. gal. Q_w - Q_e	Energy, in coulombs
Time, in days t_w - t_e	Time, in seconds
Length, in feet l_w - l_e	Length, in feet

where $S_s = \gamma(\alpha_0 + n_0\beta)$.

SCALING

The analogous quantities are made equivalent through the use of proportionality constants or scaling factors. These scaling factors are arbitrary, but must be selected so that the range of values of the electrical analog components are commercially available.

The four scale factors SC_1, SC_2, SC_3, and SC_4 are defined as follows (Walton and Prickett, 1963):

$$Q_w = SC_1\, Q_e \quad SC_1 = \text{Imp. gal./coulomb} \quad (16)$$
$$\phi = SC_2\, V \quad SC_2 = \text{feet/volt} \quad (17)$$
$$q_w = SC_3\, q_e \quad SC_3 = \text{lgpd/amp} \quad (18)$$
$$t_d = SC_4\, t_s \quad SC_4 = \text{days/sec} \quad (19)$$

Scale factors SC_1, SC_3, and SC_4 are related by:

$$SC_3 \times SC_4 = SC_1$$

In order to construct either a steady state or transient electric analog model, it is necessary to obtain an expression relating hydraulic conductivity to resistivity. Substituting Ohm's and Darcy's laws into equation 18 yields:

$$R_x = \frac{SC_3}{SC_2}\cdot\frac{\Delta X}{\Delta Y\cdot\Delta Z\cdot K_x} \quad (20)$$

$$R_y = \frac{SC_3}{SC_2}\cdot\frac{\Delta Y}{\Delta X\cdot\Delta Z\cdot K_y} \quad (21)$$

$$R_z = \frac{SC_3}{SC_2}\cdot\frac{\Delta Z}{\Delta Y\cdot\Delta X\cdot K_z} \quad (22)$$

Equations 20, 21, and 22 can therefore be used to calculate values of resistors for both interior and boundary nodes of the electric analog model.

The values of the capacitors for interior and boundary nodes for transient solutions are derived by using equations 16 and 17 plus the definitions of the storage and capacitance coefficients:

$$C = 6.23\,\Delta X \cdot \Delta Y \cdot \Delta Z \cdot S_s \cdot \frac{SC_2}{SC_1} \qquad (23)$$

where C is in farads and S_s, the specific storage, in ft^{-1}.

Therefore, in order to construct a steady state electric analog model in three dimensions, the values of the resistors are calculated using equations 20, 21, and 22.

DESIGN

The electric analog model of the study site was constructed using approximately 2000 resistors and 550 capacitors. The model is three dimensional, in that it has two R-C (resistor-capacitor) layers interconnected by resistors in the Z direction (Figs. IV-2 and IV-3).

To calculate the values of the resistors and capacitors with equations 20, 21, 22, and 23, the following values are required:

(a) the scale factors

(b) the nodal spacings—ΔX, ΔY, and ΔZ; and

(c) the hydrogeological parameters—K, α, and n.

In light of the earlier discussion on scaling factors, the following values were chosen:

$SC_1 = 5.0 \times 10^{11}$ Imp. gal./coulomb

$SC_2 = 5.0$ feet/volt

$SC_3 = 5.0 \times 10^{7}$ lgpd/amp

$SC_4 = 1.0 \times 10^{4}$ days/sec

An analog model spacing of 1½in. = 300 ft for the X and Y directions was considered accurate enough to minimize errors due to discretizing a continuous medium (Fig. IV-4). The southeast area of the geologic model was not considered hydrologically important because of the thick section of till, therefore, a nodal spacing for ΔX and ΔY of 3 in. = 600 ft was used. Techniques for joining areas with different scales are discussed in Karplus (1958). Nodal spacings for Z vary considerably over the map area because of the change in thickness in the geologic units.

The values of the hydrogeologic parameters—K, α, and n—have been discussed in detail in the preceding sections. However, calibration of the electric analog model to known hydraulic head measurements and pump tests in the field required a change in the specific storage of the buried valley aquifer. Table IV-1 summarizes the measured parameters—K, α, and n—and also their calibrated values. Note that S, the specific storage, is used rather than α and n.

Table IV-1. Measured and Calibrated Hydrogeologic Parameters for the Till and Buried Valley Aquifer.

	Measured		Calibrated	
	Average K, lgpd/ft^2	S^1, 1/ft	Average K lgpd/ft^2	S^1, 1/ft
Till	1	7×10^{-4}	1	7×10^{-4}
Buried valley fluvial deposits	330	2×10^{-6}	330	4.9×10^{-4}

In the geologic model, the major buried valley is not bounded on the west but extends for an unknown distance. It is apparent that by terminating the analog model on the west (Fig. IV-4), errors will occur in the potential distribution in the region of interest. To avoid this problem a termination strip was used (Karplus, 1958). The termination strip extends the western portion of the buried valley aquifer approximately 9000 ft so that errors in the potential distribution in the area around the brine pond are negligible.

ELECTRICAL EQUIPMENT

Once the R-C network has been constructed, the steady state and transient analog models require different electrical generating and measuring equipment to carry out a simulation.

(i) Steady State

The steady state case requires (a) simulation of the water table, and (b) measurement of the resulting voltage at every nodal point in the analog model.

The water table is simulated by applying a voltage to each of the water table nodes (Fig. IV-5). Since there were about 450 nodal points, those points with similar voltages were attached by soldering tinned wire between nodes. This simplification results in a slightly unrealistic water table and slight errors in the resulting potential distribution.

Voltages are applied with a voltage generator and measured with a digital voltmeter (Fig. IV-6).

Figure IV-2. The front of the study site electric analog model. A topographic map has been mounted on a 4 ft x 8 ft sheet of hardboard.

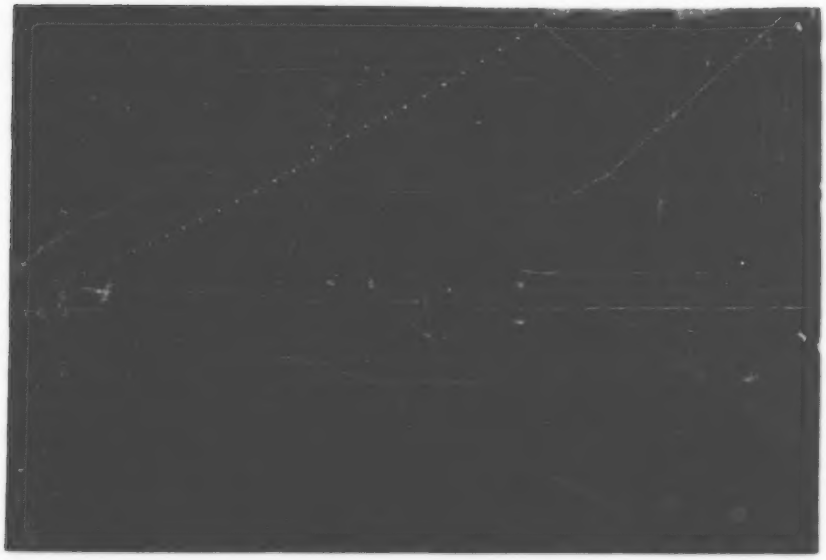

Figure IV-3. The back of the electric analog model illustrating resistors in three dimensions and a capacitor attached to each nodal point.

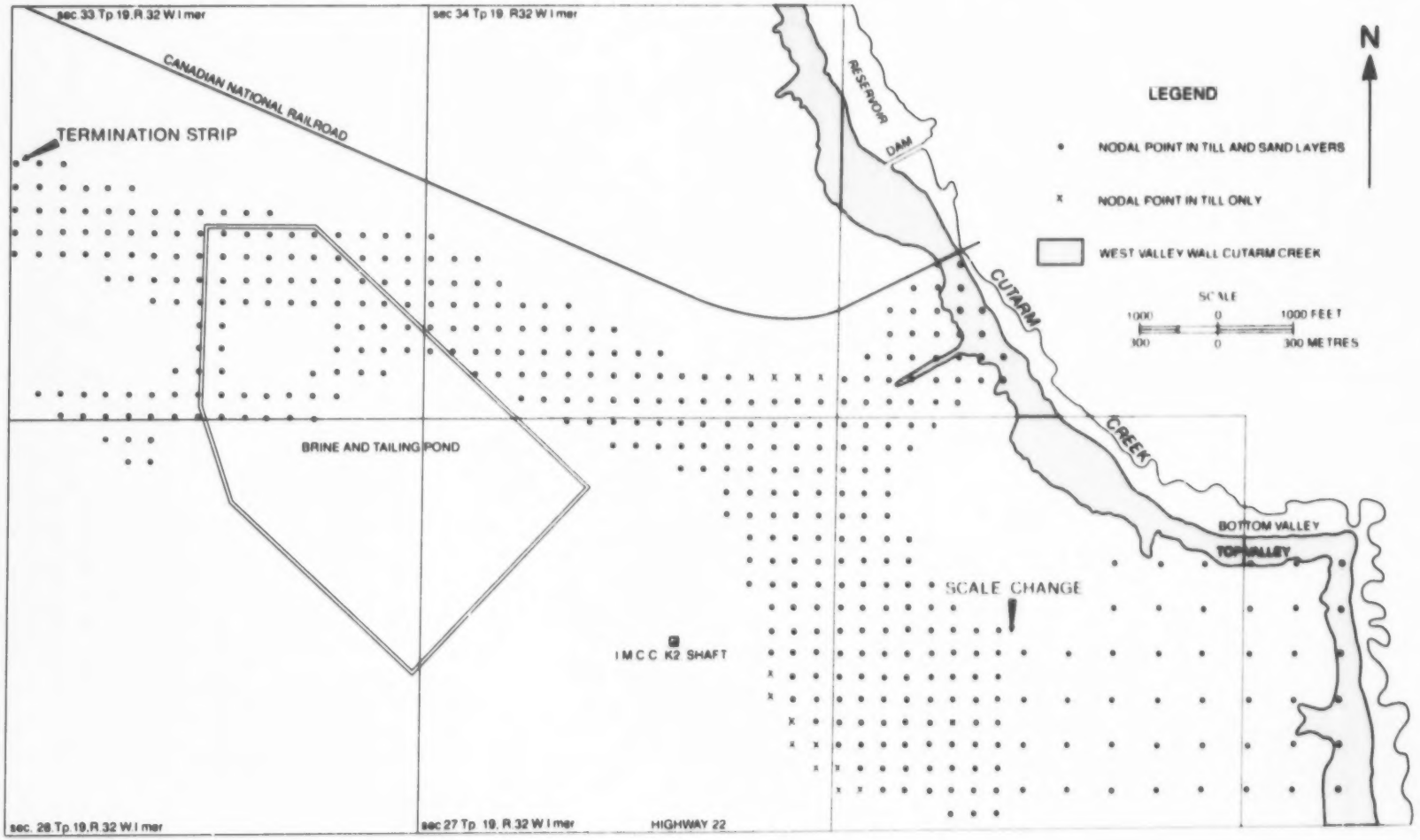

Figure IV-4. Distribution of nodes in the horizontal layers of the electric analog model.

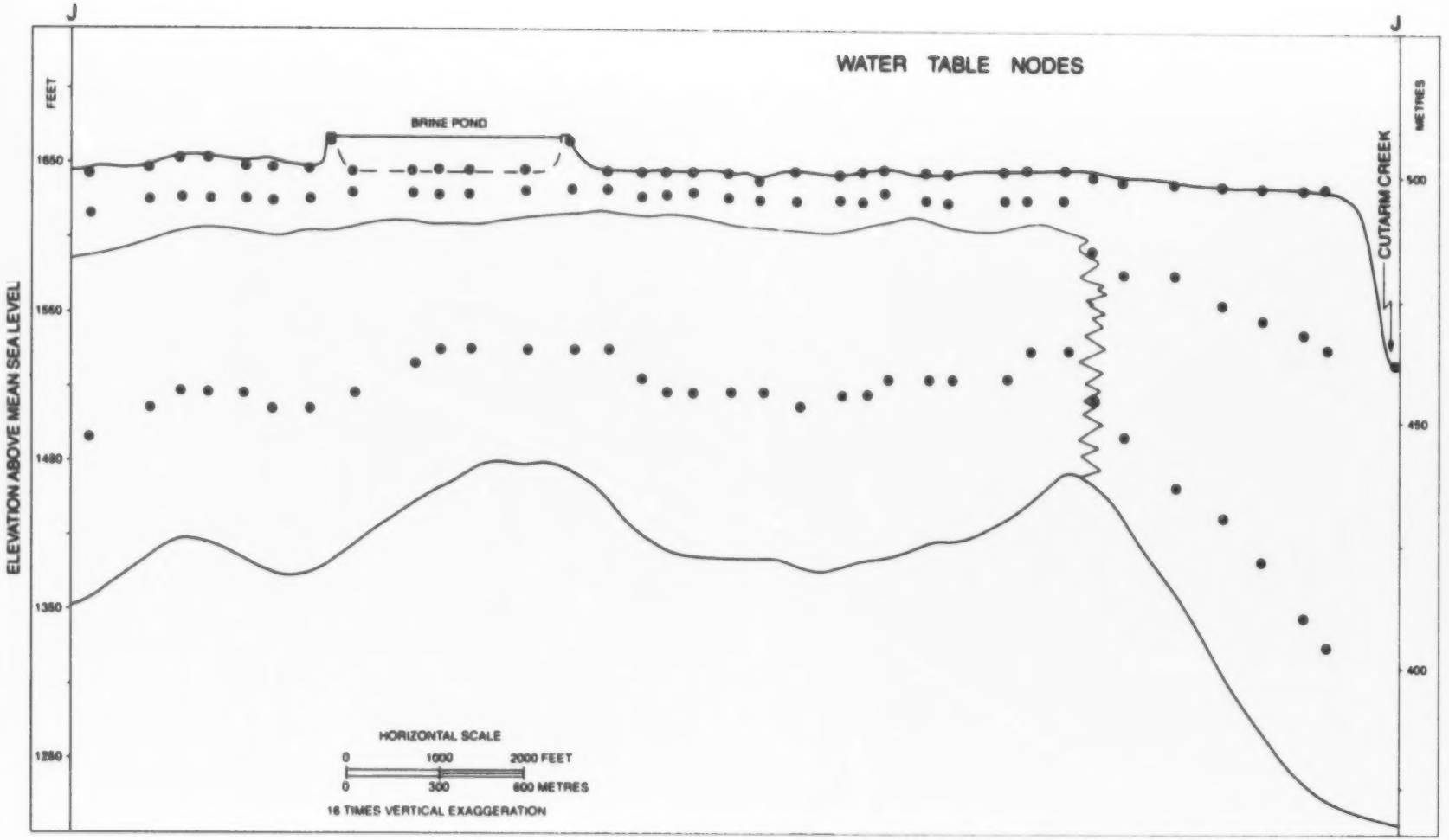

Figure IV-5. Distribution of nodes along cross section J-J'.

(ii) Transient

In the transient case, we are interested in measuring changes in voltage as a response to simulated pumping or injection of water. This requires a current-generating device, and voltage versus time plots for every nodal point in the model. This equipment is called the excitation-response apparatus. It requires that the water table simulator, used in the steady state case, be detached.

Excitation-response apparatus forces electrical energy, in the form of current, into the analog model and measures the response or energy levels throughout the energy-dissipative, resistor-capacitor network. The excitation-response apparatus, Figure IV-7, consists of a power supply, a waveform generator, a pulse generator, and an oscilloscope.

The following sequence of events occurs during the transient testing of an electric analog model:

1. The waveform generator sends a positive pulse to the oscilloscope, and simultaneously, a negative or positive sawtooth waveform is sent to the pulse generator.
2. The pulse generator is set to trigger when the voltage of the input sawtooth from the waveform generator exceeds a preselected level, thereby producing a rectangular pulse of desired duration and amplitude. The duration and amplitude of the pulse are analogous to the volume of water pumped or injected into the model.
3. Model response to the rectangular pulse from the pulse generator is monitored on the oscilloscope as a time-voltage curve, analogous to a time-drawdown graph for an observation well. To construct distance versus change in hydraulic head maps for time, t, a sufficient number of nodal points must be monitored.

Either pumping or injection of water can be simulated using the above apparatus by producing either a negative (pumping) or positive (injection) current pulse output from the pulse generator.

Since the excitation-response apparatus produces only pulses of voltage, current is calculated by substituting Ohm's law into equation 18, which yields:

$$q_w = \frac{V}{R_i} SC_3 \qquad (24)$$

where q_w = pumping rate, in lgpd

V = voltage, in volts

R_i = resistance in ohms

SC_3 = scale factor 3 in lgpd/amp

Therefore, a known voltage drop (V), which is selected using the pulse generator, across a predetermined resistance (R_i) produces a current that is analogous to the injection or pumping rate (q_w).

CONSTRUCTION TECHNIQUES

Two electric analog models, a prototype and a final, were constructed. The prototype model was constructed using 24-gauge tin plate as a mounting medium or base. A square grid was drawn on the tin plate and ceramic capacitors were soldered to the appropriate node. The unattached end of the capacitor served as a nodal point for the resistors. The tin plate proved satisfactory as an electrical grounding medium, however, the nodes were difficult to relate to topographic locations so this model was not an effective display and communication tool.

The base of the final model consisted of 1/8-in. tempered masonite or hardboard (Figs. IV-2 and IV-3). Holes (0.093 in. diameter) were drilled in a 1½ in. grid pattern. A topographic map of the area was glued onto the masonite and vectorboard push-in terminals (#T9.4) were inserted in the holes to serve as nodal junctions or terminals. The hardboard was mounted onto a wooden frame for construction and display purposes. Tinned copper wire (16 gauge) was placed the full length on the back of the model between alternate rows of nodes to provide a common ground.

Fixed carbon resistors (tolerance ± 5%) ranging from 10 ohms to 1.0×10^7 ohms, and ceramic disc capacitors, ranging from 0.22×10^{-6} to 1.0×10^{-11} farads were fastened and soldered to the terminals.

In general, leakage of electricity is the main source of error. To determine the extent of leakage from the terminals through the masonite, three terminals were inserted and soldered one node apart on the hardboard. The resistance between these terminals was measured and recorded before each electric analog model run. Results show that the resistance between terminals is 10^{10} ohms. This resistance is 3 orders of magnitude larger than the highest value resistor in the electric analog model, therefore demonstrating that leakage would be insignificant.

Other points to consider when constructing an electric analog model are:

1. The total capacitance of the model should be kept as low as possible because the larger the total capacitance of the model, the greater the chance for leakage from the capacitors to ground.

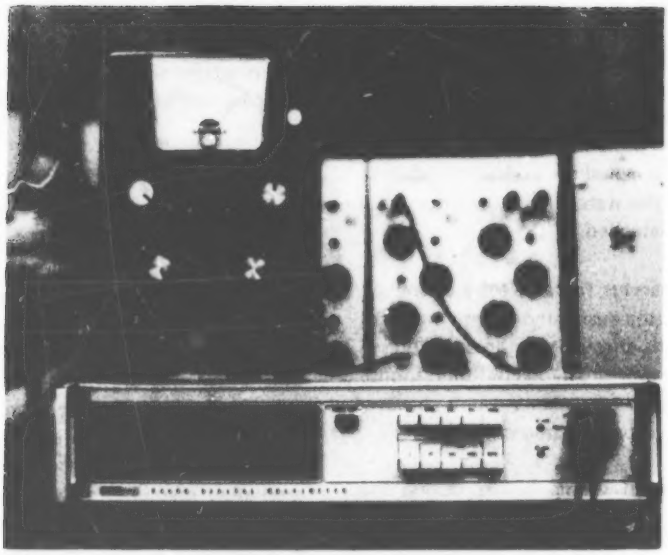

Figure IV-6. The steady state electric analog model response equipment showing a voltage generator resting on a digital readout voltmeter.

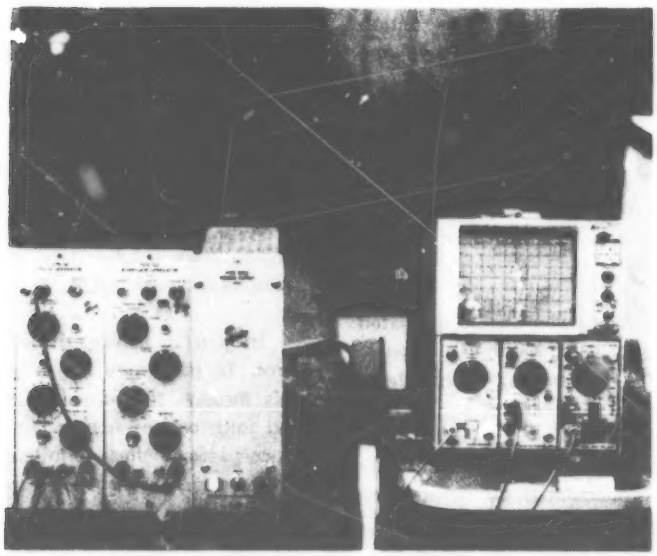

Figure IV-7. The excitation-response apparatus for the transient ground-water case showing, from left to right, pulse generator, a waveform generator, a power supply, and an oscilloscope.

2. The total resistance of the model should be kept low so that the current drawn by the model is small.

3. Spring clips and mechanical fasteners, although time saving, do not give a reliable electrical contact. Soldering is the best electrical connecting device.

APPENDIX V

Summary Field Analyses Hydrochemical Sampling Program 1972-1974

Summary Field Analyses Hydrochemical Sampling Program 1972-1974

FLOWING WELL 1—EXPLANATION OF TABLE

Day = no. of days since beginning of monitoring period, i.e., 1 = November 1, 1972.

Temp. = °C.

pH is in terms of pH units.

Eh is expressed as mV.

All concentrations are as ppm.

Day	Temp.	pH	Eh	Cond.	Ca	Mg	Na	K	Mn	Fe	HCO_3	SO_4	Cl
4	6.0	7.10	+ 20	----	153	72	---	---	---	6.4	595	408	---
5	5.8	7.00	+ 20	1277	157	71	---	---	---	5.7	618	397	---
8	7.0	7.25	- 10	1352	157	68	---	---	---	6.1	599	391	---
9	7.0	7.15	- 25	1395	155	69	---	---	---	6.0	628	395	---
10	6.1	7.20	- 35	1458	158	70	---	---	---	5.7	610	396	---
13	5.8	7.30	- 35	1351	166	64	---	---	---	6.4	634	388	---
14	6.0	7.35	- 35	1285	162	66	---	---	---	5.8	621	393	---
15	6.0	7.40	- 10	1418	170	62	---	---	---	5.5	628	394	---
16	6.2	7.35	- 30	1425	165	65	---	---	---	6.0	622	395	---
17	5.8	7.40	- 20	1432	164	65	---	---	---	5.8	626	399	---
18	6.0	7.30	- 35	1433	164	65	---	---	---	5.9	618	402	---
205	11.0	7.08	----	1347	---	---	---	---	---	---	---	---	---
207	9.0	7.00	----	1365	---	---	---	---	---	---	---	---	---
208	8.0	7.10	----	1400	160	---	---	---	---	5.5	617	---	---
209	11.0	7.34	----	1290	158	---	---	---	---	6.1	642	---	---
210	8.0	7.09	----	1450	167	---	---	---	---	5.5	643	---	---
211	8.1	7.28	----	1372	162	---	---	---	---	5.7	625	---	---
212	10.0	7.10	----	1380	162	---	---	---	---	5.5	655	---	---
213	9.0	7.01	----	1406	---	---	---	---	---	5.5	---	---	---
214	10.1	7.09	----	1388	---	---	---	---	---	5.7	---	---	---

Day	Temp.	pH	Eh	Cond.	Ca	Mg	Na	K	Mn	Fe	HCO_3	SO_4	Cl
215	10.0	7.23	----	1373	164	---	---	---	---	5.6	647	---	---
216	10.0	7.00	----	1386	166	90	---	---	---	5.5	644	---	---
217	14.9	7.05	----	1375	193	81	---	---	---	5.1	671	---	---
218	11.2	7.05	----	1388	169	73	---	---	---	5.7	653	---	---
219	10.1	7.00	----	1359	---	---	---	---	---	5.7	632	---	---
220	10.0	7.08	----	1351	---	---	---	---	---	7.1	---	---	---
221	8.0	7.00	----	1456	---	---	---	---	---	---	---	---	---
222	8.9	7.17	----	1362	156	103	---	---	---	7.2	624	---	---
223	9.0	7.04	----	1414	---	---	---	---	---	5.7	---	---	---
224	9.6	6.92	----	1353	167	92	---	---	---	6.9	642	---	---
225	9.2	6.98	----	1382	157	80	---	---	---	5.7	626	---	---
226	11.2	7.03	-100	1331	158	75	---	---	---	5.5	625	---	---
227	11.0	6.95	- 20	1403	152	79	---	---	---	5.5	629	---	---
228	11.0	6.96	+ 10	1316	159	81	---	---	---	6.0	619	---	---
229	9.0	7.13	+ 16	1368	158	75	---	---	---	5.7	639	---	---
230	11.0	7.01	+ 34	1336	158	76	---	---	---	5.7	625	---	---
231	10.0	7.03	+ 14	1328	154	76	---	---	---	5.8	631	---	---
233	11.0	7.03	+ 8	1398	151	80	---	---	---	5.6	626	---	---
234	9.1	6.95	- 4	1354	156	78	---	---	---	5.9	626	---	---
235	12.1	7.13	- 50	1310	150	82	---	---	---	5.9	617	---	---

Day	Temp.	pH	Eh	Cond.	Ca	Mg	Na	K	Mn	Fe	HCO_3	SO_4	Cl
236	11.0	6.96	- 3	1323	158	73	---	---	---	5.6	621	---	---
237	10.0	7.05	+ 6	1352	159	73	---	---	---	5.7	623	---	---
238	10.2	7.05	- 20	1310	158	73	---	---	---	5.8	627	---	---
239	10.3	7.04	- 40	1354	151	79	---	---	---	5.5	634	---	---
240	10.5	7.05	- 23	1320	156	76	---	---	---	5.9	626	---	---
241	10.0	6.96	- 10	1330	155	76	---	---	---	5.7	628	---	---
243	12.0	7.06	- 34	1290	156	76	---	---	---	5.6	622	---	---
244	10.4	7.06	- 40	1250	160	73	---	---	---	5.9	634	---	---
245	9.8	7.06	- 40	1230	153	79	---	---	---	5.8	648	---	---
246	9.0	7.10	- 35	1290	150	82	---	---	---	5.8	642	---	---
247	7.9	7.02	- 17	1300	155	78	---	---	---	5.8	615	---	---
249	9.1	7.00	- 40	1230	158	79	---	---	---	5.8	611	---	---
250	9.0	7.13	- 34	1300	162	71	---	---	---	5.8	611	---	---
251	9.5	7.12	- 44	1290	161	75	---	---	---	5.5	623	---	---
252	8.5	7.18	- 41	1310	157	78	---	---	---	5.7	634	---	---
253	9.2	7.10	- 35	1300	158	76	---	---	---	5.2	642	---	---
254	10.0	7.10	- 50	1450	147	84	---	---	---	5.6	621	---	---
255	9.1	7.00	- 34	1395	153	80	---	---	---	5.7	628	---	---
257	10.1	7.13	- 34	1400	154	80	---	---	---	5.7	628	---	---
258	11.5	7.14	- 18	1400	157	76	---	---	---	5.7	617	---	---

Day	Temp.	pH	Eh	Cond.	Ca	Mg	Na	K	Mn	Fe	HCO_3	SO_4	Cl
259	11.4	7.09	- 30	1400	154	80	---	---	---	5.7	627	---	---
260	10.0	7.21	- 25	1380	156	79	---	---	---	5.8	626	---	---
261	10.1	7.00	- 33	1400	142	86	---	---	---	5.8	627	---	---
264	11.0	7.18	- 30	1390	153	80	---	---	---	5.6	626	---	---
265	11.1	7.18	- 35	1450	155	78	---	---	---	5.6	623	---	---
266	10.3	7.11	- 24	1390	154	79	---	---	---	5.5	629	---	---
267	9.9	7.08	- 28	1380	159	75	---	---	---	5.5	623	---	---
268	10 2	7.10	- 13	1380	152	79	---	---	---	5.7	636	---	---
269	10.0	7.08	- 39	1420	153	78	---	---	---	5.7	619	---	---
271	8.3	7.20	+ 4	1470	156	76	---	---	---	---	605	---	---
272	8.3	7.11	0	1370	153	80	---	---	---	---	612	---	---
273	8.9	7.13	+ 5	1410	153	79	---	---	---	---	620	---	---
274	10.7	7.16	+ 30	1410	155	78	---	---	---	---	627	---	---
275	8.1	7.03	+ 65	1450	157	76	---	---	---	---	631	---	---
277	8.4	7.05	+ 14	1450	148	83	---	---	---	5.7	639	---	---
278	8.4	7.12	- 19	1420	155	79	---	---	---	5.8	629	---	---
279	9.0	7.16	- 30	1360	157	78	---	---	---	5.6	631	---	---
280	8.0	7.16	- 59	1390	154	79	---	---	---	5.5	620	---	---
281	9.9	7.18	- 47	1400	153	81	---	---	---	5.6	617	---	---
282	8.7	7.20	- 49	1460	154	78	---	---	---	5.6	626	---	---

Day	Temp.	pH	Eh	Cond.	Ca	Mg	Na	K	Mn	Fe	HCO_3	SO_4	Cl
283	9.0	7.16	- 48	1490	153	80	---	---	---	5.6	608	---	---
284	9.7	7.10	- 59	1440	152	81	---	---	---	5.6	628	---	---
285	8.5	7.10	- 50	1396	155	80	---	---	---	5.6	593	---	---
286	10.0	7.13	- 51	1400	157	80	---	---	---	---	625	---	---
287	8.7	7.19	- 57	1400	155	79	---	---	---	---	622	---	---
288	8.0	7.28	- 50	1440	153	81	---	---	---	---	601	---	---
289	8.1	7.11	- 48	1400	153	80	---	---	---	---	625	---	---
290	8.4	7.20	- 60	1390	154	79	---	---	---	---	616	---	---
291	8.4	7.05	- 56	1400	153	79	---	---	---	---	608	---	---
292	9.5	7.20	- 55	1397	154	78	---	---	---	---	612	---	---
571	7.5	7.10	+130	1180	154	---	---	11.4	---	5.5	---	---	---
575	7.0	7.10	+132	1500	157	---	88	11.6	0.30	5.5	---	---	---
578	7.0	7.24	+122	1590	152	---	93	10.4	0.25	5.5	---	---	---
584	8.0	7.30	+110	1220	152	72	105	12.2	0.27	5.9	---	---	---
590	7.0	7.20	+130	1390	150	70	93	10.6	0.24	5.7	---	---	14.0
592	6.0	7.35	+100	1520	157	63	96	11.8	0.28	6.3	---	---	14.0
596	6.8	7.30	+ 70	1100	155	76	85	12.0	0.32	5.8	565	---	15.0
598	7.0	6.85	+ 50	1440	148	65	85	10.4	0.34	5.8	566	---	13.8
600	6.5	6.85	+140	1310	151	70	93	11.1	0.28	5.7	578	---	13.6
603	6.5	6.70	+105	1310	153	69	93	10.5	0.28	5.3	566	---	14.4

Day	Temp.	pH	Eh	Cond.	Ca	Mg	Na	K	Mn	Fe	HCO_3	SO_4	Cl
604	6.5	6.71	+117	1380	154	66	93	10.4	0.25	5.5	532	---	13.6
605	6.7	7.05	+137	1310	148	64	87	10.6	0.29	5.5	---	---	13.2
606	7.2	6.80	+132	1310	156	61	75	10.7	0.28	6.8	569	---	13.0
607	6.1	6.92	+138	1350	151	64	95	11.0	0.45	5.3	558	---	13.0
610	5.8	6.60	+171	1380	157	71	90	9.6	0.32	4.3	569	---	12.6
611	6.3	7.10	+145	1340	157	70	90	10.2	0.31	5.6	565	---	13.2
312	6.2	6.89	+143	1320	154	73	93	9.2	0.20	5.1	584	---	13.0
613	6.9	6.78	+161	1250	142	73	90	10.3	0.25	5.8	572	---	13.0
614	5.9	6.80	+170	1360	170	70	95	10.3	0.25	5.7	581	---	13.2
624	6.5	6.90	+100	1200	153	68	113	10.7	0.27	5.8	564	---	14.0
625	6.8	6.90	+144	1260	154	67	105	10.7	0.24	5.3	565	---	13.2
626	6.6	6.85	+170	1300	157	80	90	10.2	0.24	6.1	564	---	13.6
627	6.2	6.83	+150	1330	160	80	90	10.0	0.26	6.1	560	---	13.6
628	6.9	6.80	+142	1310	156	77	93	10.8	0.25	6.0	577	---	13.2
631	6.4	6.51	+142	1260	150	73	80	10.7	0.25	5.9	591	---	13.4
632	6.6	6.81	+145	1300	153	74	70	11.2	0.27	5.8	578	---	13.8
634	6.5	6.92	+155	1260	165	89	100	10.4	0.28	5.6	592	---	12.8
635	7.1	6.74	+175	1280	152	88	100	10.3	0.28	5.1	576	---	12.8
637	6.3	6.80	+145	1240	154	78	100	11.4	0.25	4.7	565	---	12.8
638	6.5	6.83	+179	1230	153	---	---	11.0	0.24	5.3	571	---	13.4
639	6.3	6.93	+135	1240	158	76	95	10.9	0.28	6.1	572	---	13.4
640	6.4	6.74	+165	1210	149	72	95	14.0	0.25	6.8	593	---	13.4
641	6.3	6.80	+165	1280	152	69	95	10.6	0.28	5.5	573	---	15.0
642	6.9	6.86	+144	1220	153	69	88	10.5	0.29	6.1	576	---	15.0

FLOWING WELL 2–EXPLANATION OF TABLE

Day = no. of days since beginning of monitoring period, i.e., 1 = November 1, 1972.

Temp. = °C.

pH is in terms of pH units.

Eh is expressed as mV.

All concentrations are as ppm.

Day	Temp.	pH	Eh	Cond.	Ca	Mg	Na	K	Mn	Fe	HCO_3	SO_4	Cl
12	---	7.85	-115	2373	109	28	---	---	---	---	399	1001	---
13	---	7.90	-125	2380	106	29	---	---	---	4.9	400	998	---
14	---	7.85	- 70	2388	108	29	---	---	---	3.7	395	996	---
15	---	7.85	-110	2337	110	29	---	---	---	3.7	398	1008	---
16	---	8.00	- 95	2366	108	29	---	---	---	3.7	396	1011	---
17	---	7.90	-100	2348	109	28	---	---	---	3.1	396	1010	---
18	---	7.90	-125	2367	108	31	---	---	---	---	400	1006	---
205	11.0	7.90	----	2348	---	---	---	---	---	---	---	----	---
207	8.0	7.62	----	2296	---	---	---	---	---	---	---	----	---
208	7.3	7.56	----	2394	105	---	---	---	---	3.2	398	----	---
209	9.0	7.61	----	2315	106	---	---	---	---	3.3	407	----	---
210	6.9	7.68	----	2417	109	---	---	---	---	3.3	392	----	---
211	8.0	7.70	----	2318	109	---	---	---	---	3.3	429	----	---
212	9.0	7.64	----	2331	116	---	---	---	---	3.3	421	----	---
213	8.0	7.57	----	2358	---	---	---	---	---	2.3	---	----	---
214	9.2	7.58	----	2480	---	---	---	---	---	3.0	---	----	---
215	8.5	7.85	----	2307	108	---	---	---	---	3.3	401	----	---
216	8.4	7.60	----	2355	107	50	---	---	---	3.3	403	----	---
217	10.1	7.60	----	2434	123	43	---	---	---	---	454	----	---
218	9.2	7.63	----	2317	110	33	---	---	---	3.3	404	----	---

Day	Temp.	pH	Eh	Cond.	Ca	Mg	Na	K	Mn	Fe	HCO_3	SO_4	Cl
219	9.0	7.52	----	2299	106	40	---	---	---	3.2	394	----	---
220	10.9	7.50	----	2283	---	---	---	---	---	2.5	---	----	---
221	10.1	7.57	----	2438	---	---	---	---	---	---	---	----	---
222	8.0	7.66	----	2251	109	34	---	---	---	2.9	406	----	---
223	8.1	7.56	----	2285	---	---	---	---	---	2.8	---	----	---
224	8.2	----	----	2243	110	36	---	---	---	---	405	----	---
225	8.1	----	----	2302	104	38	---	---	---	3.3	404	----	---
226	11.1	7.70	- 20	2281	105	31	---	---	---	5.6	409	----	---
227	10.0	7.50	- 20	2409	105	27	---	---	---	3,5	410	----	---
228	9.3	7.62	- 8	2241	102	40	---	---	---	5.3	410	----	---
229	9.9	7.63	- 8	2162	105	33	---	---	---	5.3	416	----	---
230	9.6	7.54	- 18	2219	106	32	---	---	---	5.4	386	----	---
231	9.0	7.66	- 40	2293	104	35	---	---	---	5.1	407	----	---
233	10.0	7.61	- 53	2231	103	35	---	---	---	5.5	410	----	---
234	10.0	7.59	- 59	2242	100	38	---	---	---	5.3	412	----	---
235	10.7	7.69	- 64	2132	99	38	---	---	---	---	405	----	---
236	10.4	7.61	- 60	2164	103	35	---	---	---	---	411	----	---
237	10.9	7.57	- 63	2193	103	34	---	---	---	---	405	----	---
238	10.8	7.52	- 70	2161	104	33	---	---	---	---	407	----	---
239	11.0	7.60	- 79	2193	101	36	---	---	---	---	410	----	---

Day	Temp.	pH	Eh	Cond.	Ca	Mg	Na	K	Mn	Fe	HCO_3	SO_4	Cl
240	10.3	7.53	- 90	2200	100	38	---	---	---	---	405	----	---
241	8.7	7.67	- 73	2190	105	33	---	---	---	---	412	----	---
243	9.2	7.57	- 80	2180	103	35	---	---	---	---	410	----	---
244	9.0	7.60	- 84	2050	105	32	---	---	---	4.9	412	----	---
245	9.1	7.61	- 72	2090	104	34	---	---	---	5.4	411	----	---
246	10.0	7.66	- 81	2130	101	36	---	---	---	5.4	431	----	---
247	9.0	7.69	- 37	2100	100	35	---	---	---	5.1	409	----	---
249	9.0	7.69	- 88	2110	105	33	---	---	---	5.5	403	----	---
250	8.9	7.63	- 82	2170	106	32	---	---	---	4.5	405	----	---
251	9.0	7.67	- 79	2200	105	34	---	---	---	4.4	401	----	---
252	8.1	7.70	- 60	2200	102	36	---	---	---	4.4	403	----	---
253	8.8	7.54	- 48	2200	107	33	---	---	---	3.3	412	----	---
254	9.9	7.60	- 40	2300	100	38	---	---	---	3.3	404	----	---
255	8.0	7.61	- 35	2390	106	33	---	----	---	4.4	405	----	---
257	9.0	7.60	- 45	2330	105	33	---	----	---	3.3	406	----	---
258	9.1	7.65	- 40	2400	105	33	---	---	---	3.4	391	----	---
259	10.0	7.59	- 53	2320	106	33	---	---	---	3.3	411	----	---
260	9.5	7.63	- 58	2300	104	36	---	---	---	3.3	412	----	---
261	12.0	7.60	- 45	2270	102	35	---	---	---	3.3	393	----	---
262	8.6	7.58	- 50	2280	106	33	---	---	---	3.2	394	----	---

Day	Temp.	pH	Eh	Cond.	Ca	Mg	K	Na	Mn	Fe	HCO_3	SO_4	Cl
264	8.3	7.51	- 40	2410	106	32	---	---	---	3.2	403	----	---
265	10.9	7.61	- 39	2380	107	32	---	---	---	3.3	397	----	---
266	10.0	7.59	- 39	2390	107	33	---	---	---	3.3	399	----	---
267	10.1	7.58	- 44	2380	109	31	---	---	---	3.2	401	----	---
268	9.7	7.60	- 42	2400	105	32	---	---	---	3.4	398	----	---
269	10.4	7.53	- 49	2300	106	34	---	---	---	3.9	393	----	---
271	7.9	7.60	- 43	2320	105	34	---	---	---	---	398	----	---
272	7.7	7.59	- 45	2400	107	32	---	---	---	---	392	----	---
273	11.0	7.62	- 30	2420	106	33	---	---	---	---	398	----	---
274	8.0	7.58	- 40	2400	107	32	---	---	---	---	398	----	---
275	8.0	7.61	- 53	2300	106	34	---	---	---	---	386	----	---
277	7.9	7.55	- 56	2320	105	34	---	---	---	3.3	400	----	---
278	8.0	7.60	- 80	2380	105	34	---	---	---	3.3	395	----	---
279	8.4	7.57	- 76	2250	105	33	---	---	---	3.5	404	----	---
280	8.8	7.51	- 90	2380	106	34	---	---	---	3.4	406	----	---
281	8.9	7.54	- 95	2400	107	34	---	---	---	3.5	392	----	---
282	9.0	7.54	- 98	2200	110	34	---	---	---	3.3	404	----	---
283	8.1	7.58	- 98	2380	107	33	---	---	---	3.4	393	----	---
284	7.4	7.67	- 99	2395	104	35	---	---	---	3.3	394	----	---
285	7.7	7.57	- 91	2300	107	34	---	---	---	3.3	398	----	---

Day	Temp.	pH	Eh	Cond.	Ca	Mg	Na	K	Mn	Fe	HCO_3	SO_4	Cl
286	9.0	7.59	- 93	2400	110	32	---	---	---	---	390	----	---
287	8.9	7.60	- 90	2400	108	33	---	---	---	---	390	----	---
288	8.0	7.60	- 98	2350	109	33	---	---	---	---	389	----	---
289	8.0	7.62	- 90	2400	109	31	---	---	---	---	384	----	---
290	8.8	7.60	- 98	2390	107	32	---	---	---	---	397	----	---
291	9.4	7.61	- 81	2394	106	33	---	---	---	---	395	----	---
292	9.7	7.66	- 90	2395	107	33	---	---	---	---	398	----	---
571	7.0	7.18	+ 70	2200	110	---	---	9.3	---	3.4	---	----	---
575	8.0	7.35	+110	2460	112	---	490	10.1	0.17	3.3	---	----	---
578	7.5	7.45	+ 71	2200	108	33	523	10.8	0.15	3.7	---	----	---
585	7.0	7.40	+ 20	2460	104	32	488	10.5	0.11	3.9	---	----	---
590	7.5	7.24	+ 30	2460	105	30	500	9.5	0.16	3.0	---	----	---
592	7.0	7.60	+ 30	2500	113	24	500	9.8	0.15	4.6	---	----	63
596	7.0	7.70	+ 60	2230	110	27	495	9.8	0.17	4.8	375	----	64
598	7.5	7.30	+ 10	2900	105	32	495	9.4	0.13	4.8	372	----	64
600	6.8	7.50	+ 80	2380	109	29	458	9.5	0.17	3.6	375	----	64
603	8.0	7.24	+ 75	2210	110	27	458	9.5	0.13	3.4	379	----	64
604	7.5	7.23	- 7	2350	113	33	458	9.8	0.14	4.1	367	----	58
605	7.5	7.26	+ 37	2150	107	28	470	10.2	0.11	3.8	---	----	61
606	6.9	7.21	+ 49	2250	119	21	480	10.1	0.17	4.4	381	----	61

Day	Temp.	pH	Eh	Cond.	Ca	Mg	Na	K	Mn	Fe	HCO_3	SO_4	Cl
607	6.8	7.61	+ 99	2260	110	27	470	10.0	0.17	3.4	346	----	66
610	7.2	7.15	+ 59	2210	115	29	485	11.3	0.16	2.5	379	----	50
611	6.8	7.45	----	2310	112	29	485	9.1	0.10	3.6	399	----	53
612	7.5	7.50	+ 59	2030	120	41	533	8.6	0.09	3.5	379	----	61
613	6.8	7.22	+ 71	2030	112	29	513	10.3	0.12	5.0	381	----	61
614	7.4	7.18	+ 88	2220	110	37	478	8.5	0.10	3.9	386	----	64
624	7.0	7.40	+ 32	2200	109	24	470	8.8	0.10	3.7	431	----	57
625	7.2	7.29	+108	2190	114	23	480	9.1	0.10	3.4	371	----	60
626	7.1	7.10	+118	2100	110	30	475	11.8	0.09	3.6	370	----	63
627	7.3	7.24	+148	2010	110	30	460	8.7	0.09	3.7	358	----	65
628	8.1	7.43	+ 59	2200	116	32	460	11.5	0.10	3.4	381	----	64
631	7.1	7.15	+ 92	2020	107	34	475	10.0	0.10	3.3	392	----	63
632	7.0	7.41	+102	2180	110	47	458	9.3	0.10	3.3	381	----	64
634	6.9	7.48	+ 61	2230	117	25	508	12.7	0.12	3.5	393	----	65
635	7.1	7.32	+132	2020	100	37	500	8.8	0.13	3.5	376	----	65
637	7.2	7.38	+100	2080	107	28	508	9.5	0.11	3.5	372	----	68
638	7.1	7.43	+119	2030	112	26	480	11.4	0.10	3.3	375	----	58
639	6.8	7.51	+118	2190	106	28	470	15.2	0.13	3.9	376	----	88
640	6.8	7.33	+138	2200	106	27	470	16.8	0.10	3.6	382	----	64
641	6.5	7.42	+ 99	2190	105	27	470	19.5	0.14	3.6	373	----	67
642	6.0	7.49	+ 10	2160	109	31	460	10.0	0.14	3.8	377	----	67

OBSERVATION WELL G—EXPLANATION OF TABLE

Day = no. of days since beginning of monitoring period, i.e., 1 = November 1, 1972.

Temp. = °C.

pH is in terms of pH units.

Eh is expressed as mV.

All concentrations are as ppm.

Day	Temp.	pH	Eh	Cond.	Ca	Mg	Na	K	Mn	Fe	HCO_3	SO_4	Cl
584	8.0	7.87	-125	1120	124	77	93	11.2	0.57	28	---	----	---
590	10.0	7.60	- 10	1400	158	68	83	11.7	0.37	9	---	----	12
592	10.0	7.90	- 80	1500	167	62	85	12.3	0.47	21	---	----	12
596	8.5	7.80	-150	1430	162	70	80	12.8	0.62	20	620	----	15
598	10.0	7.20	- 70	1410	153	71	80	11.5	0.62	18	615	----	14
600	8.5	7.28	- 70	1380	156	73	85	10.8	0.55	22	615	----	13
603	9.0	7.25	-100	1330	158	75	83	11.6	0.56	21	621	----	12
604	10.5	6.95	- 47	1320	162	66	78	10.5	0.56	20	612	----	13
605	8.2	6.94	-151	1390	155	69	78	11.1	0.51	26	---	----	13
606	7.5	6.92	-100	1380	160	63	80	12.5	0.50	21	622	----	14
607	7.2	7.35	-118	1390	164	74	83	11.8	0.90	20	570	----	14
610	7.5	7.13	-120	1390	170	72	83	11.0	0.59	24	623	----	12
611	7.9	7.11	-139	1340	166	72	80	9.4	0.60	24	622	----	12
612	8.2	7.22	- 88	1250	172	80	85	9.1	0.60	22	614	----	12
613	8.1	7.17	-145	1380	165	82	84	10.7	0.54	29	621	----	12
614	7.2	7.19.	- 94	1350	183	79	88	10.3	0.54	31	623	----	12
619	8.5	7.25	-120	1380	151	74	88	10.4	0.65	32	628	----	14
624	8.5	7.30	-200	1350	161	71	100	10.7	0.55	27	611	----	10
625	7.5	7.20	- 63	1300	178	71	105	12.3	0.47	26	621	----	14
626	8.2	7.02	-195	1300	168	82	93	11.3	0.56	33	614	----	14

Day	Temp.	pH	Eh	Cond.	Ca	Mg	Na	K	Mn	Fe	HCO_3	SO_4	Cl
627	7.9	7.21	- 80	1230	166	80	85	10.7	0.56	30	592	----	13
628	7.9	7.25	-103	1340	164	80	93	12.3	0.53	24	625	----	15
631	7.8	6.91	-181	1320	163	78	70	11.1	0.57	31	644	----	13
632	7.9	7.13	-187	1320	155	82	75	14.4	0.54	32	626	----	13
634	7.8	7.25	-171	1300	202	92	95	11.3	0.65	32	676	----	12
635	7.9	7.13	-158	1300	156	84	95	11.2	0.57	31	620	----	11
637	7.0	7.36	-110	1320	160	82	95	14.3	0.57	31	627	----	17
638	8.1	7.22	- 95	1230	158	82	83	13.1	0.60	30	620	----	12
639	7.5	7.28	- 99	1310	158	77	93	11.4	0.60	37	604	----	13
640	7.1	7.12	-120	1300	155	72	80	10.8	0.58	38	633	----	13
641	7.2	7.23	- 63	1350	164	72	80	11.3	0.57	34	631	----	15
642	7.5	7.28	-129	1350	161	75	83	10.5	0.50	32	630	----	15

APPENDIX VI

Indirect Determination of Cl and SO_4 in Aqueous Solutions by Atomic Absorption Spectroscopy

Indirect Determination of Cl and SO_4 in Aqueous Solutions by Atomic Absorption Spectroscopy

During this study Cl and SO_4 were determined in aqueous solutions in the field laboratory using indirect AAS (atomic absorption spectroscopy) techniques (Dunk, *et al.*, 1967; Barefoot, 1974, pers. comm.). Chloride was determined in the range 1-20 μg/ml by the addition of a known amount of excess Ag. The preparation vials were allowed to sit in a dark cool place overnight to allow $AgCl_s$ to settle. An aliquot of supernatant solution was decanted and Ag was analyzed in the range 1-5 μg/ml by flame AAS on a Jarrell-Ash Dial Atom II Spectrophotometer. Reproducibility was found to be ± 1% for the range 1-20 μg/ml Cl, using a lean air-acetylene flame. Higher Cl concentrations were determined by dilution down to this range. The AAS results for Cl were comparable with those obtained by the Western Laboratory for the same samples using the automated thiocyanate method.

Sulphate was determined in the range 10-1000 μg/ml by the addition of a predetermined excess of Ba to precipitate $BaSO_{4(s)}$. Excess Ba was determined by flame AAS in the range 10-100 μg/ml. The SO_4 determinations lacked sufficient reproducibility in this study to be included in the chemical analysis of the aqueous samples. Sensitivity was poor for Ba determinations using the Jarrell-Ash Ba hollow cathode source and acetylene-air flame. Ba sensitivity is increased by the use of a nitrous oxide-air flame, but this was unavailable during this study. Also, the finely divided precipitate did not settle sufficiently during overnight storage. Centrifugation would likely have eliminated this latter problem. Unfortunately, a centrifuge unit was not available in the field laboratory.

APPENDIX VII

Standard Addition Method to Detect and Correct for Interference Effects in Flame Atomic Absorption Spectroscopy Determination of Ca, Mg, and K (R. R. Barefoot)

EXAMPLE

Standard Addition Method for Ca Determination by AAS.

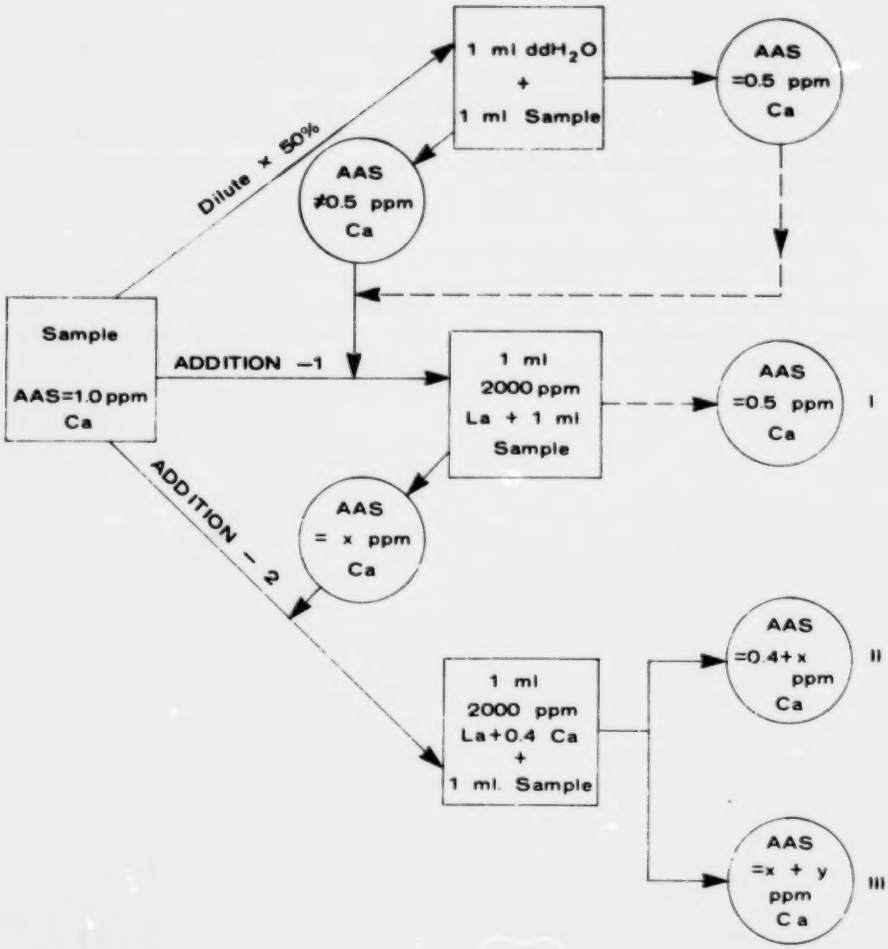

If I: No standard addition is necessary.

If II: La addition has removed interference problems. The true Ca (Ca_T) in the sample is $Ca_T = x \times$ dilution.

If III: La addition has not removed interference and a correction factor must be applied to calculate the true Ca (Ca_{T_r}) in the sample.

Correction Factor

After La addition, an addition of 0.4 ppm. Ca did not give a 0.4 p.p.m. Ca increase in the AAS determination. Instead, the increase was y ppm Ca. The correction factor is expressed as $f = \frac{0.4}{y}$ in this case. Therefore, the true concentration of Ca in the sample can be calculated:

$Ca_{T_r} = x \times f \times$ dilution.

APPENDIX VIII

Calcium and Magnesium Analyses of Unpreserved Stored Groundwater Samples (C. C. Davison)

Calcium and Magnesium Analyses of Unpreserved Stored Groundwater Samples (C. C. Davison)

Chemical analyses were done on the precipitate, suspended and dissolved fractions in a number of water samples to determine the magnitude of the loss of Ca or Mg in unpreserved groundwater samples during storage.

PROCEDURE

Groundwater samples were collected from flowing wells 1 and 2. The samples were stored unpreserved in tightly capped 100-ml polyethylene bottles for 3 months at ambient air temperature. At the end of this period the samples were shaken vigorously and uncapped. For each sample, the supernatant solution was passed through a prerinsed 0.45-μm Millipore filter, acidified with a predetermined quantity of reagent grade HNO_3 and saved for subsequent Ca and Mg analyses.

The filter paper for each sample was placed in a dilute HNO_3 solution and washed for a period of 2 weeks. At the end of the washing period the filter paper was removed, the solution was diluted to 100 ml with double distilled H_2O and saved for atomic absorption spectroscopy analysis.

The inside of the polyethylene sample bottle was coated with clear amorphous-looking precipitate; 0.6 ml conc. HNO_3 was pipetted into the sample bottle and diluted to approximately 10 ml with double-distilled H_2O. The bottles were capped and shaken vigorously for about 10 min, or until no precipitate was visible on the walls of the bottle. Double-distilled H_2O was added to bring the volume up to 100 ml and the sample was saved for analysis.

All Ca and Mg analyses were done by AAS, using a Perkin-Elmer 360 spectrophotometer, and standard addition techniques were used to eliminate interference effects. Standards were prepared from reagent grade chemicals and checked against U.S. Geological Survey standard reference values. Samples and standards were normalized with a predetermined quantity of HNO_3 to avoid viscosity and matrix interferences.

APPENDIX IX

Field Laboratory and Western Laboratory Analyses of Split Groundwater Samples, Summer 1973

Field Laboratory and Western Laboratory Analyses of Split Groundwater Samples, Summer 1973

EXPLANATION OF TABLE

Day – Number of days since the beginning of water quality monitoring programme (i.e., 0 – November 1, 1972)

$\bar{X}$ – Sample population mean.

S – Standard deviation.

V_T^2 – Coefficient of total variation of sample population.

Spec. Cond. – Specific Conductance (in μmhos/cm)

All concentrations expressed in ppm.

Split Samples – Flowing Well 1 – Field Laboratory Analyses (1973)

Day	Ca	Mg	Fe	HCO_3	Spec. Cond.
225	157	80	5.7	642	1382
226	158	75	5.5	626	1331
233	151	80	5.6	626	1392
240	156	76	5.9	626	1320
246	150	82	5.8	642	1290
254	147	84	5.6	621	1450
265	155	78	5.6	623	1450
279	157	78	5.6	631	1360
286	157	80	–	625	1400
292	154	78	–	612	1397
$\bar{X}$	154.2	79.1	5.66	627.4	1377
S	3.7	2.7	0.16	9.14	52.8
V_T^2	5.7	11.5	8.2	2.1	14.7

Split Samples – Flowing Well 2 – Field Laboratory Analyses (1973)

Day	Ca	Mg	Fe	HCO_3	Spec. Cond.
219	106	40	3.2	394	2299
225	104	38	3.3	404	2302
226	105	31	5.6	409	2281
233	103	35	5.5	410	2231
240	100	38	–	405	2200
246	101	36	5.4	431	2130
254	100	38	3.3	404	2300
265	107	32	3.3	397	2380
279	105	33	3.5	404	2250
286	110	32	–	390	2400
292	107	33	–	398	2395
$\bar{X}$	104.4	35.1	4.14	404	2288
S	3.6	3.1	1.10	10.8	84
V_T^2	11.6	77.0	692.00	7.1	13.44

Split Samples – Flowing Well 1 – Water Quality Laboratory (1973)

Day	Ca	Mg	Na	K	Fe	Mn	HCO_3	SO_4	Cl	Spec. Cond.
219	152	57	97	9.4	–	–	491	410	14	1520
225	202	56	84	9.0	–	–	–	400	13	1604
226	199	57	91	9.0	6.0	0.24	597	400	–	1620
233	202	54	90	9.9	5.4	0.24	599	400	15	1640
240	172	60	80	9.3	5.6	0.24	552	360	13	1750
246	204	53	90	10.0	7.7	0.24	604	400	14	1450
254	196	57	92	13.0	5.9	–	606	395	10	1540
265	211	51	82	10.0	5.8	0.25	611	380	15	1560
279	148	52	82	10.0	5.6	0.24	471	332	15	1343
286	177	46	88	11.0	5.0	0.23	489	369	14	1566
292	193	62	84	9.5	5.9	0.24	580	380	13	1432
$\bar{X}$	186.9	55.0	87.3	10.0	5.9	0.24	559.9	384.4	13.6	1548
S	21.6	4.5	3.2	1.2	0.76	0.01	55.5	22.1	1.6	111.3
V_T^2	133.0	67.8	13.4	132.3	167.4	4.95	98.4	33.0	140.4	51.7

Split Samples – Flowing Well 2 – Water Quality Laboratory (1973)

Day	Ca	Mg	Na	K	Fe	Mn	HCO_3	SO_4	Cl	Spec. Cond.
219	112	26	454	7.5	–	–	347	960	63	2720
225	131	24	395	7.0	–	–	384	950	62	2777
226	130	24	389	7.0	3.6	0.11	390	950	61	2760
233	133	21	470	7.5	3.8	0.51	388	920	62	2790
240	132	24	460	7.4	4.7	0.10	–	900	61	2790
246	134	27	470	7.4	6.5	0.10	398	970	62	2620
254	129	57	464	7.6	3.3	0.11	396	970	64	2610
265	139	21	456	7.3	3.2	0.11	399	960	60	2630
279	128	19	480	7.4	0.11	0.95	356	960	62	2615
286	144	13	470	7.6	3.2	0.10	376	950	62	2605
292	128	27	478	7.4	3.3	0.24	388	1000	60	2619
$\bar{X}$	130.9	25.8	454.0	7.4	3.6	0.25	383.0	954.0	61.7	2685
S	7.9	11.2	30.0	0.20	1.9	0.29	36.0	26.0	1.2	81
V_T^2	36.8	891.5	44.6	7.72	2840	13621	87.5	7.5	3.7	9.1